AIR FORCE INSTITUTE OF TECHNOLOGY

AIR UNIVERSITY
UNITED STATES AIR FORCE

SCHOOL OF ENGINEERING

WRIGHT-PATTERSON AIR FORCE BASE, OHIO

GRAVITY-ASSISTED TRAJECTORIES FOR SOLAR PROBE MISSIONS

THESIS

GA/AE/67-4 Kenneth A. Myers
1/Lt USAF

AFLC--WPAFB--AUG 67 35

GRAVITY-ASSISTED TRAJECTORIES FOR SOLAR PROBE MISSIONS

THESIS

Presented to the Faculty of the School of Engineering of
the Air Force Institute of Technology
Air University
in Partial Fulfillment of the
Requirements for the Degree of
Master of Science

By
Kenneth A. Myers, B.S.
1/Lt USAF
Graduate Astronautics

June 1967

Preface

This thesis is the result of a suggestion by Dr. Corrado R. Poli, of the Department of Aeronautical Engineering at AFIT, for a study on gravity-assisted solar probe trajectories. The need for this investigation was established at the NASA-Stanford University Summer Training Program in Systems Engineering which he attended in the summer of 1966. Results of this program, a systems analysis of a solar probe mission, are reported in the ICARVS design study (Ref 12).

The thesis is written on a level which should provide no difficulty to a reader who has completed a first course in astrodynamics. The method developed for gravity-assisted trajectories is useful in feasibility studies, and can be applied to any ballistic flyby mission. Gravity assist has been found to be useful (Ref 17) in many types of missions such as: deep-space probes, trips to the outer planets, grand tours or trajectories which pass several planets on a single flight, and out-of-ecliptic trajectories. If the reader finds an interest in this area, I can suggest two thesis topics which would supplement this work: 1) application of the gravity-assist equations to continuous-thrust missions and 2) a linear error analysis of gravity-assisted trajectories.

A discussion on computer programming is included with each mission study in the thesis, and the programs with

sample output are given in Appendix E. These sections are provided for the reader who may wish to continue the study, and if desired, may be skipped with no discontinuity in the subject material.

I wish to express my appreciation to Dr. Poli for his suggestions and continued interest in my work, and to the computational staff at Building 57, Wright-Patterson Air Force Base, for their assistance in programming the equations. Finally, I thank my wife for the intangible contributions she has made to this study, and for the typing of the manuscript.

Kenneth A. Myers

Contents

List of Figures

Figure Page

List of Tables

List of Symbols and Subscripts

Symbols

A - transformation matrix from xyz to XYZ

a - semi-major axis

B - transformation matrix from XYZ to X'Y'Z'

C - transformation matrix from xyz to $X_2Y_2Z_2$

D - transformation matrix from $x_2y_2z_2$ to $X_2Y_2Z_2$

d - distance of closest approach or DOCA

e - eccentricity

$\bar{e}$ - unit vector (subscript indicates direction)

f - heliocentric true anomaly

i - inclination of orbital plane with respect to ecliptic

l_1, l_2 - heliocentric longitudes of P_1 and P_2

m - number of solar circuits of P_2 in a multiple assist

n - number of solar circuits of spacecraft in a multiple assist

P_1 - departure planet

P_2 - assist planet

P_3 - second assist planet

q_m - perihelion after assist maneuver

q_{mm} - perihelion after assist at P_3

R - equatorial radius of a planet

r - orbital radius

r_A - aphelion

r_m - distance from center of mass of P_2 to intersection of inbound and outbound asymptotes of assist hyperbola

Symbols

S - synodic period

T - transfer time

t_L - launch time

t_o - epoch

V - orbital velocity

V_b - burnout velocity

V_∞ - hyperbolic excess velocity (HEV)

XYZ - ecliptic system with origin O at Sun

xyz - orbital reference system with origin O at Sun

$X'Y'Z'$ ecliptic system with origin O' at Sun

$X_1Y_1Z_1$ planetocentric system with origin O_1 at center of mass of P_1

$X_2Y_2Z_2$ system located near P_2 with origin O_2 at intersection of inbound and outbound assist hyperbola asymptotes

$x_2y_2z_2$ assist orbit system with origin at O

α - angle between $\bar{V}_{P_1}$ and $\bar{V}_{\infty P_1}$ in two-dimensional analysis; right ascension of $\bar{V}_{\infty_i}$ at P_2 in three-dimensional analysis

β - assist orbit plane orientation angle

γ - heliocentric angle between P_1 at launch and P_2 at intercept measured in ecliptic

δ - declination of $\bar{V}_{\infty i}$ at P_2

η - angle between $\bar{V}_o$ and $\bar{V}_{\infty P_1}$ in two-dimensional analysis; angle between XYZ and X'Y'Z' systems in three-dimensional analysis

θ - heliocentric transfer angle

θ_L - lead angle between P_1 to P_2 at time of launch

θ_P - angle between P_1 and P_2 at time of intercept

μ - gravitational parameter

Symbols

ν - angle between asymptote and conjugate axis of assist hyperbola

ρ - radius of sphere of influence (SOI)

τ - orbital period

Υ - vernal equinox

ϕ - flight path angle measured clockwise from inward orbital radius vector to orbital velocity vector

ψ - angle measured clockwise from assist planet velocity vector to outbound HEV vector

ω_1, ω_2 - mean daily motion of P_1 and P_2

Subscripts

i - applies to inbound HEV at P_2

o - applies to outbound HEV at P_2

sc - spacecraft

0 - heliocentric departure conditions at P_1

1 - heliocentric arrival conditions at P_2

2 - assist orbit conditions at P_2

3 - heliocentric departure conditions at P_2

4 - assist orbit conditions at P_3 for combination assist; second assist orbit conditions at P_2 for multiple assist

5 - heliocentric arrival conditions at P_3 for combination assist; heliocentric departure conditions at P_2 in double assist

6 - third assist orbit conditions at P_2 for multiple assist

7 - heliocentric departure conditions at P_3 in combination assist; heliocentric departure conditions at P_2 in triple assist

Subscripts

OP - applies to transfer from P_1 to final perihelion

12 - applies to transfer from P_1 to P_2

23 - applies to transfer from P_2 to P_3

Abbreviations

DOCA - distance of closest approach

HEV - hyperbolic excess velocity

SOI - sphere of influence

Abstract

An investigation of direct-transfer trajectories for solar probe missions indicates that expensive launch vehicles such as the $125-million Saturn V are required to achieve perihelia less than 0.25 AU and inclination angles above 20°. Methods are developed for two- and three-dimensional gravity-assisted trajectories (trajectories which pass through one or more planetary gravitational fields), and are applied to solar probe missions in an attempt to reduce launch vehicle costs. The analysis is based on the pieced-conic approximation and the assumption of circular coplanar planetary orbits. It is found that a perihelion of 0.16 AU can be obtained with the $16-million Atlas/Centaur/TE-364-3 by using a Venus assist. Even greater reductions in perihelia are attained with multiple passes at Venus; in addition, these missions allow the exploration of several regions near the Sun with a single launch. Venus-Mercury combination-assisted trajectories are of little value in solar probe missions. A Venus assist is useful for 10°-out-of-ecliptic trajectories when the pre-assist orbit lies in the ecliptic. For a pre-assist orbit out of the ecliptic, an inclination angle of 25° and a perihelion of 0.53 AU can be achieved with the Atlas/Centaur/TE-364-3 launch vehicle. Solar impact and 90°-out-of-ecliptic trajectories can be attained with a Jupiter assist; however, traversal of the asteroid belt and a three-year mission time decreases spacecraft reliability.

GA/AE/67-4

GRAVITY-ASSISTED TRAJECTORIES FOR SOLAR PROBE MISSIONS

I. Introduction

Background Information

The current NASA Pioneer program (Ref 22:69) is designed to explore solar effects on the space environment between 0.8 and 1.2 AU from the Sun. Plans for advanced missions in this program include the exploration of regions as close as 0.5 AU from the Sun, both in and out of the ecliptic plane. The trajectories for these missions can be achieved with the Thrust-Augmented Delta and Atlas launch vehicles, but larger and more expensive booster systems are required for the exploration of regions closer to the Sun.

The perihelion which can be attained for a given burnout velocity is shown on the graph in Fig. 1 for a hyperbolic ascent departure and Hohmann transfer orbit. Burnout velocities in excess of 41,000 ft/sec are necessary for solar probe missions to regions less than 0.5 AU from the Sun. The reason for this high velocity requirement is that the spacecraft velocity must not only exceed the velocity for Earth escape (36,700 ft/sec), but also counteract the high orbital velocity of the Earth about the Sun (97,700 ft/sec).

For missions to the 0.2 to 0.1 AU region, the range of required burnout velocities is from 55,000 to 67,000 ft/sec, respectively. This requirement can be met with the Saturn V

launch vehicle, but the cost of this system ($125 million) and the small payload for a solar probe (200 lb) warrant an investigation for less expensive techniques.

Purpose of the Thesis

The purpose of this thesis is to investigate the use of gravity assist as a means of reducing the cost (see Table I) and/or burnout velocity requirements for booster vehicles in solar probe missions. Gravity assist is defined as a significant trajectory perturbation between launch and target positions caused by a close approach to an intermediate planet. This concept is also referred to as a planet fly-by or swing-by. The basic purpose of gravity assist is to change the spacecraft velocity vector with respect to the Sun; the effectiveness of the maneuver depends primarily on the mass and velocity of the assist planet and on the DOCA (distance of closest approach) of the spacecraft to the surface of the planet.

The primary goal is to achieve the smallest possible perihelion with the least expensive booster vehicles; for out-of-ecliptic missions it is also desired to achieve the largest possible inclination angle.

History of Fly-By Missions

The first planetary fly-by was achieved in December, 1962, when the Mariner 2 spacecraft (Ref 4:695-699) passed within 21,600 mi (18,800 NM) from the surface of Venus. The purpose of this flight was to collect data on the Venusian atmosphere,

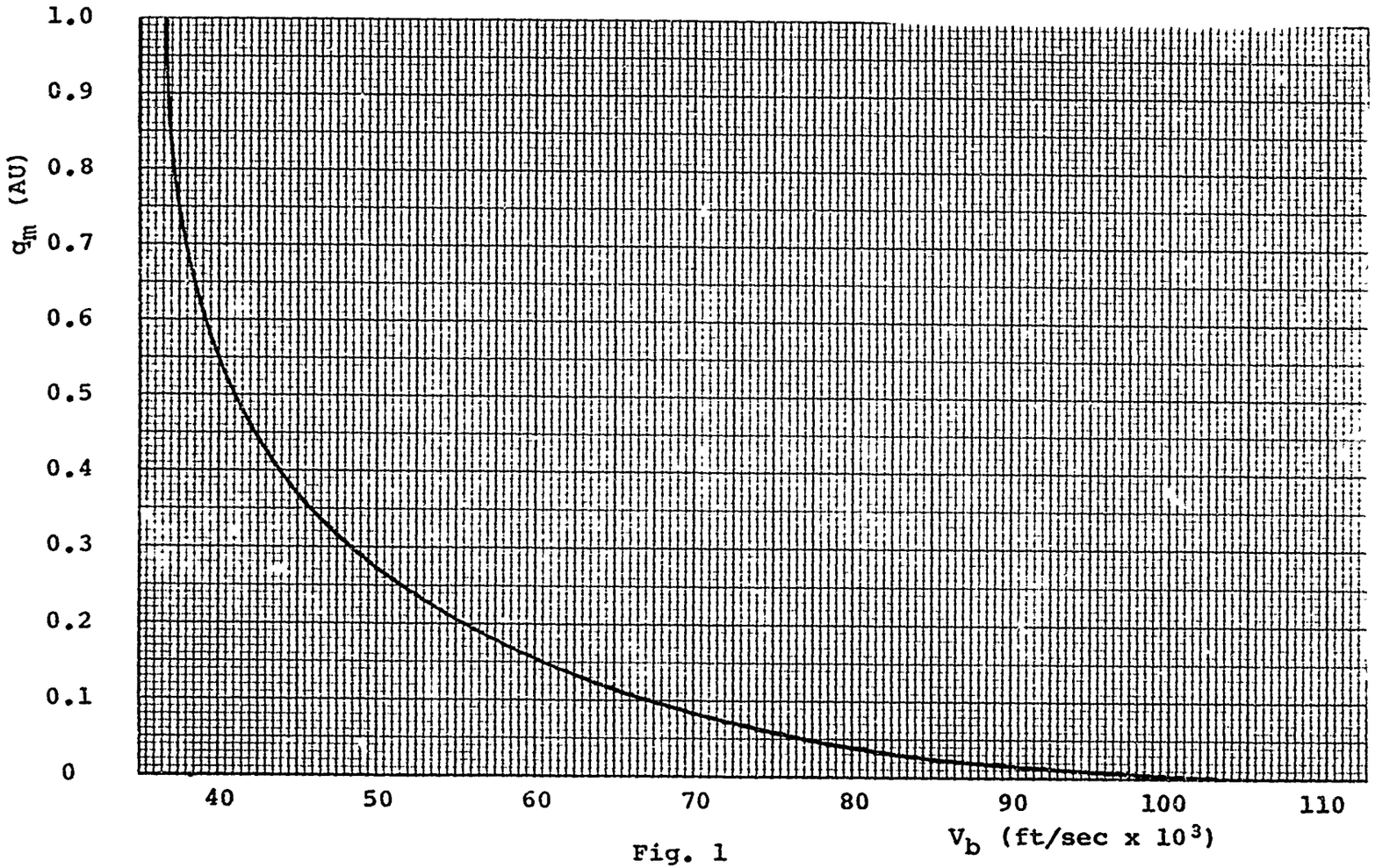

Fig. 1

Burnout Velocity Requirement for Direct-Transfer Solar Probe Trajectories

so the mission was completed after the encounter, and the spacecraft was left to orbit the Sun. Mariner 4 (Ref 24: Fall 1965) completed a similar mission when it passed within 5400 mi (4690 NM) from the surface of Mars in July, 1965.

Survey of the Literature

Minovitch (Ref 10,11) has conducted a two-part investigation on gravity-assisted trajectories. The first part of his investigation is devoted to the development of theory and the calculation of gravity-assisted trajectories to the inner planets. The second part is devoted to deep-space and solar probe trajectories in which Jupiter is used as an assist planet for missions in and out of the ecliptic plane. Niehoff (Ref 13) has continued the work done by Minovitch for gravity-assist missions in the ecliptic plane by using Jupiter as either a target or an assist planet. The results of these studies show that 90°-out-of-ecliptic trajectories with perihelia less than 0.1 AU can be attained with a Jupiter assist and an Atlas/Centaur/Kick launch vehicle ($16 million).

Thus, Jupiter-assisted solar probe trajectories have been thoroughly investigated. The excellent performance attained in these miss .s is due to the large mass of Jupiter (318 times the mass of Earth), but these missions have two disadvantages: first, the flight time is about three years, and second, the vehicle must pass through the asteroid belt twice on its path to the Sun.

Ross (Ref 15) has presented a detailed study on round

Table I

ESTIMATED COST OF LAUNCH VEHICLES (1967)

Launch Vehicle	Launch Cost ($ Million)	Performance (lbs payload escape)	($/lb to escape)
Delta	3.1	100	31,000
TAID	3.4	300	11,300
Atlas/SLV-3A/Agena D	7.9	1,450	5,500
Atlas/SLV-3C/Centaur	11.9	2,850	4,000
Atlas/Centaur/Kick	16.0 **	----	----
Titan II/Centaur	20.0 *	----	----
Titan IIIA/Agena D	8.6	1,200	7,100
Titan IIIC	17.6	5,000	3,500
Uprated Saturn I	29.8	13,000	2,300
Saturn IB/Centaur	41.0 **	----	----
Saturn V	125.0	93,000	1,300

(From Ref 23:58)

* (From Ref 22:84)

** (From Ref 12:93)

trips to the inner planets and an introduction to Venus-assisted trajectories for solar probes. The Jupiter-assist disadvantages are avoided by using the inner planets for gravity assist in solar probe missions.

Plan of Development

The over-all plan of the thesis is to investigate inner-planet gravity-assist missions, and to compare them with direct-transfer and Jupiter-assist missions. The body of the report contains a discussion of the theory and results of the mission studies. Detailed derivations of the equations are given in the appendices.

Chapter II is an investigation of direct-transfer solar probe trajectories. This chapter serves to illustrate the departure orbit technique used in the report, and it provides a standard with which gravity-assisted solar probe trajectories may be compared.

The method of analysis for two-dimensional gravity-assisted trajectories is discussed in Chapter III. This method is applied to the following solar probe missions:

1. Venus Assist in the Ecliptic (Chapter IV)
2. Venus-Mercury Combination Assist (Chapter V)
3. Multiple Venus Assist (Chapter VI)
    a. Double Pass at Venus
    b. Triple Pass at Venus

The method in Chapter III is extended to the case of three-dimensional gravity assist in Chapter VII, and is

applied to the following out-of-ecliptic solar probe missions:

1. Out-of-ecliptic Venus Assist (Chapter VIII)
    a. Pre-Assist Orbit in the Ecliptic Plane
    b. Pre-Assist Orbit out of the Ecliptic Plane
2. Jupiter Assist (Chapter IX)

It has been shown (Ref 11:39) that Mars offers little or no benefit as an assist planet for solar probe trajectories, so these missions have not been investigated in this study.

Conclusions are made in Chapter X, and favorable missions are recommended for further consideration.

The derivation of the equations for gravity-assisted trajectories is included in Appendix A, B, and C, and a method for the generation of launch opportunities is described in Appendix D. Computer programs used in the numerical calculations are given in Appendix E.

Mathematical Model

The assumptions and limitations used in this study are as follows:

1. Planetary orbits are assumed to be circular and coplanar, except for Mercury which is assumed to have a coplanar orbit with an eccentricity of 0.2.

2. The pieced-conic approximation is used, so that the calculation of each gravity-assisted trajectory is a sequence of two-body problems.

3. It is assumed that a planet and its SOI (sphere of influence) may be approximated as a point mass on the planetary orbit when viewed on a heliocentric scale. Thus, a given pre-assist trajectory (the trajectory from Earth departure to the SOI of the assist planet) may be assumed to intersect the SOI at any desired point. The actual point of intersection may be controlled by mid-course guidance maneuvers or by small variations in the launch time. The validity of this assumption is analyzed in Chapter III.

4. The length of time which the spacecraft spends in the SOI of the assist planet is assumed to be negligible compared to the length of the total mission time. Thus, the spacecraft position vector with respect to the Sun can be approximated by the planetary position vector at the time of closest approach to the assist planet.

5. Ballistic trajectories with a single impulse at Earth launch are employed in all missions. The gravity-assist techniques which are developed can also be applied to continuous-thrust missions; the idea of applying an impulse during planetary encounter has been investigated by Ross (Ref 15:149).

6. The departure orbit is a direct-ascent hyperbola from Earth; thus, the HEV (hyperbolic excess velocity) for the departure orbit is a function only of a specified burnout velocity. The determination of azimuth, flight path angle, right ascension, and declination at burnout

is left for more detailed investigations (Refs 5, 9).

7. The trajectories are designed so that perihelion lies inside the Earth's orbit about the Sun. That is, the heliocentric flight path angle (angle between spacecraft velocity vector and inner radial line from Sun to Earth) at the time of Earth launch is always equal to or less than 90°. Modification of the equations for trajectories outside the Earth's orbit is illustrated in the Jupiter-assist missions of Chapter IX.

8. Only Type I trajectories (heliocentric transfer angle from Earth to the assist planet $\theta_{12} \leq 180°$) are investigated in this report. Additional circuits about the Sun before interception of the assist planet serve only to increase the time and reliability requirements of the spacecraft.

General Method

In general the thesis is a collection of preliminary mission studies. Trajectories are calculated for each mission by selecting four arbitrary parameters: a burnout velocity V_b, departure flight path angle ϕ_o, inclination angle i, and distance of closest approach d.

For convenience, the equations derived in the appendices are programmed on the IBM 7094 digital computer, and trajectories are generated for the desired range of V_b, ϕ_o, i, and d. Each chapter includes a discussion of the program for the particular mission under consideration, and results

are presented in graphical form.

A list of solar system data used for the computations is given in Table II. Gravitational parameters and the astronomical unit are taken from Reference 8, Chapter III, pp. 2 and 3; equatorial radii are from Reference 16, p. 371; all other data are from Reference 2, p. 378. The perihelion and aphelion for Mercury, 0.30750 and 0.46670 AU, respectively, are taken from Reference 23, p. 14.

Table II

PHYSICAL CHARACTERISTICS OF THE PLANETS

Planet	Symbol	Gravitational Parameter (ft^3/sec^2)	Equatorial Radius (km)	Sphere of Influence Radius (mi)
Mercury	☿	7.7230×10^{14}	2,420	70,500
Venus	♀	1.1488×10^{16}	6,100	383,000
Earth	⊕	1.4077×10^{16}	6,371	574,000
Jupiter	♃	4.4670×10^{18}	71,370	29,937,000

ORBITAL CHARACTERISTICS OF THE PLANETS

Planet	Mean Orbital Radius (AU)	Mean Orbital Velocity (ft/sec)	Synodic Period (days)	Mean Daily Motion (deg/day)	Mean Longitude at Epoch * (deg)
Mercury	0.38710	157,110	115.88	4.09234	222.62
Venus	0.72332	114,930	583.92	1.60213	174.29
Earth	1.00000	97,751		0.98561	100.16
Jupiter	5.20280	42,809	398.88	0.08309	259.83

Gravitational Parameter of Sun ⊙: 4.6868×10^{21} ft^3/sec^2

Astronomical Unit: 92.901×10^6 mi

* Epoch: 1.5 Jan 1960 - J. D. 2,436,935.0

II. Direct-Transfer Trajectories for Solar Probe Missions

Purpose and Scope

The purpose of this chapter is threefold: first, to investigate the velocity requirements for solar probe missions; second, to introduce the equations which are used for Earth departure orbits; third, to develop a set of reference trajectories which may be compared with gravity-assisted trajectories in later chapters.

The trajectories for direct-transfer missions are broken into two phases:

1. Geocentric escape orbit - direct-ascent hyperbolic orbit from the surface of the Earth to the boundary of its SOI.

2. Heliocentric transfer orbit - an elliptical orbit which originates at a point on the Earth's orbit about the Sun.

Geocentric Escape Orbit

The initial phase of a solar probe mission involves escape from the Earth's gravitational field. A direct-ascent hyperbola is employed in all the trajectories; it is assumed here that parking orbits, used primarily for storage dumps and pre-departure checkout, are seldom used in solar probe missions.

Velocity on a Direct-Ascent Hyperbola. From two-body theory, it is known that parabolic velocity is the limiting velocity for escape from the Earth's gravitational field.

However, hyperbolic velocity is usually employed in order to avoid the long time interval required for escape on a parabolic orbit. Also, the hyperbolic excess velocity (HEV) for a parabolic orbit is zero, so it is necessary that the escape orbit be hyperbolic if it is desired to achieve a perihelion less than 1.0 AU.

The velocity of a spacecraft on a hyperbolic orbit is given by (Ref 16:96)

$$V^2 = \mu_{P_1} \left(\frac{2}{r} + \frac{1}{a} \right) \tag{2-1}$$

where r is distance between the spacecraft position and the center of mass of the planet P_1. When the spacecraft approaches the SOI of P_1, $r \to \infty$, and the velocity becomes

$$V^2_{\infty_{P_1}} = \frac{\mu_{P_1}}{a} \tag{2-2}$$

which is the HEV. Thus, for any point on the hyperbolic orbit,

$$V^2 = V^2_{\infty_{P_1}} + \frac{2\mu_{P_1}}{r} \tag{2-3}$$

Selection of V_b. The vehicle is launched in an easterly direction, as shown in Fig. 2, to take advantage of the Earth's rotational velocity. Burnout usually occurs from 50 to 100 mi above the surface, but the radius of the

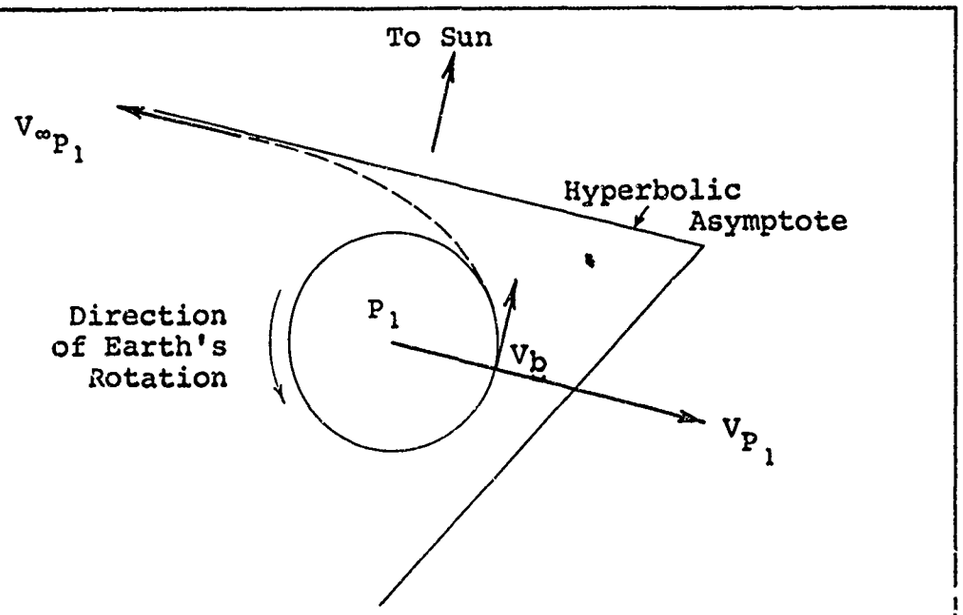

Fig. 2

Direct-Ascent Escape Orbit

Earth (R_{P_1} = 3960 mi) serves as a good approximation for the actual burnout radius. Thus,

$$V_b^2 = V_{\infty_{P_1}}^2 + \frac{2\mu_{P_1}}{R_{P_1}} \qquad (2\text{-}4)$$

The use of Eq (2-4) avoids the sometimes conflicting definitions of ideal, mission, and total velocities. V_b is the actual velocity of the vehicle with respect to the Earth when burnout occurs. The velocity required to accomplish the mission is greater than V_b because of gravity and drag losses, engine inefficiencies, and the Earth's rotational velocity (Ref 19:136-138).

The values of V_b used in Eq (2-4) may be compared directly with data for existing launch vehicles in Fig. 3.

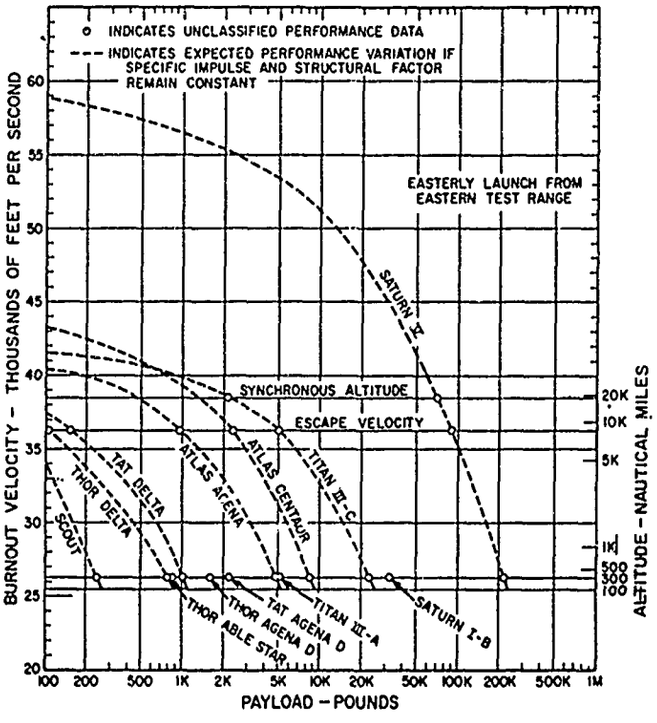

Fig. 3

Launch Vehicle Performance

(From Ref 25:Chap. II, p. 46)

In turn, the cost of these vehicles may be found in Table I. An expanded view of the region of interest (solar probe payloads less than 500 lb) is given on the chart in Fig. 4.

Selection of V_b fixes the value of the HEV, $V_{\infty p_1}$, (see Fig. 5) which is then used in calculating the heliocentric transfer orbit.

Heliocentric Transfer Orbit

After the escape phase of the mission is completed, the vehicle enters a heliocentric elliptic orbit. The actual

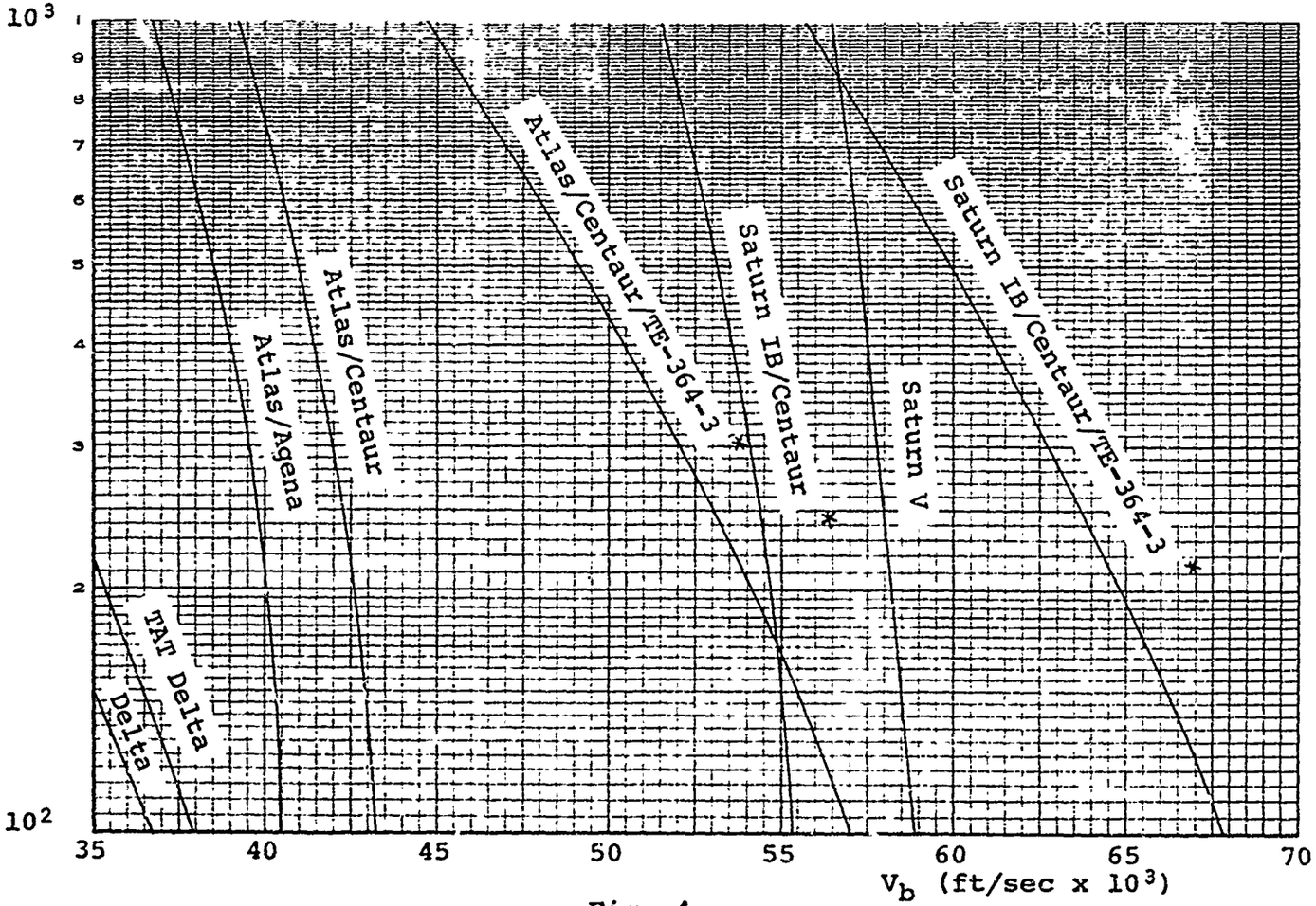

Fig. 4
Launch Vehicle Performance for Solar Probe Missions

(From Ref 25:Chap. II, P. 46)
* (From Ref 12:91,97,98)

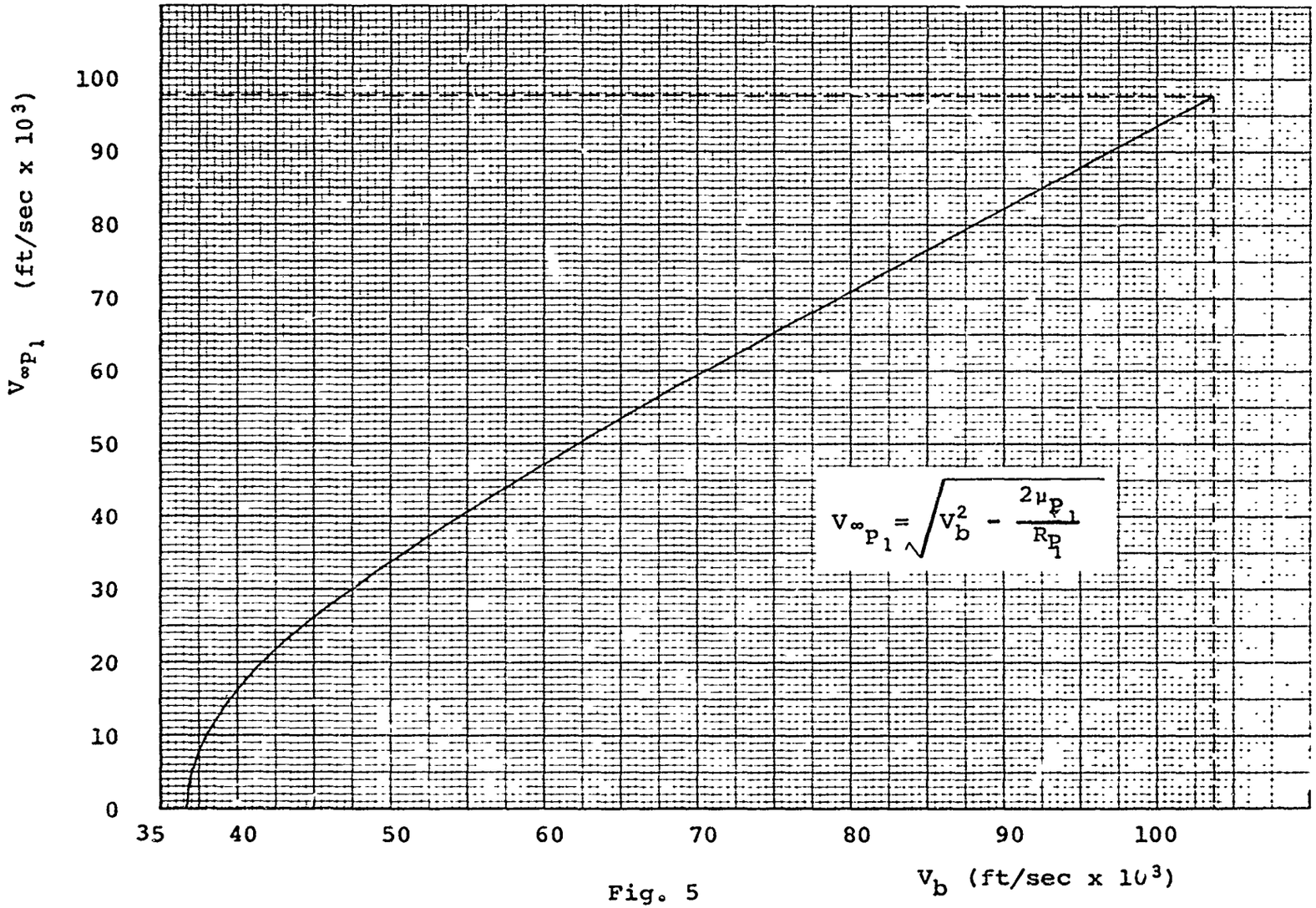

Fig. 5

HEV as a Function of V_b for Direct-Ascent Hyperbola

departure trajectory, shown as a heavy line in Fig. 6, is

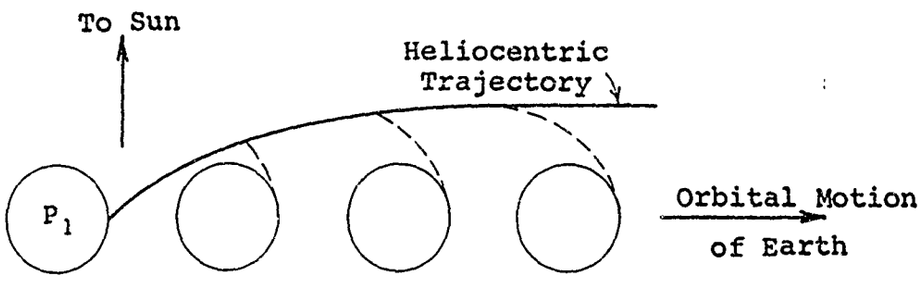

Fig. 6

Launch Trajectory of a Solar Probe

(From Ref 4:696)

a combination of the motion of the vehicle on its escape hyperbola and the motion of the Earth about the Sun. The thin lines represent the hyperbolic escape orbit with respect to the Earth for a sequence of observations after launch.

Selection of ϕ_0, i. As stated in the introduction, the trajectories investigated in this report depend upon the choice of a burnout velocity V_b, departure flight path angle ϕ_0, and an inclination angle i. The parameter V_b specifies a departure orbit which, in turn, fixes the magnitude of $V_{\infty_{P_1}}$. The selection of ϕ_0 and i defines the geometry of a heliocentric orbit which is assumed to originate from a point on the Earth's orbit about the Sun.

Calculation of $\bar{V}_0$. The vector geometry, shown in Fig. 7, is used to calculate $\bar{V}_0$, the velocity of the spacecraft with respect to the Sun after Earth escape. The $X_1Y_1Z_1$

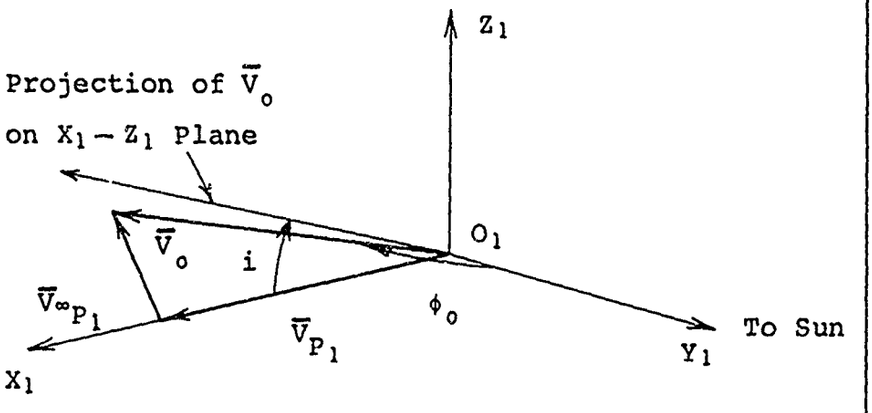

Fig. 7

Velocity Vector Geometry at Launch

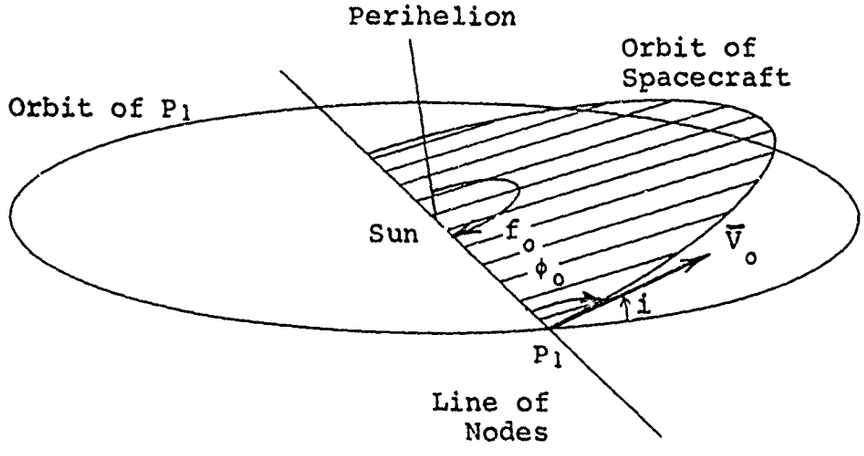

Fig. 8

Heliocentric Transfer Orbit

coordinate system is located with its origin O_1 at the center of mass of P_1. The X_1 axis lies along $\bar{V}_{P_1}$ (the velocity of P_1 about the Sun), the Y_1 axis points toward the Sun, and the Z_1 axis completes the right-hand system. From the figure,

$$\bar{V}_o = \bar{V}_{P_1} + \bar{V}_{\infty_{P_1}}$$

$$= V_o \sin \phi_o \cos i \, \bar{e}_{X_1} + V_o \cos \phi_o \, \bar{e}_{Y_1} +$$

$$V_o \sin \phi_o \sin i \, \bar{e}_{Z_1} \qquad (2\text{-}5)$$

where $$\bar{V}_{P_1} = V_{P_1} \bar{e}_{X_1} \qquad (2\text{-}6)$$

Combination of Eqs (2-5) and (2-6), and use of the dot product to find an expression for the square of the magnitude of $V_{\infty_{P_1}}$, gives

$$V^2_{\infty_{P_1}} = \left(V_o \sin \phi_o \cos i - V_{P_1}\right)^2 + \left(V_o \cos \phi_o\right)^2 +$$

$$\left(V_o \sin \phi_o \sin i\right)^2 \qquad (2\text{-}7)$$

The value of V_o must satisfy Eq (2-7) which reduces to the following quadratic equation:

$$V_o^2 - 2V_{P_1} \sin \phi_o \cos i \, V_o + V^2_{P_1} - V^2_{\infty_{P_1}} = 0 \qquad (2\text{-}8)$$

The solutions to this equation are given by

$$V_o = V_{P_1} \sin \phi_o \cos i \pm \sqrt{V_{P_1}^2 \sin^2 \phi_o \cos^2 i + V_{\infty P_1}^2 - V_{P_1}^2} \qquad (2\text{-}9)$$

The plus sign in Eq (2-9) applies to orbits which lie outside the Earth's orbit about the Sun (V_o is perihelion velocity for $\phi_o = 90°$); the negative sign, for orbits which lie inside the Earth's orbit (V_o is aphelion velocity for $\phi_o = 90°$), is used for most solar probe trajectories.

If the selected values of ϕ_o and i make V_o a complex number, then V_b (or $V_{\infty P_1}$) is not large enough to attain a heliocentric orbit, and the vehicle is unable to escape the Earth's gravitational field.

Orbit Characteristics. Now that the V_o, ϕ_o, and r_{P_1} (the distance of the Earth from the Sun) are known, the geometrical characteristics of the heliocentric transfer orbit (see Fig. 8) may be calculated.

The true anomaly at launch is given by (Ref 21:62)

$$\tan f_o = \frac{\left(r_{P_1} V_o^2 / \mu_\odot\right) \cos \phi_o \sin \phi_o}{1 - \left(r_{P_1} V_o^2 / \mu_\odot\right) \sin^2 \phi_o} \qquad (2\text{-}10)$$

where f_o is measured from perihelion, and is a negative angle for elliptic orbits inside Earth's circular orbit, that is, $-180° \leq f_o \leq 0°$.

The semi-major axis of the heliocentric orbit (Ref 21:73) is given by

$$a_1 = \frac{r_{p_1}}{2 - r_{p_1} V_o^2 / \mu_\odot} \tag{2-11}$$

and the eccentricity is

$$e_1^2 = \left(r_{p_1} V_o^2 / \mu_\odot - 1 \right)^2 \sin^2 \phi_o + \cos^2 \phi_o \tag{2-12}$$

The transfer time on an elliptic orbit is found by integrating the moment of momentum equation for the orbiting body (Ref 21:73). The result of this integration is

$$t = \sqrt{\frac{a^3}{\mu}} \left[2 \arctan \left(\sqrt{\frac{1 - e}{1 + e}} \tan \frac{f}{2} \right) - \frac{e \sqrt{1 - e^2} \sin f}{1 + e \cos f} \right] \tag{2-13}$$

which gives the time measured from periapsis to the true anomaly f. Inspection of this equation reveals that negative true anomalies ($-180° \leq f < 0°$) produce negative time values, so a negative sign must be placed in front of Eq (2-13) when the spacecraft is traveling from aphelion to perihelion.

For convenience, Eq (2-13) is written in functional form, that is,

$$t = t(a, \mu, e, f) \tag{2-14}$$

Thus, for direct-transfer trajectories in this chapter

$$T_{OP} = - t(a_1, \mu_\odot, e_1, f_o) \tag{2-15}$$

which gives the time from launch to perihelion.

The aphelion of the heliocentric transfer orbit is given by

$$r_A = a_1 (1 + e_1) \tag{2-16}$$

and finally, for the perihelion,

$$q_m = a_1 (1 - e_1) \tag{2-17}$$

Computer Programming

As shown on the flow chart in Fig. 9, Program 1 (see Appendix E) consists of a parametric variation of V_b, ϕ_o, and i, respectively. Characteristics of the orbits resulting from the choice of these parameters are printed in rows of data which vary with i for each selected value of V_b and ϕ_o. A line of asterisks across the page of output is used to separate the results for each choice of V_b, as shown in the sample printout.

Control provisions are made in the program for cases in which the values of V_b, ϕ_o, or i are such that escape from P_1 is not possible. The increments for the independent

variables may be selected as desired, and in this program are

$$\Delta i = 5°$$

$$\Delta \phi_o = 10°$$

$$\Delta V_b = 1000 \text{ ft/sec}$$

where the initial values are

$$i = 0°$$

$$\phi_o = 90°$$

$$V_b = 36{,}000 \text{ ft/sec}$$

Special precautions must be taken to find the true anomaly f_o from Eq (2-10) on the computer, since tan f_o is a double-valued function. The arc tangent function subroutine in the IBM 7094 system is designed so that the output angle for a given argument is less than + $\pi/2$ and greater than - $\pi/2$. Thus, by considering the double-valuedness of the tangent of any angle, it is reasoned that

$$\begin{aligned} f_o &= \text{arc tan } (\tan f_o), \text{ if } \tan f_o < 0 \\ f_o &= \text{arc tan } (\tan f_o) - \pi, \text{ if } \tan f_o > 0 \end{aligned} \qquad (2\text{-}18)$$

An arithmetic statement function is used to find the time on an elliptical orbit. The function is defined like Eqs (2-13) and (2-14), above, and it appears at the beginning of each program in the thesis.

In general, the variable names in the programs and the output correspond to the notation used in the report. The following list relates the notation on the computer output

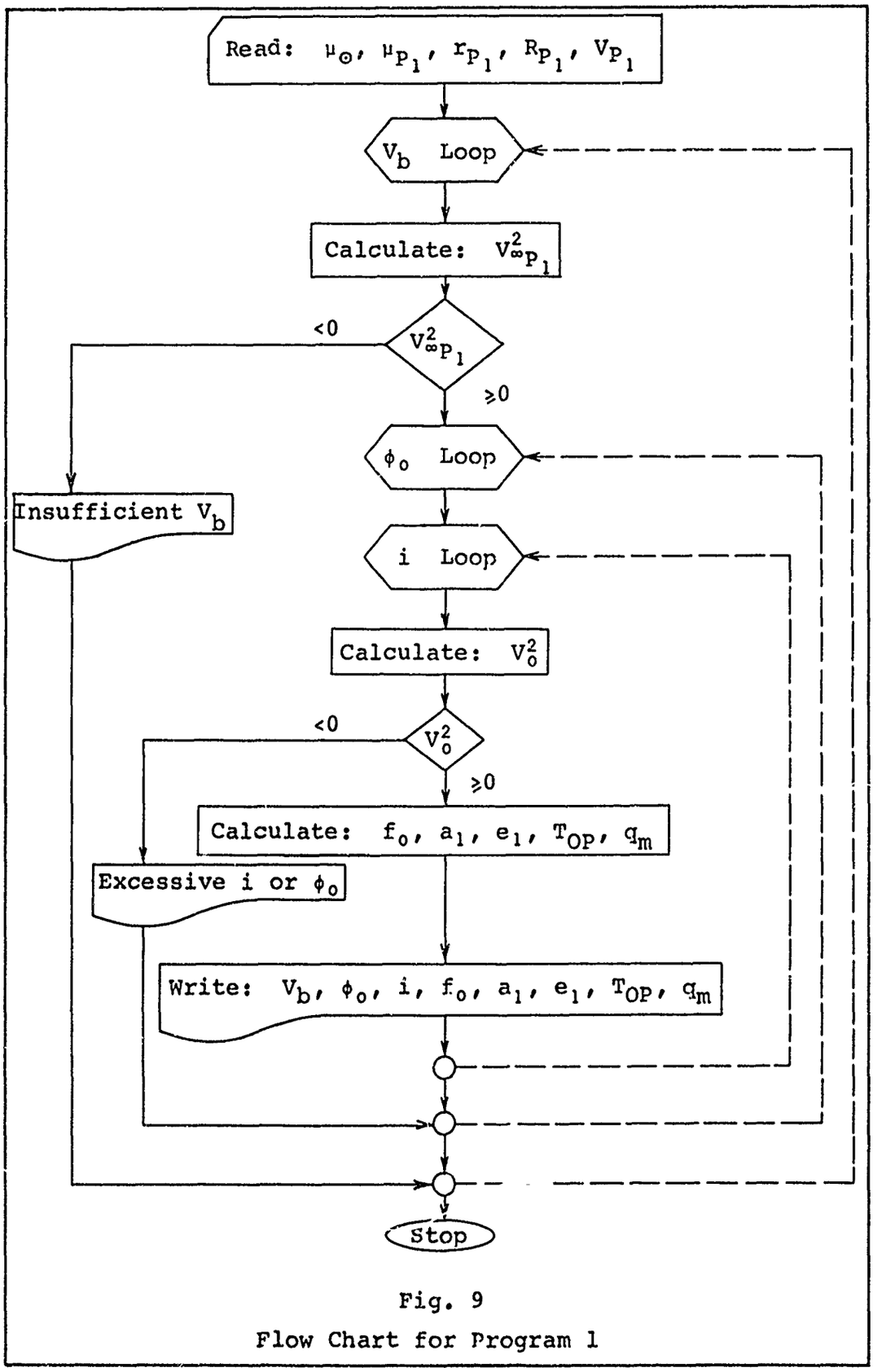

Fig. 9
Flow Chart for Program 1

with symbols defined in the text:

VB ∿ V_b	XI ∿ i	El ∿ e_1
VlNFPl ∿ $V_{\infty P_1}$	FO ∿ f_o	TlMOP ∿ T_{OP}
PH ∿ ϕ_o	Al ∿ a_1	RP ∿ q_m

Output quantities in all programs are given in the same units used in the text.

Conclusions

The graph in Fig. 10, plotted from computer output, illustrates the perihelion which can be achieved with a given V_b for several values of ϕ_o. Fig. 11 is plotted with the same data, except that mission time is plotted as a function of ϕ_o for various burnout velocities. Examination of these two graphs (both for transfers in the ecliptic) indicates some interesting properties of direct-transfer orbits.

The primary reason for using non-tangential ($\phi_o < 90°$) transfers is to decrease the mission time. Fig. 11 illustrates that mission time is strongly influenced by small changes in ϕ_o for low values of V_b. For instance, at V_b = 37,000 ft/sec, a change in ϕ_o from 90° to 88° decreases the mission time from 140 to 120 days. However, at V_b = 50,000 ft/sec, this same change in ϕ_o produces a mission time decrease of only 0.2 days.

As shown in Fig. 10, perihelion is significantly increas.d when ϕ_o departs from 90°. For example, at V_b = 41,000 ft/sec a decrease in ϕ_o from 90° to 80° reflects

an increase in perihelion from 0.50 AU to 0.66 AU. It appears that the advantage of shorter mission time for non-tangential transfers is outweighed by the disadvantage of increased perihelion distance.

Fig. 12 gives the V_b requirements for direct-transfer out-of-ecliptic missions with $\phi_o = 90°$. It illustrates that velocity requirements are heavily imposed for inclination angles above 10°.

From Fig. 10, tangential transfers to 0.5 AU in the ecliptic require burnout velocities less than 41,000 ft/sec (Atlas/Centaur). However, more sophisticated boosters must be used for missions closer to the Sun; that is, Saturn V is required for a direct mission to 0.1 AU.

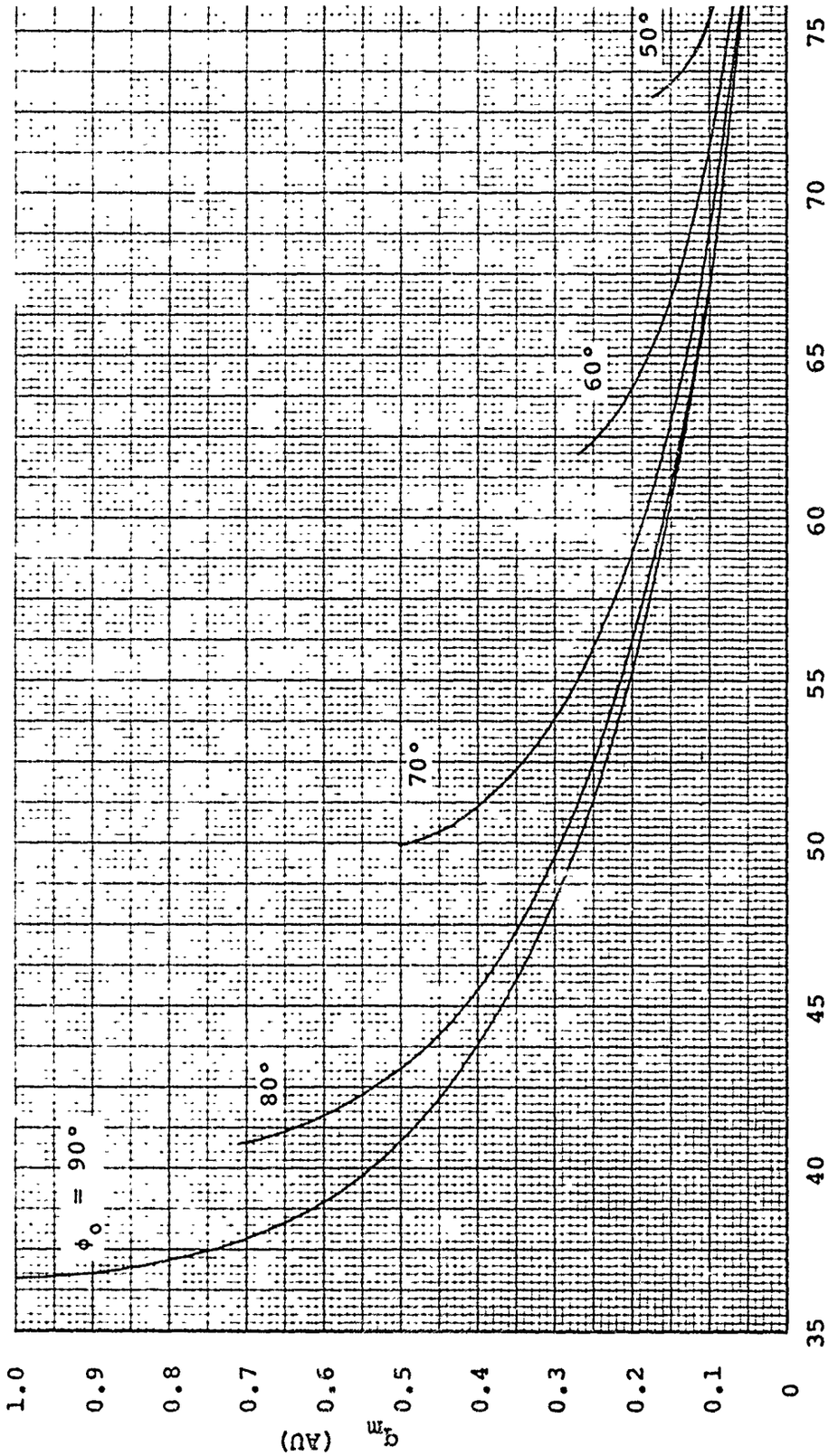

Fig. 10 Perihelion vs. Burnout Velocity for Trajectories in the Ecliptic

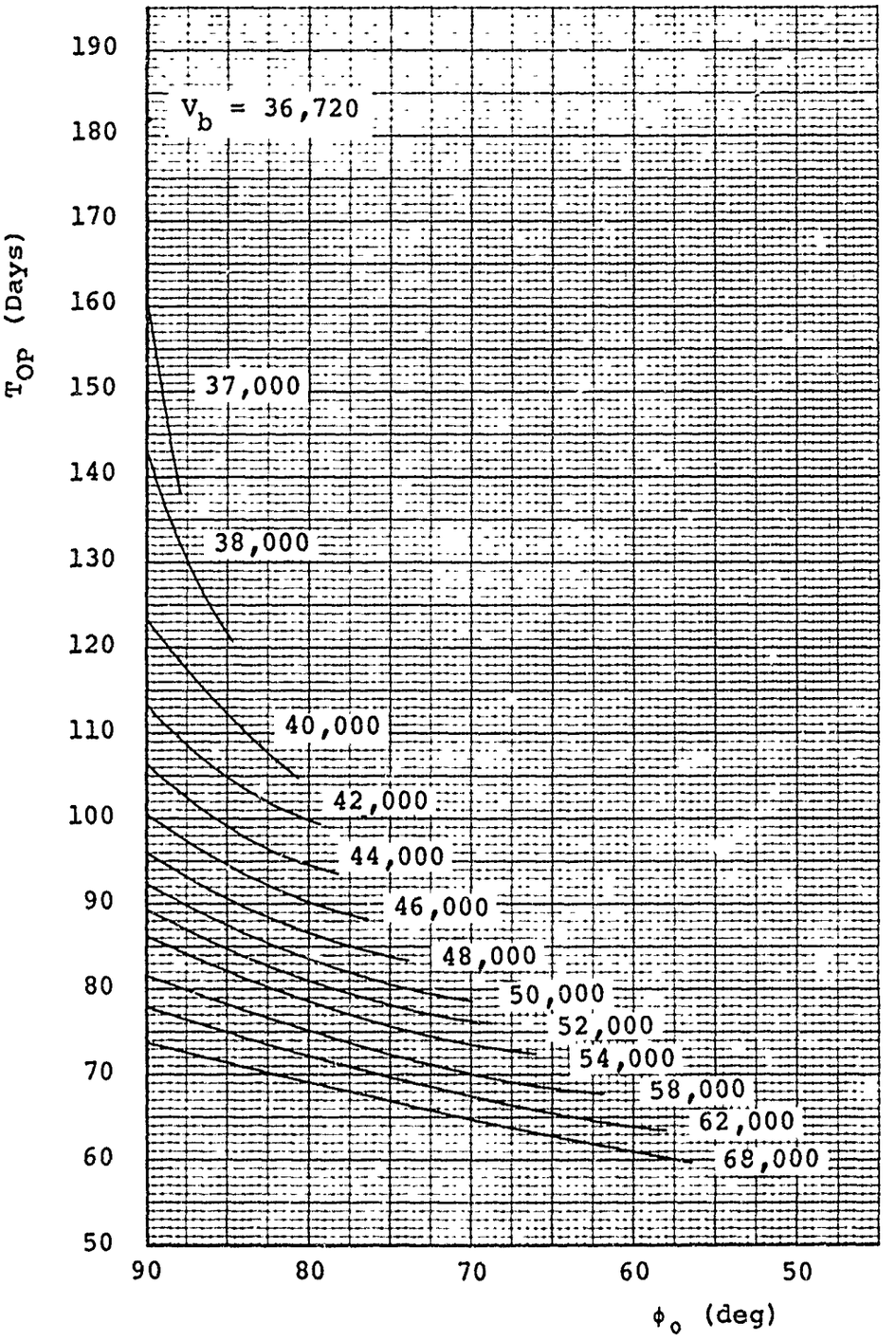

Fig. 11

Mission Time Requirements for Direct-Transfer in the Ecliptic

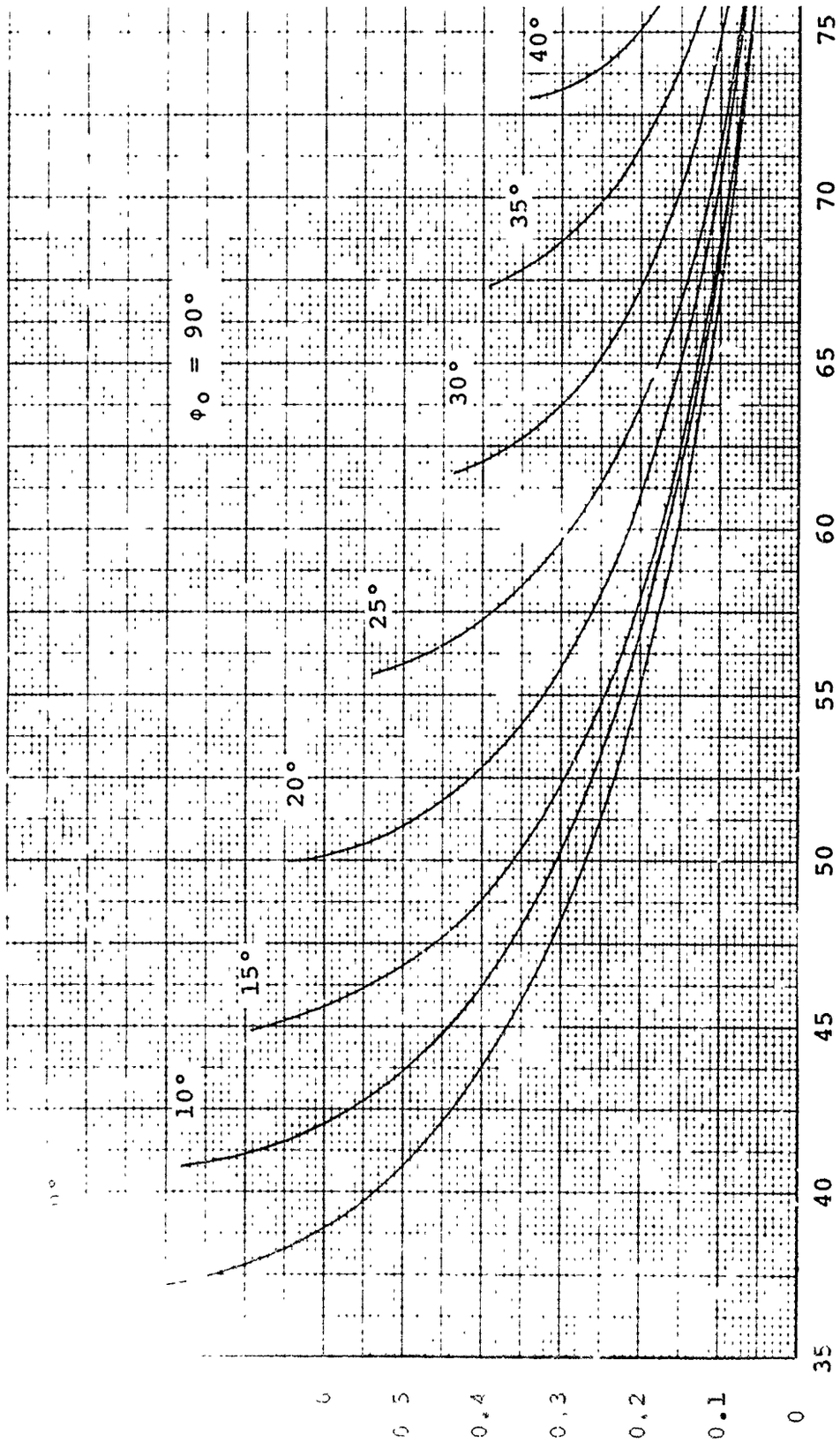

Fig. 12

Perihelion vs. Burnout Velocity for Direct-Transfer Out of the Ecliptic

III. Two-Dimensional Gravity-Assisted Trajectories

Purpose and Scope

The burnout velocity and cost requirements for direct-transfer solar probe trajectories were studied in the previous chapter. It is hoped that these requirements may be relaxed by using the gravitational attraction of one or more planets to reduce the spacecraft perihelion.

The purpose of this chapter is to outline the method which is used for gravity-assisted solar probe trajectories in the ecliptic and to clarify the assumptions made in the analysis. A detailed derivation of the equations is given in Appendix A.

Two-Dimensional Gravity Assist

It is assumed that a gravity-assisted trajectory can be separated into a series of conic orbits. The accuracy of this assumption was investigated by Sturms and Cutting (Ref 18) who computed a precise trajectory and midcourse guidance requirements for an unmanned probe to Mercury with a gravity assist at Venus. In their report it is shown that conic trajectories are an excellent approximation to the actual trajectories, and percentage differences for the orbital elements are within 2%.

The approach taken here is to divide the entire trajectory into four conic orbits:

1. Departure Orbit - planetocentric hyperbola at

departure planet P_1.

2. Pre-Assist Orbit - heliocentric ellipse from P_1 to the assist planet P_2.

3. Assist Orbit - planetocentric hyperbola at P_2.

4. Post-Assist Orbit - heliocentric ellipse after the spacecraft passes P_2.

Departure Orbit and Pre-Assist Orbit. The procedure which was used to determine a geocentric escape orbit and a heliocentric transfer orbit in Chapter II is used again in this chapter; however, the heliocentric transfer orbit, defined by the selection of V_b and ϕ_o, is now called a pre-assist orbit. Since this analysis is two-dimensional, the inclination i is zero.

The point of intersection A of the pre-assist orbit and the orbit of P_2, shown in Fig. 13, is assumed to be the point at which the pre-assist orbit intersects the SOI of P_2. This assumption (no. 5 in the Introduction) is more meaningful when the SOI radius of P_2 is compared with the distance of P_2 from the Sun. For example, Venus has a SOI radius of 383,000 mi, and a mean orbital radius of 67,100,000 mi. If the SOI radius is assumed to be the chord of a circular sector, it subtends a heliocentric angle of only 0.33°. A similar calculation for Jupiter reveals that its SOI radius subtends an angle of 3.5°.

The geometry of the pre-assist orbit is used to calculate true anomaly f_1, velocity V_1, and flight path

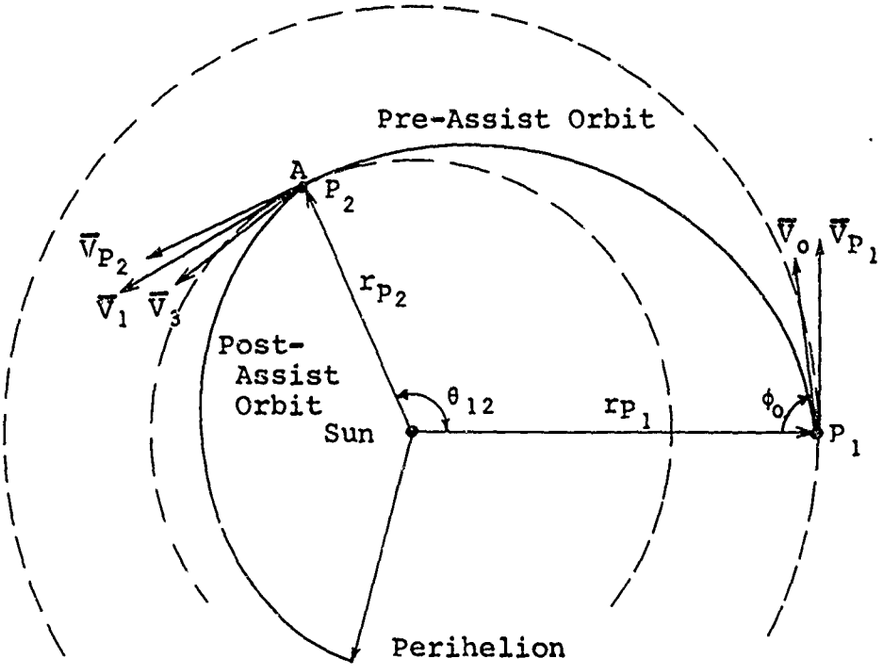

Fig. 13

Pre-Assist and Post-Assist Orbits

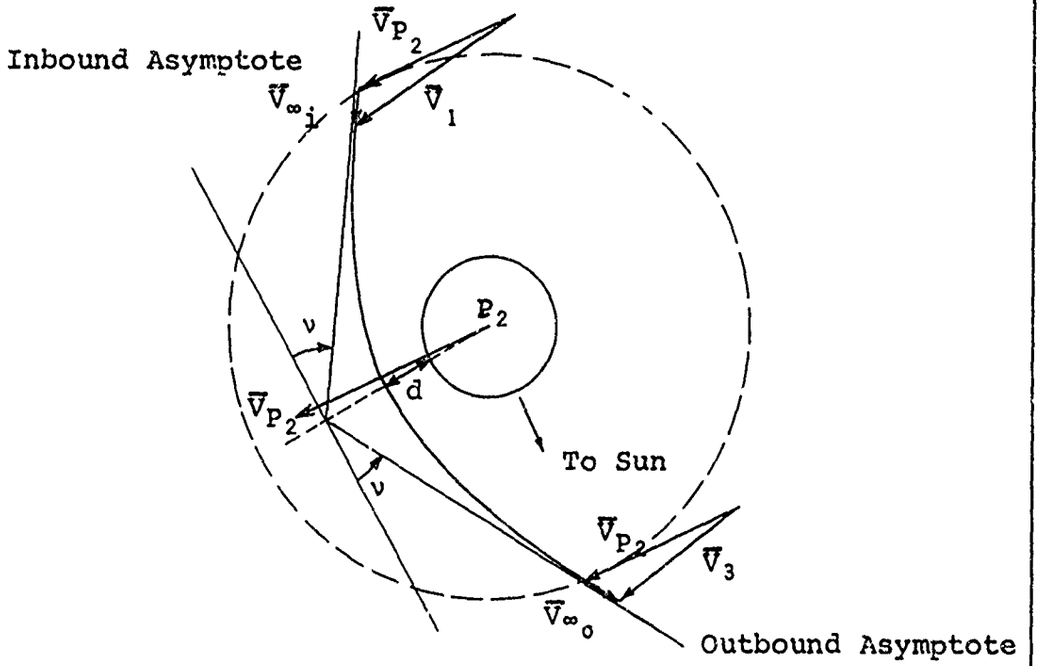

Fig. 14

Assist Orbit

angle ϕ_1 at point A. These quantities are taken as pre-assist orbit conditions at the time the spacecraft enters the SOI of P_2.

Assist Orbit. The velocity of the spacecraft with respect to P_2 as it enters the SOI is

$$\bar{V}_{\infty_i} = \bar{V}_1 - \bar{V}_{P_2} \tag{3-1}$$

This velocity (at an infinite distance from P_2) is the inbound HEV for a hyperbolic orbit at P_2 called the assist orbit.

From considerations on hyperbolic orbits (Ref 16:96) it is known that the outbound HEV vector is equal to $\bar{V}_{\infty_i}$ in magnitude, but differs by an angle of 2ν in direction (see Fig. 14). This angle is determined by choosing a value for d, the DOCA; after this choice has been made, the geometry of the assist orbit is completely specified.

Post-Assist Orbit. Point A in Fig. 13 is assumed to be fixed in heliocentric space during the time that the spacecraft is within the SOI of P_2 (assumption no. 4 of the Introduction). It has been shown (Ref 10) that a spacecraft spends approximately one day on an assist orbit in the SOI of Venus. The above assumption is reasonable when it is considered that the mean daily motion of Venus is 1.602°.

Thus, neglecting small changes in the position and velocity of P_2 about the Sun, the post-assist orbit can be assumed to originate at point A. Also, by using the same

arguments which were applied to the pre-assist orbit, point A is assumed to be the point at which the post-assist orbit intersects the SOI of P_2.

In accordance with the above assumptions, the following expression is written for the velocity of the spacecraft with respect to the Sun as it exits the SOI of P_2:

$$\bar{V}_3 = \bar{V}_{P_2} + \bar{V}_{\infty_o} \tag{3-2}$$

This expression and the geometry of the assist orbit are used to find the true anomaly f_3, velocity V_3, and flight path angle ϕ_3 on the post-assist orbit at P_2. Finally, these conditions are used to determine the geometry and perihelion of the post-assist orbit.

Total mission time T_{OP} is defined as the elapsed time from launch at P_1 to perihelion of the post-assist orbit. The time spent in the SOI of P_1 and P_2 is neglected, since it is much less than T_{OP}. Thus, use of the functional notation in Eqs (2-13) and (2-14) gives

$$T_{OP} = T_{12} - t(a_3, \mu_\odot, e_3, f_3) \tag{3-3}$$

where T_{12} is the time from P_1 to P_2:

$$T_{12} = t(a_1, \mu_\odot, e_1, f_1) - t(a_1, \mu_\odot, e_1, f_o) \tag{3-4}$$

Corollary

As explained in the previous section, the pre-assist

orbit (determined by the choice of V_b and ϕ_0) defines the geometry of the velocity vector diagram in Fig. 15(a) at the time of entry to the SOI of P_2. The actual point of entry is not specified until d is chosen. Thus, an implicit result in the above analysis is that a given pre-assist orbit may be assumed to enter the SOI at any point. This corollary is the basis for the third assumption in the Introduction, and will be of more importance in the three-dimensional discussion of Chapter VII.

In precision trajectory calculations the point of entry and DOCA are determined by a pre-assist orbit. During an actual flight the point of entry must be controlled by midcourse guidance and small deviations in the launch time.

Geometry of the Gravity-Assist Maneuver

Locus of Outbound HEV Vectors. Since $|\bar{V}_{\infty_0}| = |\bar{V}_{\infty_i}|$ a circular locus of $\bar{V}_{\infty_0}$ vectors may be drawn for a given pre-assist orbit. As shown in Fig. 15(b), the center of this circle lies at the tip of the vector $\bar{V}_{P_2}$. The selection of d automatically fixes the angle ν, and the resulting $\bar{V}_{\infty_0}$ vector is drawn in Fig. 15(c). Finally, in Fig. 15(d), $\bar{V}_3$ is drawn from the base of $\bar{V}_{P_2}$ to the tip of $\bar{V}_{\infty_0}$.

It should be noted that physical limitations are imposed on the angle ν, so that only an arc of the circle in Fig. 15(b) represents possible $\bar{V}_{\infty_0}$ vectors. The maximum turn angle $2\nu_{max}$ for a given pre-assist orbit occurs when

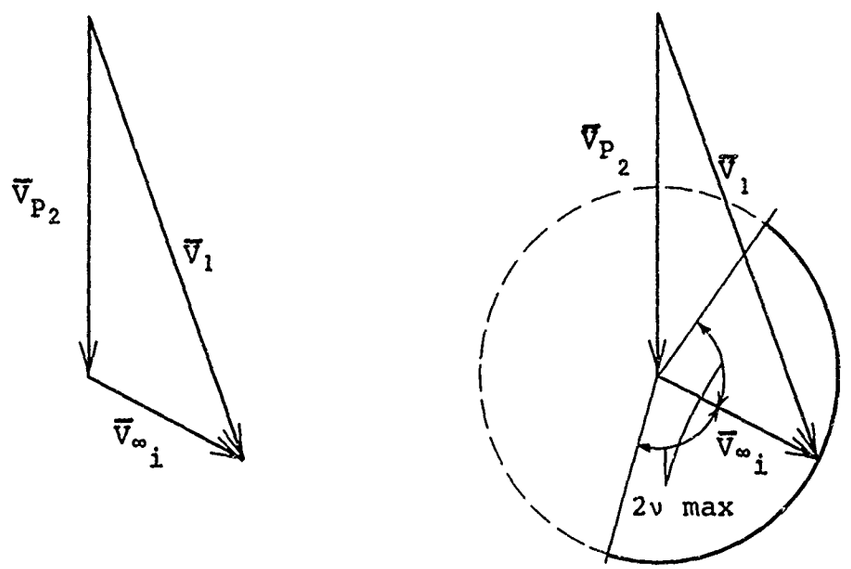

(a) Pre-Assist Vectors

(b) Locus of $\bar{V}_{\infty_o}$ Vectors

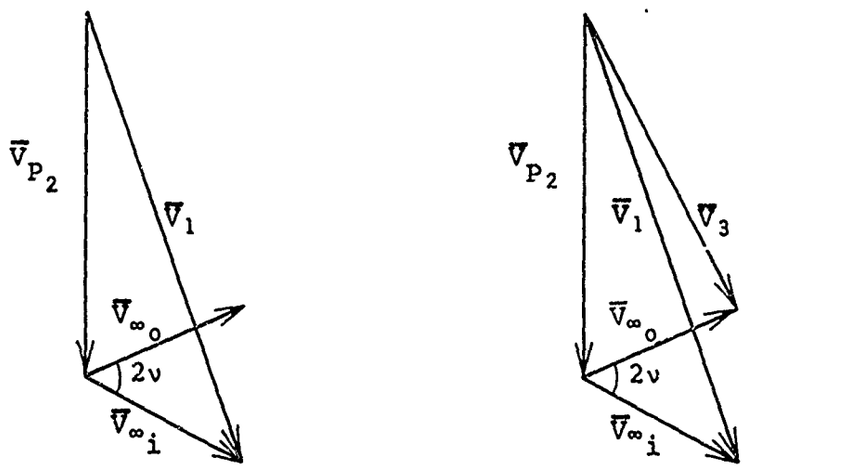

(c) Selection of d

(d) Determination of $\bar{V}_3$

Fig. 15

Gravity-Assist Geometry

$d = 0$ (grazing pass at P_2). This can be seen analytically by inspection of Eqs (A-18) and (A-19).

Effect of Gravity Assist. The effect of gravity assist is to rotate $\bar{V}_{\infty_i}$ through an angle of 2ν in the plane of motion. The direction of rotation can increase or decrease the spacecraft velocity with respect to the Sun, and is controlled by the side of the planet which is passed by the spacecraft (dark-side or light-side passage).

Some interesting observations may be made in the velocity vector diagram of Fig. 15(d). First of all, the minimum $|\bar{V}_3|$ for a given pre-assist orbit is attained when $\bar{V}_{\infty_o}$ is directed opposite to $\bar{V}_{P_2}$. Similarly, the maximum $|\bar{V}_3|$ is attained when $\bar{V}_{\infty_o}$ is in the same direction as $\bar{V}_{P_2}$. Also, the maximum heliocentric velocity change $|\bar{V}_3 - \bar{V}_1|$ is achieved when $\nu = \nu_{max}$ (or $d = 0$).

Another observation is that if $|\bar{V}_{\infty_i}| > |\bar{V}_{P_2}|$, and if ν (or d) can be chosen within its range of physically possible values ($d > 0$) such that $\bar{V}_{\infty_o}$ lies opposite $\bar{V}_{P_2}$, then $\bar{V}_3$ also lies opposite to $\bar{V}_{P_2}$, and a retrograde orbit is obtained. This is found to be the case for some Jupiter-assisted trajectories (Ref 11).

Visualization. The gravity-assist maneuver may be visualized by separating the velocity vector diagram of Fig. 15(d) into two reference frames: one with respect to the Sun, and the other with respect to P_2. This procedure is best illustrated with a hypothetical example.

Suppose that a gravity-assisted trajectory has been calculated and that the above procedures have been followed to obtain the velocity vector diagram in Fig. 16(a). Since all vectors in this figure are drawn relative to heliocentric space, they may be referenced to the P_2 - Sun line and translated into two separate diagrams as shown in Figs. 16(b) and (c). All angles in Fig. 16(a) have been preserved in the translation, and now the entire maneuver may be easily visualized by viewing it from two different frames of reference.

Comparison with Other Methods

The method used for gravity-assisted trajectories in this study is similar to that used by Minovitch and Niehoff (Refs 10, 11, 13). Their investigations, however, are primarily concerned with interception of a target planet after a close approach to one or more intermediate planets. The target planet rendezvous imposes a constraint which need not be considered in solar probe missions.

Minovitch has conducted a very thorough study or gravity-assisted trajectories, and his approach includes the inclinations and eccentricities of planetary orbits. However, the analysis may yield physically unrealizable trajectories with negative DOCA values.

Niehoff has derived expressions for the maximum velocity and energy change at the assist planet, but satisfaction of these expressions constrains the geometry of the assist orbit which also fixes a DOCA for a given pre-assist orbit.

Thus, trajectories which have maximum velocity or energy change are not necessarily those trajectories which have minimum perihelia.

Ross (Ref 15) has devised a systematic approach to the study of non-stop interplanetary round-trip trajectories. His analysis includes the inclinations and eccentricities of planetary orbits, and results are presented in design manuals (Planetary Flight Handbook, Vol. III, Parts 1, 2, and 3, NASA SP-35) for manned missions to Venus and Mars. He has conducted a short investigation on Venus-assisted solar probe missions for the 1965-66 time period.

The method developed in this thesis lends itself nicely to feasibility studies, and is designed so that gravity-assisted trajectories may be calculated as a function of specified burnout conditions at Earth and DOCA at the assist planet. The equations are derived in a general form, and may be applied not only to solar probe missions, but also to any of the target-planet or round-trip missions which were studied by Minovitch, Niehoff, and Ross.

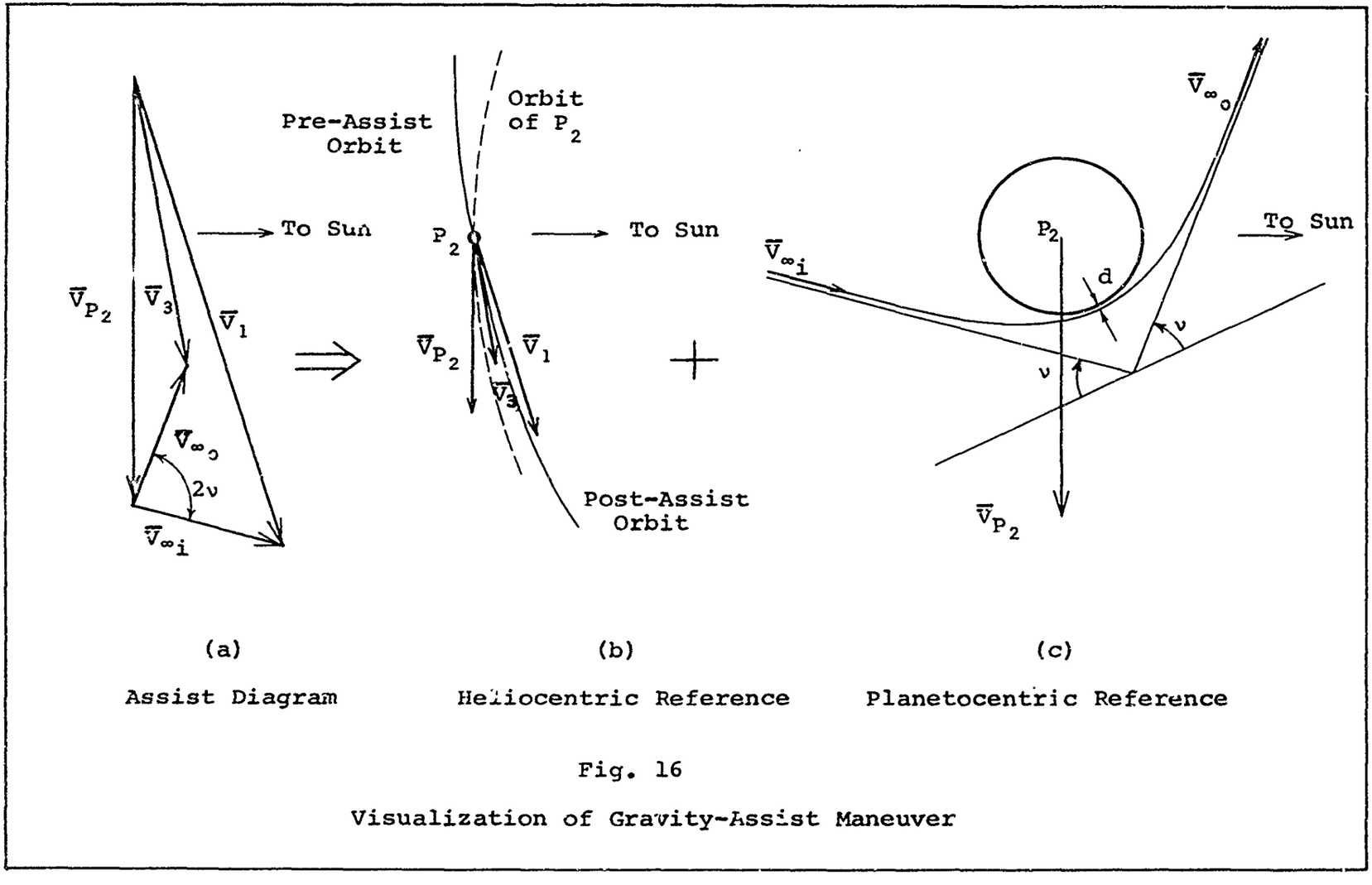

(a) Assist Diagram

(b) Heliocentric Reference

(c) Planetocentric Reference

Fig. 16

Visualization of Gravity-Assist Maneuver

IV. Venus Assist in the Ecliptic

A method of analysis for gravity-assisted trajectories was described in the preceeding chapter. It is the purpose of this chapter to apply that method to the specific problem of a Venus assist for solar probe missions in the ecliptic. This problem has been investigated in other reports (Refs 3, 11), but is included here to serve as a foundation for the development of other Venus-assist missions which are studied in later chapters.

Also, this chapter is designed to outline the feasibility of gravity-assist missions and some of the additional considerations which must be made in the selection of a trajectory for more precise design study.

Additional Considerations for Gravity-Assist Missions

Guidance Requirements. The most significant difference between direct-transfer and gravity-assist missions, as far as hardware is concerned, is guidance requirements. A gravity-assist mission would have no hope of success without some form of midcourse maneuvering capability.

This problem is not as formidable as it appears, for it has been shown that guidance requirements for the gravity-assist maneuver are modest, and are within the capabilities of present-day technology. Sturms and Cutting (Ref 18) have shown that 180 lb of additional midcourse guidance equipment and fuel are required to accomplish a Venus assist for a

1120-lb Mercury-probe payload. A design study (Ref 3) on Venus-assist missions for solar probes indicates that an 80-lb guidance system is sufficient for a 460-lb payload.

From this discussion it is assumed that the payload for Venus-assisted solar probe missions in this thesis weighs approximately 250 to 300 lb (200 lb for the probe and 50 to 100 lb for additional guidance equipment). The probe weight is based on findings in the ICARVS design study (Ref 12:103), where a 150- to 200-lb spacecraft is designed for a direct-transfer mission to 0.1 AU.

DOCA. It is found in this and all of the following chapters on gravity-assist missions that the post-assist orbit perihelion decreases with a decrease in DOCA at the assist planet. As mentioned in the previous chapter, a grazing pass represents the physical lower limit for DOCA, but a planetary atmosphere may represent an additional limitation.

Little is known about the Venusian atmosphere, but it has been estimated (Ref 4:680) that the atmospheric pressure at an altitude of 120 km (65 NM) above the surface of Venus is about 2×10^{-6} atm. For Earth this pressure is found at an altitude of about 107 km (58 NM) from the 1959 ARDC Model Atmosphere (Ref 25:Chap. II, p. 8). The Earth's atmosphere effectively ends at 400,000 ft or 65.8 NM (reentry altitude in Ref 23:104). From this data it should be safe to assume for Venus that atmospheric effects are insignificant for a DOCA above 100 NM.

Communications. It is shown in the two design studies mentioned above (Ref 3, 12) that a solar probe must have data handling and storage capability for the transmission of information at a suitable time after perihelion. Thus, the actual mission time may be longer than that defined in this report (time from launch to perihelion).

The communications necessary to effect a midcourse maneuver for a planetary flyby have been demonstrated in the Mariner missions. For many of the gravity-assisted trajectories in this study the spacecraft-Sun elongation angle from Earth is large enough to allow communication with the spacecraft at the time of planetary encounter.

Computer Programming

As shown on the flow chart in Fig. 17 the program for gravity assist in the ecliptic (Program 2 in Appendix E) consists of a parametric variation in V_b, ϕ_o, and d, respectively. The first portion of the program is designed to calculate and store the departure orbit and pre-assist orbit conditions at launch for various values of V_b and ϕ_o.

The value of d is parametrically varied for each value of V_b and ϕ_o, and a line of printed output (sample follows Program 2) consists of trajectory characteristics for a given value of d.

As in Program 1, control provisions are made for cases in which escape from P_1 is not possible. Also, provision is made for the cases in which the pre-assist orbit does

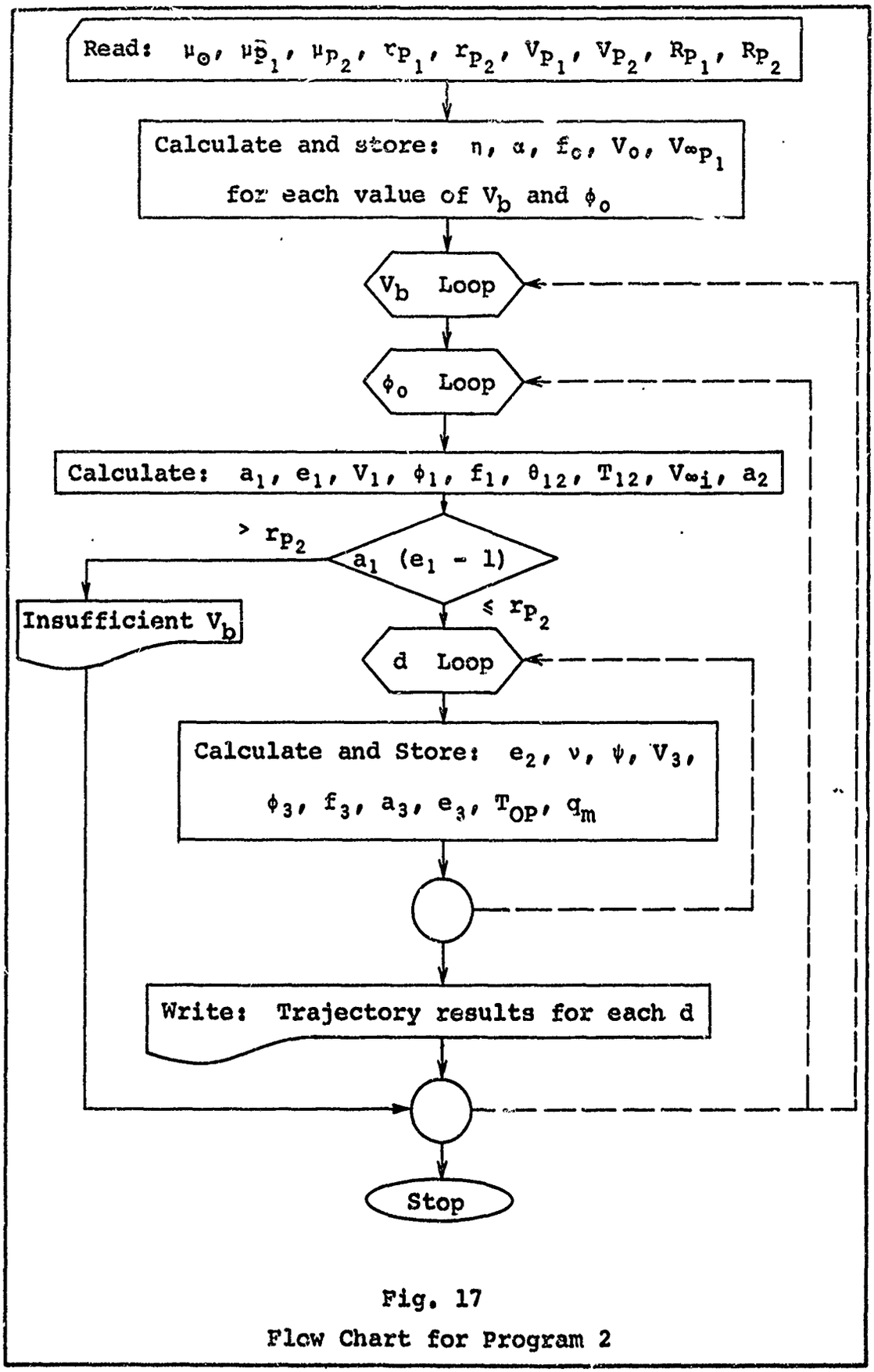

Fig. 17

Flow Chart for Program 2

not intersect the orbit of P_2. That is, the perihelion of the pre-assist orbit must be at least as small as the orbital radius of P_2 (see Eq (A-6)).

The comments above Eq (2-18) regarding the arc tan subroutine and the calculation of f_o in Program 1 are also applicable in Program 2. These considerations apply again to the calculation of f_1 and f_3, the true anomalies of the pre- and post-assist orbits at P_2, respectively. That is, the programmed expressions for f_1 and f_3 may be obtained by replacing f_o in Eq (2-18) by f_1 or f_3.

The calculation of the angle ψ in Eq (A-22) requires a procedure similar to that used in the calculation of f_o. The arc sin subroutine on the IBM 7094 is designed so that the output angle for a given argument is less than $+\pi/2$ and greater than $-\pi/2$. From Fig. 64 and Eq (A-22), the following condition must hold:

$$\begin{aligned} &(\psi + 2\nu) > \pi/2, \quad \text{if} \quad V_1 \sin \phi_1 > V_{P_1} \\ &(\psi + 2\nu) < \pi/2, \quad \text{if} \quad V_1 \sin \phi_1 < V_{P_1} \end{aligned} \tag{4-1}$$

and thus, for the program,

$$\begin{aligned} &\psi = \pi - \arcsin [\sin (\psi + 2\nu)] - 2\nu, \quad \text{if} \\ &\qquad V_1 \sin \phi_1 > V_{P_1} \\ &\psi = \arcsin [\sin (\psi + 2\nu)] - 2\nu, \quad \text{if} \\ &\qquad V_1 \sin \phi_1 < V_{P_1} \end{aligned} \tag{4-2}$$

Notation on the printed output for Program 2 is the same as that used in Program 1 of Chapter II. Additional and revised notation is as follows:

VO ∿ V	VINF ∿ V_{∞_i}, V_{∞_o}	NU ∿ ν
A ∿ α	DOCA ∿ d	E2 ∿ e_2
ET ∿ η	F3 ∿ f_3	PSI ∿ ψ
TH12 ∿ θ_{12}	A3 ∿ a_3	TIM12 ∿ T_{12}
F1 ∿ f_1	E3 ∿ e_3	TOP ∿ T_{OP}
V1 ∿ V_1	V3 ∿ V_3	QM ∿ q_m

Mission Profile

A trajectory from the computer data is illustrated in the mission profile of Fig. 18. An Atlas/Centaur/TE-364-3 launch vehicle is selected for the mission; from Fig. 4 it is found that the burnout velocity of this vehicle is 53,000 ft/sec for a 250 lb payload. A tangential departure is used ($\phi_o = 90°$) in order to obtain the smallest possible perihelion with the given burnout velocity.

The launch date for this mission (30 August 1970) is selected from computer printout of Program 8 in Appendix E. Heliocentric longitudes of Earth and Venus at the time of launch are taken from Reference 1. The angles in Fig. 18 have been drawn carefully with a protractor, but are not indicated because they serve only to clutter the drawing.

Conclusions

From the success of the Mariner Program and the results of the reports discussed above (Refs 3, 18), it can be

Trajectory Data

Launch Date: 30 Aug 1970 (JD2440828.8)
Launch Vehicle: Atlas/Centaur/TE-364-3
V_b = 53,000 ft/sec, ϕ_o = 90°
Payload = 250 lb
T_{12} = 52.7 days
T_{OP} = 87.4 days
d = 100 NM
q_m = 0.161 AU

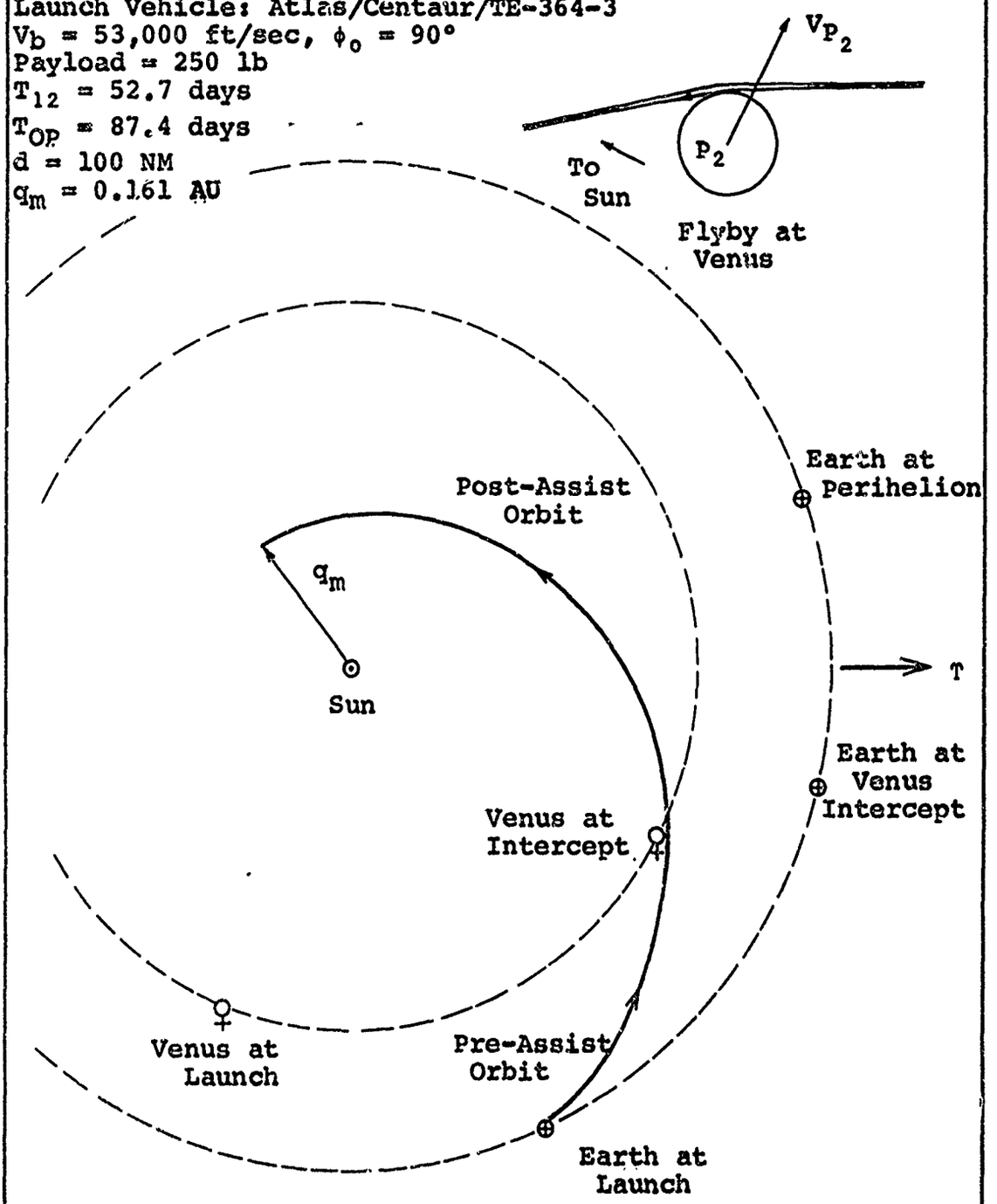

Fig. 18

Mission Profile for Venus-Assisted Trajectory

concluded that gravity-assist missions to Venus are within the capability of present-day technology.

The example mission indicates that a perihelion of 0.161 AU can be achieved with the Atlas/Centaur/TE-364-3 launch vehicle ($16 million) and a Venus assist; whereas a Saturn V ($125 million) or a Saturn I/Centaur/Kick (no cost data, but Saturn I/Centaur alone costs $41 million) is required for a direct-transfer to this perihelion.

A graph of perihelion versus burnout velocity for varying DOCA in Fig. 19 indicates that the performance (achieved perihelion) of gravity assist at Venus changes only slightly for DOCA variations below 1000 NM. Thus, the performance results for a DOCA of 100 NM are fairly representative of the results for any DOCA less than 1000 NM.

A plot for direct-transfer missions (dot-dashed line) is shown in the figure. A comparison of the curves reveals that a DOCA above 100,000 NM offers no significant advantage in solar probe missions. A horizontal measurement on the graph for any given perihelion below 0.35 AU indicates that the reduction in V_b is approximately 6500 ft/sec, that is

$$V_{b_{Direct}} - V_{b_{DOCA=0}} \approx 6500 \text{ ft/sec.}$$

Fig. 19 also illustrates that the most significant reductions in perihelion are achieved with the lower values of V_b (less than 55,000 ft/sec). This point is further illustrated with the plot of perihelion versus

DOCA in Fig. 20. The horizontal dashed lines in this figure indicate perihelion for direct-transfer missions; these lines are asymptotes for the solid lines which are for gravity-assist missions.

Mission time for any V_b and DOCA can be found in Fig. 21. This plot indicates that for a given V_b the mission time is relatively invariant with DOCA. A cross-plot of this graph is found in Fig. 22 for a DOCA of 100 NM. Also shown in Fig. 22 is mission time for direct-transfer orbits. It can be seen that the mission time requirements for a Venus assist are, for all practical purposes, about the same as direct transfer.

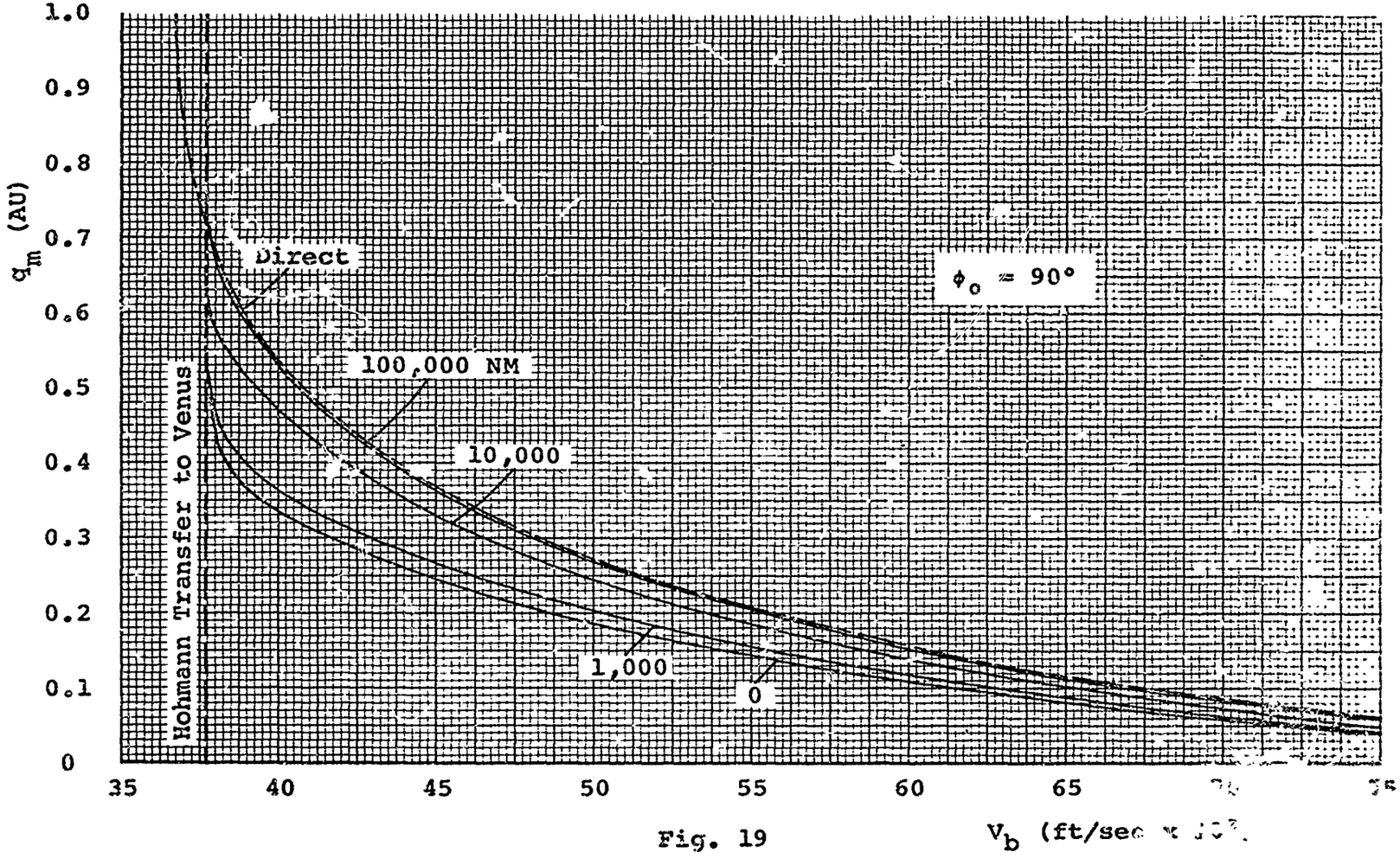

Fig. 19

Perihelion vs. Burnout Velocity for Gravity-Assist at Venus

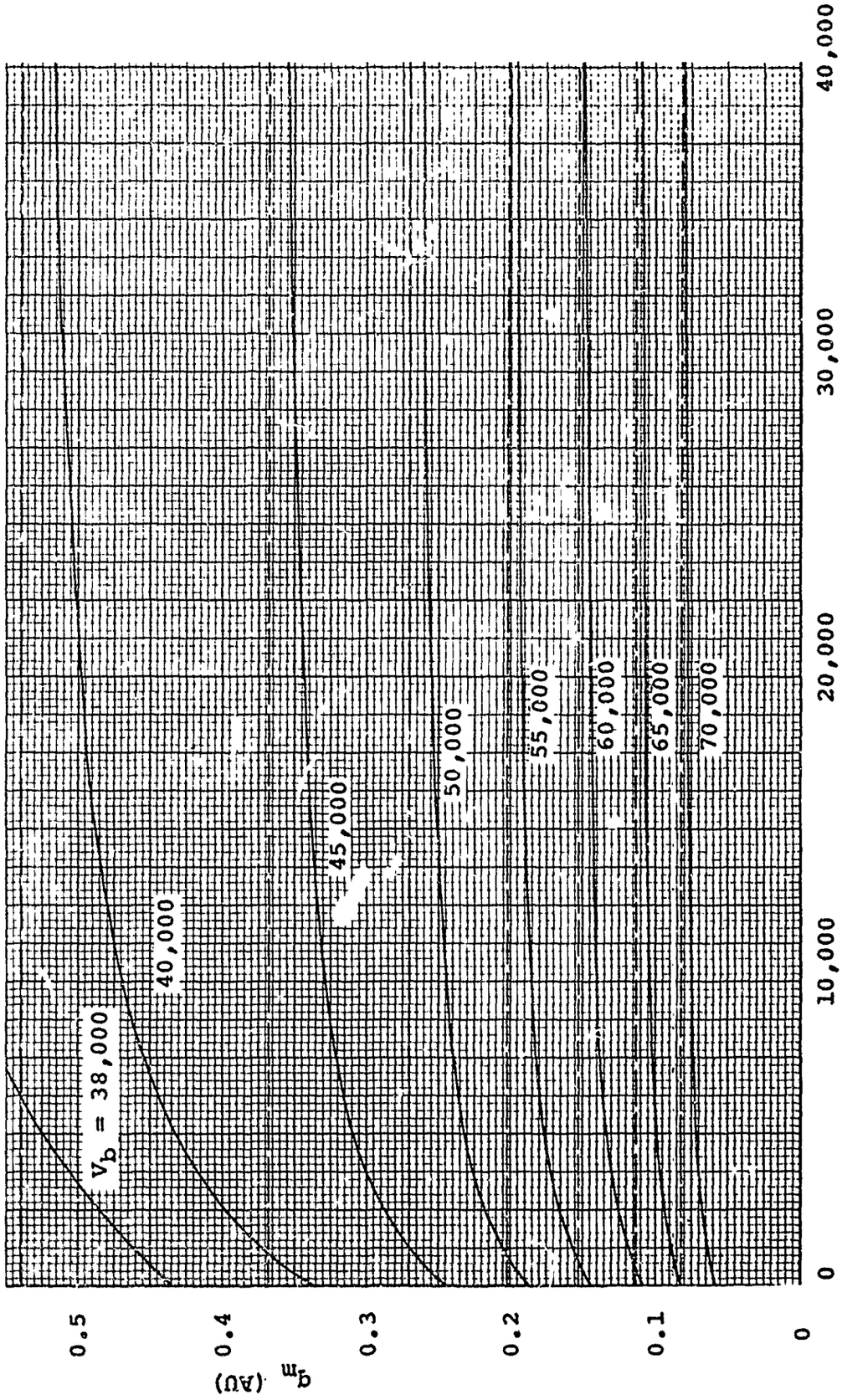

Fig. 20
Perihelion vs. DOCA for Various Burnout Velocities

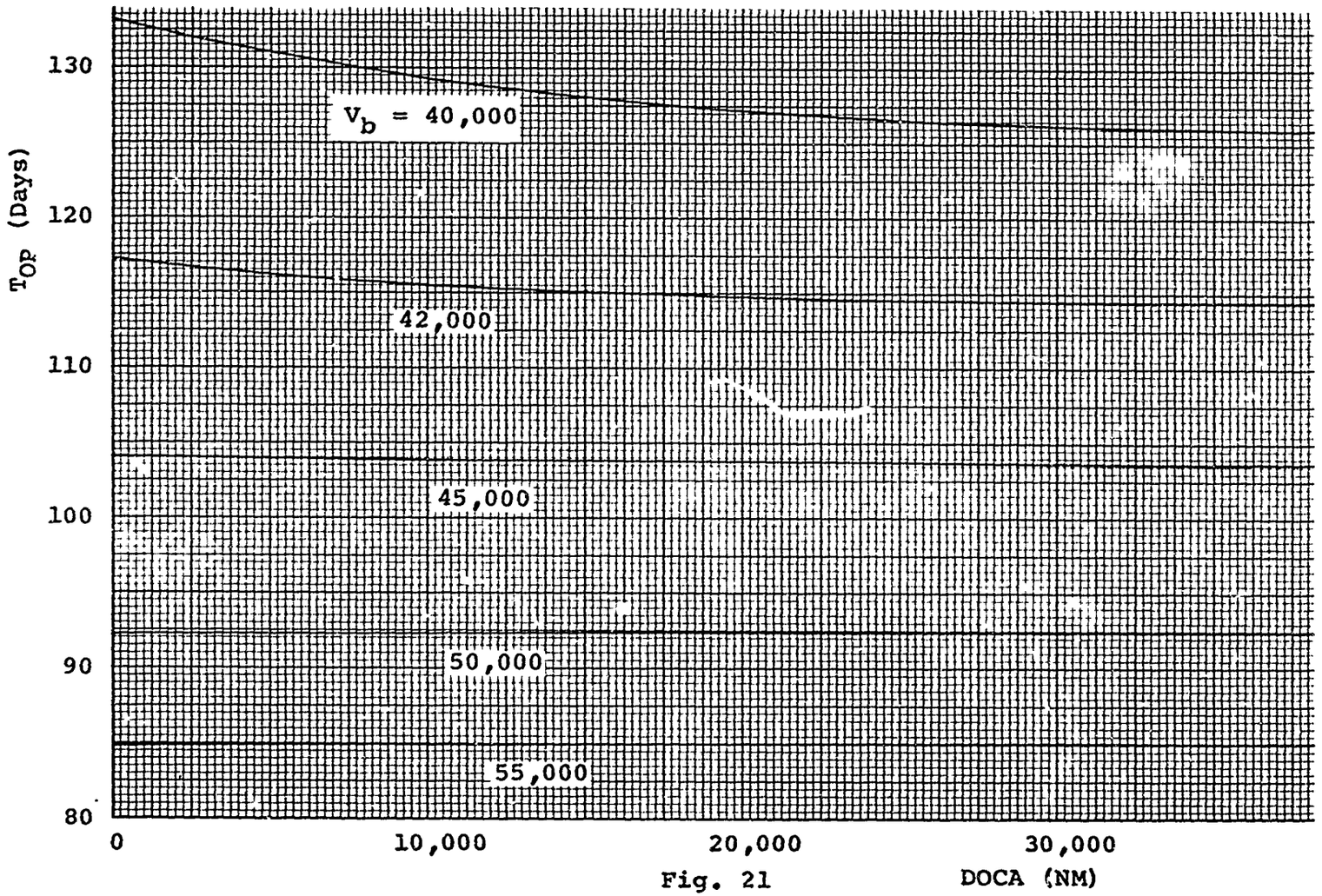

Fig. 21

Mission Time vs. DOCA for Various Burnout Velocities

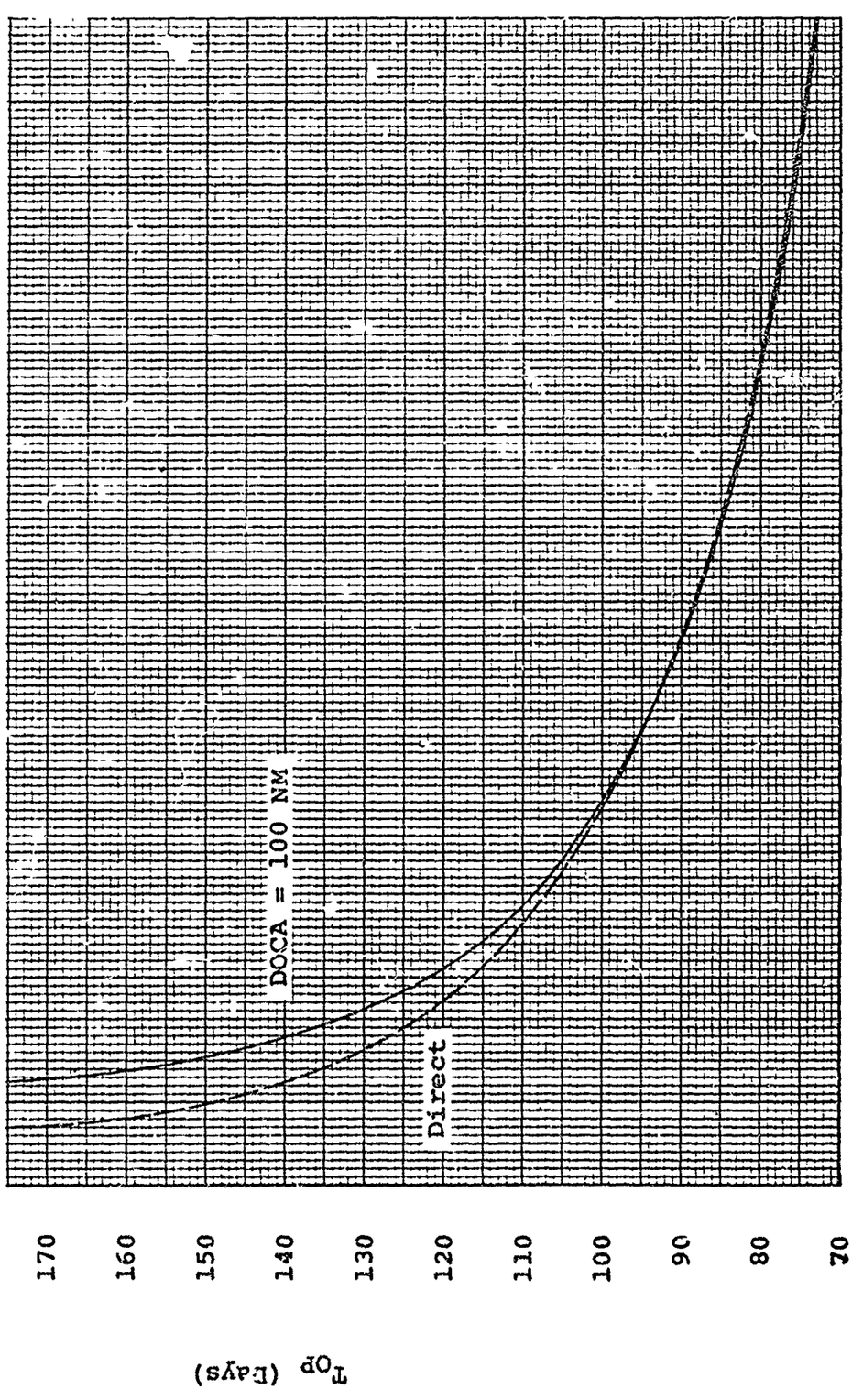

Fig. 22 Mission Time for Venus Assist Compared with Direct-Transfer

V. Venus-Mercury Combination Assist

The theory developed in Appendix A and the Venus-assist mission in the preceeding chapter is easily extended to the case of a second assist at Mercury. The post-assist orbit for the Venus assist is treated as a pre-assist orbit for the Mercury assist, and the procedures for a single assist are repeated. Thus, each Venus-assisted trajectory and a chosen DOCA at Mercury determines a combination-assist trajectory.

General Method

The general method may be described by reference to the equations derived in Appendix A. First of all, a value is selected for V_b, ϕ_o, and d at the first assist planet P_2. This determines the post-assist orbit characteristics a_3 and e_3; if the post-assist orbit intersects the orbit of a second assist planet, P_3, it is treated as a pre-assist orbit at P_3, and

$$r = r_{P_3} \tag{5-1}$$

Eqs (A-8) through (A-13) are used to find the orbit conditions at intercept of P_3:

$$V_5^2 = \mu_\odot\left(\frac{2}{r_{P_3}} - \frac{1}{a_3}\right) \tag{5-2}$$

$$\text{Sin } \phi_5 = \left[\frac{a_3^2 \ (1 - e_3^2)}{r_{p_3} \ (2a_3 - r_{p_3})} \right]^{1/2} \tag{5-3}$$

$$\tan f_5 = \frac{\left(r_{p_3} \ V_5^2 \ / \mu_\odot \right) \cos \phi_5 \sin \phi_5}{1 - \left(r_{p_3} \ V_5^2 \ / \mu_\odot \right) \sin^2 \phi_5} \tag{5-4}$$

The heliocentric transfer angle and time from P_2 to P_3, respectively, are given by

$$\theta_{23} = f_5 - f_3 \tag{5-5}$$

$$T_{23} = t \ (a_3, \ \mu_\odot, \ e_3, \ f_5) - t \ (a_3, \ \mu_\odot, \ e_3, \ f_3) \tag{5-6}$$

To determine the assist orbit at P_3, as shown in Fig. 23, use is made of Eqs (A-14) and (A-15) as follows:

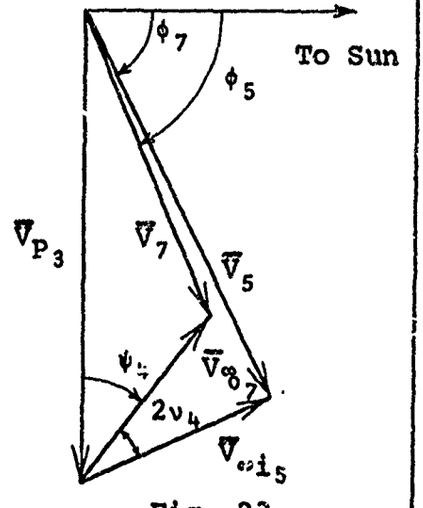

Fig. 23

Assist Geometry at P_3

$$V_{\infty_{i_5}}^2 = V_5^2 + V_{P_3}^2 - 2V_5 \ V_{P_3} \sin \phi_5 \tag{5-7}$$

and $$a_4 = \mu_{P_3} / V_{\infty_{i_5}}^2 \tag{5-8}$$

After selection of d_3, the DOCA at P_3, the eccentricity of the second orbit is calculated as in Eq (A-18):

$$e_4 = \frac{1}{a_4}\left(R_{p_3} + a_4 + d_3\right) \tag{5-9}$$

and

$$\sin \nu_4 = \frac{1}{e_4} \tag{5-10}$$

The final post-assist orbit conditions at P_3 are found with Eqs (A-22) through (A-26):

$$\psi_4 = \arcsin\left[\frac{V_5}{V_{\infty_{i_5}}} \cos \phi_5\right] - 2\nu_4 \tag{5-11}$$

$$V_{\infty_{o_7}} = V_{\infty_{i_5}} \tag{5-12}$$

$$V_7^2 = V_{p_3}^2 + V_{\infty_{o_7}}^2 - 2V_{p_3} V_{\infty_{o_7}} \cos \psi_4 \tag{5-13}$$

$$\cos \phi_7 = \frac{V_{\infty_{o_7}}}{V_7} \sin \psi_4 \tag{5-14}$$

$$\tan f_7 = \frac{\left(r_{p_3} V_7^2 / \mu_\odot\right) \cos \phi_7 \sin \phi_7}{1 - \left(r_{p_3} V_7^2 / \mu_\odot\right) \sin^2 \phi_7} \tag{5-15}$$

Finally, the post-assist orbit characteristics after the second assist are determined from Eqs (A-27) through (A-31),

$$a_5 = \frac{r_{p_3}}{2 - \left(r_{p_3} V_7^2 / \mu_\odot\right)} \tag{5 16}$$

$$e_5^2 = \left(r_{p_3} V_7^2 / \mu_\odot - 1\right)^2 \sin^2 \phi_7 + \cos^2 \phi_7 \tag{5-17}$$

$$T_{OP} = T_{12} + T_{23} - t(a_5, \mu_\odot, e_5, f_5) \qquad (5\text{-}18)$$

$$r_{a_5} = a_5 (1 + e_5) \qquad (5\text{-}19)$$

and for the final perihelion,

$$q_{mm} = r_{p_5} = a_5 (1 - e_5) \qquad (5\text{-}20)$$

Computer Programming

The program for combination-assisted trajectories (Program 3) is illustrated with the flow chart in Fig. 24. The first half of Program 3 is identical to Program 2, so that single-assist trajectories are generated by a parametric variation of V_b, ϕ_o, and d. Each trajectory calculated in the first half of the program is used to generate a set of combination-assisted trajectories by a parametric variation in d_3, the DOCA at P_3.

In addition to the control provisions made in Program 2, a provision is made for the case in which the post-assist orbit from P_2 does not intersect the orbit of P_3. The perihelion of the post-assist orbit from P_2 must be at least as small as the orbital radius of P_3.

A sample of the computer printout is given in Appendix E after Program 3. The first list of results for each V_b and ϕ_o is a set of Venus-assisted trajectories for varying d. Below this is a listing of Venus-Mercury-assisted trajectories for varying d_3 for each value of d.

The notation on the printed output is the same as that

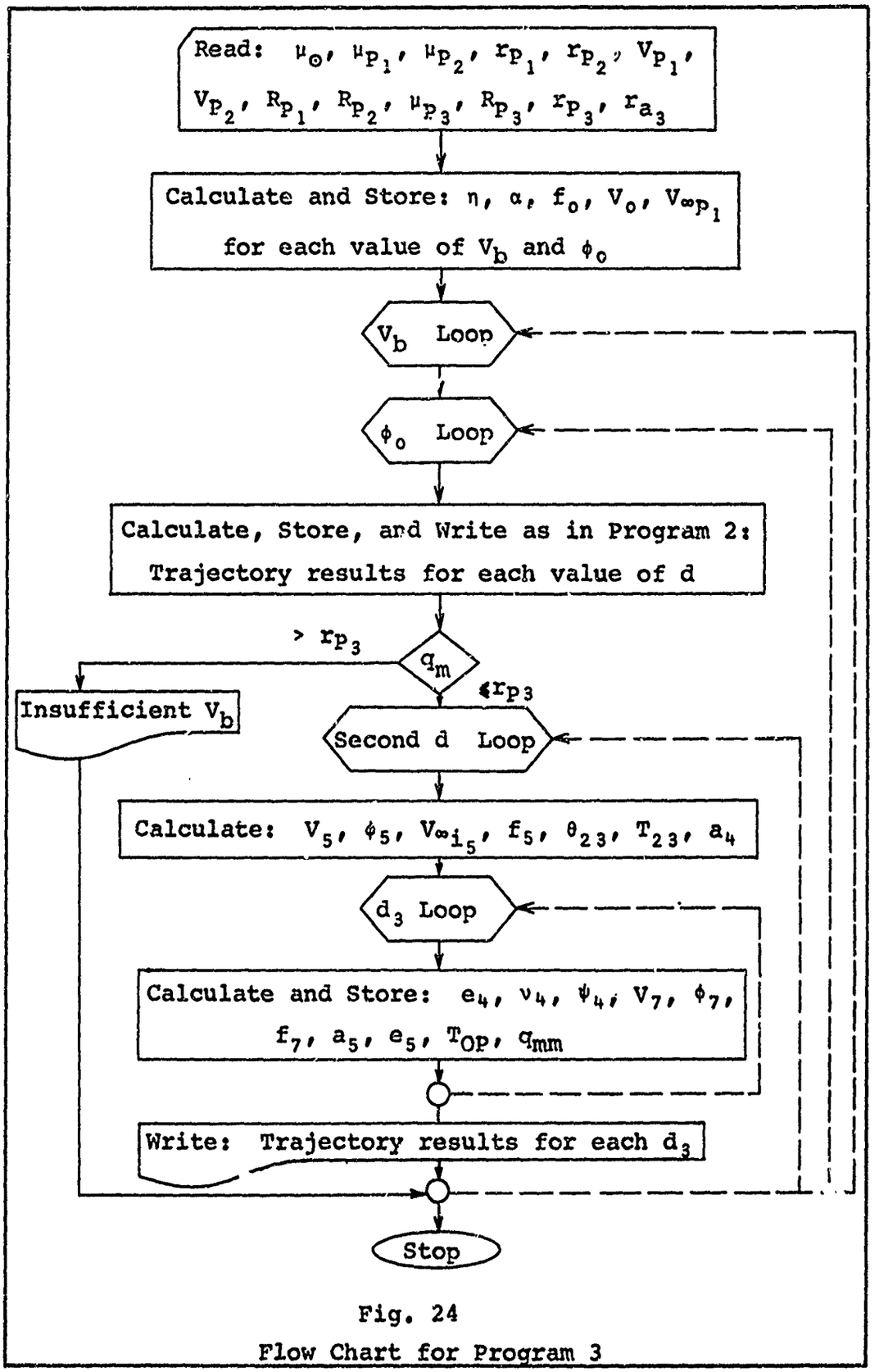

Fig. 24
Flow Chart for Program 3

used in Programs 1 and 2 with the following additions or changes:

N ∿ ν	T23 ∿ T_{23}	E5 ∿ e_5
T12 ∿ T_{12}	QMM ∿ q_{mm}	V7 ∿ V_7
TH23 ∿ θ_{23}	D3 ∿ d_3	N4 ∿ ν_4
F5 ∿ f_5	F7 ∿ f_7	PSI4 ∿ ψ_4
VINF5 ∿ $V_{\infty_{i_5}}$, $V_{\infty_{o_5}}$	A5 ∿ a_5	THOP ∿ θ_{OP}

TOP ∿ T_{OP} (Venus-Mercury Assist)

TTOT ∿ T_{OP} (Venus Assist with no Mercury Assist)

Eccentricity of Mercury's Orbit

When Program 3 is applied to the Venus-Mercury combination-assist problem, it is necessary to consider the eccentricity of Mercury's orbit, since it is not nearly circular.

In order to obtain a range of possible results, two cases are studied: Mercury at perihelion $r_{p_{\mathbb{Q}}}$ and Mercury at aphelion $r_{a_{\mathbb{Q}}}$. Thus, for the perihelion case,

$$r_{p_3} = r_{p_{\mathbb{Q}}} \tag{5-21}$$

and for the velocity of Mercury (Ref 8:Chap. II, pp. 11,12, Eqs (1-134) and (1-153)),

$$V_{p_3} = V_{p_{\mathbb{Q}}} = \sqrt{\frac{2\mu_{\odot}\, r_{a_{\mathbb{Q}}}}{r_{p_{\mathbb{Q}}}\left(r_{a_{\mathbb{Q}}} + r_{p_{\mathbb{Q}}}\right)}} \tag{5-22}$$

For the aphelion case,

$$r_{p_3} = r_{a_{\mathbb{Q}}} \tag{5-23}$$

and for the velocity,

$$V_{p_3} = V_{a_{\mathbb{H}}} = \sqrt{\frac{2\mu_\odot \, r_{p_{\mathbb{H}}}}{r_{a_{\mathbb{H}}} \left(r_{a_{\mathbb{H}}} + r_{p_{\mathbb{H}}} \right)}} \qquad (5\text{-}24)$$

Conclusions

The three missions which have been studied thus far (direct-transfer, Venus-assist, and Venus-Mercury assist) are compared in Fig. 25 on a plot of perihelion versus burnout velocity. Results for both the Venus-Mercury-at-aphelion and Venus-Mercury-at-perihelion missions are shown. Of the two cases, smaller perihelia are achieved when Mercury is at aphelion, but the difference is almost insignificant.

It can be concluded immediately from the figure that the Venus-Mercury combination-assist missions are not worthwhile. Not only is the reduction in perihelion insignificant when compared to the single Venus-assist missions, but also the added problems of guidance at a second assist planet and launch opportunities make these missions more trouble than they are worth.

Thus, the only useful result of this chapter is that a method has been outlined for the calculation of Venus-Mercury-probe trajectories, and equations have been derived for duel combination-assisted trajectories. However, the analysis has contributed little for solar probe missions.

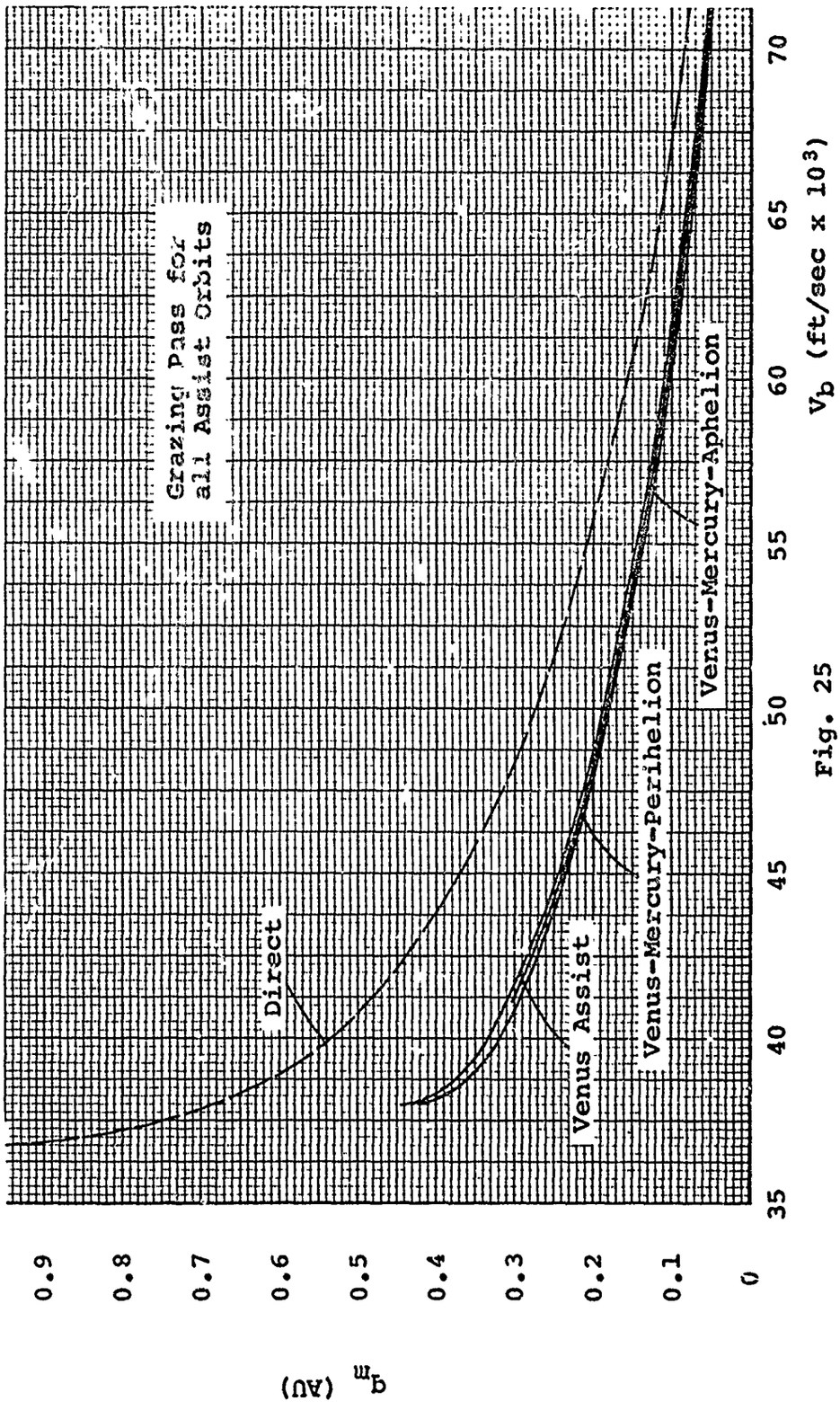

Fig. 25 Comparison of Direct-Transfer, Venus Assist, and Mercury-Venus Combination Assist Missions

VI. Multiple Venus Assist

The theory for gravity-assisted trajectories in Appendix A was extended in the preceeding chapter for the case of a combination of gravity assists at several planets. In this chapter, the same theory is extended for another case - multiple gravity assists at a single planet.

The problem here is to determine a DOCA at the assist planet (for given values of burnout velocity V_b and departure flight path angle ϕ_o) which will cause the spacecraft to intercept P_2 a second time at the same point in space. As shown below, this requires a post-assist orbit whose period is m/n times the orbit period of P_2; the quantities m and n are integers, where m is the number of solar circuits of P_2 and n is the number of solar circuits of the spacecraft before the second intercept.

This procedure may be repeated for additional passes at P_2 until the spacecraft aphelion is too small for interception. Of course, the DOCA for a final pass is arbitrary, just as it was for a single pass.

The theory and computer programs in this chapter are developed for multiple assist at any planet, but application is made only to a double and a triple assist at Venus. It has already been shown that little benefit is derived with a Mercury or Mars assist; a multiple assist at Jupiter is impractical because of excessive flight time and also because Sun impact can be achieved with just a single assist.

Double Assist at Venus

As stated above, the pre-assist orbit is determined by selecting V_b and ϕ_c. The next parameter for a double assist is the orbit ratio m/n. If the spacecraft and P_2 are to intercept a second time at the same point in space, then necessarily,

$$n\ \tau_{sc} = m\ \tau_{P_2} \tag{6-1}$$

where τ_{sc} is the first post-assist orbit period and τ_{P_2} is the orbit period of P_2.

Thus, for the orbit ratio selected, the required post-assist orbit period is

$$\tau_{sc} = \frac{m}{n}\ \tau_{P_2} \tag{6-2}$$

where τ_{P_2} is known from planetary data. From Kepler's Laws, this also specifies the semi-major axis of the post-assist orbit:

$$a_3 = \sqrt[3]{\frac{\mu_\odot\ \tau_{sc}^2}{4\pi^2}} \tag{6-3}$$

The heliocentric velocity at P_2 on the post-assist orbit is found with the vis-viva integral:

$$V_3^2 = \mu_\odot \left(\frac{2}{r_{P_2}} - \frac{1}{a_3} \right) \tag{6-4}$$

As shown in Fig. 26 there are two possible directions for $\bar{V}_3$. The $\bar{V}_3'$ case (dotted line) is discarded, because it serves to increase rather than decrease the perihelion of the post-assist orbit. If

$$|\bar{V}_3| < |\bar{V}_{P_2} - \bar{V}_{\infty_i}| \qquad (6\text{-}5)$$

then the trajectory cannot be realized and another orbit ratio must be selected.

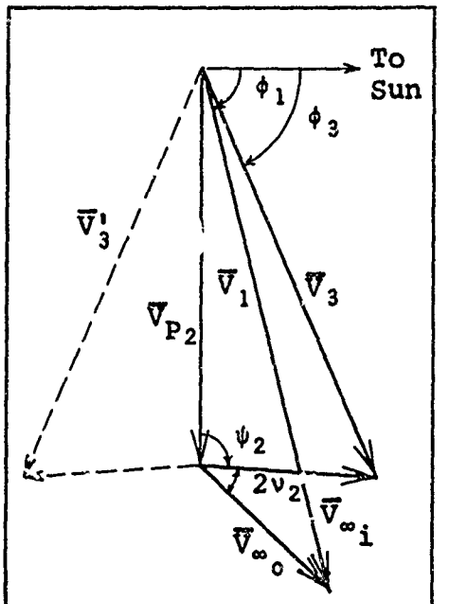

Fig. 26
Vector Geometry for First Assist

Conservation of energy of the flyby orbit gives

$$V_{\infty_o} = V_{\infty_i} \qquad (6\text{-}6)$$

and the flight path angle ϕ_3, is determined from the Law of Cosines:

$$\sin \phi_3 = \frac{1}{2V_3 V_{P_2}} \left[V_3^2 + V_{P_2}^2 - V_{\infty_o}^2 \right] \qquad (6\text{-}7)$$

The angle ψ_2 in the figure is given by

$$\sin \psi_2 = \frac{V_3}{V_{\infty_o}} \cos \phi_3 \qquad (6\text{-}8)$$

and from the Law of Sines, the turn angle is

$$2\nu_2 = \arcsin\left(\frac{V_1}{V_{\infty_i}} \cos \phi_1 \right) - \psi_2 \qquad (6\text{-}9)$$

Thus, Eqs (A-15) and (A-19) give

$$a_2 = \frac{\mu_{P_2}}{V_{\infty_i}^2} \tag{6-10}$$

$$e_2 = \frac{1}{\sin \nu_2} \tag{6-11}$$

and finally, from Eqs (A-16) and (A-17), the required DOCA at P_2 is

$$d = a_2 (e_2 - 1) - R_{P_2} \tag{6-12}$$

If a negative value is obtained for d, then, again, another value of m/n must be chosen.

The remaining characteristics of the post-assist orbit are calculated with Eqs (A-26) through (A-31).

If only minor guidance corrections are made, the first and second intercepts may be assumed to occur at the same point in space. Thus, the post-assist orbit for the first pass becomes a pre-assist orbit for the second pass with the new pre-assist conditions V_3 and ϕ_3 (see Fig. 27). The remainder of the problem is now identical to the single assist mission, and the DOCA for the second pass, d_2, may be selected arbitrarily. The post-assist conditions (V_5, ϕ_5) and the final post-assist orbit characteristics are computed with Eqs (A-18) through (A-31). The final perihelion is given by

$$q_{m_2'} = a_5 \ (1 - e_5) \tag{6-13}$$

It should be noted here that subscript notation in this chapter has a different meaning than that used in Chapter V.

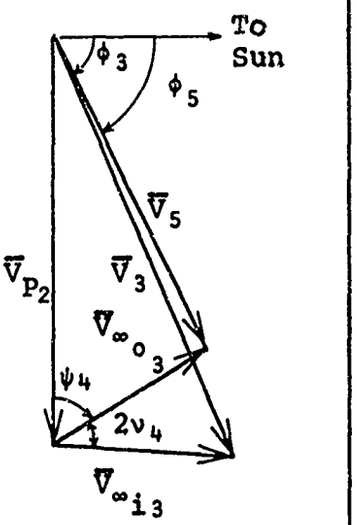

Fig. 27
Vector Geometry for Second Assist

Computer Program. The computer program for a double assist (Program 4), illustrated in the flow chart of Fig. 28, does not entirely follow the method outlined in this chapter. The values of V_b and ϕ_o are parametrically varied as before, but d is found by iteration rather than direct calculation for given values of m and n.

A value is selected for d, and the first assist orbit is computed; next, m is selected, and n is varied until Eq (6-1) is satisfied. If no value of n is found to satisfy the equation, the next highest integer is selected for m, and so on until all values of m and n up to a limiting integer have been tried for the value of d. If no combinations of m and n produce the desired orbit, then d is increased by an increment, and the procedure is repeated until all combinations of m and n are found with a corresponding value for d.

This procedure demands more computer time than would be required for the method developed in the chapter, but it also avoids a major rewrite of the basic program which is used in the two previous chapters.

In this program, m was allowed to vary from 1 to 5, and n from 1 to 9. Obviously, the trajectories with low values of m have the more satisfactory mission times. It is found in the computations that Venus-assisted trajectories are not physically realizable for m or n equal to one.

Notation changes or additions on the output of Program 4 are:

DOCA1 ∿ d	NSP ∿ n	VINF3 ∿ $V_{\infty_{i_3}}$, $V_{\infty_{o_3}}$
TAUP2 ∿ τ_{P_2}	TAUP ∿ τ_{sc}	T1MOP ∿ Mission Time
MP1 ∿ m	DOCA2 ∿ d_2	QM2 ∿ Final Perihelion

T ∿ Time from Launch to Perihelion of First Pre-Assist Orbit

THTOT ∿ Heliocentric Angle from Launch to Final Perihelion

Mission Profile. The mission profile in Fig. 29 illustrates the trajectory for a burnout velocity of 42,000 ft/sec and a tangential departure. From Fig. 4 this trajectory may be achieved by an Atlas/Centaur launch vehicle with a 300-lb payload. This payload allows for additional guidance equipment which may be required for a second pass (Ref 3).

A significant advantage of this trajectory is that the semi-major axis of the first pre-assist orbit (0.728 AU) is very nearly that of Venus' orbit (0.723 AU). The value of

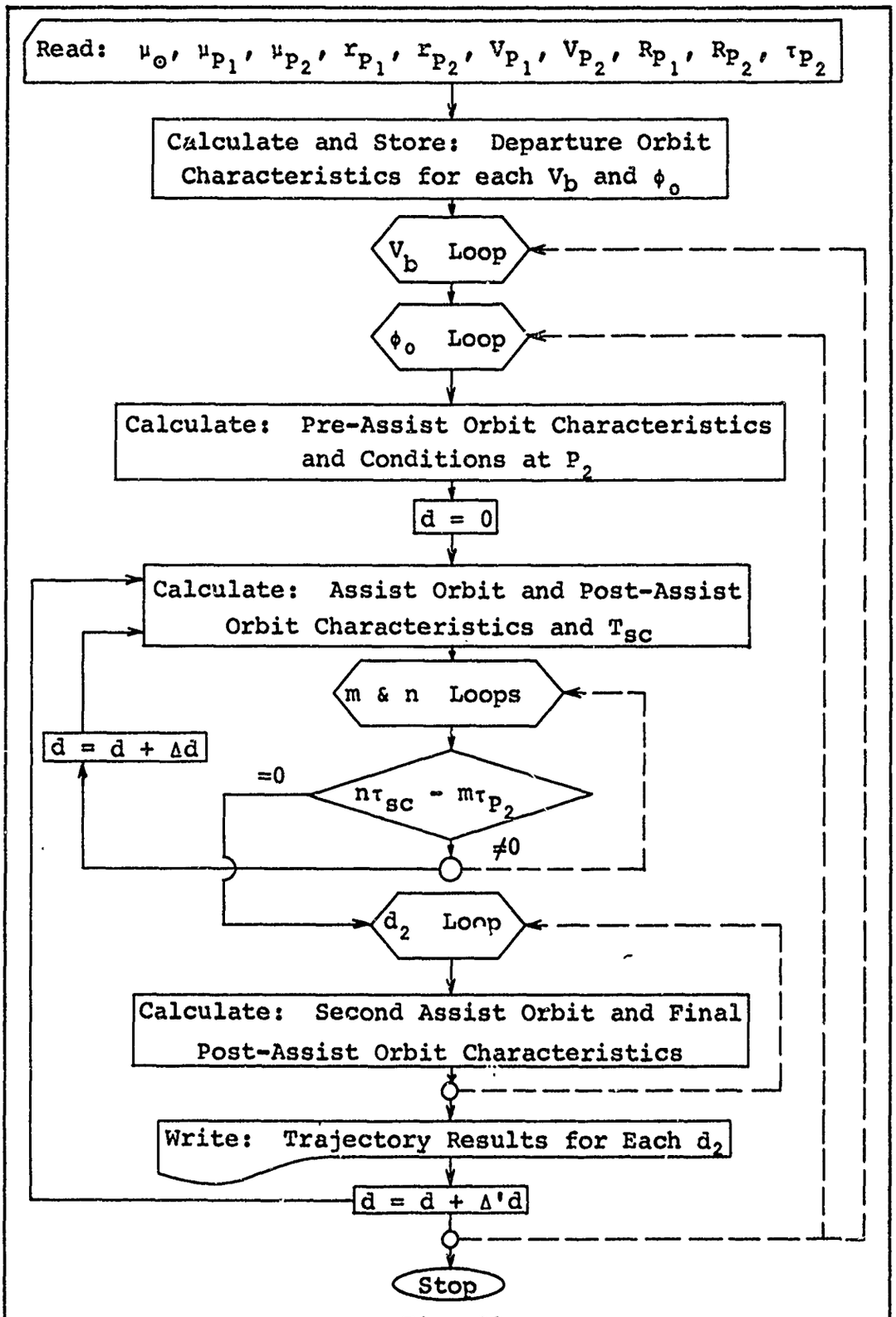

Fig. 28

Flow Chart for Program 4

Trajectory Data

Launch Date: 24 Jan 1969 (JD 2440246.2)
Launch Vehicle: Atlas/Centaur
V_b = 42,000 ft/sec, ϕ_o = 90°
Payload = 300 lb
T_{12} = 70.7 days
T_{OP} = 567.4 days = 1.55 years

d_1 = 65 NM
d_2 = 100 NM
q_{m_1} = 0.294 AU
q_{m_2} = 0.201 AU
Orbit Ratio = $\frac{2}{3}$

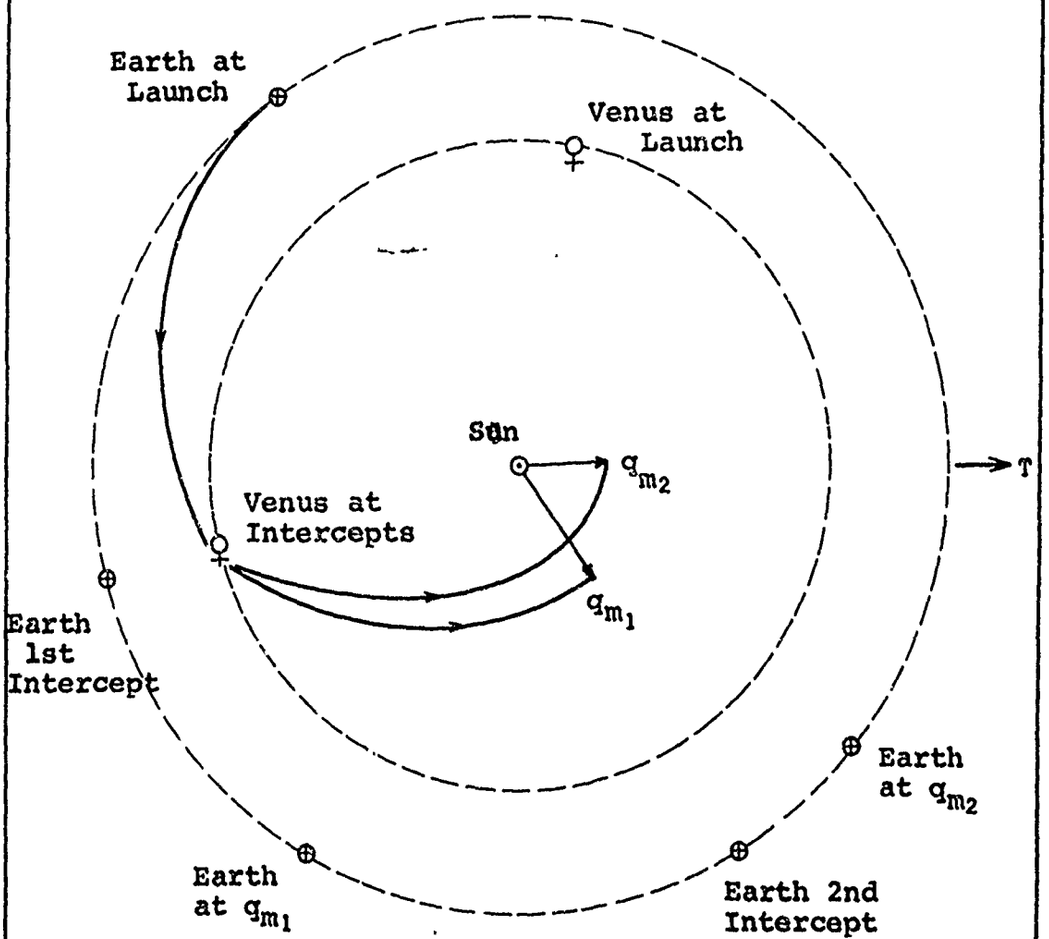

Fig. 29

Mission Profile for Double Venus Assist

V_b which gives exactly $a_1 = 0.723$ AU may be found with a few calculations, but suppose that this has been done. Then by Kepler's Third Law, the period of the pre-assist orbit matches the period of Venus. Thus, if midcourse maneuvers fail to establish the initial intercept at Venus, a second attempt may be made one Venus year later.

Conclusions. In the double-assist mission profile it was found that a perihelion of 0.201 AU can be established with the Atlas/Centaur ($11.9 million). A direct-transfer to this perihelion, from Figs. 4 and 10, requires a much larger booster such as the Saturn I/Centaur with an added kick stage or a Saturn V.

The double-assist missions not only reduce booster vehicle costs, but also provide the opportunity to explore two regions of the solar system with a single launch. For the mission profile above, data can be obtained from the 0.3 AU region after the first pass at Venus and from the 0.2 AU region after the second pass.

Double-assist missions with different orbit ratios are compared in Fig. 30. The left-hand end of each curve represents the smallest value of V_b with which the desired orbit ratio can be achieved; the right-hand end represents an upper limit on d (5000 NM) in the computations. If d is increased, the curves may be extended as far to the right as desired.

From this graph the most promising orbit ratio is 2/3, because it offers short mission times, and gives physically

realizable trajectories for almost the entire spectrum of V_b which is used in Venus-assist missions. The 3/5 ratio is also attractive because of the small perihelia which can be achieved; however, V_b for these missions must be greater than 55,000 ft/sec which automatically demands a more expensive booster. The 5/8 missions are discounted for their unreasonable time requirements.

One additional note of interest on this graph is that perihelion distance decreases (for a given V_b) with the value of the orbit ratio.

Results of the 2/3 missions are illustrated on the graphs in Figs. 31 through 34. In Fig. 31 double-assist missions are compared with direct-transfer missions for various values of d_2. The most significant reductions in perihelia are achieved for the lower values of V_b.

The value of d required to establish a post-assist orbit of period 2/3 τ_{φ} is indicated in Fig. 32 for any value of V_b. From this graph, it can be seen that d increases with V_b; therefore, the effect of the first assist diminishes as V_b increases, and only the second assist serves to decrease the perihelion. This trade-off property is also evident in Fig. 33, where the double-assist missions (solid lines) are compared with the single-assist (dot-dashed lines) and direct-transfer missions (dashed lines) for a few values of V_b. From this graph, if V_b = 55,000 ft/sec, then a single-assist mission is

more beneficial than a double-assist mission for d_2 > 4000 NM.

An inherent disadvantage in double-assist missions is the time requirements, as illustrated in Fig. 34 for $m/n = 2/3$ and $d_2 = 100$ NM. Double-assist missions require approximately 550 days or 1.15 years, whereas direct missions require less than 160 days.

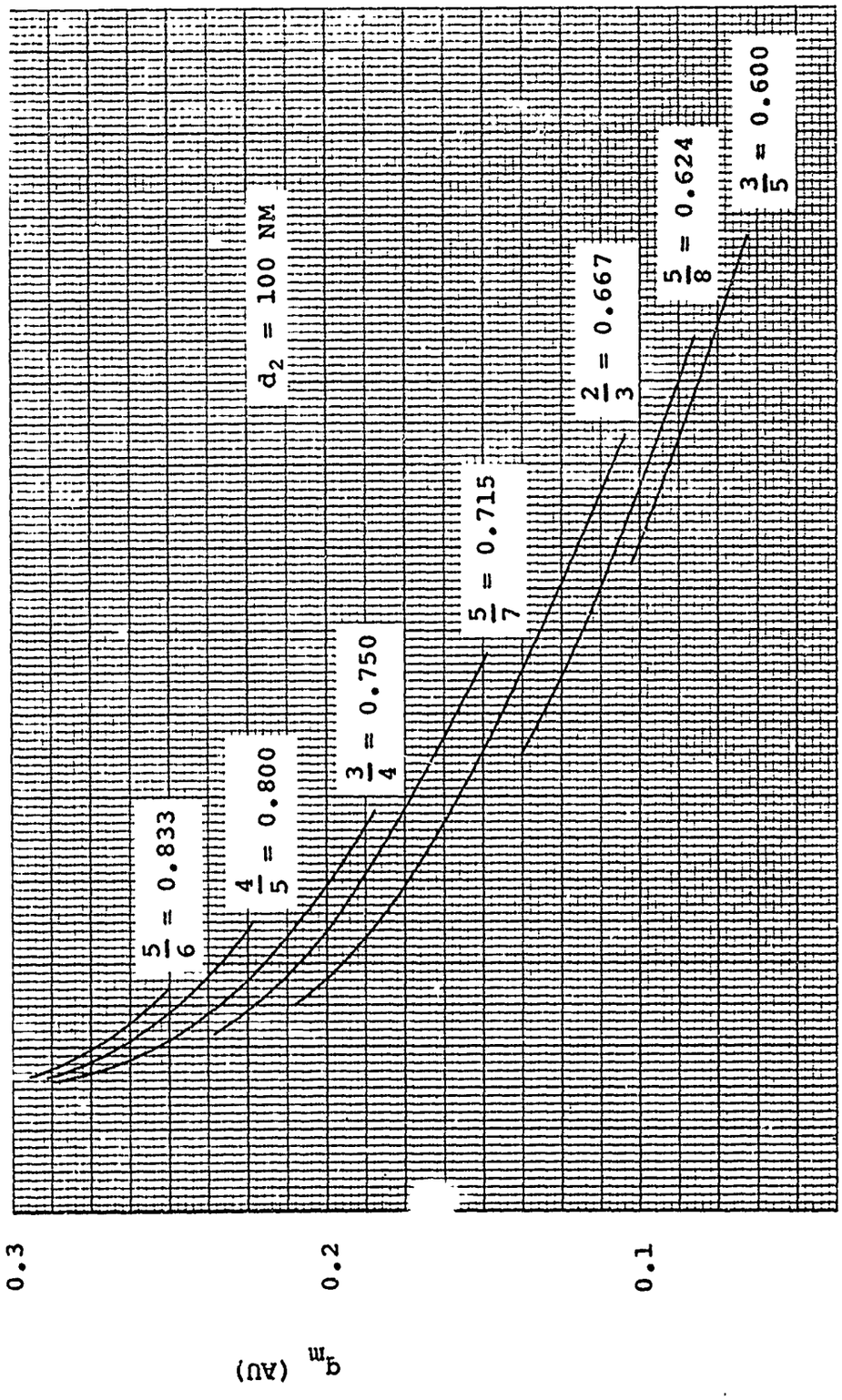

Fig. 30 Comparison of Venus Double-Assist Missions with Various Orbit Ratios

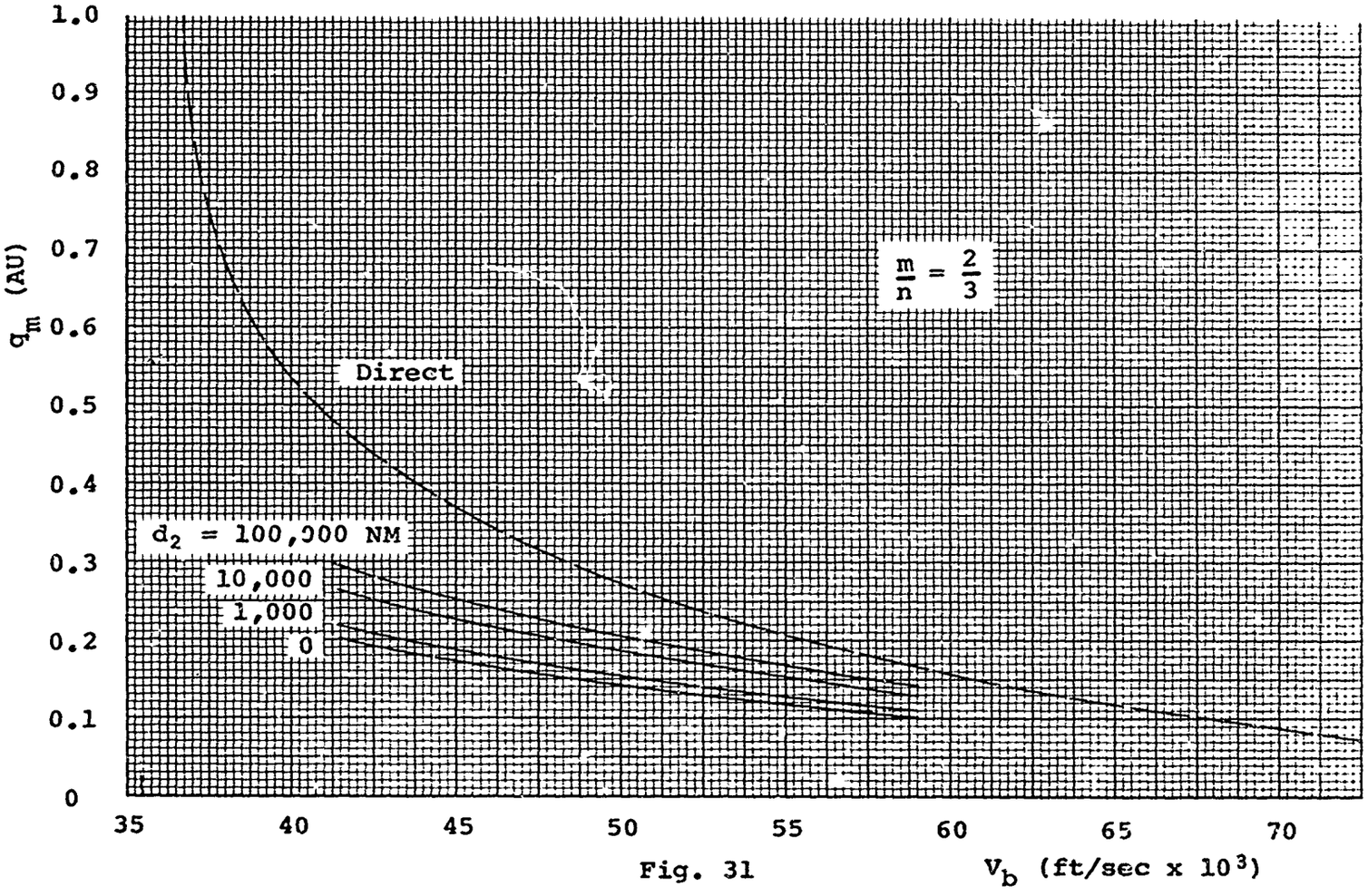

Fig. 31

Perihelion vs. Burnout Velocity for Double-Assist at Venus

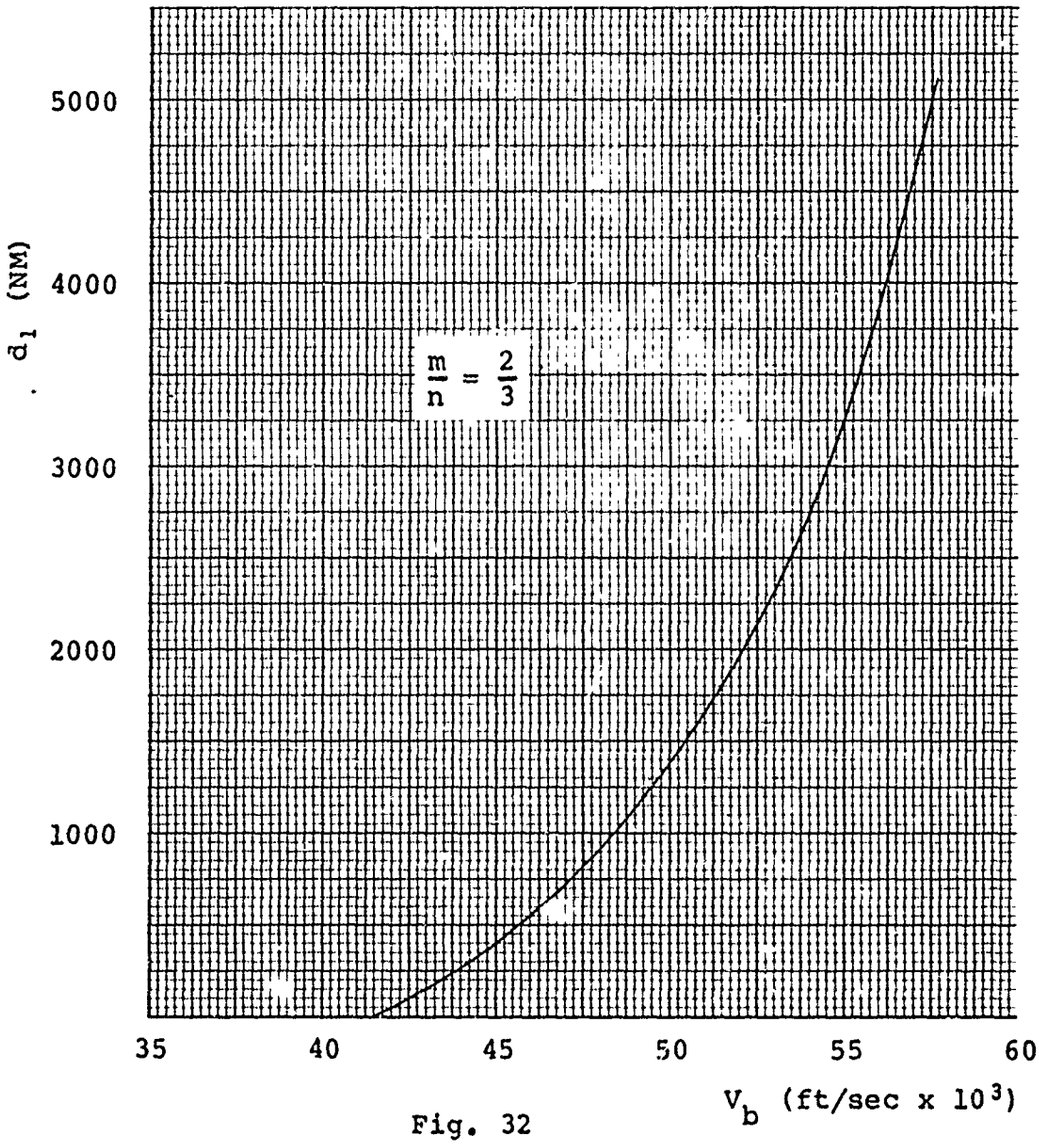

Fig. 32

Required d_1 for Double-Assist Missions to Venus

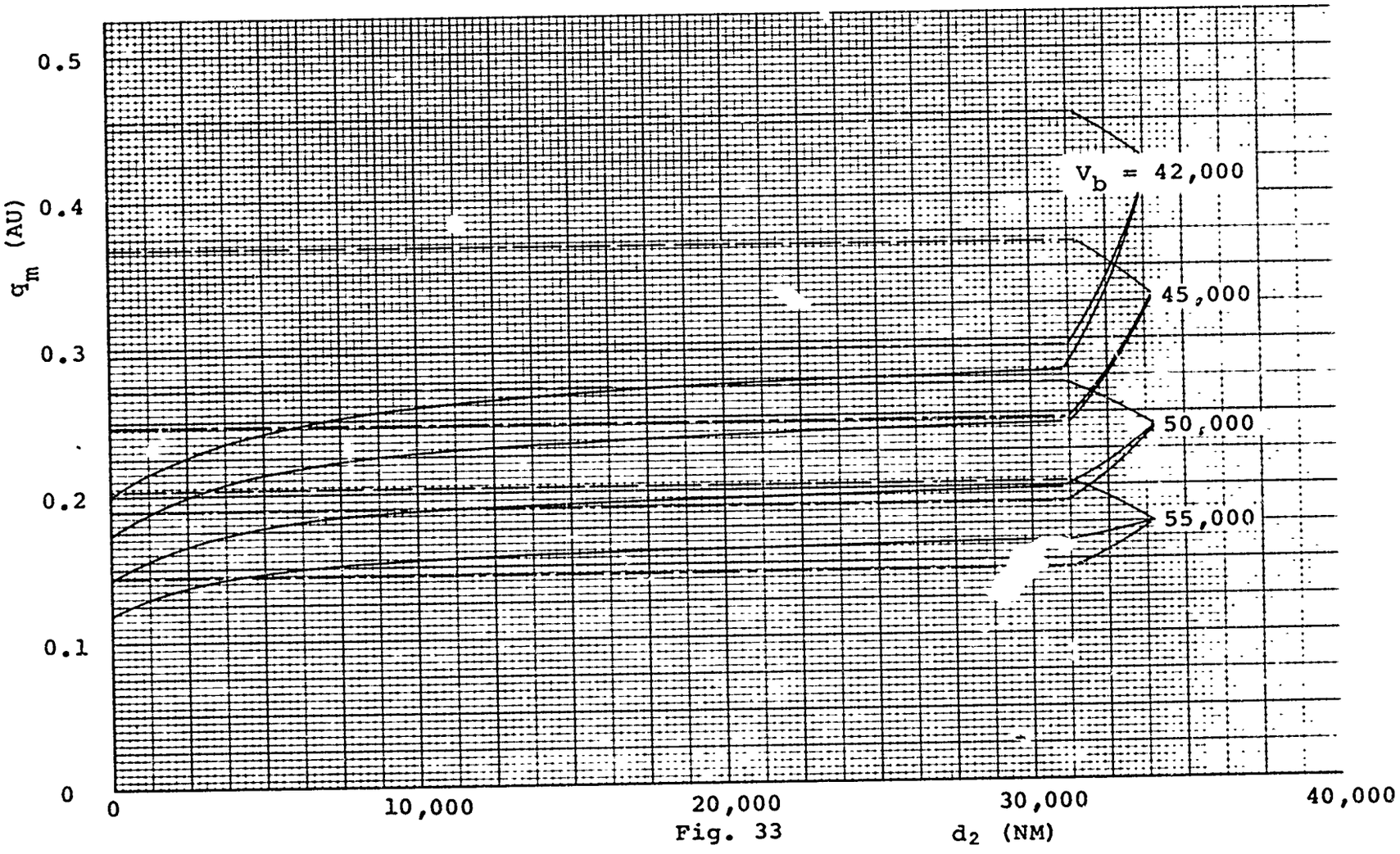

Fig. 33

Comparison of Double-Assist, Single-Assist (d = 100 NM), and Direct-Transfer Missions

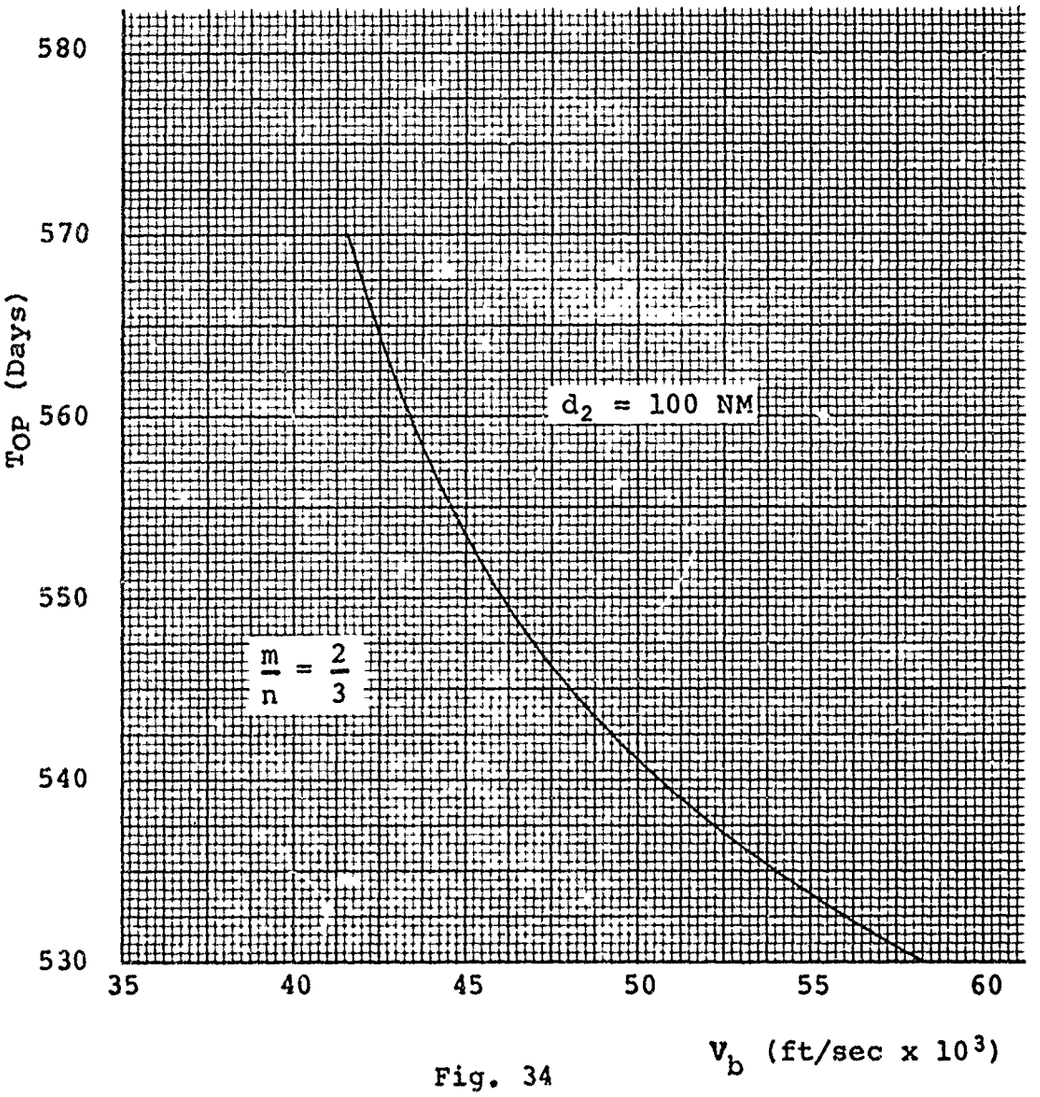

Fig. 34

Time Requirements for Double-Assist Missions

Triple Assist at Venus

The analysis for a double assist extends easily to the case of a triple assist. The method used to determine the first DOCA for a second intercept is again used to determine the second DOCA for a third intercept.

For a triple assist, two relations similar to Eq (6-1) or (6-2) must be satisfied

$$\tau_{sc_1} = \frac{m_1}{n_1} \tau_{P_2} \tag{6-14}$$

$$\tau_{sc_2} = \frac{m_2}{n_2} \tau_{P_2} \tag{6-15}$$

where m_i is the number of solar circuits of P_2, and n_i is the number of solar circuits of the spacecraft after the ith intercept (i = 1,2). From the double-assist procedures then, it follows that

$$a_3 = \sqrt[3]{\frac{\mu_\odot \tau_{sc_1}^2}{4\pi^2}} \tag{6-16}$$

$$a_5 = \sqrt[3]{\frac{\mu_\odot \tau_{sc_2}^2}{4\pi^2}} \tag{6-17}$$

for the semi-major axes of the first and second post-assist orbits, respectively. The heliocentric velocity at P_2 on the first and second post-assist orbits, respectively, is

$$V_3^2 = \mu_\odot \left(\frac{2}{r_{P_2}} - \frac{1}{a_3} \right) \tag{6-18}$$

$$V_5^2 = \mu_\odot \left(\frac{2}{r_{P_2}} - \frac{1}{a_5} \right) \tag{6-19}$$

The HEV is the same for each pass due to conservation of energy. Thus, the flight path angles ϕ_3 and ϕ_5 may be calculated with relations similar to Eq (6-7).

The hyperbolic assist orbit at each pass is found with Eqs (6-8) through (6-11), which give

$$e_2 = \frac{1}{\sin \nu_2} \tag{6-20}$$

$$e_4 = \frac{1}{\sin \nu_4} \tag{6-21}$$

Finally, the required DOCA for the first two passes, respectively, are given by

$$d_1 = a_2 \ (e_2 - 1) - R_{P_2} \tag{6-22}$$

$$d_2 = a_4 \ (e_4 - 1) - R_{P_2} \tag{6-23}$$

Again, if a negative value is obtained for either DOCA, then another combination of m_i or n_i must be selected.

The DOCA for the final pass, d_3, may be chosen as desired, and the problem again takes the form of a single assist. Thus, the selection of d_3 determines the third

post-assist orbit conditions V_7 and ϕ_7 shown in Fig. 35. Finally, the post-assist orbit characteristics are found with Eqs (A-26) through (A-31), and the final perihelion is

$$q_{m_3} = a_7 (1 - e_7) \qquad (6\text{-}24)$$

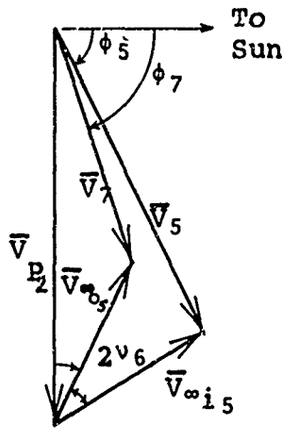

Fig. 35
Vector Geometry for
Third Assist

Computer Program. Program 5 (for a triple assist) is summarized in the flow chart of Fig. 36. The program is identical to Program 4, except that a section has been added to calculate the second DOCA for a third intercept.

After the first post-assist is computed (d_1, m_1, n_1 determined), a value is selected for d_2, and m_2 and n_2 are varied up to some limiting integer (5 and 9, respectively) until Eq (6-15) is satisfied. If no orbit is found for all combinations of m_2 and n_2, then d_2 is increased by an increment, and so on as in Program 4. After Eqs (6-14) and (6-15) have been satisfied, a final post-assist orbit is computed for various values of d_3.

Notation on the output is as follows:

DOCA2 ∿ d_2	MP2 ∿ m_2	N6 ∿ ν_6
TAUP ∿ τ_{sc_1}	NS2 ∿ n_2	QM3 ∿ q_{m_3}
TAUPP ∿ τ_{sc_2}	DOCA3 ∿ d_3	TIMO2 ∿ Mission Time

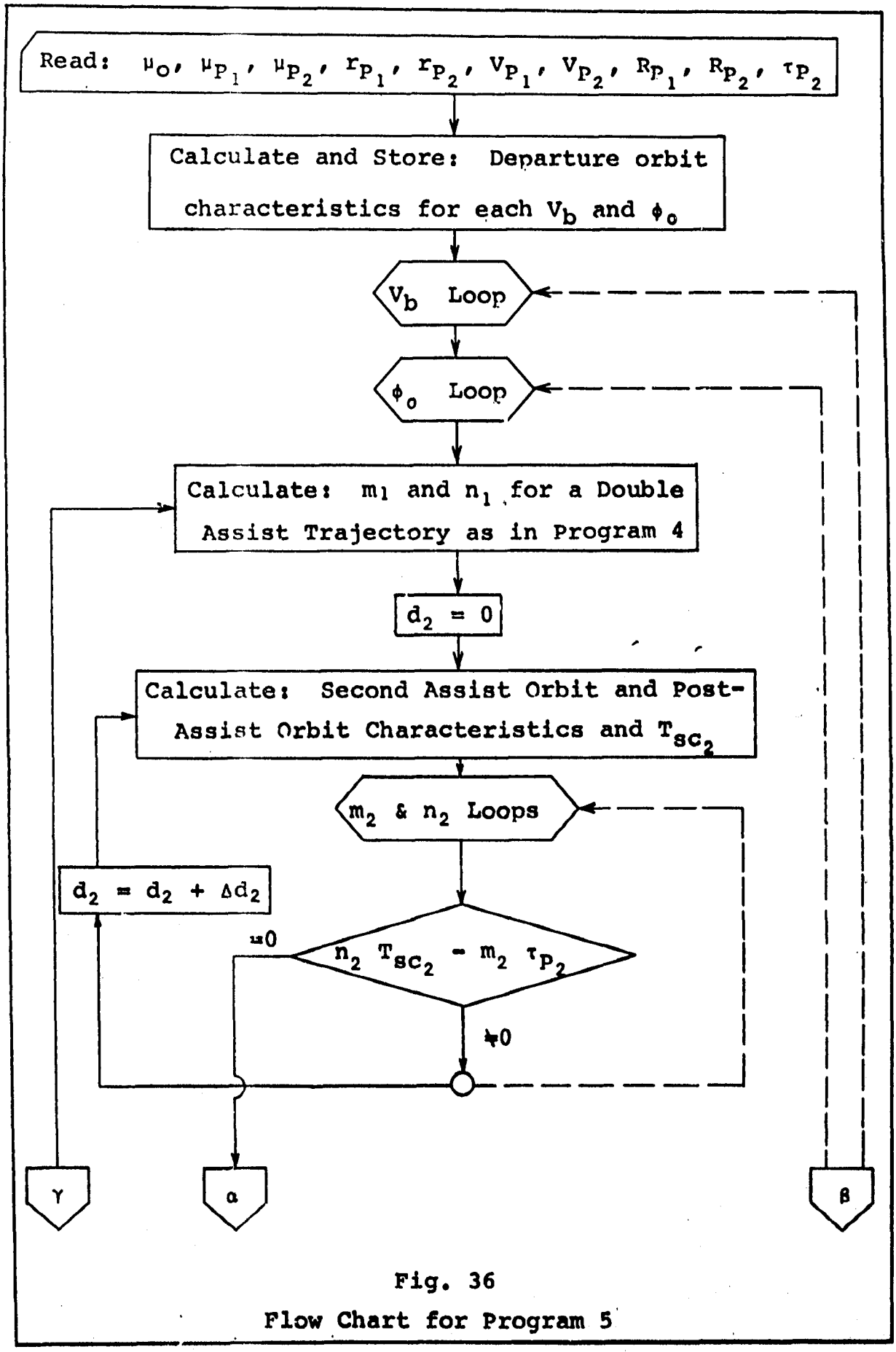

Fig. 36

Flow Chart for Program 5

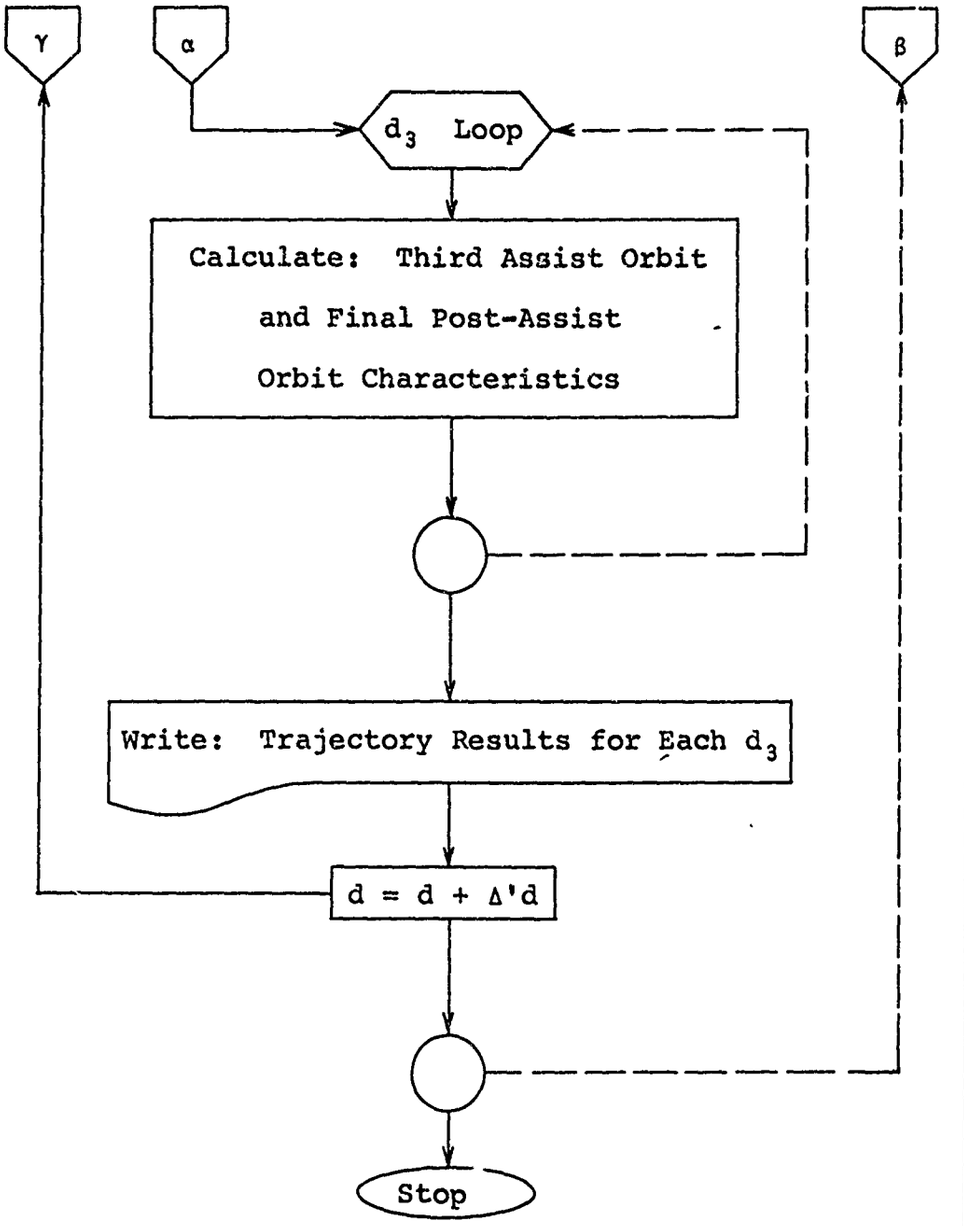

Fig. 36 (Continued)

Flow Chart for Program 5

THTO2 ∿ Heliocentric Angle from Launch to Final Perihelion

Mission Profile. A triple-assist mission is illustrated in Fig. 37 for a tangential departure and a burnout velocity of 53,000 ft/sec. An orbit ratio of (2/3) (5/9) is selected so that the second assist may be completed early in the flight; thus, a partial success is assured if capability for a third intercept is lost during the mission.

The Atlas/Centaur/TE-364-3 is used for this mission with a payload of 250 lb. It is assumed here that this payload weight can be realized for a triple-assist by the 1972 time period. A heavier package would require either a larger booster or an additional kickstage (Ref 6, Ref 12:89-101).

Conclusions. In the triple-assist mission profile it was found that a perihelion of 0.096 AU can be attained with a burnout velocity of 53,000 ft/sec. A direct transfer to this perihelion requires a burnout velocity of 68,000 ft/sec; thus, triple assist has reduced the booster vehicle requirement from Saturn V/Kick Stage to Atlas/Centaur/TE-364-3. This mission also allows the exploration of three regions (0.183 AU, 0.134 AU, 0.096 AU) near the Sun with a single launch.

Various orbit ratios are compared in Fig. 38, and again the left-hand end of the curves represents a physical lower limit on V_b for each orbit ratio, and the right-hand end is limited by the highest values of d_1 and d_2 in the computations (5000 NM for each). The (2/3) (5/9) orbit ratio is

Trajectory Data

Launch Date: 6 Apr 1972 (JD 2441412.8)
Launch Vehicle: Atlas/Centaur/TE-364-3
V_b = 53,000 ft/sec, ϕ_o = 90°
Payload = 250 lb
T_{12} = 52.7
T_{OP} = 1659.2 days = 4.54 years
Orbit Ratio = $\frac{2}{3}\frac{5}{9}$

d_1 = 2315 NM
d_2 = 540 NM
d_3 = 100 NM
q_{m_1} = 0.183 AU
q_{m_2} = 0.134 AU
q_{m_3} = 0.096 AU

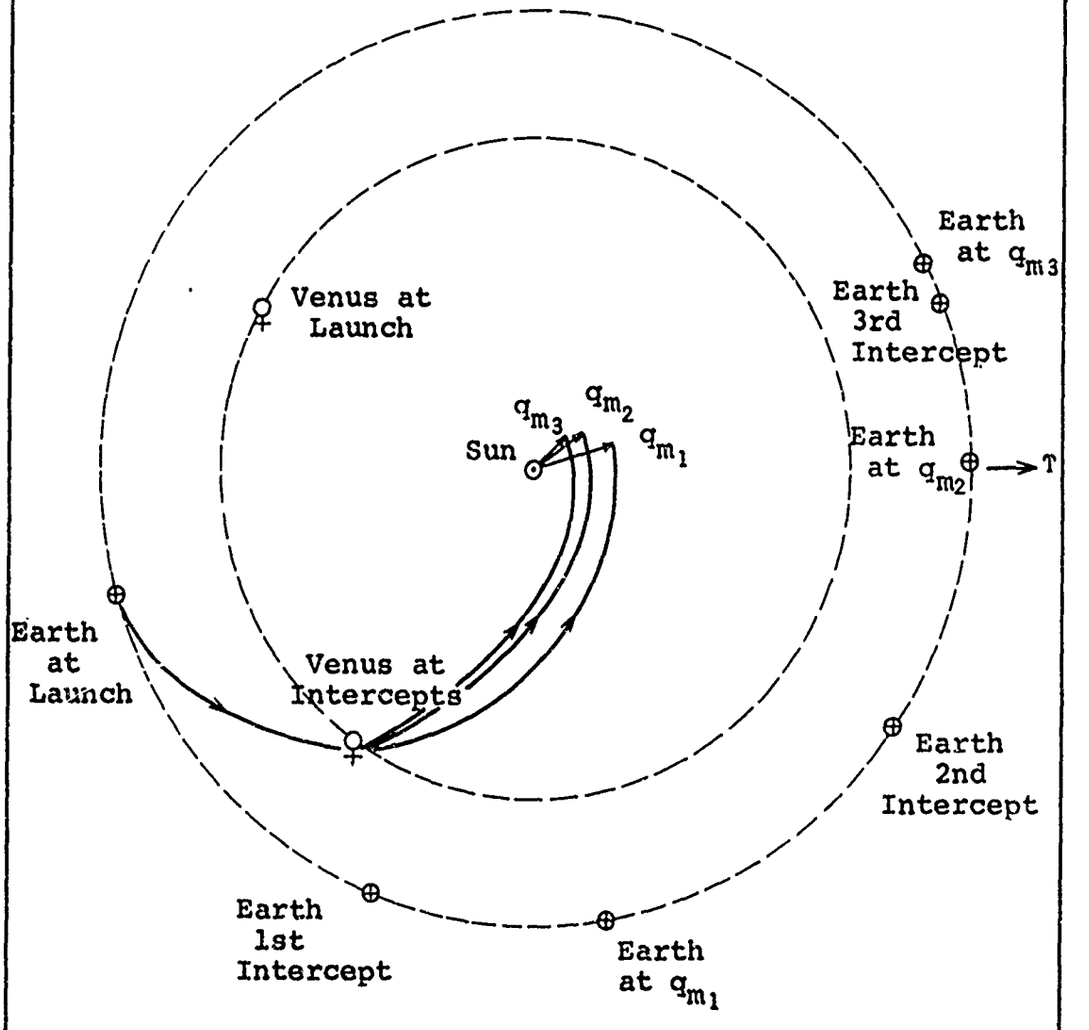

Fig. 37

Mission Profile for Triple Venus Assist

the most favorable for two reasons: mission time is comparitively short, and trajectories are realizable for a wide range of V_b. From the figure there are three orbit ratios which yield smaller perihelia, but these cases are discarded because of long mission times ((5/8) (5/9) and (3/5) (5/9)) or high burnout velocity requirements ((4/7) (1/2)).

Results for the (2/3) (5/9) missions, illustrated in Fig. 39 through 42, indicate the same trends which were found in the 2/3 double-assist missions.

Triple-assist and direct-transfer missions are compared in Fig. 39; it is found that the perihelion may be reduced by as much as 0.28 AU with a triple assist.

The required values of the first and second DOCA are shown in Fig. 40. The value of d_1 increases with V_b, whereas d_2 decreases with V_b. If it turns out that the multiple-assist navigation system is limited to one particular DOCA for each intercept, then a burnout velocity of 48,500 ft/sec must be used and $d_1 = d_2 = d_3 = 1000$ NM. This trajectory has a perihelion of 0.125 AU.

The trade-off property for double-assist missions is also found in the triple-assist missions. This is illustrated in Fig. 41, where the triple-assist missions (solid lines) for any value of d_3 are compared with double-assist missions (dot-dashed lines) with $d_2 = 100$ NM. At a burnout velocity of 45,000 ft/sec, the perihelion for a triple assist is

smaller than the perihelion for a double assist only if $d_3 < 11{,}000$ NM.

The time requirements for triple-assist missions, shown in Fig. 42, indicate that these trajectories are of questionable value. Mission time is about 1670 days (4.6 years) which demands a spacecraft reliability well beyond present-day capability.

It is probable that the mission time for a multiple assist can be shortened by effecting one or more of the assists at the point where the post-assist orbit makes its first crossing of the assist planet orbit (rather than the point of the second crossing which was used for each assist in the above investigation). This possibility is left for further study; however, it is doubtful that the perihelia obtained in these missions will be smaller than those found above.

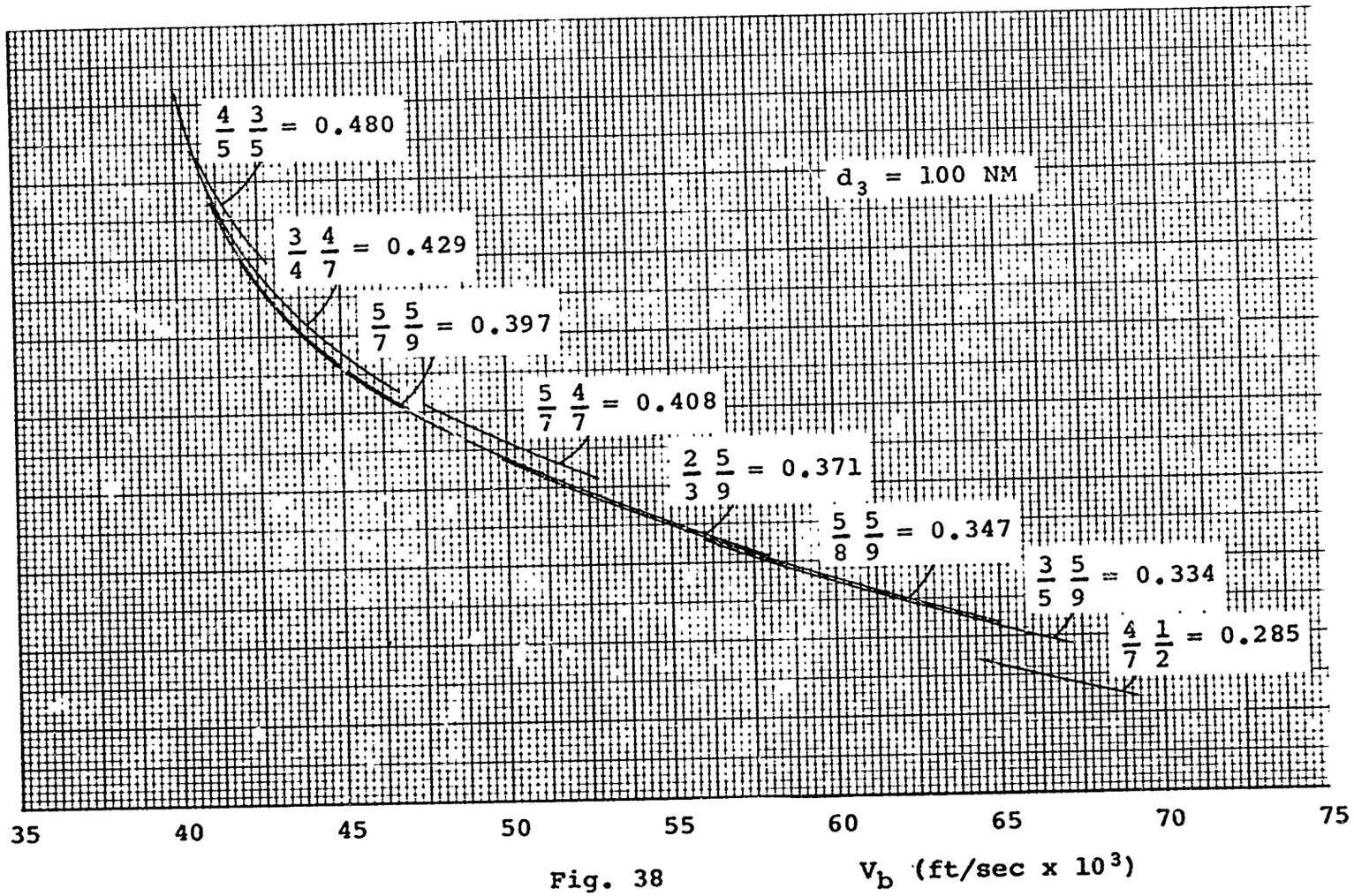

Fig. 38

Comparison of Venus Triple-Assist Missions with Various Orbit Ratios

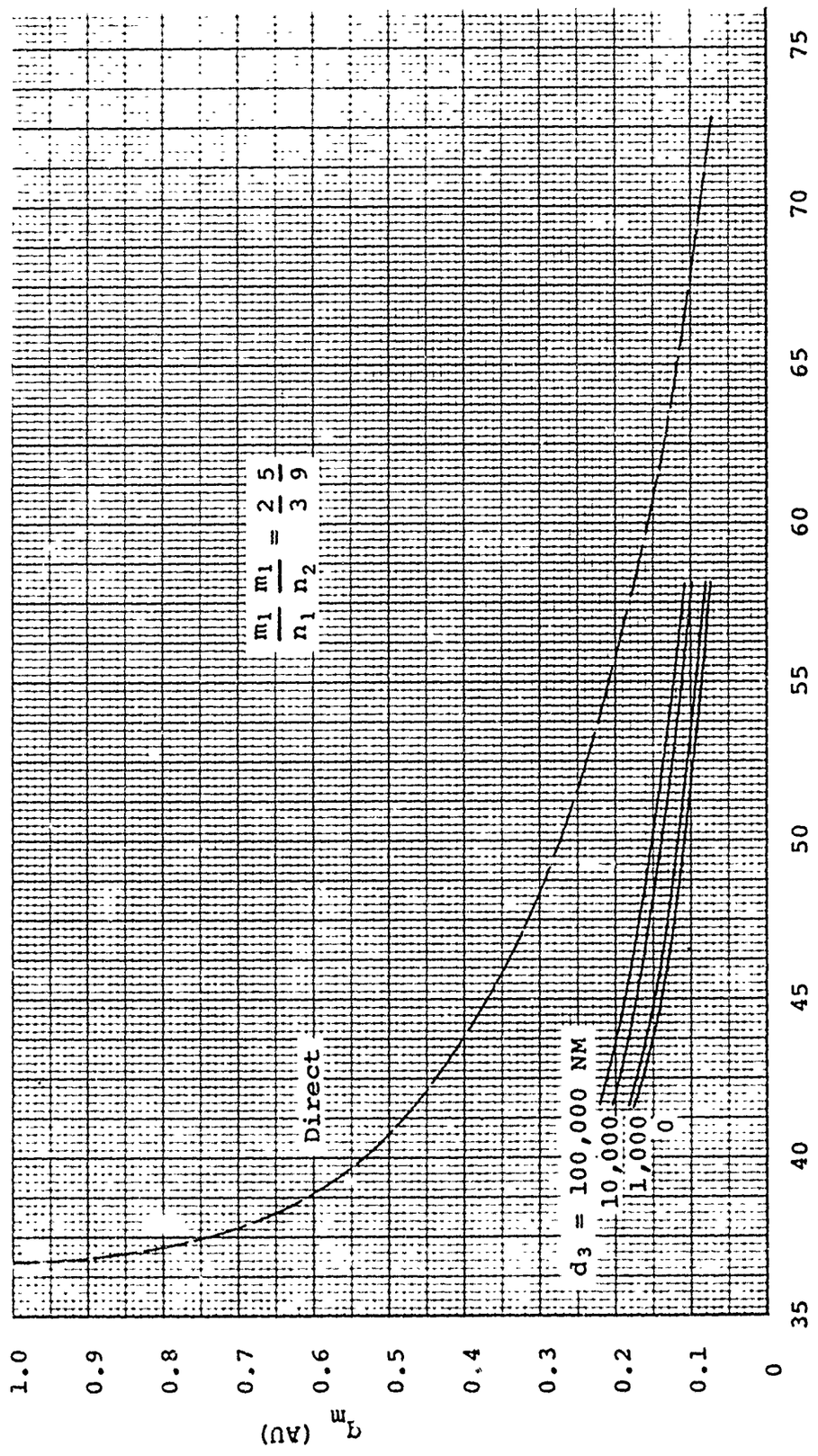

Fig. 39 Perihelion vs. Burnout Velocity for Triple Assist at Venus

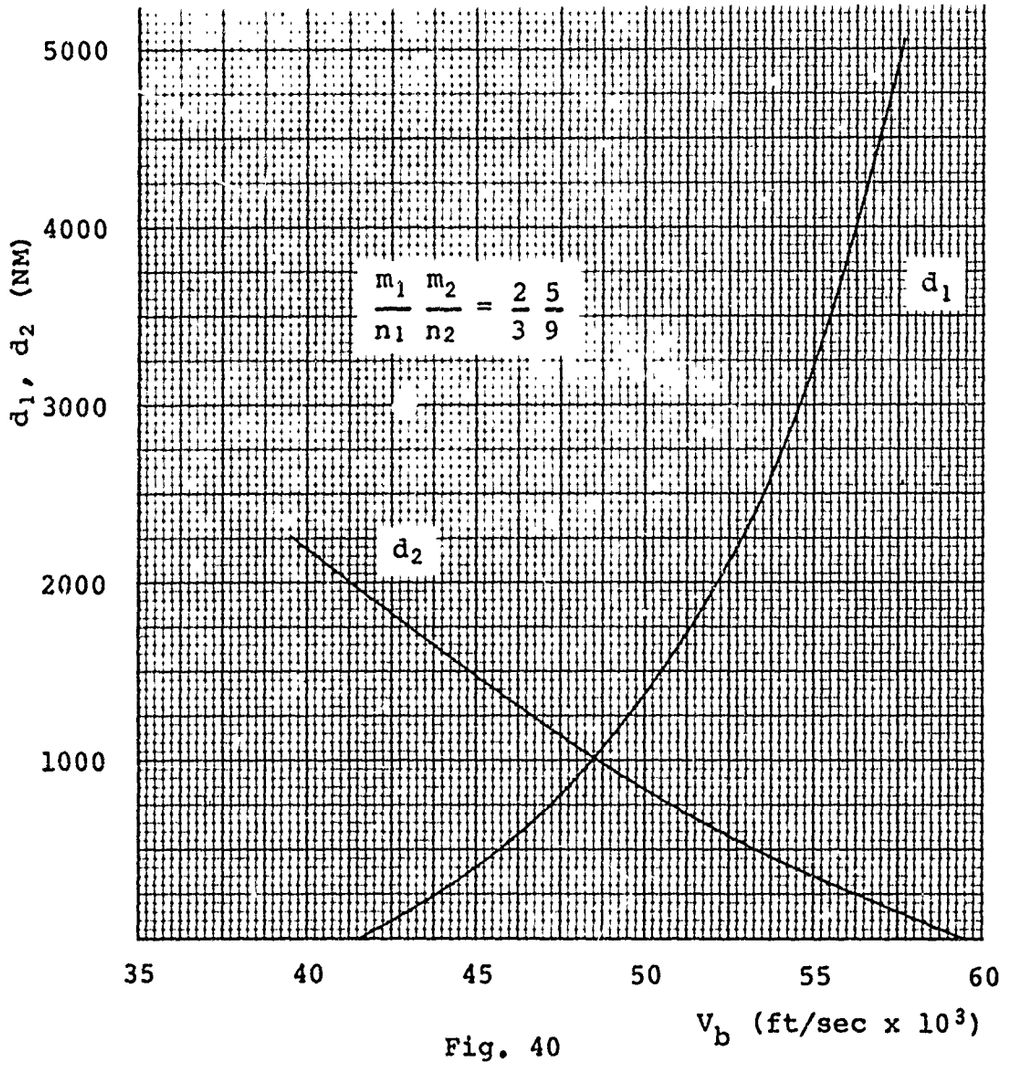

Fig. 40

DOCA Required for Triple Assist at Venus

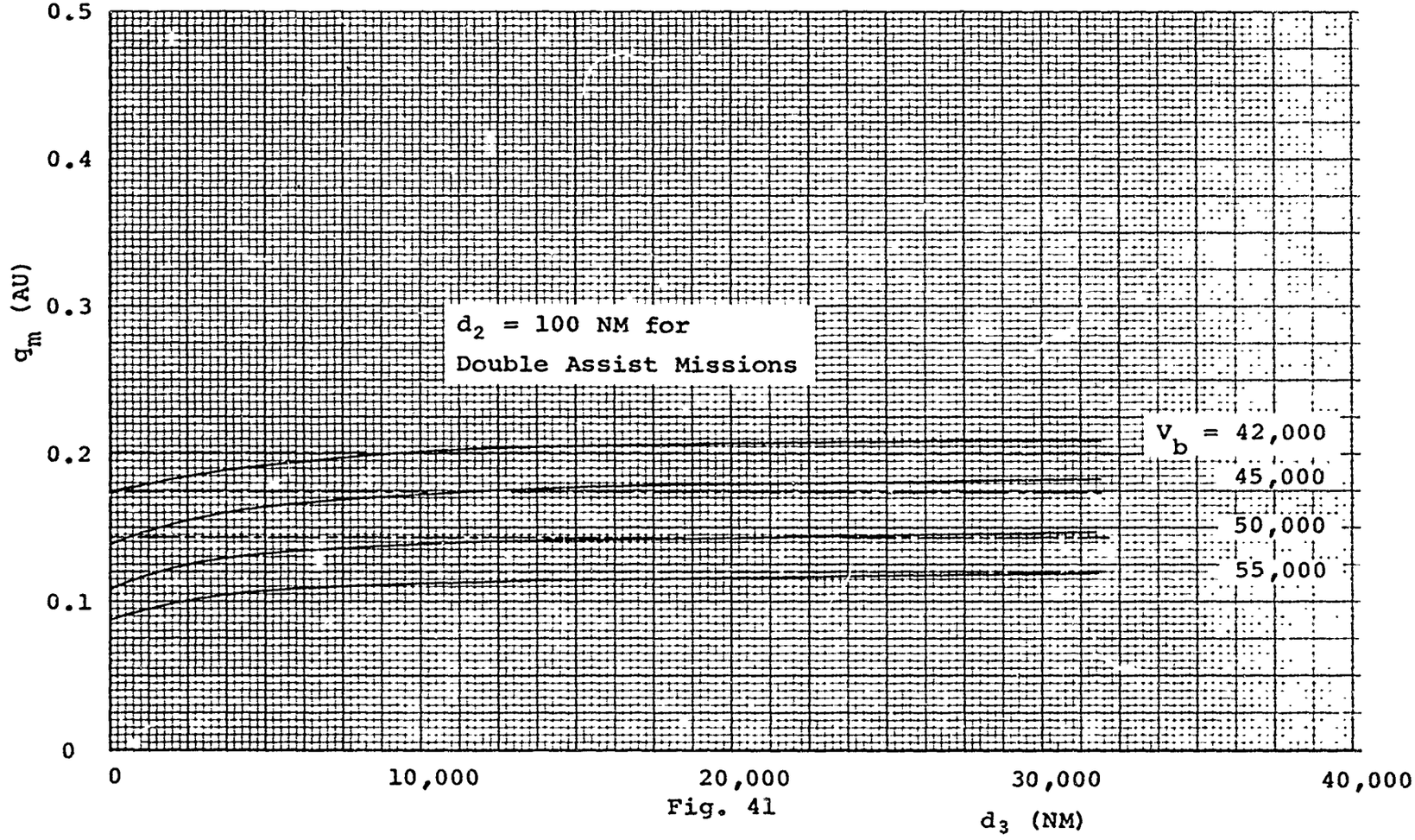

Fig. 41

Comparison of Triple-Assist and Double-Assist Missions

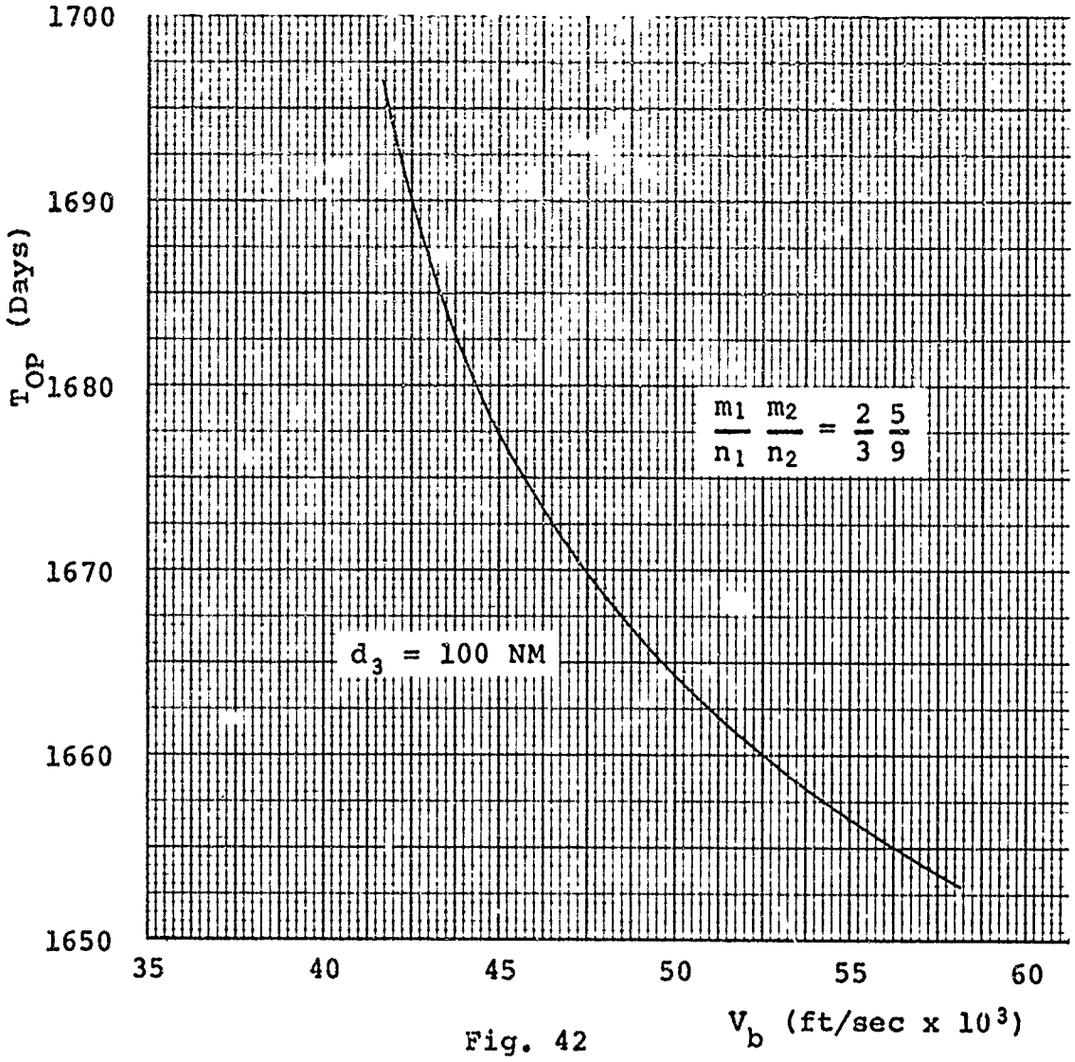

Fig. 42

Time Requirements for Triple-Assist Missions at Venus

VII. Three-Dimensional Gravity-Assisted Trajectories

Purpose and Scope

The method outlined in Chapter III for two-dimensional gravity-assisted trajectories was applied to specific missions in Chapters IV through VI. The purpose of this chapter is to outline an extension of that method for the case of three-dimensional gravity-assisted trajectories. This development will then be used in the out-of-ecliptic mission studies of Chapters VIII and IX.

Coordinate Systems

The coordinate systems (see Fig. 43) which are used in the three-dimensional analysis are as follows:

1. The $X_1Y_1Z_1$ coordinate system is a planetocentric system with its origin O_1 located at the center of mass of the departure planet P_1. The X_1 axis lies along $\bar{V}_{P_1}$ (the velocity of P_1 about the Sun), the Y_1 axis points toward the Sun, and the Z_1 axis forms a right-hand system.

2. XYZ is an ecliptic coordinate system with origin O at the Sun. The Z axis is directed towards the north-pole of the ecliptic; the X-Y plane lies in the ecliptic such that the Y axis points toward P_1 at launch, and the X axis forms a right-hand system.

3. The pre-assist orbit system, xyz, is an orbital reference system located at the Sun. This system defines the heliocentric longitude of the spacecraft between the

time of launch at P_1 and intercept at P_2. The z axis points to the north pole of the pre-assist orbit plane; the x-y plane lies in the pre-assist orbit plane so that the y axis lies along the Sun-spacecraft line, and x forms a right-hand system.

4. The X'Y'Z' coordinate system is another ecliptic system with its origin O' at the Sun. The X'-Y' plane lies in the ecliptic so that the X' axis points in the direction of a line drawn from P_2 to the Sun at intercept and the Y' axis lies opposite to the direction of $\bar{V}_{P_2}$. The Z' axis is perpendicular to the ecliptic and forms a right-hand system.

5. The axes of the $X_2Y_2Z_2$ coordinate system are parallel to the respective axes of the X'Y'Z' system, but the origin O_2 lies near P_2 at the point of intersection of the inbound and outbound asymptotes of the assist hyperbola. The system moves with P_2 about the Sun and the X_2-Y_2 plane lies parallel to the ecliptic (not necessarily in the ecliptic).

6. The origin of the $x_2y_2z_2$system is also located at O_2, but the x_2-y_2 plane lies in the plane of the assist orbit. The y_2 axis points opposite to the $\bar{V}_{\infty_i}$ vector, the x_2 axis lies in the direction of the x_2 component of $\bar{V}_{\infty_o}$, and the z_2 axis forms a right-hand system.

A General Approach to the Problem

The problem of three-dimensional gravity assist is best introduced with a discussion of the underlying motivations for the technique presented in the next section. The plan

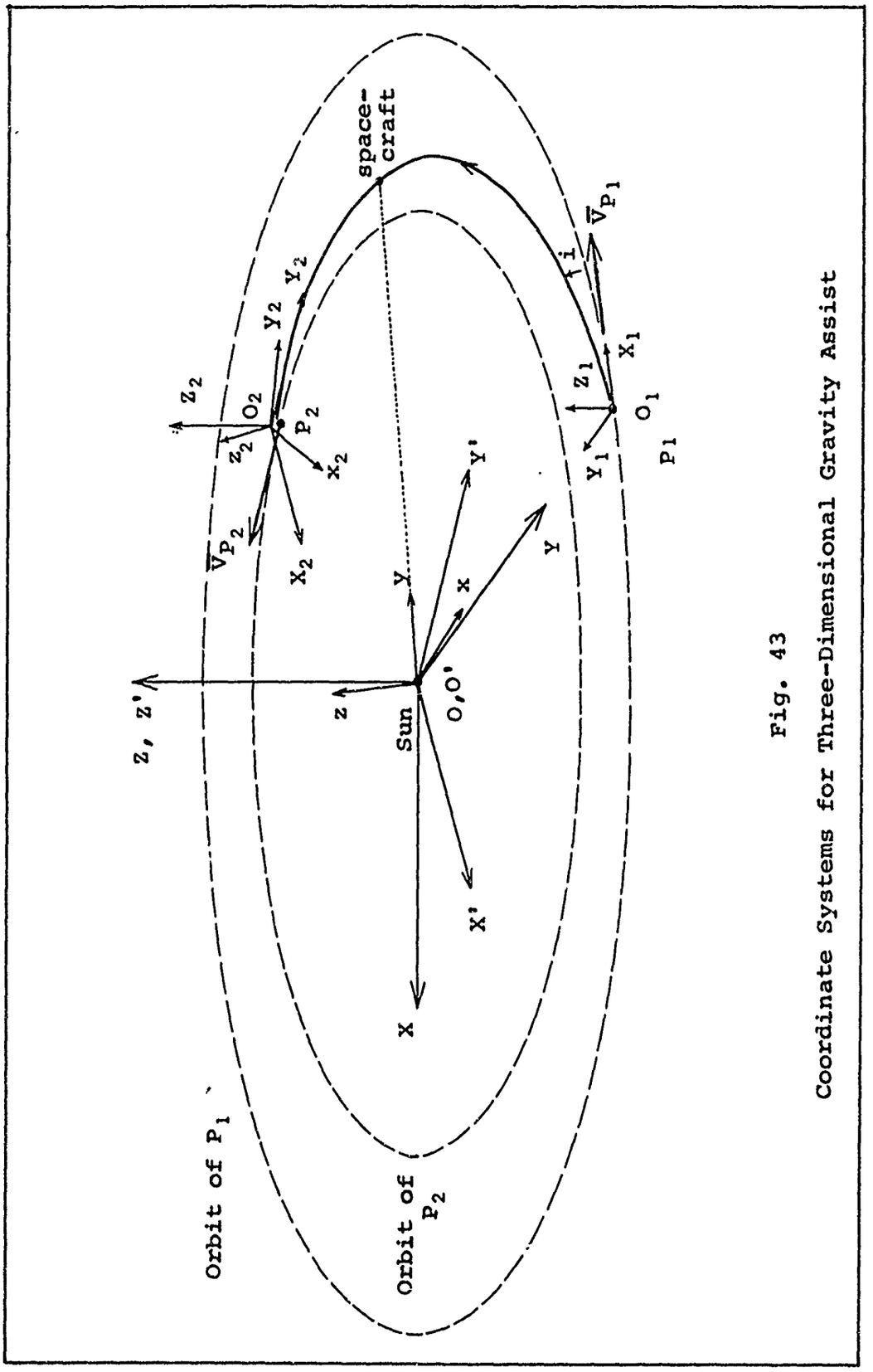

Fig. 43

Coordinate Systems for Three-Dimensional Gravity Assist

here is to construct two example problems, and to describe a method of attack for each.

For the first example (see Fig. 44), consider an assist orbit which lies in a plane perpendicular to the ecliptic, such that the spacecraft enters the SOI above the ecliptic (with $\overline{V}_{\infty_i}$ in a plane parallel to the ecliptic), passes P_2 along a north-south meridian, and exits the SOI below the ecliptic. Addition of $\overline{V}_{\infty_i}$ to the planet's velocity $\overline{V}_{P_2}$, as in Eq (3-1), gives $\overline{V}_1$, the required velocity of a pre-assist orbit at P_2.

From the corollary presented in Chapter III it is argued that the pre-assist orbit may be assumed to enter the SOI at any point. Thus, it is safe in this example to choose a pre-assist orbit which lies in the ecliptic. The assumption of circular and coplanar planetary orbits contradicts the possibility of this scheme; however, minor velocity corrections (which have little influence on the burnout conditions at P_1) serve to establish the slight pre-assist orbit inclination necessary to achieve the desired entry point.

For a more general example, consider the assist orbit in Fig. 45 which has a given DOCA and orientation within the SOI of P_2. The plane of the assist orbit may be related to the ecliptic by three Euler angle rotations (α, δ, β as described in Appendix B), from the $x_2y_2z_2$ orbit system to the $X_2Y_2Z_2$ planet system, where the origin of these systems is located at the intersection of the inbound and outbound

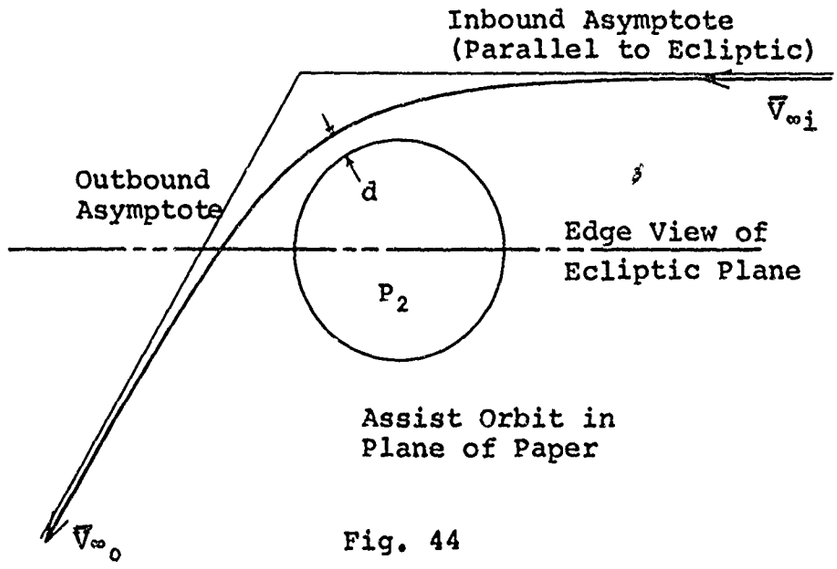

Fig. 44

Assist Orbit Example

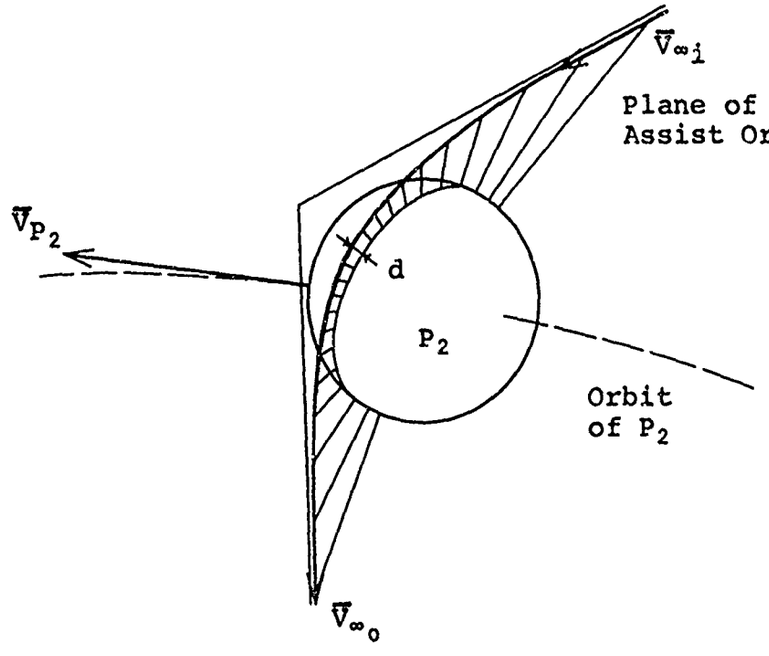

Fig. 45

General Assist Orbit

asymptotes of the assist hyperbola.

The assist orbit again defines $\bar{V}_{\infty_i}$, and addition of this vector to $\bar{V}_{P_2}$ gives $\bar{V}_1$ which determines the conditions of a pre-assist orbit at P_2. In general, this orbit is inclined at some angle i which can be determined from the components of $\bar{V}_1$ in the XYZ ecliptic system. If this inclination is small (a fraction of a degree as shown in the next section), the pre-assist orbit may be assumed to lie in the ecliptic like the previous example, but if it is not small then either a large midcourse correction (broken-plane transfer) or a 180° transfer (from P_1 to P_2) is necessary.

In a similar fashion, the given assist orbit defines $\bar{V}_{\infty_0}$ which is added to $\bar{V}_{P_2}$ for the post-assist velocity $\bar{V}_3$. Components of this vector give the post-assist orbit inclination i_3.

The inclination of planetary orbits serves only to enhance the feasibility of the above examples when the pre-assist orbit lies nearly in the ecliptic plane. A launch date may be selected such that the spacecraft enters the SOI at a time when P_2 is sufficiently below the ecliptic. However, the assumption of circular coplanar planetary orbits is retained, because it is desired to investigate the effects of gravity assist alone.

Three-Dimensional Gravity Assist Method

A three-dimensional gravity-assisted trajectory is broken into the same conic orbits which were defined in

Chapter III: departure orbit, pre-assist orbit, assist orbit, and post-assist orbit.

Departure Orbit. The departure orbit is defined, as before, with the selection of a burnout velocity V_b. The choice of a departure flight path angle ϕ_o and an inclination angle i for the pre-assist orbit determines $\bar{V}_o$, the heliocentric velocity at P_1. These quantities are illustrated in the $X_1Y_1Z_1$ system in Fig. 7.

Pre-Assist Orbit. A necessary condition for the pre-assist orbit is that it must intercept the SOI of P_2. This condition is satisfied for either of the following classifications:

1. Category I Trajectories - the pre-assist orbit for these trajectories lies in the ecliptic or slightly out of the ecliptic, as explained below.

2. Category II Trajectories - the pre-assist orbit for these trajectories lies out of the ecliptic and the heliocentric transfer angle θ_{12} is 180°.

For Category I trajectories the specified inclination angle must be small enough to allow the spacecraft to pass no further than a distance ρ_{P_2} above P_2, where ρ_{P_2} is the SOI radius. As shown in Chapter III, the SOI radius for Venus subtends a heliocentric angle of about 0.33°; this angle is also the maximum allowable inclination for a transfer of $\theta_{12} = 90°$. The maximum inclination increases as the transfer angle increases or decreases from 90°.

For Category II trajectories, when $\theta_{12} = 180°$, the required inclination angle must be computed for given values of V_b and ϕ_o. Details of this computation are found in Appendix C.

The velocity V_1 and flight path angle ϕ_1 at entry to the SOI of P_2 ($r = r_{P_2}$) are computed from the pre-assist orbit characteristics. In order to find the components of $\bar{V}_1$ in the $X_2Y_2Z_2$ system, a coordinate transformation is made from the xyz pre-assist orbit system to the XYZ ecliptic system, and from the XYZ to the X'Y'Z' ecliptic system. Finally, the components of $\bar{V}_1$ in the X'Y'Z' system are translated to the $X_2Y_2Z_2$ system.

Assist Orbit. The inbound HEV at P_2 is found by adding the components of $\bar{V}_1$ and $\bar{V}_{P_2}$ in the $X_2Y_2Z_2$ system with the usual relation

$$\bar{V}_{\infty_i} = \bar{V}_1 - \bar{V}_{P_2} \qquad (3\text{-}1)$$

The orientation of $\bar{V}_{\infty_I}$ with respect to P_2 is given by the right ascension α and declination δ shown in Fig. 46.

As mentioned in the previous section, three Euler angles must be used to relate the position of the $x_2y_2z_2$ system to the $X_2Y_2Z_2$ system. Two of these angles are found above (α and δ), but the third (β) must be specified and is used as an arbitrary parameter in the calculations. This procedure allows the computation of all possible assist orbits for a given pre-assist orbit, and subsequently determines the range of gravity-assist performance for any

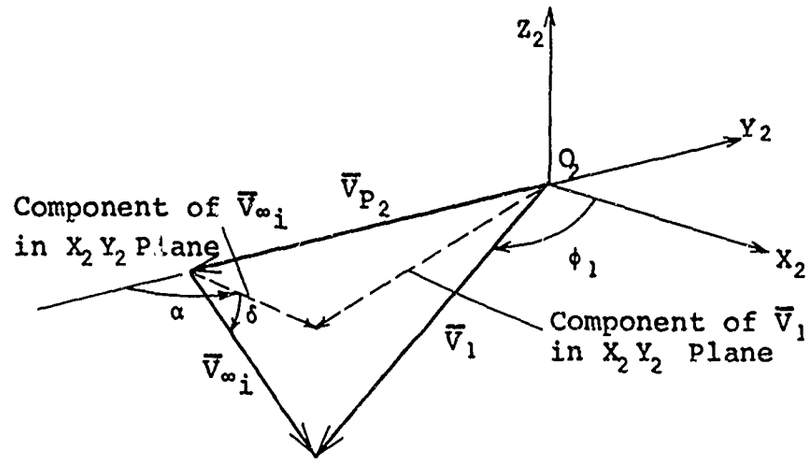

Fig. 46

Pre-Assist Velocity Vectors

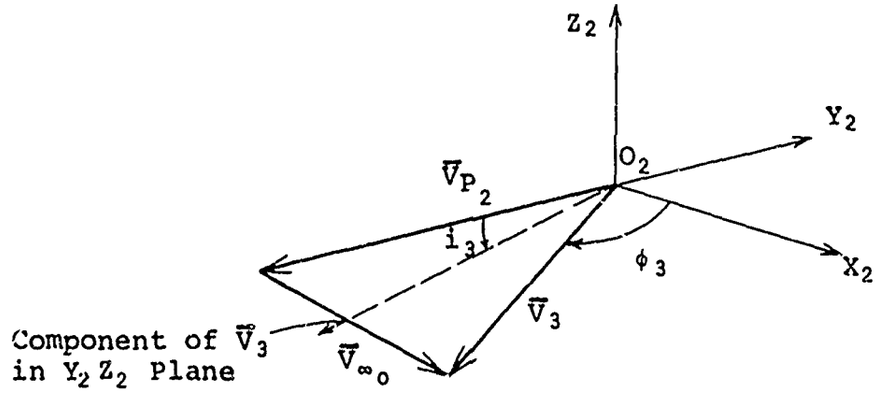

Fig. 47

Post-Assist Velocity Vectors

planet P_2.

The selection of a DOCA, as for the two-dimensional case, determines the turn angle 2ν which gives the direction of $\bar{V}_{\infty_0}$ in the $x_2y_2z_2$ system.

Post-Assist Orbit. The components of $\bar{V}_{\infty_0}$ are transformed from the $x_2y_2z_2$ to the $X_2Y_2Z_2$ system, and the heliocentric velocity of the spacecraft as it leaves the SOI is

$$\bar{V}_3 = \bar{V}_{P_2} + \bar{V}_{\infty_0} \qquad (3\text{-}2)$$

The components of $\bar{V}_3$ in the $X_2Y_2Z_2$ frame (see Fig. 47) are used to determine the flight path angle ϕ_3 and the inclination i_3 of the post-assist orbit with respect to the ecliptic.

Visualization of Three-Dimensional Gravity Assist

The velocity vector diagrams in Fig. 16 for two-dimensional trajectories extend logically to three-dimensional trajectories; the circular locus of outbound HEV vectors here becomes a spherical locus. A complete summary of the velocity vectors at P_2 is shown in Fig. 70 of Appendix B. As in Fig. 16 the diagram may be broken into two frames of reference: one with respect to the Sun (Fig. 43) and one with respect to P_2 (Fig. 45).

VIII. Out-of-Ecliptic Assist at Venus

In this chapter the three-dimensional method is applied to Venus-assisted solar probe trajectories. The purpose here is to investigate the effectiveness of a Venus assist for both a reduction in perihelion and an increase in the inclination angle. The trajectories are divided into the two classifications defined in Chapter VII: Category I trajectories and Category II trajectories.

Category I Trajectories

As mentioned in the previous chapter, the pre-assist orbit for Category I trajectories may lie no more than 0.33° out of the ecliptic for $\theta_{12} = 90°$. As θ_{12} increases or decreases from 90° (but does not approach 180°) the maximum allowable inclination increases by less than about 0.2°.

It was found in the investigation that a 0.1° change in pre-assist orbit inclination produces less than a 0.1% change in the characteristics of the post-assist orbit. Therefore, only the results for zero inclination angle are included, since they are sufficiently representative of all trajectories in this category.

Also, the results for non-tangential departure are not reported, since time requirements are of less concern here than burnout velocity requirements.

Computer Program. The program for Category I trajectories (see Fig. 48) includes a parametric variation of five quantities in the order listed: burnout velocity V_b, flight

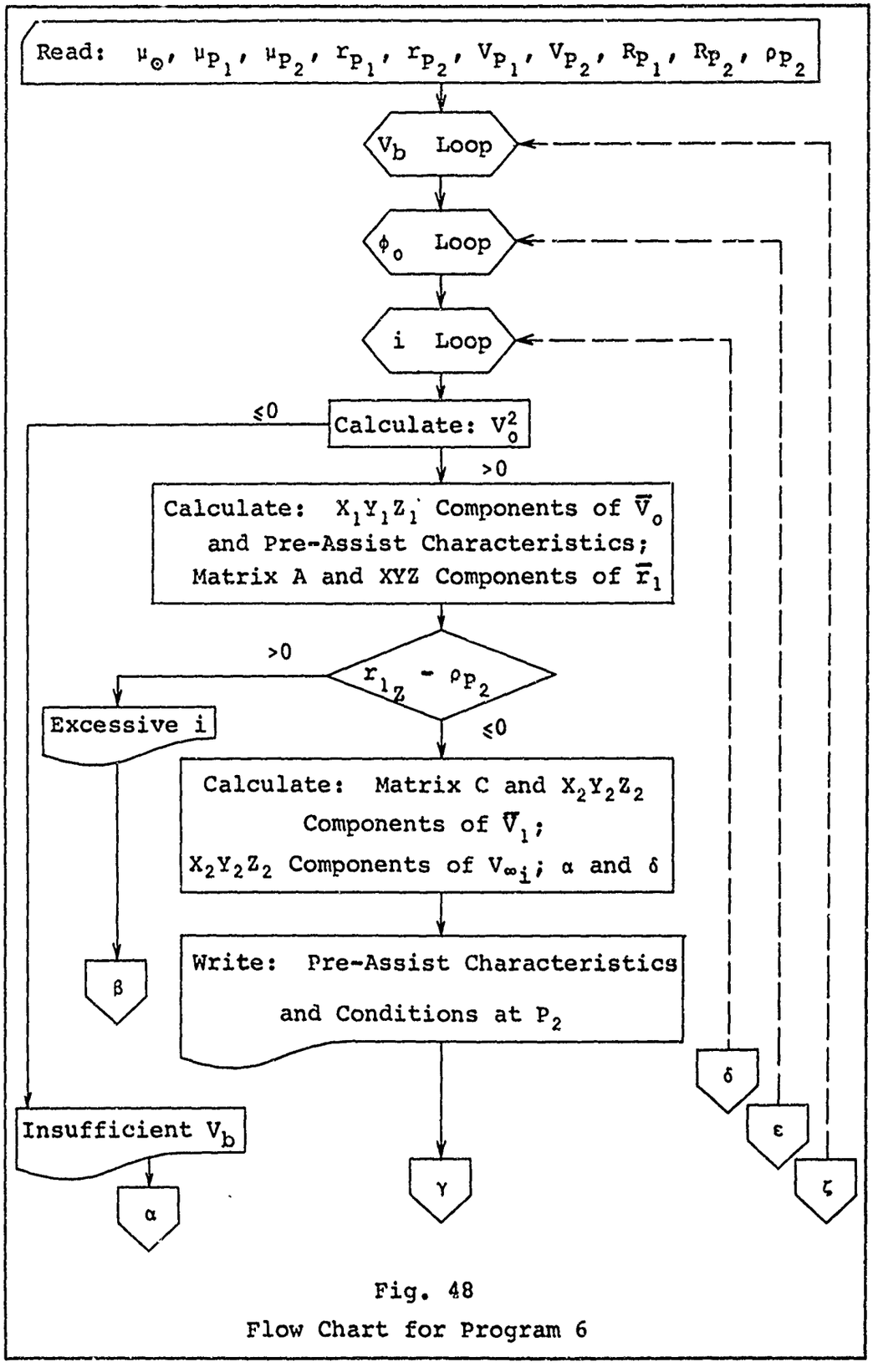

Fig. 48
Flow Chart for Program 6

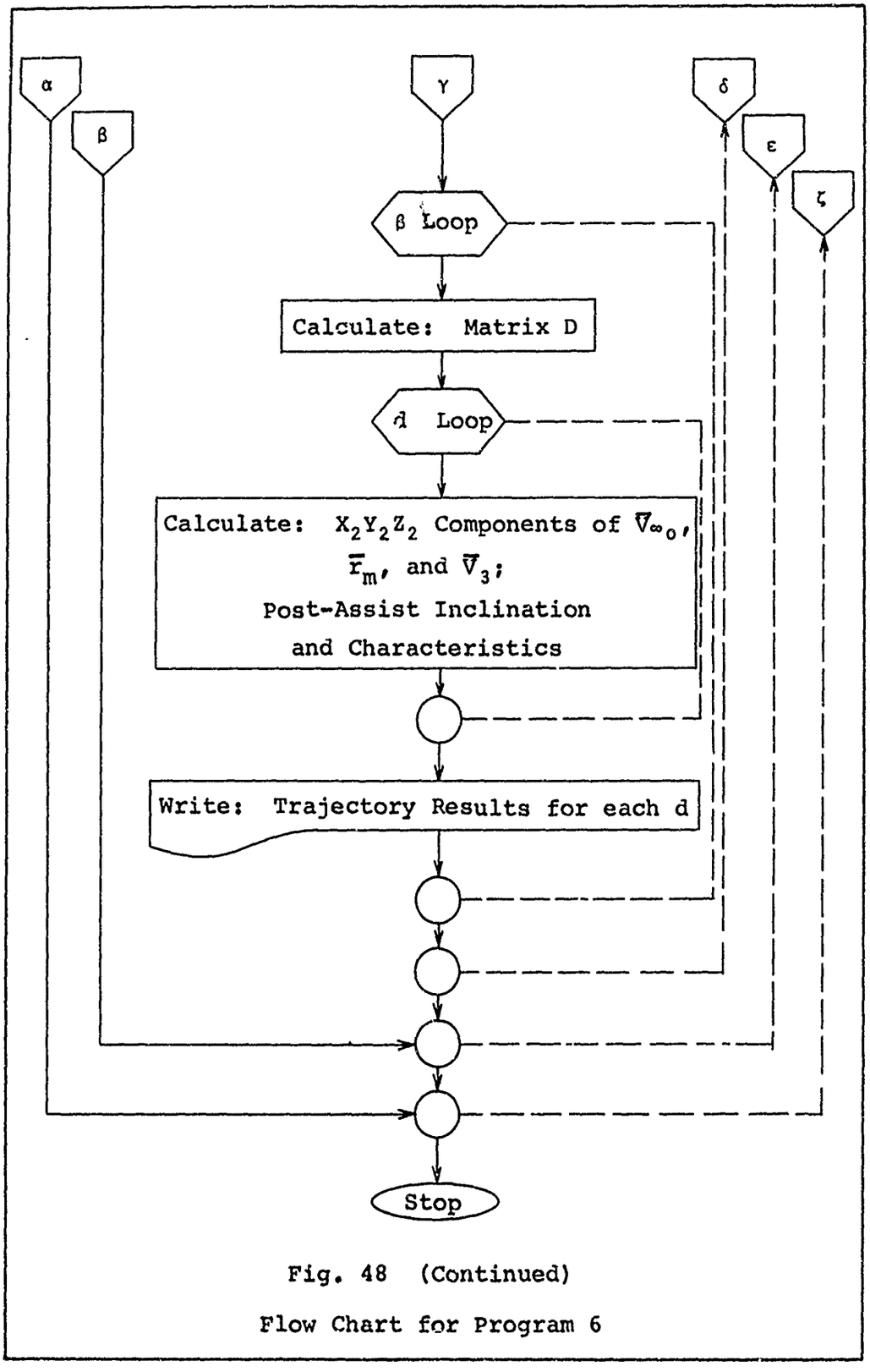

Fig. 48 (Continued)

Flow Chart for Program 6

path angle ϕ_o, pre-assist orbit inclination i, assist orbit orientation angle β, and DOCA d.

The pre-assist orbit is calculated by the same techniques used in Program 1 for out-of-ecliptic direct-transfer trajectories. If $r_{1_Z} > \rho_{P_2}$ (Eq B-5) at the assist planet, then the pre-assist inclination is too large for an intercept and a new value of ϕ_o is selected.

The transformation matrix C, denoted by E in Program 6, is used to find the components of $\bar{V}_1$ in the $X_2Y_2Z_2$ reference system. The right ascension α and declination δ are calculated, and a value is selected for the angle β. These angles determine the transformation matrix D, denoted by F in the program, which is used with a selected DOCA to find components of $\bar{V}_{\infty_o}$ and $\bar{r}_m$ in the $X_2Y_2Z_2$ system. Finally, the components of $\bar{V}_3$ give i_3 and the post-assist orbit characteristics.

Notation on the printed output is as follows:

VOX,VOY,VOZ ∿ Components of $\bar{V}_o$ in $X_1Y_1Z_1$ system

V1X,V1Y,V1Z ∿ Components of $\bar{V}_1$ in $X_2Y_2Z_2$ system

R1XP,R1YP,R1ZP ∿ Components of $\bar{r}_1$ in XYZ system

V3X,V3Y,V3Z ∿ Components of $\bar{V}_3$ in $X_2Y_2Z_2$ system

DX,DY,DZ ∿ Components of $\bar{r}_m$ in $X_2Y_2Z_2$ system in units of P_2 radii

I3 ∿ Inclination of Post-Assist Orbit

A2 ∿ Semi-Major axis of Assist Orbit in P_2 Radii

V1NFXY ∿ $V_{\infty i_{X_2Y_2}}$ ALP ∿ δ

PSI ∿ α BETA ∿ β

Mission Profile. The mission profile in Fig. 49 is designed for an Atlas/Agena launch vehicle and a 200-lb payload with a burnout velocity of 40,000 ft/sec.

It is assumed that the guidance and navigation requirements for missions out of the ecliptic are the same as those for missions in the ecliptic, so that no additional payload is required for a three-dimensional assist.

The assist at Venus has tilted the heliocentric orbit of the spacecraft to an inclination of 10.6°, and has increased the perihelion from 0.540 AU for the pre-assist orbit to 0.552 AU for the post-assist orbit.

Conclusions. The graph in Fig. 12 indicates that a perihelion of 0.552 AU and an inclination angle of 10.6° for a direct-transfer orbit requires a burnout velocity of a little more than 43,000 ft/sec. An Atlas/Agena ($7.9 million) was used in the mission profile above, but an Atlas/Centaur ($11.9 million) with a small kick stage is required for the direct-transfer. Thus, a few million dollars can be saved by using a Venus assist rather than a direct transfer for this mission.

Fig. 50 is a plot of post-assist orbit inclination angle i_3 and perihelion q_m for various values of burnout velocity V_b (solid lines) and orientation angle β (dashed lines). These curves are plotted directly from computer output for a DOCA of 100 NM. The dotted line on the right-hand side of the graph is a locus of maximum i_3 for any V_b.

Trajectory Data

Launch Date: 22 Jan 1969 (JD 2440243.8)
Launch Vehicle: Atlas/Agena
Payload = 200 lb
V_b = 40,000 ft/sec
$\phi_o = 90°$, $i = 0°$
T_{12} = 81.1 days
T_{OP} = 128.4 days
d = 100 NM
q_m = 0.552 AU
$i_3 = 10.6°$

$\alpha = 92.9°$
$\delta = 0°$
$\beta = 80°$

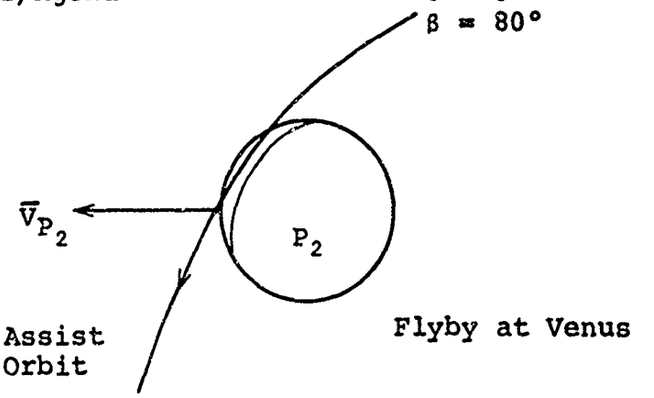

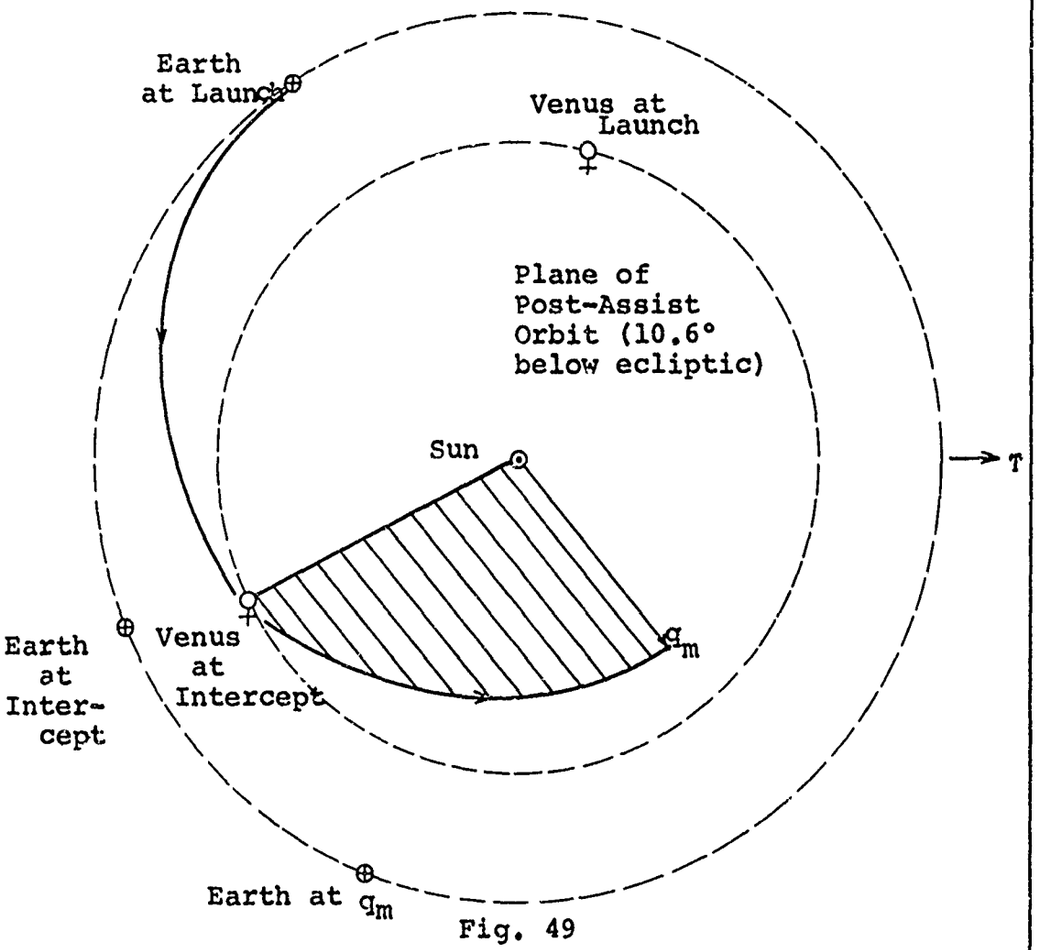

Fig. 49

Mission Profile for Venus-Assisted Category I Trajectory

This line indicates that the highest inclination angles are achieved with either low or high burnout velocities (approximately 40,000 or 70,000 ft/sec respectively). It can be concluded from this graph that a Venus assist produces, at best, an inclination of about 10°.

Fig. 50 also indicates that a large gain in i_3 reflects a substantial increase in perihelion. For instance, at V_b = 40,000 ft/sec, perihelion increases slightly from 0.337 AU to 0.357 AU for a change in i_3 from 0° to 5°, respectively; however, the perihelion increases rapidly to 0.550 AU for i_3 = 10.55°.

A plot of maximum inclination angle versus burnout velocity is given in Fig. 51 for various DOCA values. These curves are obtained from a plot of β versus i_3 for each value of V_b and d; the maximum value of i_3 is then transferred to Fig. 51 and a locus is obtained for each value of d. The double maximum observed in Fig. 50 is again evident in Fig. 51 for each value of d.

The perihelion for maximum-inclination missions and ecliptic direct-transfer missions (dashed line) is compared in Fig. 52. From these curves it is found that perihelion may be significantly reduced for the lower range of V_b. For instance, at V_b = 41,000 ft/sec and d = 100 NM, perihelion is reduced from 0.71 AU for direct transfer (10° inclination) to 0.50 AU (10.45° inclination) for Venus assist.

Figs. 51 and 52 also indicate that variations in DOCA below 1000 NM do not strongly affect the post-assist orbit.

A change in d from 0 to 100 NM decreases the inclination by about 2° and increases the perihelion by less than 0.01 AU.

A comparison of Fig. 53 with Fig. 21 indicates that the mission time for Category I trajectories is about the same as for single Venus-assist missions in the ecliptic.

In summary, Venus-assisted Category I trajectories are useful for 10° out-of-ecliptic solar probe missions with perihelia of about 0.3 AU. The best gains for these trajectories (decrease in perihelion and increase in inclination) are realized for the lower range of burnout velocities around 40,000 ft/sec.

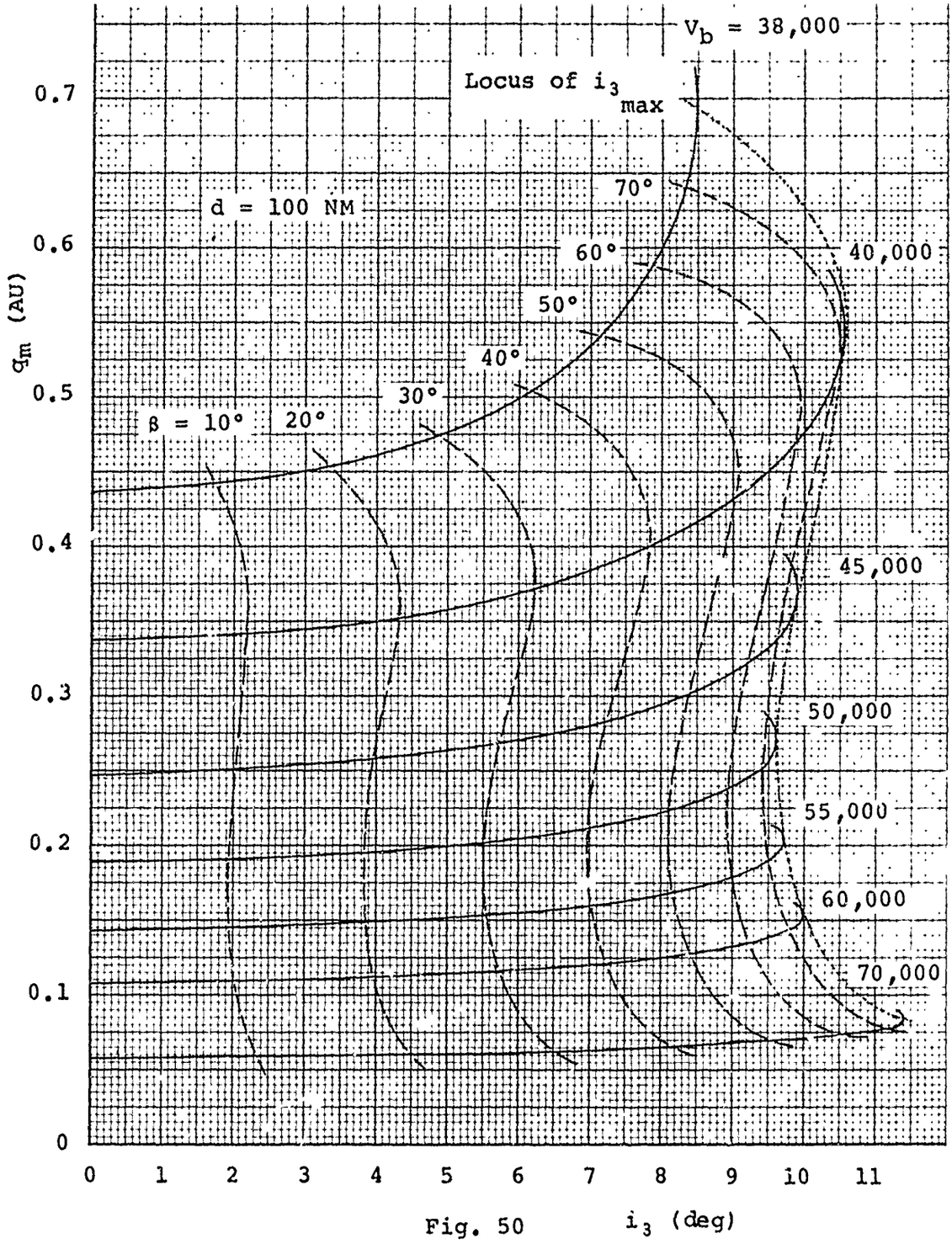

Fig. 50 Perihelion vs. Inclination for Venus-Assisted Category I Trajectories

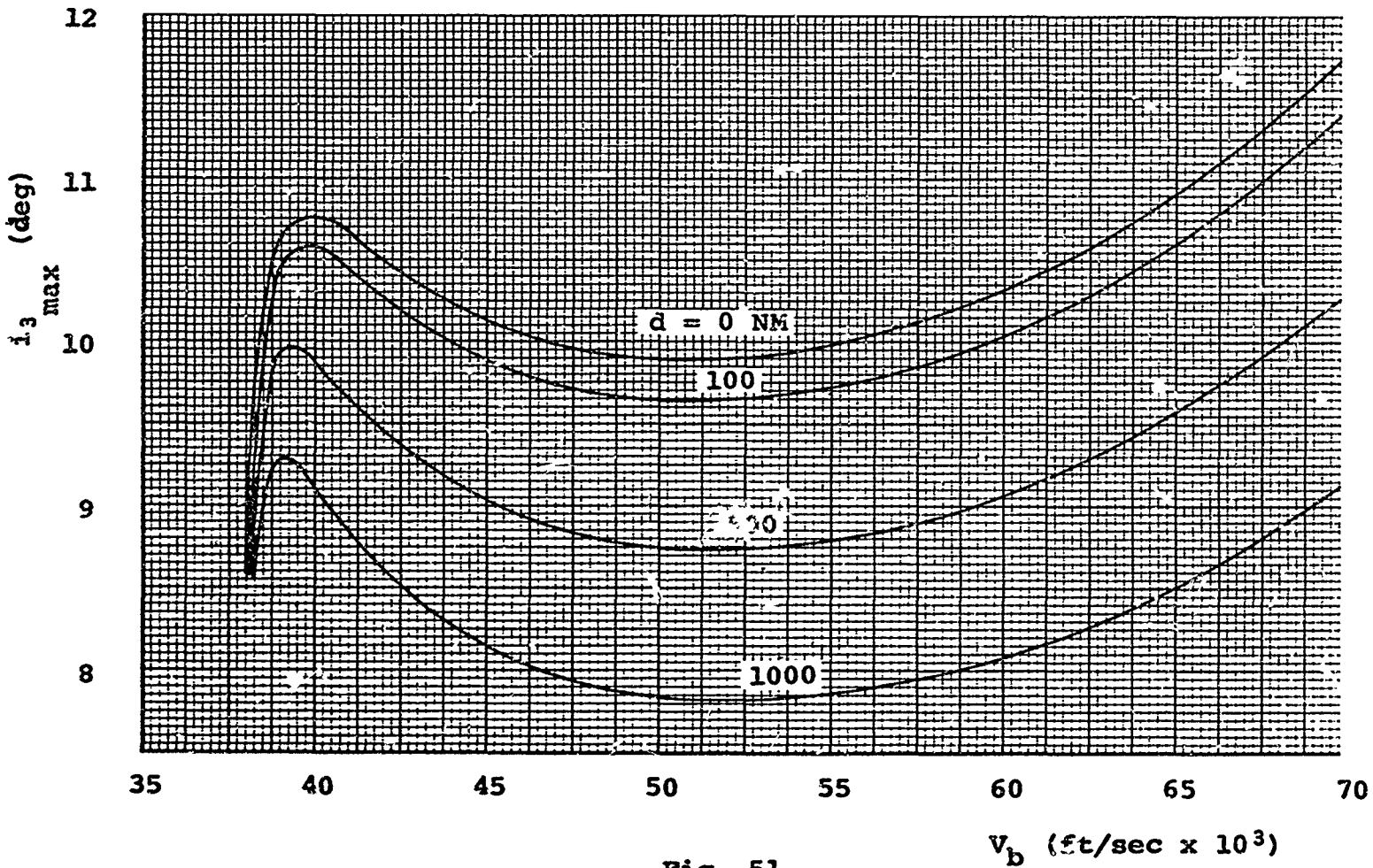

Fig. 51

Maximum Post-Assist Orbit Inclination as a Function of Burnout Velocity

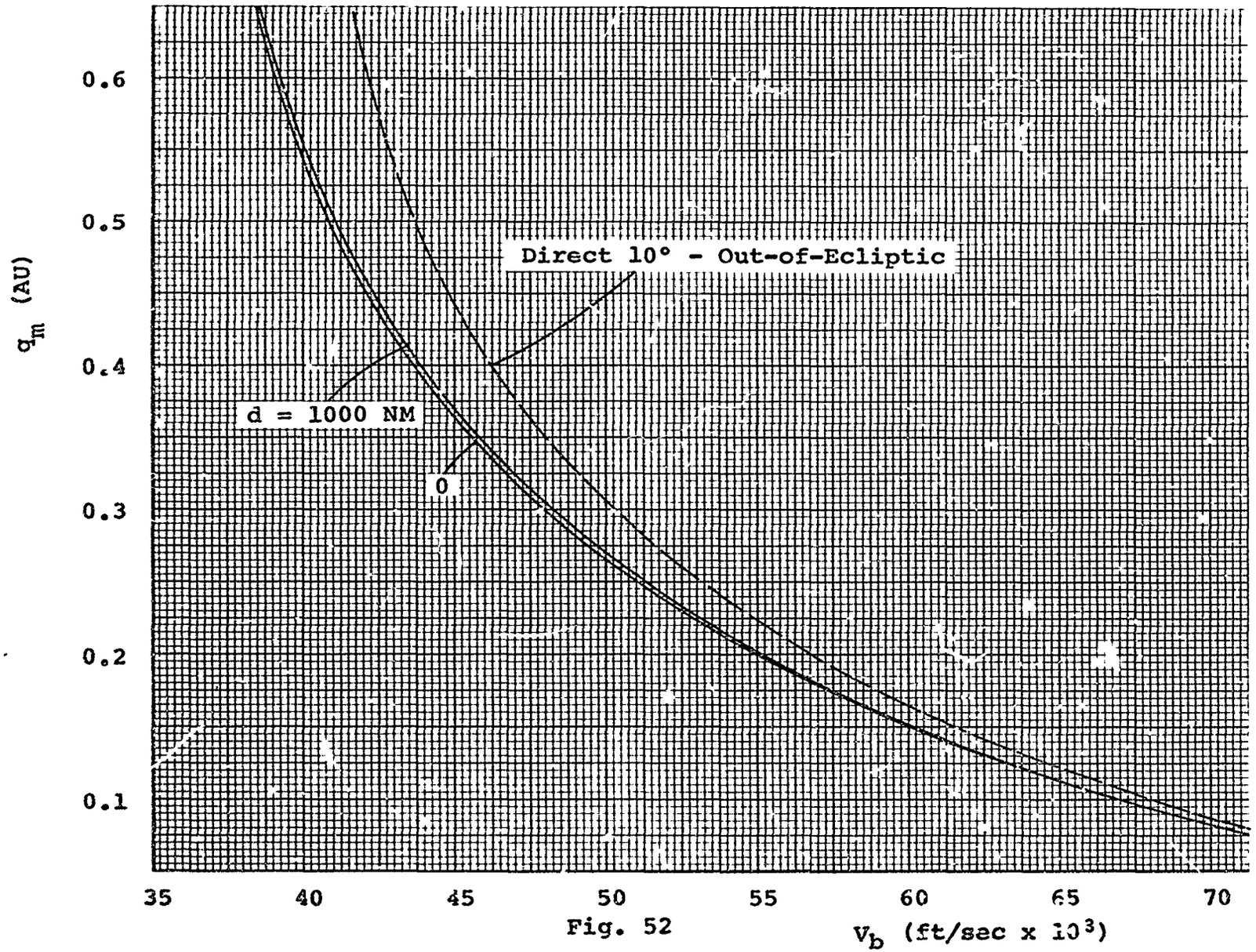

Fig. 52

Perihelion for Maximum i_3 as a Function of Burnout Velocity

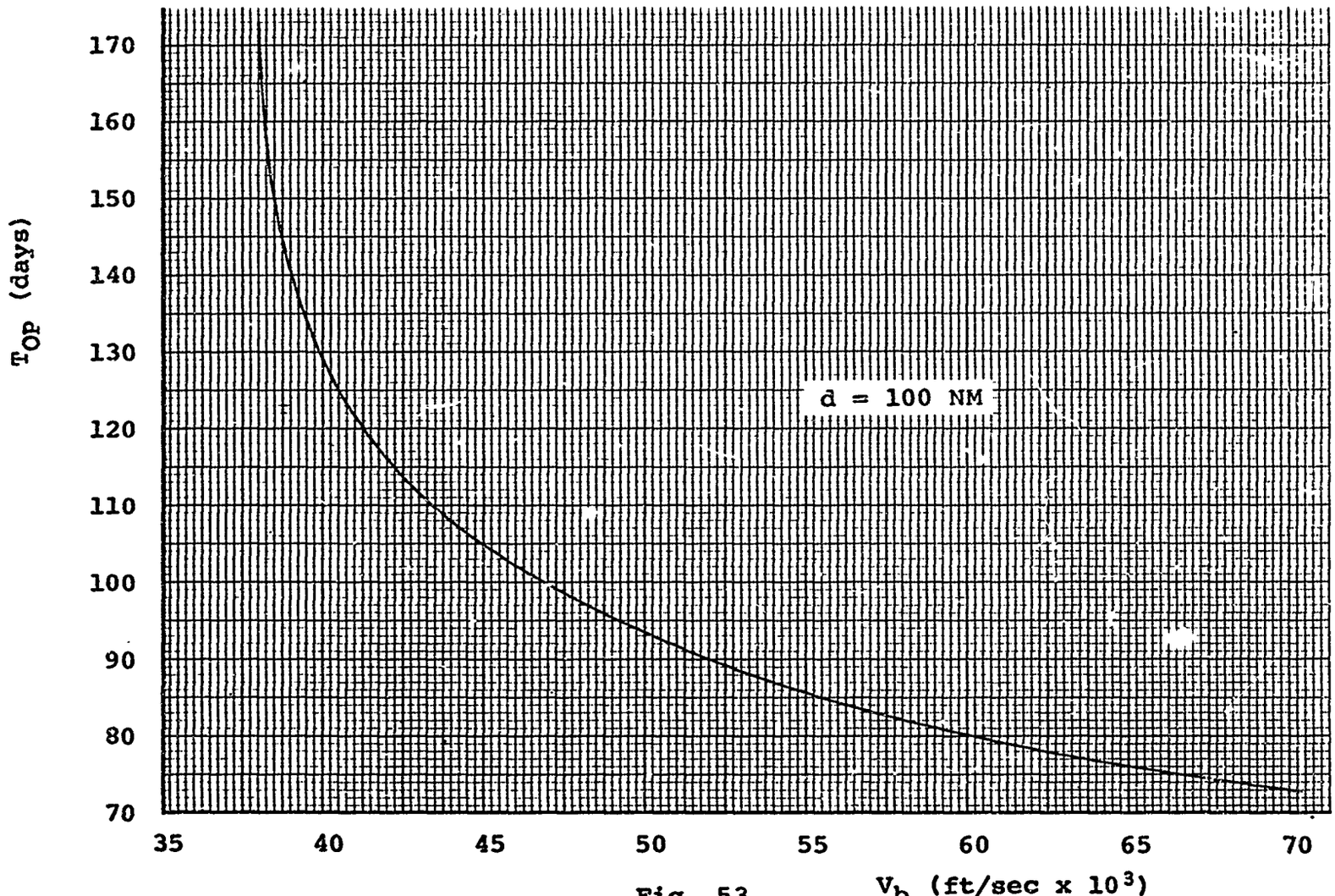

Fig. 53
Mission Time for Maximum Inclination Post-Assist Orbit

Category II Trajectories

The analysis for Category II trajectories is identical to that used for Category I trajectories, except that the pre-assist orbit inclination must now be computed, rather than specified, for the given values of burnout velocity V_b and departure flight path angle ϕ_o. This inclination angle is plotted in Fig. 54 as a function of V_b for a tangential departure; derivation of the equation for this curve is given in Appendix C.

As defined in the previous chapter, the heliocentric transfer angle θ_{12} for these missions is 180°. For a given value of ϕ_o, the pre-assist orbit inclination increases with V_b; therefore, any additional burnout velocity above the minimum V_b for a Venus intercept (Hohmann transfer which requires 37,700 ft/sec) is used to tilt the pre-assist orbit out of the ecliptic.

Computer Program. The program for Category II trajectories (Program 7 in Appendix E) is identical to Program 6, except that the pre-assist orbit inclination is calculated for each value of V_b and ϕ_o. A flow chart for this program can be obtained by replacing the i loop in Fig. 48 with a box for the calculation of i. The same transformations are made and the same notation is used for both programs.

Mission Profile. The Atlas/Centaur/TE-364-3 launch vehicle is used for the mission profile in Fig. 55. From Fig. 4 the burnout velocity for this vehicle for a 250-lb payload is 53,000 ft/sec. This velocity provides a pre-

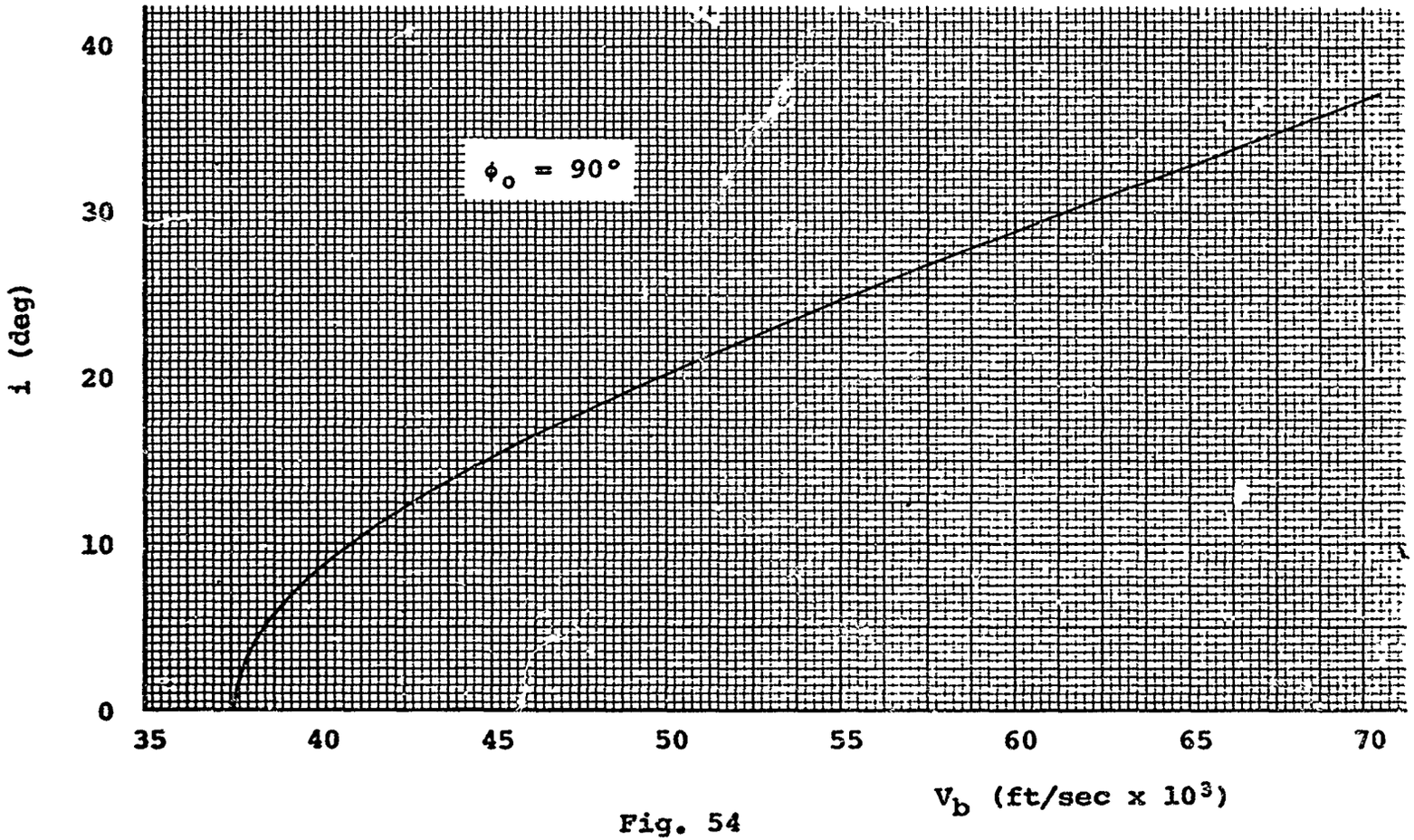

Fig. 54

Pre-Assist Inclination for Venus-Assisted Category II Trajectories

Trajectory Data

Launch Date: 16 Aug 1970 (JD 2440814.8)
Launch Vehicle: Atlas/Centaur/TE-364-3
Payload = 250 lb
V_b = 53,000 ft/sec
ϕ_o = 90°, i = 23.0°
T_{12} = 146 days
T_{OP} = 236 days
d = 100 NM
q_m = 0.529 AU
i_3 = 24.9°

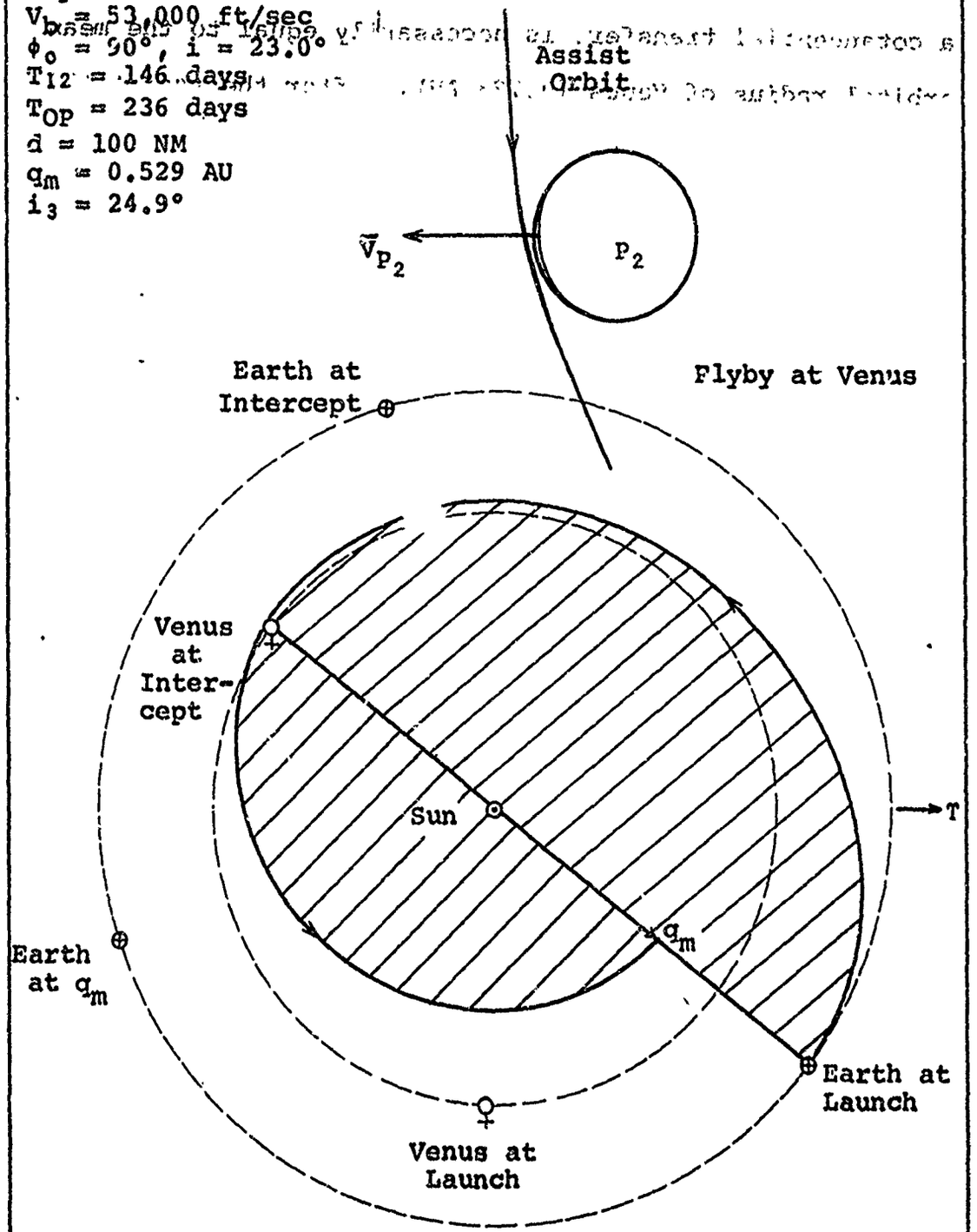

Fig. 55

Mission Profile for Venus-Assisted

assist orbit inclination of 23.0°, and the assist at Venus increases this inclination to 24.9°.

The perihelion of the pre-assist orbit, since this is a cotangential transfer, is necessarily equal to the mean orbital radius of Venus (0.723 AU). After the assist this perihelion is reduced to 0.529 AU.

Conclusions. In the mission profile above, it was found that a perihelion of 0.529 AU and an inclination of 24.9° can be achieved with an Atlas/Centaur/TE-364-3 ($16 million) by using a Venus assist. Fig. 12 indicates that a burnout velocity of 55,700 ft/sec is necessary to attain the same perihelion and inclination with a direct transfer; thus, a Saturn I ($29.8 million) is required for this mission.

Fig. 56, similar to Fig. 50, is a plot of perihelion versus post-assist orbit inclination for various values of burnout velocity V_b (solid lines) and orientation angle β (dashed lines). The heavy line which divides the right and left sides of the plot represents a V_b of 51,322 ft/sec. This particular burnout velocity and its associated pre-assist inclination combine to give

$$V_{1_{Y_2}} = V_{P_2} \qquad (8\text{-}1)$$

That is, the component of V_1 in the direction of motion of Venus is equal to the velocity of Venus about the Sun.

Burnout velocities to the left of the heavy line give $V_{1_{Y_2}} > V_{P_2}$, so that for $\phi_o = 90°$ the right ascension α of

the inbound HEV vector is 0°; that is, the spacecraft enters the SOI behind the planet and exits the SOI in front of the planet. Likewise, the right half of the plot is for burnout velocities which give $V_{1_{Y_2}} < V_{P_2}$, and $\alpha = 180°$ so that the spacecraft enters the SOI in front of P_2 and exits to the rear.

Thus, the angle α switches from 0° to 180° along the dividing line. This transition must be accompanied by a change in sign of the orientation angle β, so that aphelion, rather than perihelion, is achieved at P_2.

Fig. 56 indicates that the minimum perihelion and maximum inclination angle for a given V_b occurs for $\beta = +90°$ on the left side of the plot and $\beta = -90°$ on the right side. Thus, $\beta = \pm 90°$ represents the most desirable Category II trajectories, and further results of these missions are presented in Figs. 57 and 58.

Fig. 57 is a plot of post-assist orbit inclination i_3 as a function of V_b for various values of DOCA. A plot of pre-assist orbit inclination (dashed line) from Fig. 54 is superimposed on the graph so that i_3 may be compared with inclination before the assist. It is found that gravity assist does not significantly increase the inclination for Category II trajectories. The greatest increase, for the higher range of V_b, is only about 3 to 4 degrees.

The perihelion for Category II trajectories is shown in Fig. 58 as a function of V_b. Significant reductions in

perihelia (below the 0.723 AU perihelion of pre-assist orbits) can be obtained in these missions. The smallest perihelion is 0.439 AU at a burnout velocity of 41,500 ft/sec.

Mission times, shown in Fig. 59, are slightly longer for the Category II trajectories than for direct-transfer trajectories, but are well within reason for solar probe missions.

In conclusion, Venus-assisted Category II trajectories are useful for 20°- to 30°-out-of-ecliptic missions with perihelia of about 0.45 to 0.55 AU. A Venus assist offers little improvement in pre-assist inclination, but serves to reduce the perihelion by as much as 0.28 AU.

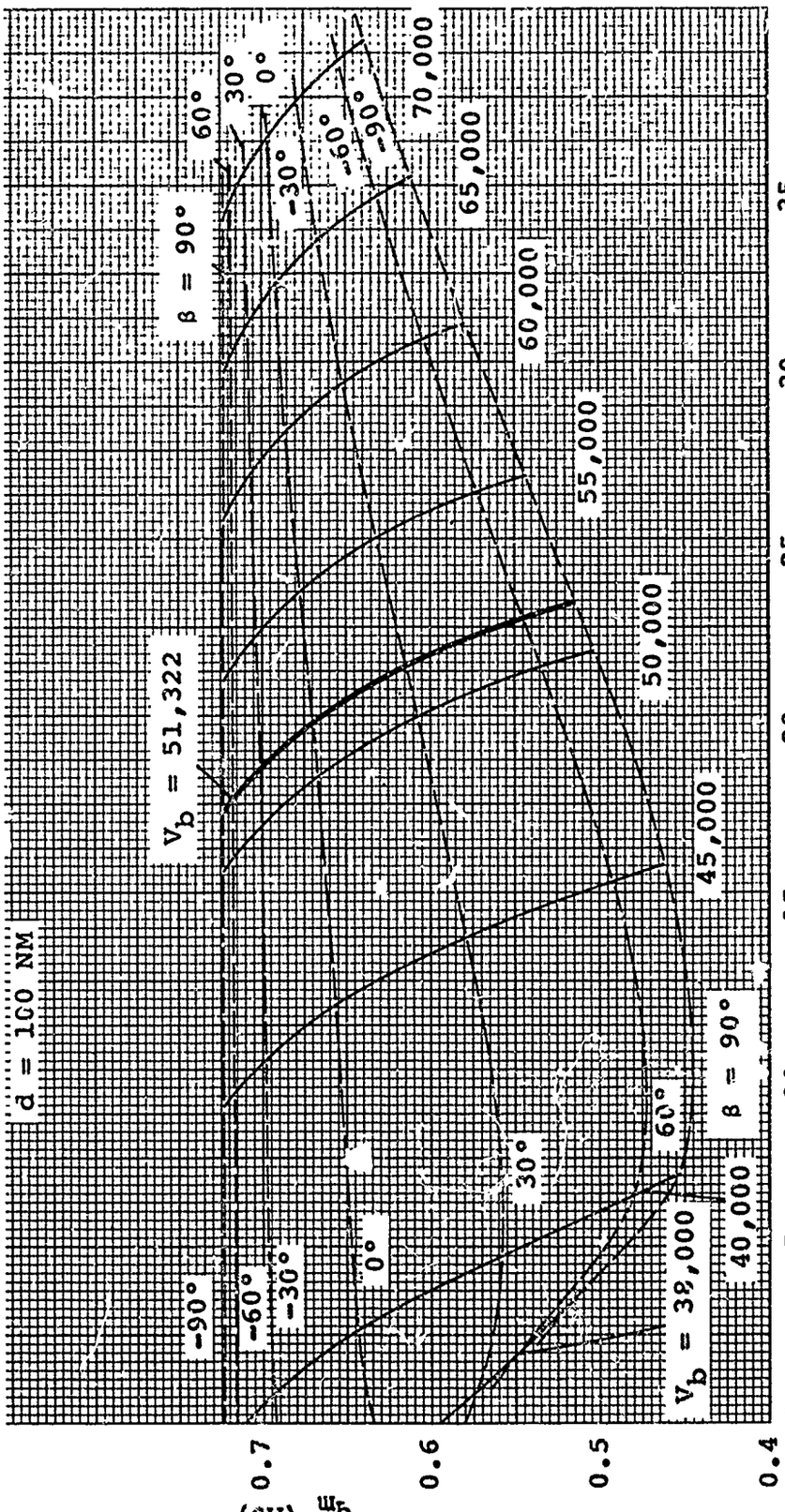

Fig. 56 Perihelion vs. Post-Assist Inclination for Venus-Assisted Category II Trajectories

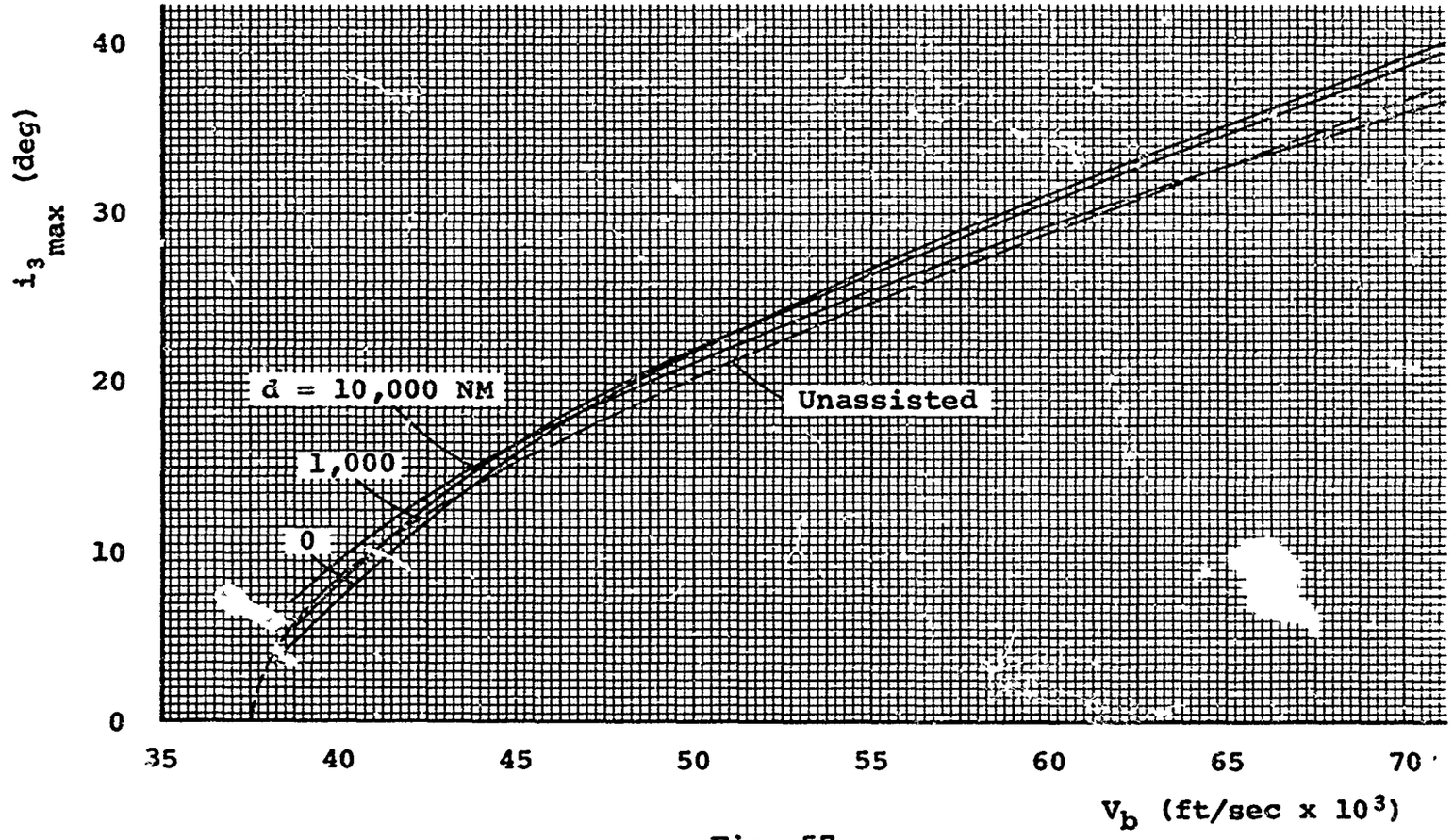

Fig. 57

Maximum Post-Assist Orbit Inclination vs. Burnout Velocity

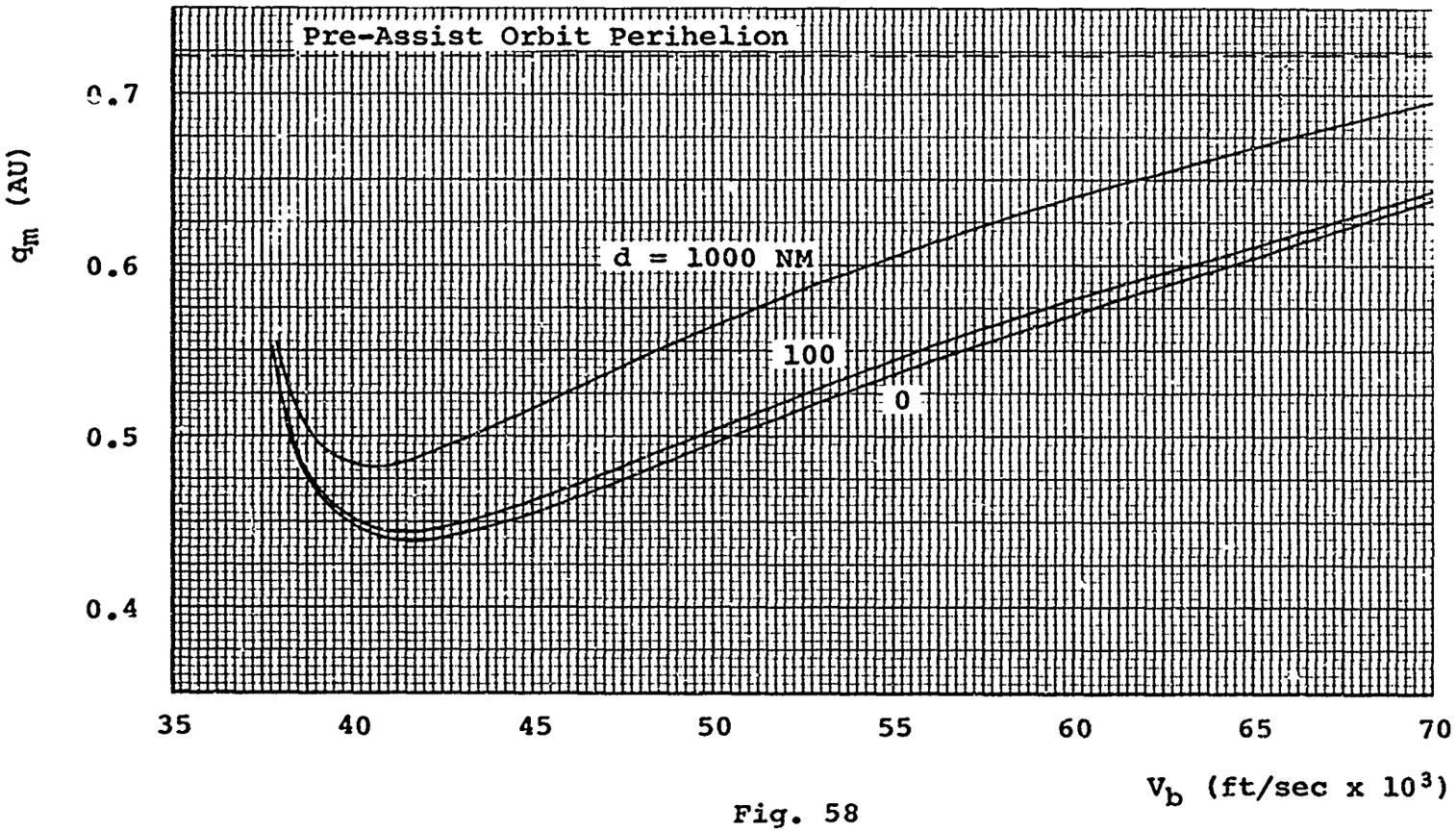

Fig. 58

Perihelion for Maximum Inclination Missions vs. Burnout Velocity

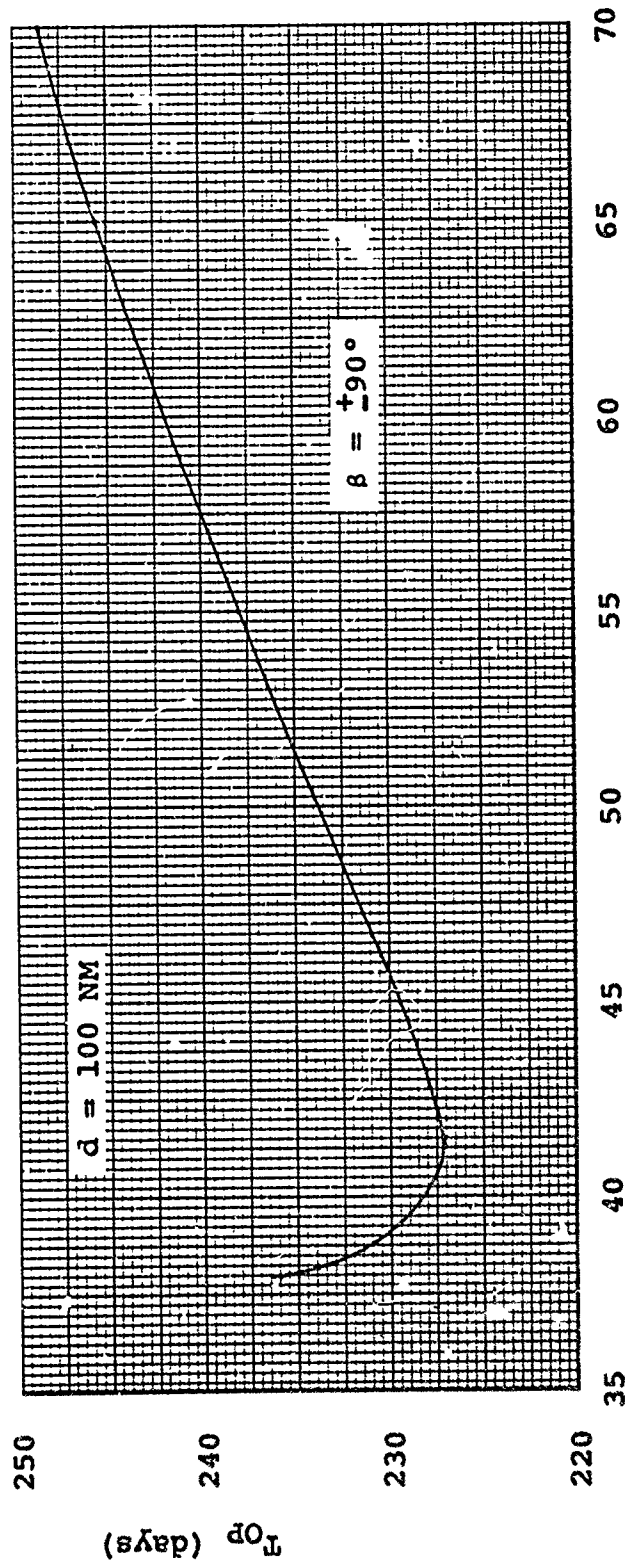

Fig. 59 Mission Time for Category II Trajectories

IX. Jupiter-Assist Missions

As stated in the introduction, Jupiter-assisted trajectories have been thoroughly investigated in the literature. However, a brief study of these missions is conducted here so that the results may be directly compared with other missions in the thesis.

Only Category I trajectories are used for Jupiter missions because of the high launch energy required for an out-of-ecliptic pre-assist orbit.

Computer Programming

The program for Jupiter-assisted missions is identical to Program 6, except that a few modifications are necessary to account for the fact that the pre-assist orbit lies outside, rather than inside, the Earth's orbit. The first of these modifications is a sign change in Eq (2-4) for the heliocentric departure velocity V_0.

Eq (2-18), for the true anomaly at Earth launch, must be modified to read as follows:

$$\begin{aligned} f_0 &= \arctan(\tan f_0), \quad \text{if } \tan f_0 > 0 \\ f_0 &= \arctan(\tan f_0) + \pi, \quad \text{if } \tan f_0 < 0 \end{aligned} \tag{10-1}$$

A similar change is required for f_1, the true anomaly at P_2.

Many of the post-assist orbits for Jupiter-assist missions are hyperbolic (solar system escape with Jupiter assist is investigated in Refs 11 and 13). These trajectories are avoided as follows: if the quantity $r_{p_2} V_3^2 / \mu_\odot$ is less than

2 (Ref 21:72), the post-assist orbit is elliptic, and the trajectory results are printed; otherwise, the traje tory is hyperbolic, and another set of parameters is selected.

Conclusions

Fig. 60 is a plot of perihelion versus burnout velocity for a Jupiter assist in the ecliptic ($i_3 = \beta = 0°$). Solar impact can be achieved with burnout velocities between 51,000 and 53,000 ft/sec for a DOCA of 500,000 NM (13 Jupiter radii). Smaller DOCA values can be used to provide retrograde post-assist orbits with small perihelia.

Out-of-ecliptic performance of Jupiter-assist missions is shown in Fig. 61, where perihelion q_m and post-assist inclination i_3 are plotted (with DOCA = 500,000 NM) for various values of orientation angle β (dashed lines) and burnout velocity V_b (solid lines). From this graph it is found that 90°-out-of-ecliptic orbits with perihelia less than 0.1 AU can be achieved with burnout velocities above 52,000 ft/sec. The best solar probe missions are attained when β is about 10°.

A summary of results for 90°-out-of-ecliptic missions is given in Table III. These missions are obtained from a plot of i_3 versus DOCA for each burnout velocity at $\beta = 10°$. The DOCA for $i_3 = 90°$ on this plot (second column in Table III) is used to interpolate the data on the computer printout for q_m and T_{OP}.

The values of T_{OP} and V_b in Table III are plotted on

the graph in Fig. 62. Also included on the graph is a plot of mission time for trajectories in the ecliptic with a DOCA of 500,000 NM. Little difference is found between the time requirements for Jupiter-assist missions in or out of the ecliptic plane.

In summary, it should be noted that Jupiter-assisted trajectories can be achieved with present-day launch vehicles. An Atlas/Centaur/TE-364-3 is capable of providing a burnout velocity of 52,000 ft/sec with a 300-lb payload. This launch velocity, combined with a Jupiter assist, can produce a perihelion of about 0.05 AU and an inclination of 90°.

The disadvantage of Jupiter assist, however, is the three-year mission time involved; also, depending on orbital inclinations, the spacecraft may be required to pass through the asteroid belt which significantly reduces the reliability of these missions.

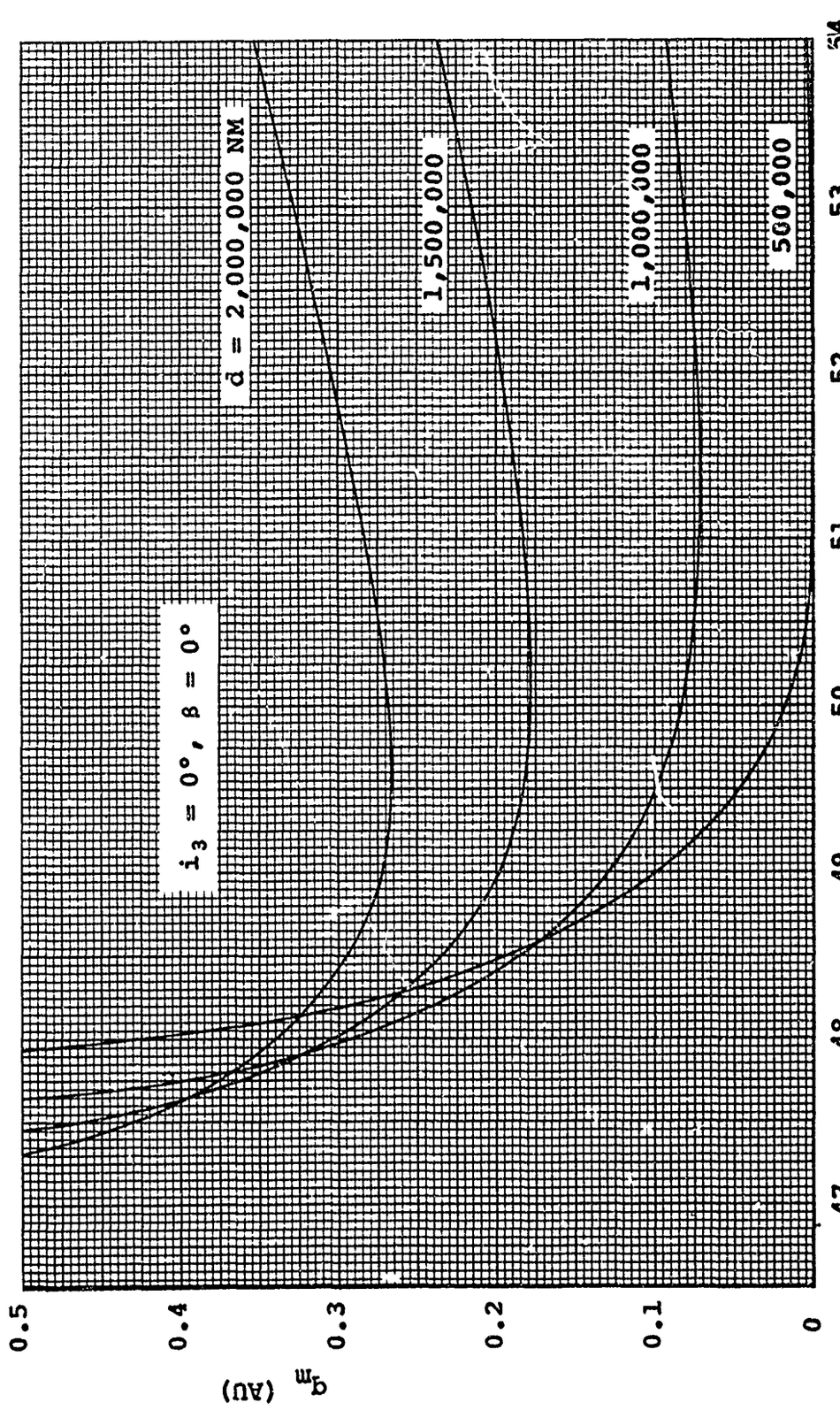

Fig. 60 Perihelion vs. Burnout Velocity for Jupiter Assist in Ecliptic

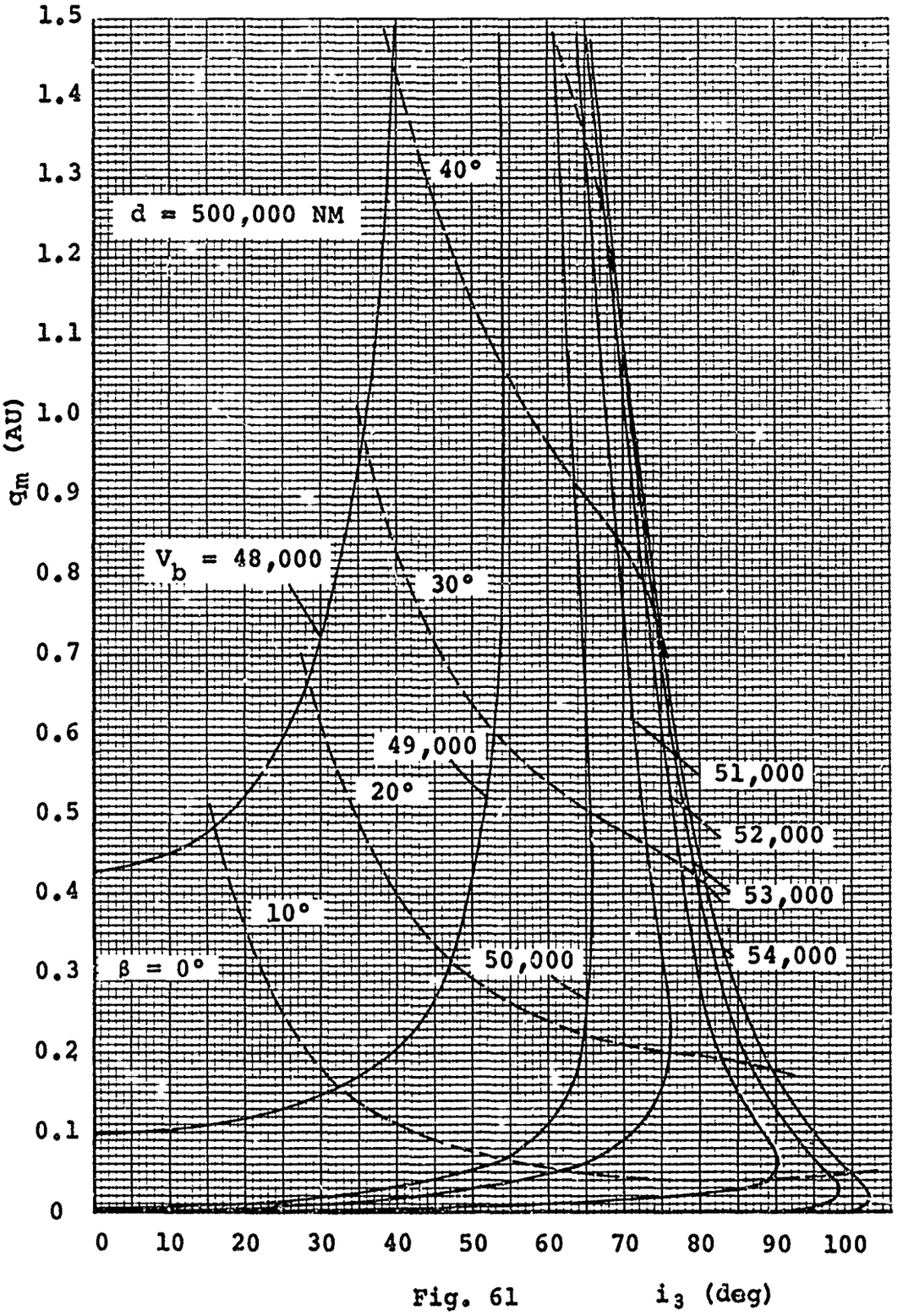

Fig. 61

Perihelion vs. Inclination for

Jupiter-Assist Missions

Table III

90°-OUT-OF-ECLIPTIC JUPITER-ASSISTED TRAJECTORIES

V_b (ft/sec)	DOCA (NM)	q_m (AU)	T_{OP} (years)
51,000	380,000	0.059	3.17
52,000	500,000	0.048	2.73
53,000	530,000	0.056	2.51
54,000	540,000	0.044	2.36

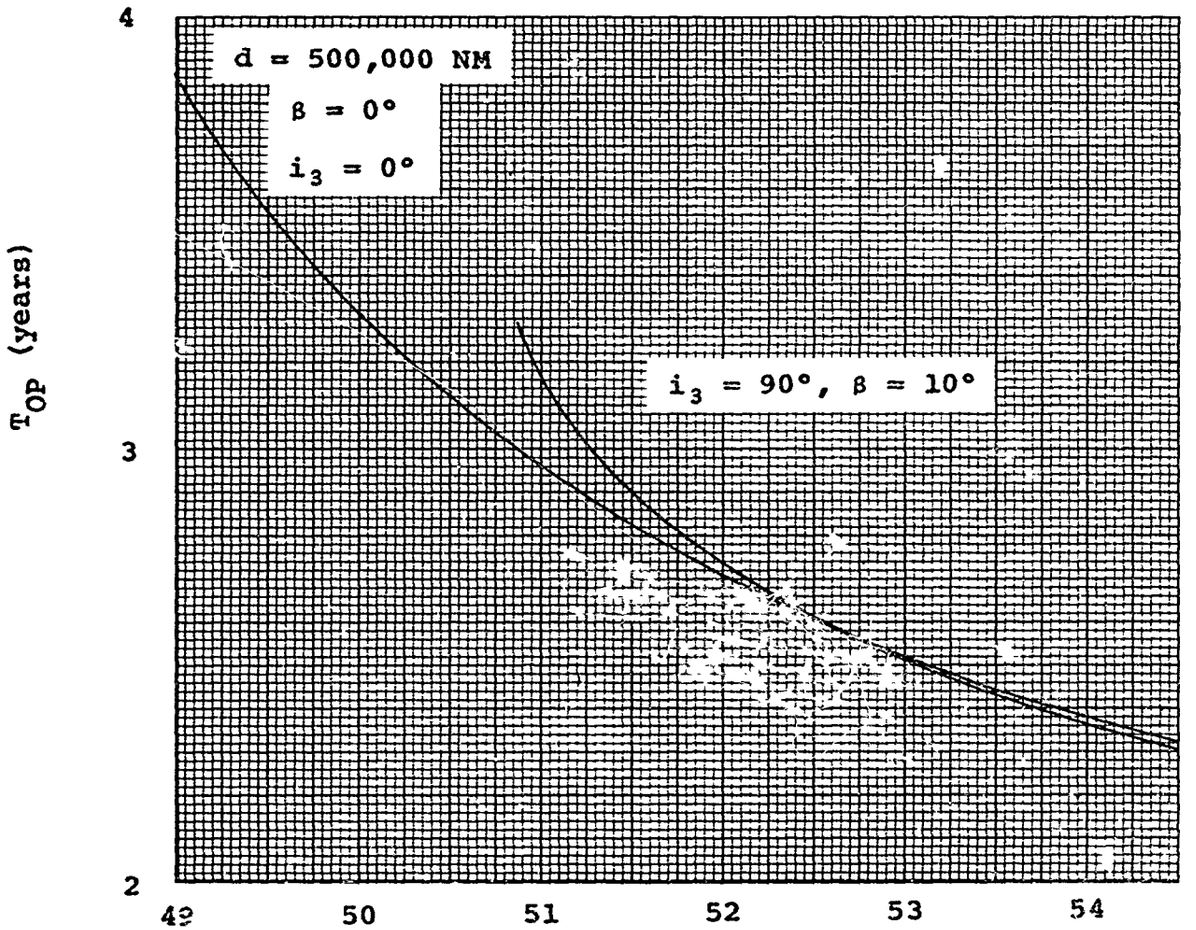

Fig. 62

Mission Time vs. Burnout Velocity for Post-Assist Orbit Inclination of 0° and 90°

X. Conclusions and Recommendations

Solar Probe Missions in the Ecliptic

Direct-transfer trajectories, characterized by high reliability and launch-date insensitivity, are preferred for solar probe missions to about 0.5 AU in the ecliptic. However, the burnout velocities required for smaller perihelia make it necessary to use expensive launch vehicles such as the Saturn I or Saturn V.

It has been shown in the thesis that a gravity assist at Venus can be used to significantly reduce the perihelion of solar probe trajectories. A few extra pounds of planetary-approach guidance equipment act as a substitute for large and expensive booster vehicles.

The multiple-assist missions at Venus offer an even greater savings in launch vehicle costs. The Atlas/Centaur/TE-364-3 ($16 million) can achieve smaller perihelia with multiple assist than a Saturn V ($125 million) with direct transfer. An additional advantage of these missions, despite their long time requirements, is that solar data can be collected over several regions of space with a single launch.

It is recommended that planetary-approach guidance techniques and space-vehicle reliability be improved for an attempted triple-assist mission. The probability of accomplishing the first passage at Venus is near certainty with present-day technology. If the second or third

passages fail, the mission can be classed as a partial success, for data will have been collected over at least one solar region.

Multiple-assist missions are the most reliable of any of the gravity-assist missions in the thesis. Trajectories can be designed, as shown in the double-assist mission profile, such that the pre-assist orbit period is equal to the period of Venus' orbit. This provides the opportunity for further attempts to pass Venus, if one should fail.

The Mercury-Venus combination-assisted trajectories were found to be more trouble than they are worth. It is also concluded from that investigation that Mercury is of little value as an assist planet.

Jupiter offers the best performance for gravity-assisted trajectories; in fact, retrograde orbits can be obtained. However, the time requirements, communication difficulties during the flyby, and penetration of the asteroid belt make these missions prohibitive. In spite of these drawbacks, a Jupiter assist is necessary to achieve perihelia less than about 0.05 AU with current launch vehicles.

Out-of-Ecliptic Solar Probe Missions

The launch energies for direct-transfer trajectories more than 20° out of the ecliptic require the use of the Saturn I or Saturn V. It has been shown that Venus-assisted Category I and II trajectories are useful in reducing this launch requirement.

The Category I trajectories are recommended for 10°-out-of-ecliptic missions. The perihelia for these trajectories is about 0.2 AU less than that obtained with direct-transfer.

It is suggested that Category II trajectories be used for 20°- to 30°-out-of-ecliptic missions. Most of the launch energy for these missions is devoted to the required pre-assist inclination, but a Venus assist serves to reduce the perihelion by as much as 0.28 AU.

A Jupiter assist is necessary to achieve inclination angles above 30°. Direct-transfer trajectories with these inclinations require launch velocities much greater than present-day technology can provide.

The attractiveness of the 90°-out-of-ecliptic trajectories obtained with a Jupiter assist cannot be overlooked. These missions are recommended for future consideration when spacecraft can be designed to withstand a three-year mission time, and when planetary-approach guidance techniques have become more perfected.

Bibliography

1. American Ephemeris and Nautical Almanac for the Year 1965. Washington:GPO, 1963.

2. Battin, Richard H. Astronautical Guidance. New York: McGraw Hill Book Co., 1964.

3. Casal, F. and Ross, Stanley. "The Use of Close Venusian Passages During Solar Probe Missions." Advances in Astronautical Sciences, 19:593-615 (1965).

4. Glasstone, Samuel. Sourcebook on the Space Sciences. New Jersey: D. Van Nostrand Co., Inc., 1965.

5. Koelle, H. H. Handbook of Astronautical Engineering. New York: McGraw Hill Book Co., 1961.

6. Kovit, Bernard. "The Coming Kick Stage." Space/Aeronautics, 44:55-61 (August 1965).

7. Magness, T. A., et al. "Accuracy Requirements for Interplanetary Ballistic Trajectories." IXth International Astronautical Congress, I:286-306 (1958).

8. Martin Company. Orbital Flight Manual. Martin Co., July 1961. AD445453.

9. Mickelwait, A. B., et al. "Three-Dimensional Interplanetary Trajectories." IRE Transactions on Military Electronics, MIL-3:149-159 (October 1959).

10. Minovitch, Michael A. The Determination and Characteristics of Ballistic Interplanetary Trajectories Under the Influence of Multiple Planetary Attractions. Technical Report No. 32-464. Pasadena, Calif.: JPL, October 1963.

11. Minovitch, Michael A. Utilizing Large Planetary Perturbations for the Design of Deep-Space, Solar Probe, and Out-of-Ecliptic Trajectories. Technical Report No. 32-849. Pasadena, Calif.: JPL, December 1965.

12. NASA-Stanford University. Inter-Planetary Craft for Advanced Research in the Vicinity of the Sun. Stanford University, August 1966.

13. Niehoff, J. An Analysis of Gravity Assisted Trajectories in the Ecliptic Plane. Report No. T-12. Chicago, Illinois: IIT Research Institute, May 1965.

14. Ragsac, R. V. and Titus, R. R. "Analysis of Planetary Flyby Missions." Advances in Astronautical Sciences, 13:572-586 (1963).

15. Ross, Stanley. "A Systematic Approach to the Study of Nonstop Interplanetary Round Trips." Advances in Astronautical Sciences, 13:104-176 (1963).

16. Roy, Archie. The Foundations of Astrodynamics. New York: The Macmillan Co., 1965.

17. Stewart, H. J. "New Possibilities for Solar-System Exploration." Astronautics and Aeronautics, 4:26-31 (December 1966).

18. Sturms, Francis M. and Cutting, Elliott. Trajectory Analysis of a 1970 Mission to Mercury via a close Encounter with Venus. Technical Report No. 32-943. Pasadena, Calif.: JPL, May 1966.

19. Sutton, George P. Rocket Propulsion Elements (Third Edition). New York: John Wiley & Sons, Inc., 1963.

20. Tanguay, Armand R. "Space Maneuvers," in Space Trajectories. New York: Academic Press Inc., 1960, pp. 163-199.

21. Thomson, W. T. Introduction to Space Dynamics. New York: John Wiley & Sons, Inc., 1963.

22. TRW Systems Group. TRW Space Data. Redondo Beach, Calif., 1965.

23. TRW Systems Group. TRW Space Data. Redondo Beach, Calif., 1967.

24. TRW Systems Group. TRW Space Log. Redondo Beach, Calif.

25. U.S. Air Force Systems Command. Space Planner's Guide. Washington: GPO, 1965.

Appendix A

Two-Dimensional Gravity-Assist Equations

Departure Orbit

The burnout velocity on a direct-ascent hyperbola at the departure planet P_1 is given by

$$V_b^2 = V_{\infty P_1}^2 + \frac{2\mu_{P_1}}{R_{P_1}} \tag{2-4}$$

Selection of V_b. After choosing a value for V_b, the HEV at P_1 becomes

$$V_{\infty P_1} = \left(V_b^2 - \frac{2\mu_{P_1}}{R_{P_1}} \right)^{1/2} \tag{A-1}$$

Pre-Assist Orbit

Characteristics of the pre-assist orbit are calculated with the same equations which were used for the heliocentric transfer orbit in Chapter II. However, the initial steps for finding $\bar{V}_0$ are more direct, since the orbit is now two-dimensional.

Selection of ϕ_0. A departure flight path angle ϕ_0 is selected, and the Law of Sines is used to determine the angle η^1 shown in Fig. 63:

$$\sin \eta^1 = \frac{V_{P_1} \cos \phi_0}{V_{\infty P_1}} \tag{A-2}$$

Calculation of V_o. Also, from Fig. 63

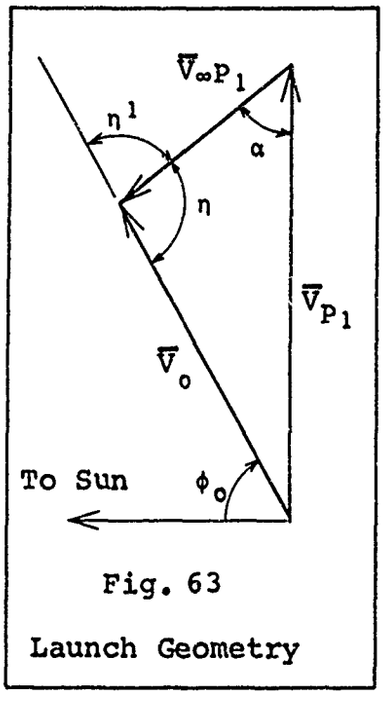

Fig. 63
Launch Geometry

$$\eta = \pi - \arcsin(\sin \eta^1) \quad \text{(A-3)}$$

and $$\alpha = \pi/2 - \eta + \phi_o \quad \text{(A-4)}$$

Finally, from the Law of Sines,

$$V_o = V_{\infty P_1} \frac{\sin \alpha}{\cos \phi_o} \quad \text{(A-5)}$$

Pre-Assist Orbit Characteristics. The equations for pre-assist orbit characteristics derived in Chapter II, are listed here for convenience:

$$\tan f_o = \frac{\left(r_{P_1} V_o^2 / \mu_\odot\right) \cos \phi_o \sin \phi_o}{1 - \left(r_{P_1} V_o^2 / \mu_\odot\right) \sin^2 \phi_o} \quad \text{(2-10)}$$

$$a_1 = \frac{r_{P_1}}{2 - r_{P_1} V_o^2 / \mu_\odot} \quad \text{(2-11)}$$

$$e_1^2 = \left(r_{P_1} V_o^2 / \mu_\odot - 1\right)^2 \sin^2 \phi_o + \cos^2 \phi_o \quad \text{(2-12)}$$

A necessary constraint on the pre-assist orbit is that its perihelion must be at least as small as the assist planet aphelion. According to the assumption of circular and coplanar planetary orbits, with the exception of Mercury, the

assist planet aphelion is taken as the mean distance of the planet from the Sun. This constraint may be expressed as

$$r_{p_2} \geq a_1 (1 - e_1) \tag{A-6}$$

where r_{p_2} is the mean distance of the assist planet from the Sun (aphelion of Mercury, if Mercury is used as the assist planet) and $a_1 (1 - e_1)$ is an expression for the perihelion of the pre-assist orbit.

Pre-Assist Orbit Conditions at the Assist Planet. As explained in Chapter III, the pre-assist orbit is assumed to end at the point where it first intersects the orbit of the assist planet. Thus, the heliocentric radius of the pre-assist orbit at the time of intercept is given by

$$r = r_{p_2} \tag{A-7}$$

Eqs (A-7) and (2-11) are used to compute the spacecraft velocity with respect to the Sun at intercept:

$$V_1^2 = \mu_\odot \left(\frac{2}{r_{p_2}} - \frac{1}{a_1} \right) \tag{A-8}$$

from the vis-viva integral. Also, for the flight path angle (Ref 16:83),

$$\sin \phi_1 = \left[\frac{a_1^2 (1 - e_1^2)}{r_{p_2} \left(2a_1 - r_{p_2} \right)} \right]^{1/2} \tag{A-9}$$

The true anomaly, using Eqs (A-8) and (A-9), is given by

$$\tan f_1 = \frac{\left(r_{P_2} V_1^2 / \mu_\odot\right) \cos \phi_1 \sin \phi_1}{1 - \left(r_{P_2} V_1^2 / \mu_\odot\right) \sin^2 \phi_1} \qquad \text{(A-10)}$$

where, $$f_1 = \arctan (\tan f_1) \qquad \text{(A-11)}$$

The heliocentric transfer angle from P_1 at launch to P_2 at intercept is

$$\theta_{12} = f_1 - f_0 \qquad \text{(A-12)}$$

and the transfer time is

$$T_{12} = t\,(a_1, \mu_\odot, e_1, f_1) - t\,(a_1, \mu_\odot, e_1, f_0) \qquad \text{(A-13)}$$

Assist Orbit

Fig. 64 which was discussed in Chapter III is used to write a vector expression for the inbound HEV of the spacecraft with respect to the assist planet

$$\bar{V}_{\infty_i} = \bar{V}_1 - \bar{V}_{P_2} \qquad \text{(3-1)}$$

The magnitude of this velocity is found by using the Law of Cosines:

$$V_{\infty_i}^2 = V_1^2 + V_{P_2}^2 - 2V_1 V_{P_2} \sin \phi_1 \qquad \text{(A-14)}$$

An expression for the HEV on a hyperbolic orbit (Ref 16:96) is used to find the semi-major axis of the assist hyperbola:

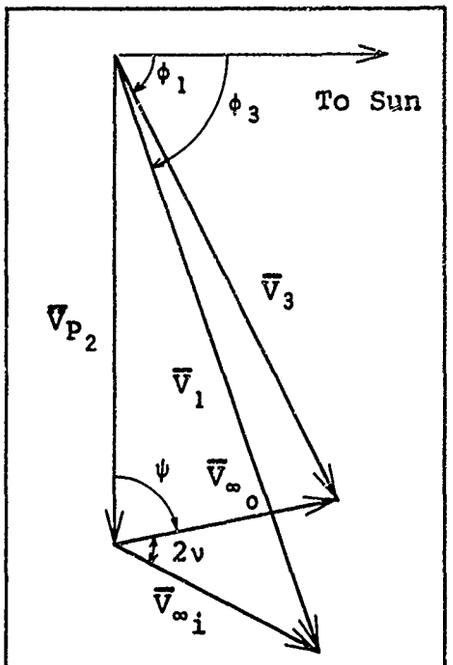

Fig. 64
Assist Geometry at P_2

$$a_2 = \frac{\mu_{P_2}}{V_{\infty_i}^2} \qquad \text{(A-15)}$$

Now an additional parameter must be selected in order to completely determine the geometry of the assist hyperbola - the DOCA which is denoted by d in the mathematical expressions.

Selection of d. The distance between the vertex and focus of the assist hyperbola is given by

$$r_m = a_2 \ (e_2 - 1) \qquad \text{(A-16)}$$

from orbital mechanics (Ref 2:152). The eccentricity, e_2, is undetermined in Eq (A-16), but can be found by assigning a value to d, where

$$r_m = R_{P_2} + d \qquad \text{(A-17)}$$

Eqs (A-16) and (A-17) are then combined as follows:

$$e_2 = \frac{1}{a_2}\left(R_{P_2} + a_2 + d\right) \qquad \text{(A-18)}$$

The angle ν between the hyperbola asymptote and conjugate axis is given by

$$\sin \nu = \frac{1}{e_2} \qquad \text{(A-19)}$$

As explained in Chapter III, the effect of gravity assist is to rotate the inbound HEV vector $\vec{V}_{\infty_i}$ through an angle 2ν in the plane of motion. The direction of this rotation depends upon the side of P_2 which is passed by the spacecraft. In this report, since it is desired to slow the spacecraft with respect to the Sun, $\vec{V}_{\infty_i}$ is rotated counter-clockwise into the vector $\vec{V}_{\infty_o}$ as shown in Fig. 64.

For navigation purposes, it is convenient to use the impact parameter or aiming vector which is the perpendicular distance from a point on the hyperbolic asymptote to the center of mass of P_2. The distance is given by (Ref 2:152)

$$r_a = r_m \sqrt{1 + \frac{2\mu_{P_2}}{r_m V_{\infty_i}^2}} \qquad \text{(A-20)}$$

The impact parameter has not been used in the computations, since this study is not concerned with navigation, but it is given here to show that it can easily be found from quantities which have been derived thus far.

Post-Assist Orbit

The post-assist orbit is assumed to originate at the end point of the pre-assist orbit, so the heliocentric radius at intercept is again given by Eq (A-7). Characteristics of this orbit are then computed from the post-assist velocity V_3, and flight-path angle ϕ_3.

Post-Assist Orbit Conditions at the Assist Planet. The heliocentric velocity $\vec{V}_3$ is determined from Fig. 64 as follows:

$$\bar{V}_3 = \bar{V}_{P_2} + \bar{V}_{\infty_o} \tag{3-2}$$

The angle ψ in Fig. 64 may be used to find the magnitude of $\bar{V}_3$. From the Law of Sines,

$$\sin (2\nu + \psi) = \frac{V_1}{V_{\infty_i}} \cos \phi_1 \tag{A-21}$$

and

$$\psi = \arcsin \left[\frac{V_1}{V_{\infty_i}} \cos \phi_1 \right] - 2\nu \tag{A-22}$$

The Law of Cosines gives

$$V_3^2 = V_{P_2}^2 + V_{\infty_o}^2 - 2V_{P_2} V_{\infty_o} \cos \psi \tag{A-23}$$

where, of course

$$V_{\infty_o} = V_{\infty_i} \tag{A-24}$$

The direction of $\bar{V}_3$ is specified by the flight path angle

$$\cos \phi_3 = \frac{V_{\infty_o}}{V_3} \sin \psi \tag{A-25}$$

The true anomaly of the post-assist orbit at P_2 is given by

$$\tan f_3 = \frac{\left(r_{P_2} V_3^2 / \mu_\odot \right) \cos \phi_3 \sin \phi_3}{1 - \left(r_{P_2} V_3^2 / \mu_\odot \right) \sin^2 \phi_3} \tag{A-26}$$

Post-Assist Orbit Characteristics. The orbit conditions in the previous section are used in the following equations for the post-assist orbit characteristics:

$$a_3 = \frac{r_{p_2}}{2 - \left(r_{p_2} V_3^2 / \mu_\odot\right)} \tag{A-27}$$

$$e_3^2 = \left(r_{p_2} V_3^2 / \mu_\odot - 1\right)^2 \sin^2\phi_3 + \cos^2\phi_3 \tag{A-28}$$

The total time from launch to perihelion is

$$T_{OP} = T_{12} - t\ (a_3,\ \mu_\odot,\ e_3,\ f_3) \tag{A-29}$$

and the aphelion and perihelion of the post-assist orbit are, respectively,

$$r_{a_3} = a_3\ (1 + e_3) \tag{A-30}$$

$$q_m = a_3\ (1 - e_3) \tag{A-31}$$

Appendix B

Three-Dimensional Gravity-Assist Equations

Departure Orbit

Selection of V_b. The HEV at the departure planet P_1 is found with the same expression used in the two-dimensional trajectories:

$$V_{\infty P_1} = \left(V_b^2 - \frac{2\mu_{P_1}}{R_{P_1}} \right)^{1/2} \qquad \text{(A-1)}$$

for a given value of V_b.

Pre-Assist Orbit

Characteristics of the pre-assist orbit are found with the heliocentric-transfer orbit equations of Chapter II. These equations are listed again for completeness of the derivation.

Selection of ϕ_o, i. The $X_1Y_1Z_1$ coordinate system, shown in Fig. 7, is used to write an equation for the heliocentric velocity at launch:

$$V_o = V_{P_1} \sin \phi_o \cos i - \sqrt{V_{P_1}^2 \sin^2\phi_o \cos^2 i + V_{\infty P_1}^2 - V_{P_1}^2} \qquad \text{(2-9)}$$

Pre-Assist Orbit Characteristics. The geometric properties of the pre-assist orbit are computed as outlined in Chapter II and Appendix A:

$$\tan f_o = \frac{\left(r_{P_1} V_o^2 / \mu_\odot\right) \cos \phi_o \sin \phi_o}{1 - \left(r_{P_1} V_o^2 / \mu_\odot\right) \sin^2 \phi_o} \tag{2-10}$$

$$a_1 = \frac{r_{P_1}}{2 - \left(r_{P_1} V_o^2 / \mu_\odot\right)} \tag{2-11}$$

$$e_1^2 = \left(r_{P_1} V_o^2 / \mu_\odot - 1\right)^2 \sin^2 \phi_o + \cos^2 \phi_o \tag{2-12}$$

with the constraint that

$$r_{P_2} \geq a_1 (1 - e_1) \tag{A-9}$$

Pre-Assist Orbit Conditions at the Assist Planet. As explained in Chapter VII, the pre-assist orbit can intersect the SOI of P_2 for only two cases: inclination angle small or heliocentric transfer angle θ_{12} equal to 180°. For either of these cases, r_1, the distance of the spacecraft from the Sun at the time it enters the SOI, is assumed to be r_{P_2}, the mean orbital radius of the assist planet. Under this assumption the heliocentric conditions of the pre-assist orbit at P_2 may be expressed as in Appendix A:

$$V_1^2 = \mu_\odot \left(\frac{2}{r_{P_2}} - \frac{1}{a_1}\right) \tag{A-8}$$

$$\sin \phi_1 = \left[\frac{a_1^2 (1 - e_1^2)}{r_{P_2} \left(2a_1 - r_{P_2}\right)}\right]^{1/2} \tag{A-9}$$

$$\tan f_1 = \frac{\left(r_{P_2} V_1^2 / \mu_\odot\right) \cos \phi_1 \sin \phi_1}{1 - \left(r_{P_2} V_1^2 / \mu_\odot\right) \sin^2 \phi_1} \qquad \text{(A-10)}$$

The transfer angle and time on the pre-assist orbit is given by the following expressions:

$$\theta_{12} = f_1 - f_0 \qquad \text{(A-12)}$$

$$T_{12} = t\,(a_1, \mu_\odot, e_1, f_1) - t\,(a_1, \mu_\odot, e_1, f_0) \qquad \text{(A-13)}$$

XYZ Components of $\bar{r}_1$ and $\bar{V}_1$. The vector components of $\bar{r}_1$ and $\bar{V}_1$ in the XYZ system are found with the following coordinate transformation (see Figs. 43 and 65):

1. The xyz orbital reference system, initially aligned with the XYZ ecliptic system, is rotated through the angle i about the line of nodes (the Y axis). This places the x-y plane in the pre-assist orbit plane.

2. The xyz system is rotated through an angle θ_{12} about the z axis, so that the y axis points toward the assist planet P_2 at the time of intercept. These rotations are expressed in the following matrix notation; where for convenience, $\theta_{12} \equiv \theta$, s represents sine, and c represents cosine:

$$\begin{Bmatrix} x \\ y \\ z \end{Bmatrix} = \begin{bmatrix} c\theta\ ci & s\theta & -c\theta\ si \\ -s\theta\ ci & c\theta & s\theta\ si \\ si & 0 & ci \end{bmatrix} \begin{Bmatrix} X \\ Y \\ Z \end{Bmatrix} \qquad \text{(B-1)}$$

Since the transformation is orthogonal, the inverse of the transformation matrix is given by its transpose.

Thus,

$$\begin{Bmatrix} X \\ Y \\ Z \end{Bmatrix} = A \begin{Bmatrix} x \\ y \\ z \end{Bmatrix} \tag{B-2}$$

where the matrix A is:

$$A = \begin{Bmatrix} c\theta\ ci & -s\theta\ ci & si \\ s\theta & c\theta & o \\ -c\theta\ si & s\theta\ si & ci \end{Bmatrix} \tag{B-3}$$

Components of $\bar{r}_1$ in the XYZ system are given by

$$\begin{Bmatrix} r_{1_X} \\ r_{1_Y} \\ r_{1_Z} \end{Bmatrix} = A \begin{Bmatrix} 0 \\ r_1 \\ 0 \end{Bmatrix} \cong A \begin{Bmatrix} 0 \\ r_{p_2} \\ 0 \end{Bmatrix} \tag{B-4}$$

The following constraint must be satisfied in Eq (B-4)

$$r_{1_Z} \leq \rho_{p_2} \tag{B-5}$$

that is, the distance of the spacecraft above the ecliptic plane must not exceed ρ_{p_2}, the radius of the SOI of P_2. If this constraint is not satisfied then the inclination i of the pre-assist orbit plane is too large for an intercept, and a smaller value must be selected.

The velocity $\bar{V}_1$, as shown in Fig. 65, has components in the negative x and negative y directions, so its components in the XYZ system are

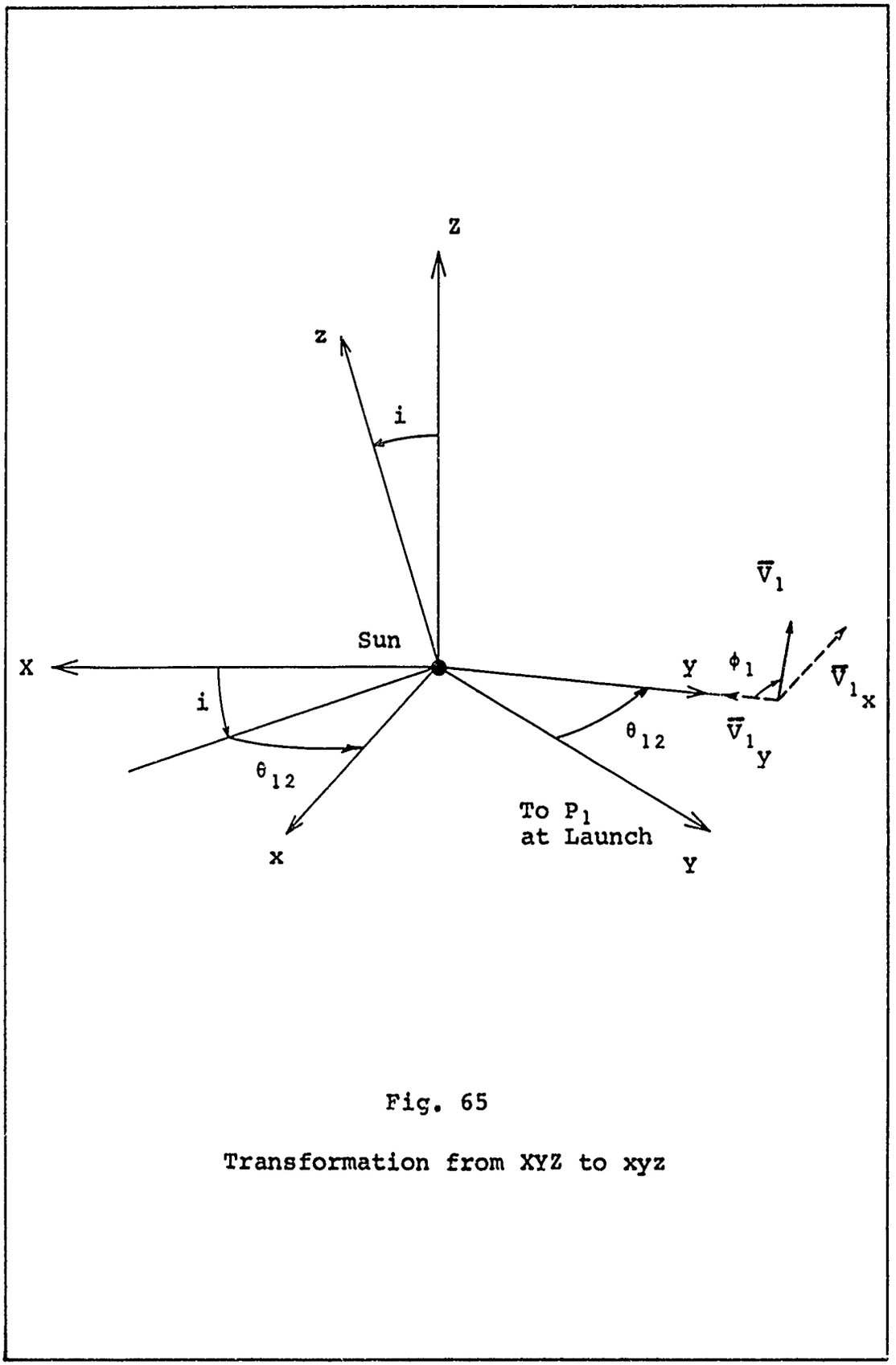

Fig. 65

Transformation from XYZ to xyz

$$\begin{Bmatrix} V_{1_X} \\ V_{1_Y} \\ V_{1_Z} \end{Bmatrix} = A \begin{Bmatrix} -V_1 \sin \phi_1 \\ -V_1 \cos \phi_1 \\ 0 \end{Bmatrix} \tag{B-6}$$

Transformation of $\bar{V}_1$ from XYZ to $X_2Y_2Z_2$. In order to define the relationship of $\bar{V}_1$ with other vectors at P_2 it is necessary to transform it from the ecliptic system XYZ to the assist planet system $X_2Y_2Z_2$. This transformation, shown in Figs. 66 and 67, is accomplished as follows:

1. The X'Y'Z' and XYZ ecliptic systems are initially aligned at the Sun. The X'Y'Z' axes are rotated about the Z axis through an angle η, where

$$\eta = \gamma - \pi/2 \tag{B-7}$$

$$\cong \theta_{12} - \pi/2 \tag{B-8}$$

so that the X' axis is directed along a line from P_2 to the Sun, and the Y' axis is directed opposite to $\bar{V}_{P_2}$, the velocity of P_2.

2. The X'Y'Z' system is translated from the Sun to a position O_2 near P_2, where the inbound and outbound assist hyperbola asymptotes intersect. This position is not defined until the DOCA and an angle β, discussed later, are selected; for the present degree of approximation, it is sufficient to know that O_2 lies within the SOI of P_2.

The relationship between the XYZ and X'Y'Z' systems is given by

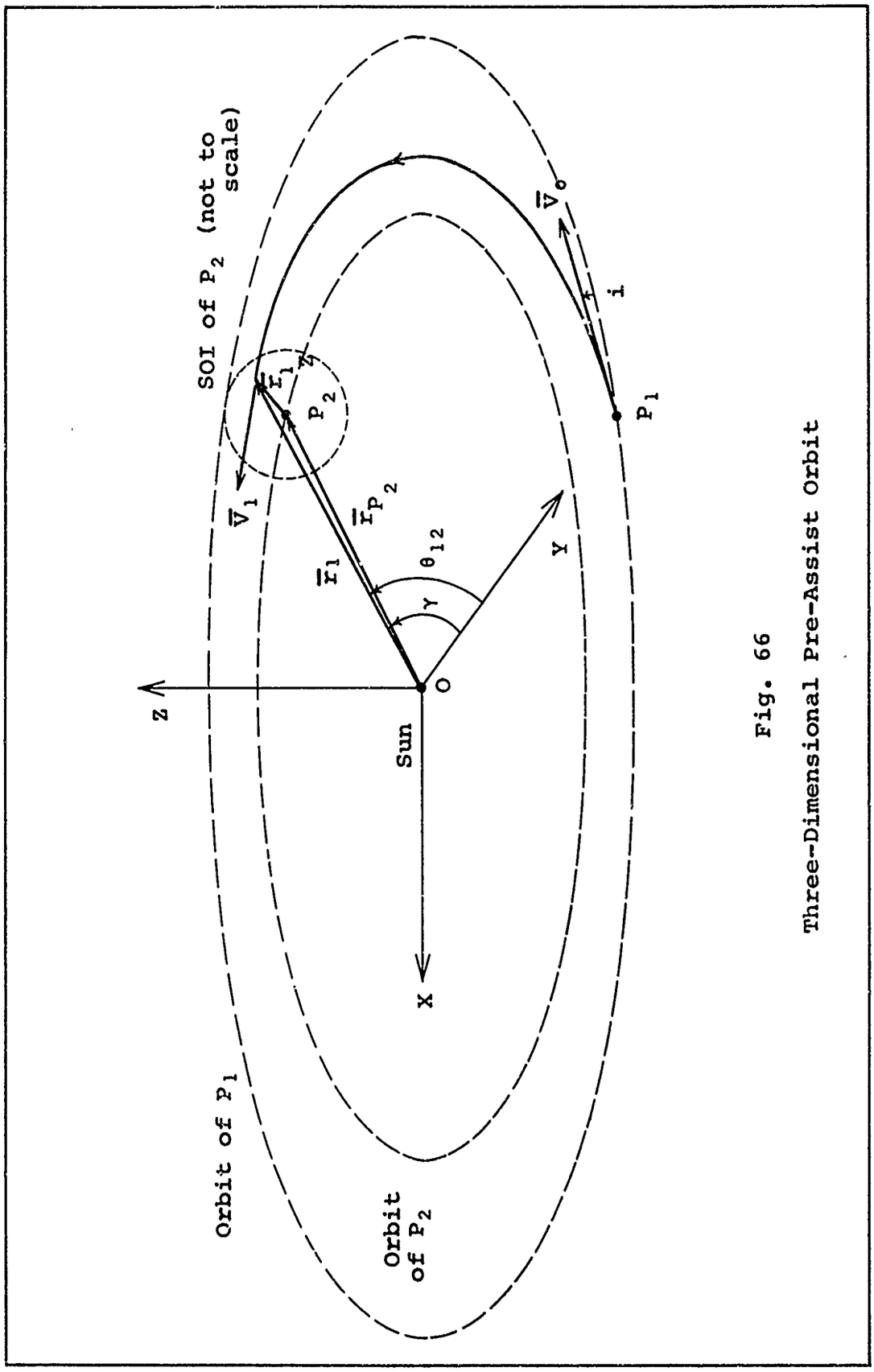

Fig. 66
Three-Dimensional Pre-Assist Orbit

$$\begin{Bmatrix} X' \\ Y' \\ Z' \end{Bmatrix} = B \begin{Bmatrix} X \\ Y \\ Z \end{Bmatrix} \tag{B-9}$$

where the transformation matrix B is defined as

$$B = \begin{Bmatrix} c\eta & s\eta & 0 \\ -s\eta & c\eta & 0 \\ 0 & 0 & 1 \end{Bmatrix} \tag{B-10}$$

The translation from X'Y'Z' to $X_2Y_2Z_2$ involves no rotation, so

$$\begin{Bmatrix} X_2 \\ Y_2 \\ Z_2 \end{Bmatrix} = \begin{Bmatrix} X' \\ Y' \\ Z' \end{Bmatrix} \tag{B-11}$$

Finally, the vector $\bar{V}_1$ in the $X_2Y_2Z_2$ system near the assist planet is

$$\begin{Bmatrix} V_{1_{X_2}} \\ V_{1_{Y_2}} \\ V_{1_{Z_2}} \end{Bmatrix} = B \begin{Bmatrix} V_{1_X} \\ V_{1_Y} \\ V_{1_Z} \end{Bmatrix} \tag{B-12}$$

$$= C \begin{Bmatrix} -V_1 \sin \phi_1 \\ -V_1 \cos \phi_1 \\ 0 \end{Bmatrix} \tag{B-13}$$

where use has been made of Eq (B-6) and the definition:

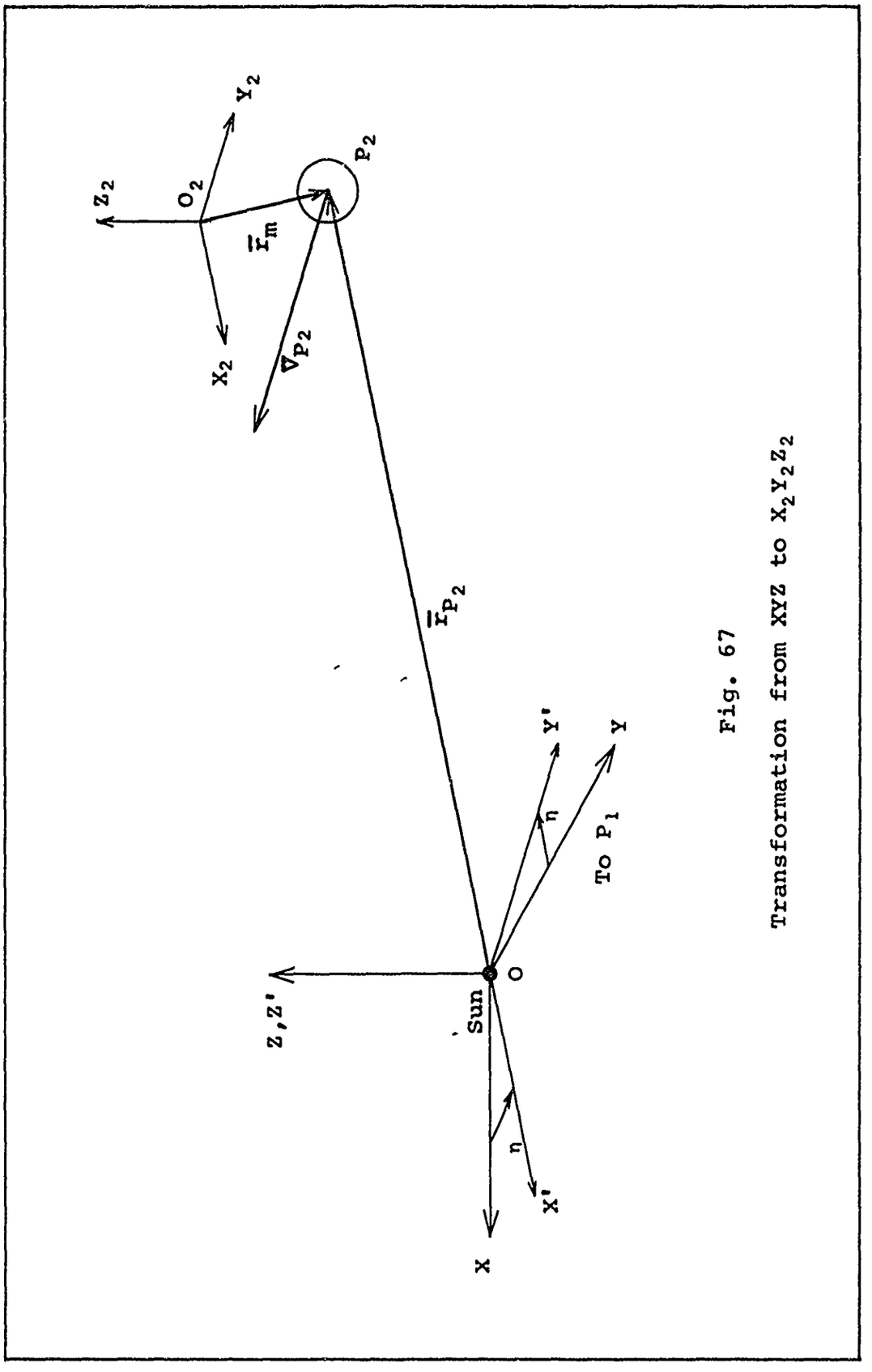

Fig. 67 Transformation from XYZ to $X_2Y_2Z_2$

$$C = BA \tag{B-14}$$

$$= \begin{Bmatrix} (\text{cn}\ c\theta\ ci + sn\ s\theta) & (-cn\ s\theta\ ci + sn\ c\theta) & (\text{cn}\ si) \\ (-sn\ c\theta\ ci + cn\ s\theta) & (\text{sn}\ s\theta\ ci + cn\ c\theta) & (-sn\ si) \\ (-c\theta\ si) & (\text{s}\theta\ si) & (ci) \end{Bmatrix} \tag{B-15}$$

Assist Orbit

Calculation of $\overline{V}_{\infty i}$. The inbound HEV at P_2 is shown in the vector diagram of Fig. 46. The vectors $\overline{V}_{P_2}$, $\overline{V}_1$, and $\overline{V}_{\infty i}$ are translated and added within the $X_2Y_2Z_2$ reference frame; the fact that the position of O_2 has not yet been defined does not affect the results, since vectors may be translated to any point in space with no change in magnitude or direction. Thus,

$$\overline{V}_{\infty i} = \overline{V}_1 - \overline{V}_{P_2} \tag{3-1}$$

In matrix notation, Eq (3-1) becomes

$$\begin{Bmatrix} V_{\infty i_{X_2}} \\ V_{\infty i_{Y_2}} \\ V_{\infty i_{Z_2}} \end{Bmatrix} = \begin{Bmatrix} V_{1_{X_2}} \\ V_{1_{Y_2}} \\ V_{1_{Z_2}} \end{Bmatrix} - \begin{Bmatrix} 0 \\ -V_{P_2} \\ 0 \end{Bmatrix} \tag{B-16}$$

which gives the magnitude of the vector,

$$V_{\infty i} = \left[V^2_{\infty i_{X_2}} + V^2_{\infty i_{Y_2}} + V^2_{\infty i_{Z_2}} \right]^{1/2} \tag{B-17}$$

Also, V_{∞_i} defines a semi-major axis for the assist hyperbola:

$$a_2 = \frac{\mu_{P_2}}{V_{\infty_i}^2} \tag{B-18}$$

Right Ascension and Declination of $\bar{V}_{\infty_i}$. For the purpose of defining the geometry of the assist hyperbola, it is necessary to determine the angles α and δ shown in Fig. 46. Later, when the assist hyperbola has been completely defined, it will be seen that these angles are, respectively, the right ascension (measured eastward on P_2 in the ecliptic plane from the direction of the Y_2 axis) and the declination (measured north (+) or south (-) of the ecliptic plane along the P_2 meridian determined by α).

Both α and δ are found with the vector $\bar{V}_{\infty_i}{}_{X_2Y_2}$ which is defined as the component of $\bar{V}_{\infty_i}$ in the X_2-Y_2 plane. As shown in the figure, the magnitude of this vector is

$$V_{\infty_i}{}_{X_2Y_2} = \left[V_{\infty_i}^2{}_{X_2} + V_{\infty_i}^2{}_{Y_2}\right]^{1/2} \tag{B-19}$$

Thus, for the right ascension,

$$\cos \alpha = \frac{-V_{\infty_i}{}_{Y_2}}{V_{\infty_i}{}_{X_2Y_2}} \tag{B-20}$$

and for the declination,

$$\cos \delta = \frac{V_{\infty_i}{}_{X_2Y_2}}{V_{\infty_i}} \tag{B-21}$$

Selection of β. The position of the assist orbit plane is defined by the center of mass of P_2. Its orientation, like any other plane, must be defined by three angles. Two of these angles, α and δ, have already been calculated, but a third angle, β (defined below), must be specified.

After β is selected, a coordinate transformation (see Fig. 68) is made from the $X_2Y_2Z_2$ system to the $x_2y_2z_2$ assist orbit system as follows:

1. The $x_2y_2z_2$ axes, initially aligned with the $X_2Y_2Z_2$ axes, are rotated about the Z_2 axis through the angle α. This rotation defines the primed system $x_2'y_2'z_2'$ shown in the figure.

2. The primed system is rotated through the angle δ about the x_2' axis. This rotation defines the double primed system $x_2''y_2''z_2''$, and aligns the y_2'' axis with the incoming HEV vector.

3. The double-primed system is rotated about the y_2'' axis through the angle β, into the $x_2y_2z_2$ system so that the x_2-y_2 plane lies in the plane of the assist orbit and z_2 forms a right-handed system.

The transformation is expressed as follows:

$$\begin{Bmatrix} x_2 \\ y_2 \\ z_2 \end{Bmatrix} = \begin{bmatrix} c\beta & 0 & -s\beta \\ 0 & 1 & 0 \\ s\beta & 0 & c\beta \end{bmatrix} \begin{bmatrix} 1 & 0 & 0 \\ 0 & c\delta & s\delta \\ 0 & -s\delta & c\delta \end{bmatrix} \begin{bmatrix} c\alpha & s\alpha & 0 \\ -s\alpha & c\alpha & 0 \\ 0 & 0 & 1 \end{bmatrix} \begin{Bmatrix} X_2 \\ Y_2 \\ Z_2 \end{Bmatrix} \qquad \text{(B-22)}$$

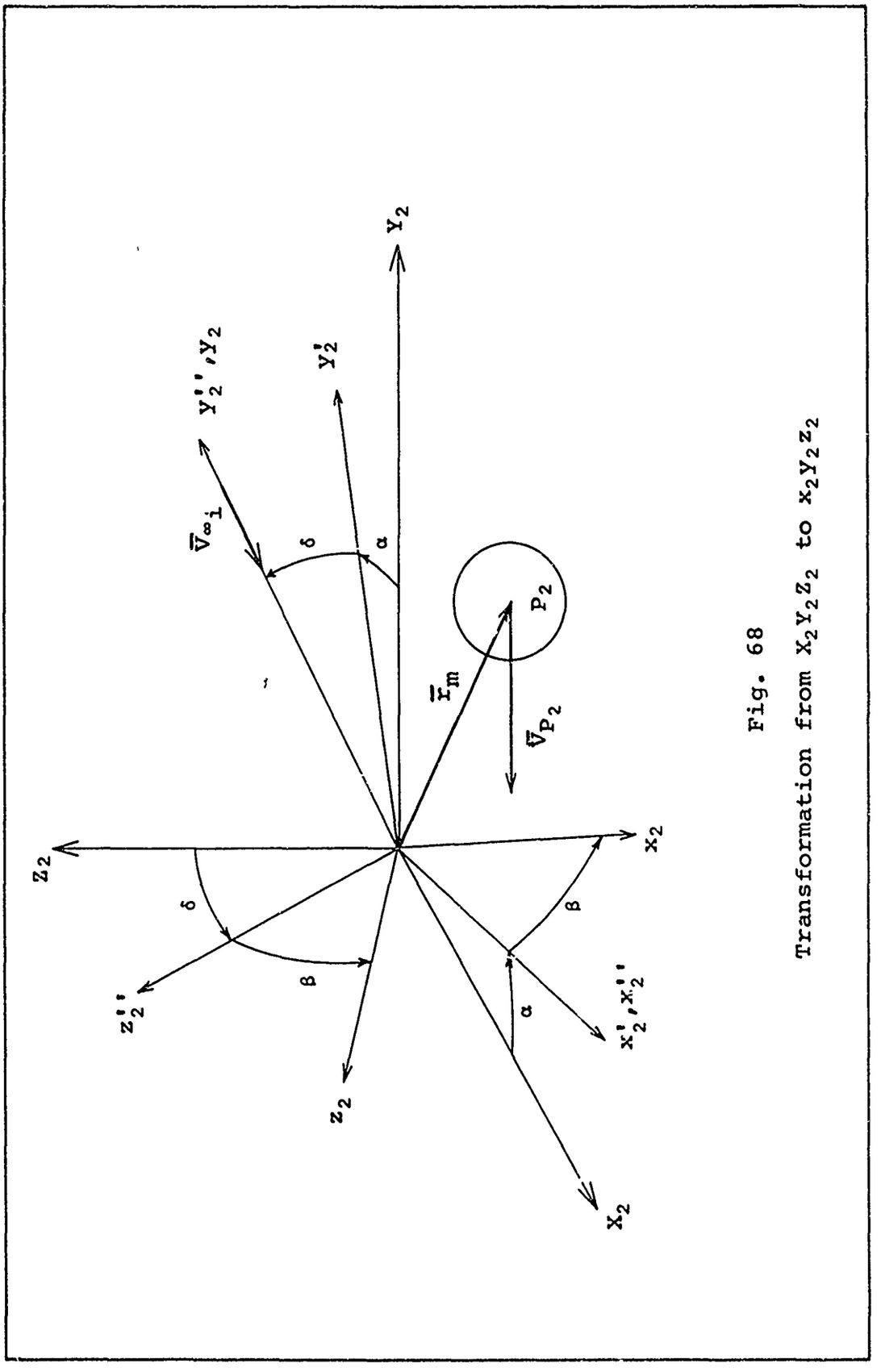

Fig. 68

Transformation from $X_2Y_2Z_2$ to $x_2y_2z_2$

$$= \begin{Bmatrix} (c\beta\ c\alpha - s\beta\ s\delta\ s\alpha) & (c\beta\ s\alpha + s\beta\ s\delta\ c\alpha) & (-s\beta\ c\delta) \\ (-c\delta\ s\alpha) & (c\delta\ c\alpha) & (\ s\delta) \\ (s\beta\ c\alpha + c\beta\ s\delta\ s\alpha) & (s\beta\ s\alpha - c\beta\ s\delta\ c\alpha) & (c\beta\ \ c\delta) \end{Bmatrix} \begin{Bmatrix} X_2 \\ Y_2 \\ Z_2 \end{Bmatrix} \quad \text{(B-23)}$$

and since the transformation is orthogonal,

$$\begin{Bmatrix} X_2 \\ Y_2 \\ Z_2 \end{Bmatrix} = D \begin{Bmatrix} x_2 \\ y_2 \\ z_2 \end{Bmatrix}$$

where D is defined as

$$D = \begin{Bmatrix} (c\beta\ c\alpha - s\beta\ s\delta\ s\alpha) & (-c\delta\ s\alpha) & (s\beta\ c\alpha + c\beta\ s\delta\ s\alpha) \\ (c\beta\ s\alpha + s\beta\ s\delta\ c\alpha) & (\ c\delta\ c\alpha) & (s\beta\ s\alpha - c\beta\ s\delta\ c\alpha) \\ (-s\beta\ c\delta) & (s\delta) & (c\beta\ c\delta) \end{Bmatrix} \quad \text{(B-24)}$$

Selection of d. The position and orientation of the assist orbit plane has been determined above, but a DOCA must be selected in order to define the assist orbit itself. This procedure is analogous to the two-dimensional case in which the assist orbit plane was automatically defined by the ecliptic, and a DOCA was selected to define the assist orbit.

The value of d determines the eccentricity of the assist orbit

$$e_2 = \frac{1}{a_2} \left(R_{P_2} + a_2 + d \right) \quad \text{(B-25)}$$

The angle between the conjugate axis and the inbound hyperbolic asymptote, as shown in Fig. 69, is given by

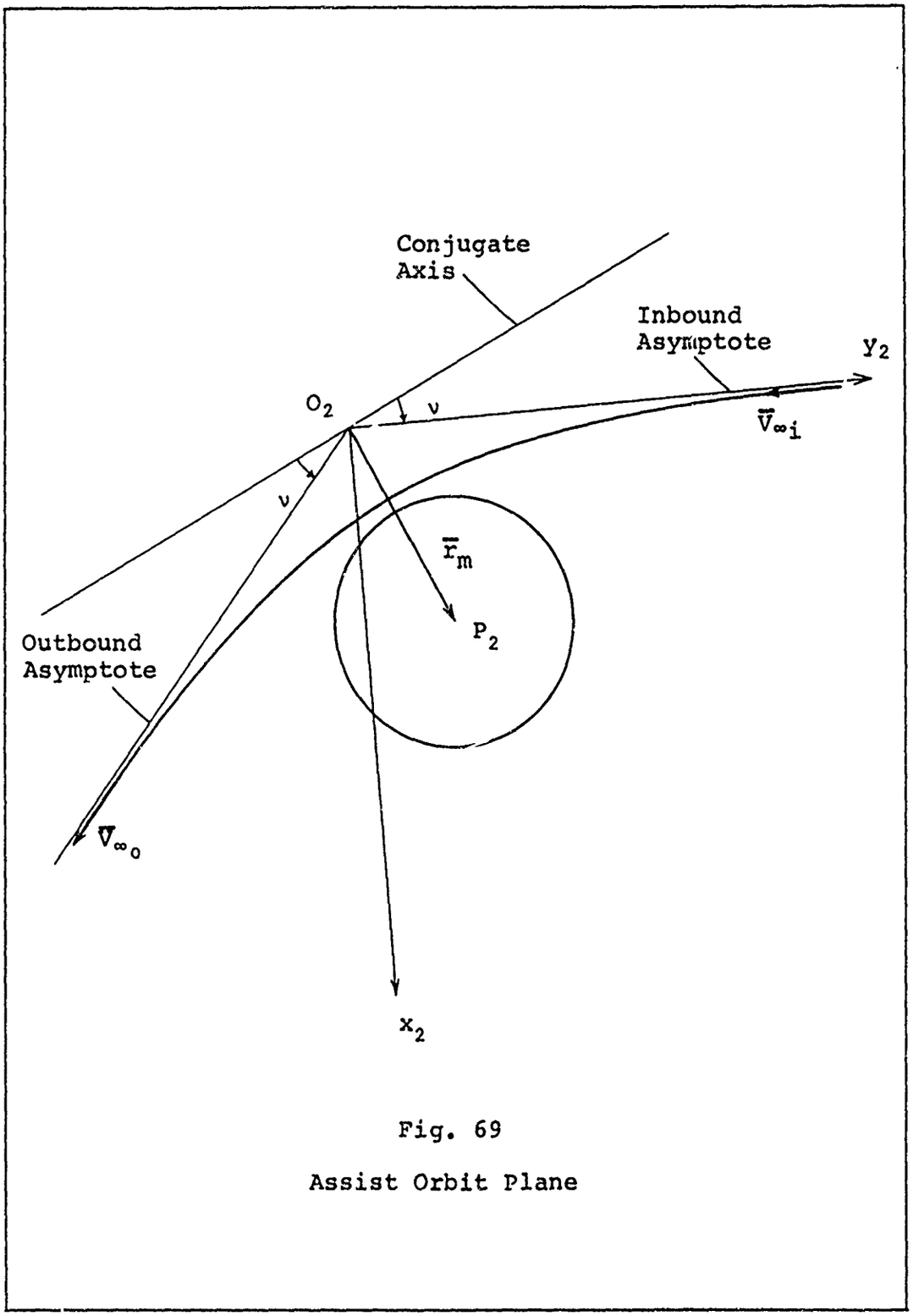

Fig. 69

Assist Orbit Plane

$$\sin \nu = \frac{1}{e_2} \tag{B-26}$$

This angle is used to find the components of $\bar{V}_{\infty_0}$ in the $x_2y_2z_2$ system,

$$\begin{Bmatrix} V_{\infty_0 x_2} \\ V_{\infty_0 y_2} \\ V_{\infty_0 z_2} \end{Bmatrix} = \begin{Bmatrix} V_{\infty_0} \sin 2\nu \\ -V_{\infty_0} \cos 2\nu \\ 0 \end{Bmatrix} \tag{B-27}$$

where, of course,

$$V_{\infty_0} = V_{\infty i} \tag{B-28}$$

The components of $\bar{V}_{\infty_0}$ in the $X_2Y_2Z_2$ system are found with the following transformation:

$$\begin{Bmatrix} V_{\infty_0 X_2} \\ V_{\infty_0 Y_2} \\ V_{\infty_0 Z_2} \end{Bmatrix} = D \begin{Bmatrix} V_{\infty_0 x_2} \\ V_{\infty_0 y_2} \\ V_{\infty_0 z_2} \end{Bmatrix} \tag{B-29}$$

Finally, the actual position of O_2, the origin of the $X_2Y_2Z_2$ system, is determined by the vector $\bar{r}_m$ from O_2 to the center of mass of P_2. For the components of this vector in the $X_2Y_2Z_2$system,

$$\begin{Bmatrix} r_{m_{X_2}} \\ r_{m_{Y_2}} \\ r_{m_{Z_2}} \end{Bmatrix} = D \begin{Bmatrix} r_m \cos \nu \\ r_m \sin \nu \\ 0 \end{Bmatrix} \tag{B-30}$$

where, $$r_m = a_2 + R_{P_2} + d \tag{B-31}$$

Post-Assist Orbit

Post-Assist Orbit Conditions at P_2. The heliocentric velocity of the spacecraft as it leaves the SOI of P_2 is given by

$$\bar{V}_3 = \bar{V}_{\infty_o} + \bar{V}_{P_2} \tag{3-2}$$

as shown in Fig. 47. This equation may be written in matrix form:

$$\begin{Bmatrix} V_{3_{X_2}} \\ V_{3_{Y_2}} \\ V_{3_{Z_2}} \end{Bmatrix} = \begin{Bmatrix} V_{\infty_{o_{X_2}}} \\ V_{\infty_{o_{Y_2}}} \\ V_{\infty_{o_{Z_2}}} \end{Bmatrix} + \begin{Bmatrix} 0 \\ -V_{P_2} \\ 0 \end{Bmatrix} \tag{B-32}$$

and $$V_3 = \left[V_{3_{X_2}}^2 + V_{3_{Y_2}}^2 + V_{3_{Z_2}}^2 \right]^{1/2} \tag{B-33}$$

The flight path angle, ϕ_3, is given by

$$\cos \phi_3 = \frac{V_{3_{X2}}}{V_3} \tag{B-34}$$

and the inclination of the post-assist orbit is

$$i_3 = \arctan \frac{V_{3_{Z_2}}}{V_{3_{Y_2}}} \tag{B-35}$$

The true anomaly, or the heliocentric angle from P_2 to perihelion is

$$\tan f_3 = \frac{\left(-r_{p_2} V_3^2 / \mu_\odot\right) \cos \phi_3 \sin \phi_3}{\left(r_{p_2} V_3^2 / \mu_\odot\right) \sin^2 \phi_3 - 1} \qquad \text{(B-36)}$$

Post-Assist Orbit Characteristics. Finally, the post-assist orbit characteristics are obtained from the following relations:

$$a_3 = \frac{r_{p2}}{2 - \left(r_{p_2} V_3^2 / \mu_\odot\right)} \qquad \text{(A-27)}$$

$$e_3^2 = \left(r_{p_2} V_3^2 / \mu_\odot - 1\right)^2 \sin^2 \phi_3 + \cos^2 \phi_3 \qquad \text{(A-28)}$$

$$T_{OP} = T_{12} - t\ (a_3, \mu_\odot, e_3, f_3) \qquad \text{(A-29)}$$

$$r_{a_3} = a_3\ (1 + e_3) \qquad \text{(A-30)}$$

$$q_m = a_3\ (1 - e_3) \qquad \text{(A-31)}$$

Summary

A complete summary of the velocity vectors at P_2 is shown in Fig. 70. This diagram is similar to Fig. 16(a), and may be used to separate the events into two reference frames: one with respect to P_2, and one with respect to the Sun.

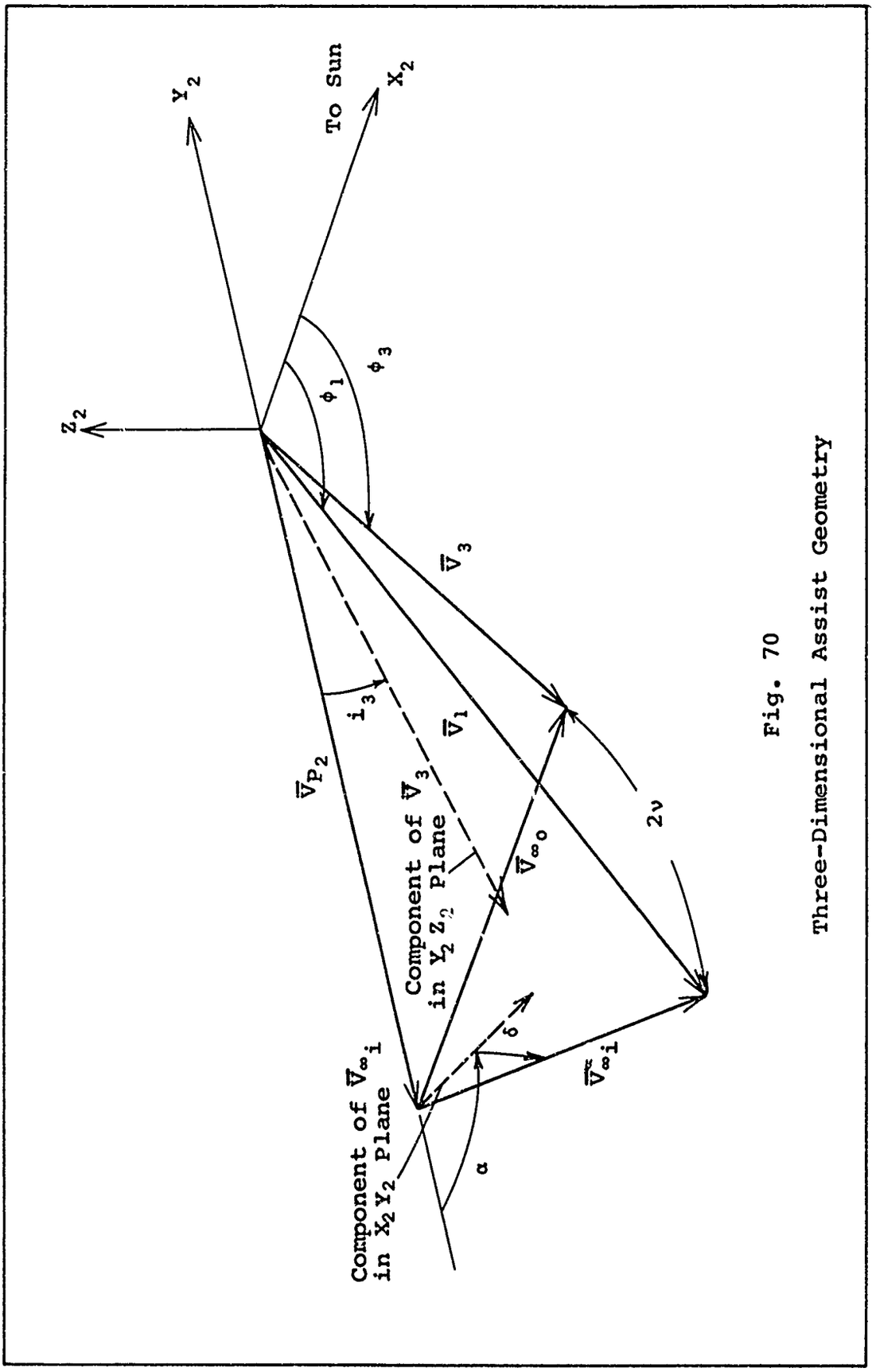

Fig. 70

Three-Dimensional Assist Geometry

Appendix C

Pre-Assist Orbit Inclination for Category II Trajectories

The purpose of this appendix is to derive an expression for the pre-assist orbit inclination i required for given values of burnout velocity V_b and departure flight path angle ϕ_o for Category II trajectories. The problem, illustrated in Fig. 71 , is to find an orbit which intersects the orbits of P_1 and P_2 at a distance of r_{P_1} and r_{P_2} from the Sun, respectively.

An expression for i is obtained from Eq (2-8):

$$V_o^2 - 2V_{P_1} \sin \phi_o \cos i \, V_o + V_{P_1}^2 - V_{\infty P_1}^2 = 0 \qquad (2\text{-}8)$$

which gives

$$i = \arccos \left(\frac{V_o^2 + V_{P_1}^2 - V_{\infty P_1}^2}{2V_{P_1} V_o \sin \phi_o} \right) \qquad (C\text{-}1)$$

The quantities V_{P_1}, ϕ_o, and $V_{\infty P_1}$ (found with given V_b in Eq (A-1)) are all known in this expression, but V_o must be calculated.

From the energy integral for elliptic orbits,

$$V_o^2 = \mu_\odot \left(\frac{2}{r_{P_1}} - \frac{1}{a_1} \right) \qquad (C\text{-}2)$$

where a_1 is the semi-major axis of the pre-assist orbit. The value of a_1 is found by first writing the basic orbital

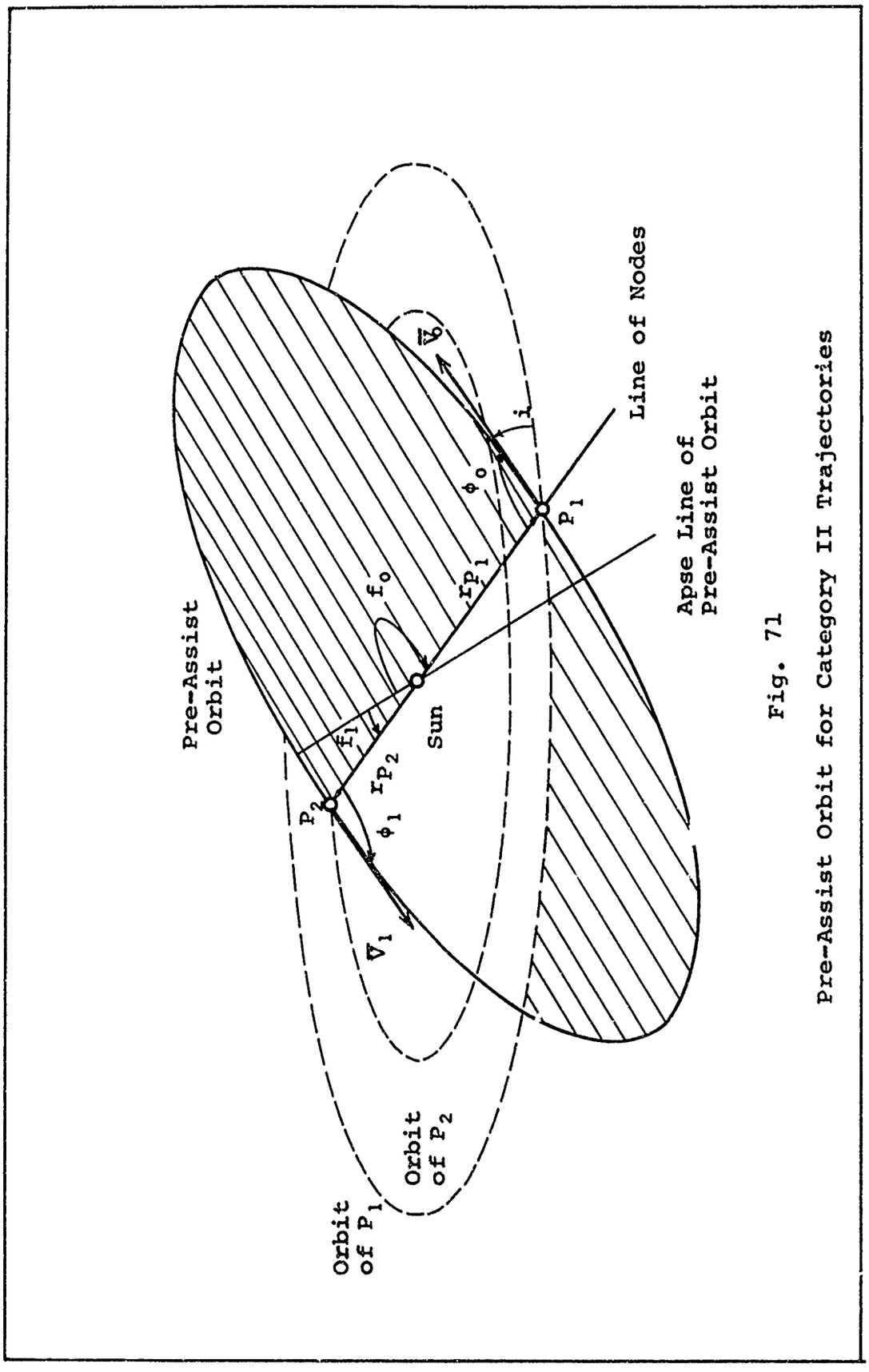

Fig. 71

Pre-Assist Orbit for Category II Trajectories

equation for the times of departure from P_1 and arrival at P_2:

$$r_{P_1} = \frac{a_1 (1 - e_1^2)}{1 + e_1 \cos f_o} \tag{C-3}$$

$$r_{P_2} = \frac{a_1 (1 - e_1^2)}{1 + e_1 \cos f_1} \tag{C-4}$$

where e_1 is the eccentricity of the pre-assist orbit.

Division of Eq (C-3) by Eq (C-4) gives

$$\frac{r_{P_1}}{r_{P_2}} = \frac{1 + e_1 \cos f_1}{1 + e_1 \cos f_o} \tag{C-5}$$

For Category II trajectories, by definition,

$$f_1 - f_o = \pi \tag{C-6}$$

where f_o is assumed to be a negative angle for pre-assist orbits inside the orbit of P_1. Substitution of Eq (C-6) into (C-5) with the definition $R \equiv r_{P_1} / r_{P_2}$ gives

$$R = \frac{1 - e_1 \cos f_o}{1 + e_1 \cos f_o} \tag{C-7}$$

which can be rearranged to give:

$$e_1 \cos f_o = \frac{(1 - R)}{(1 + R)} \tag{C-8}$$

Now, from orbital mechanics (Ref 16:83) it can be shown that

$$\sin \phi_o = \frac{1 + e_1 \cos f_o}{(1 + e_1^2 + 2e_1 \cos f_o)^{1/2}} \qquad \text{(C-9)}$$

Definition of the quantity

$$A = \frac{1 - R}{1 + R} \qquad \text{(C-10)}$$

and substitution of Eq (C-8) into (C-9) gives

$$\sin \phi_o = \frac{1 + A}{[1 + e_1^2 + 2A]^{1/2}} \qquad \text{(C-11)}$$

An expression for e_1 is found by squaring and rearranging Eq (C-11):

$$e_1 = \frac{1}{\sin \phi_o} [A^2 + (1 - \sin^2 \phi_o)(1 + 2A)]^{1/2} \qquad \text{(C-12)}$$

which can be determined from the known values of A and ϕ_o.

The value of e_1 from Eq (C-12) can now be used in the following equation (Ref 16:83) to find a_1:

$$\sin^2 \phi_o = \frac{a_1^2 (1 - e_1^2)}{r_{p_1} (2a_1 - r_{p_1})} \qquad \text{(C-13)}$$

This expression is rearranged as follows:

$$(1 - e_1^2) a_1^2 - 2r_{p_1} \sin^2 \phi_o a_1 + r_{p_1}^2 \sin^2 \phi_o = 0 \qquad \text{(C-14)}$$

which is a quadratic equation for a_1. Solution of Eq (C-14) gives

$$a_1 = \frac{r_{P_1} \sin \phi_o}{(1 - e_1^2)} \left[\sin\phi_o \pm (\sin^2\phi_o + e_1^2 - 1)^{1/2} \right] \qquad \text{(C-15)}$$

where the - (+) sign is used when the orbit of P_2 lies inside (outside) the orbit of P_1.

In summary, the sequence of calculations for the required inclination of a pre-assist orbit is as follows:

1) Given values of r_{P_1}, r_{P_2}, V_{P_1}, ϕ_o, and V_b

2) $$V_{\infty P_1} = \sqrt{V_b^2 - \frac{2\mu_{P_1}}{R_{P_1}}} \qquad \text{(A-1)}$$

3) $$e_1 = \frac{1}{\sin \phi_o} \left[A^2 + (1 - \sin^2\phi_o)\ (1 + 2A) \right]^{1/2} \qquad \text{(C-12)}$$

4) $$a_1 = \frac{r_{P_1} \sin \phi_o}{(1 - e_1^2)} \left[\sin \phi_o - (\sin^2\phi_o + e_1^2 - 1)^{1/2} \right] \qquad \text{(C-15)}$$

5) $$V_o^2 = \mu_\odot \left(\frac{2}{r_{P_1}} - \frac{1}{a_1} \right) \qquad \text{(C-2)}$$

6) $$i = \arccos \left(\frac{V_o^2 + V_{P_1}^2 - V_{\infty P_1}^2}{2 V_{P_1} V_o \sin \phi_o} \right) \qquad \text{(C-1)}$$

Appendix D

Launch Opportunities

The initial assumption of circular and coplanar planetary orbits means that any calculation of launch opportunities is only an approximation. However, this approximation is consistent with other work in the study, so the results may be followed as a guide for more precise studies.

Fig. 72 illustrates the heliocentric longitudes l_{10} and l_{20} of planets P_1 and P_2, respectively, with respect to the vernal equinox direction T at some epoch t_o. For the longitudes at any time t, after t_o:

$$l_1 = l_{10} + \omega_1 (t - t_o) \tag{D-1}$$

$$l_2 = l_{20} + \omega_2 (t - t_o) \tag{D-2}$$

where ω_1 and ω_2 are the mean daily motions of P_1 and P_2, respectively.

To accomplish some given transfer (pre-assist orbit) in time T_{12} through an angle θ_{12}, from planet P_1 to P_2,

$$-\theta_L = \omega_2 T_{12} - \theta_{12} \tag{D-3}$$

which gives the lead angle θ_L measured from Earth longitude at launch, as shown in Fig. 73.

To find a launch time t_L for the given trajectory, let

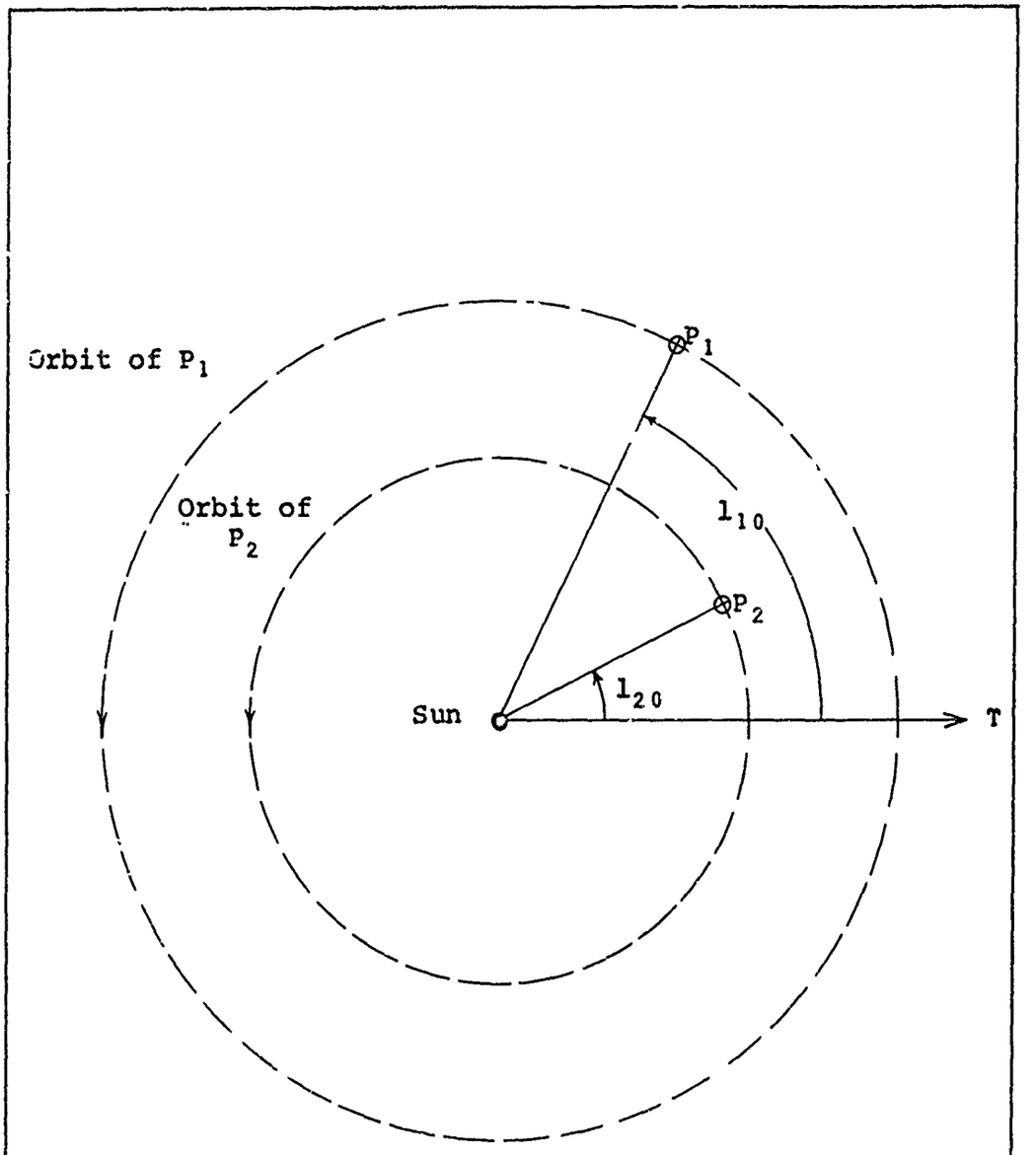

Fig. 72

Position of P_1 and P_2 at Epoch

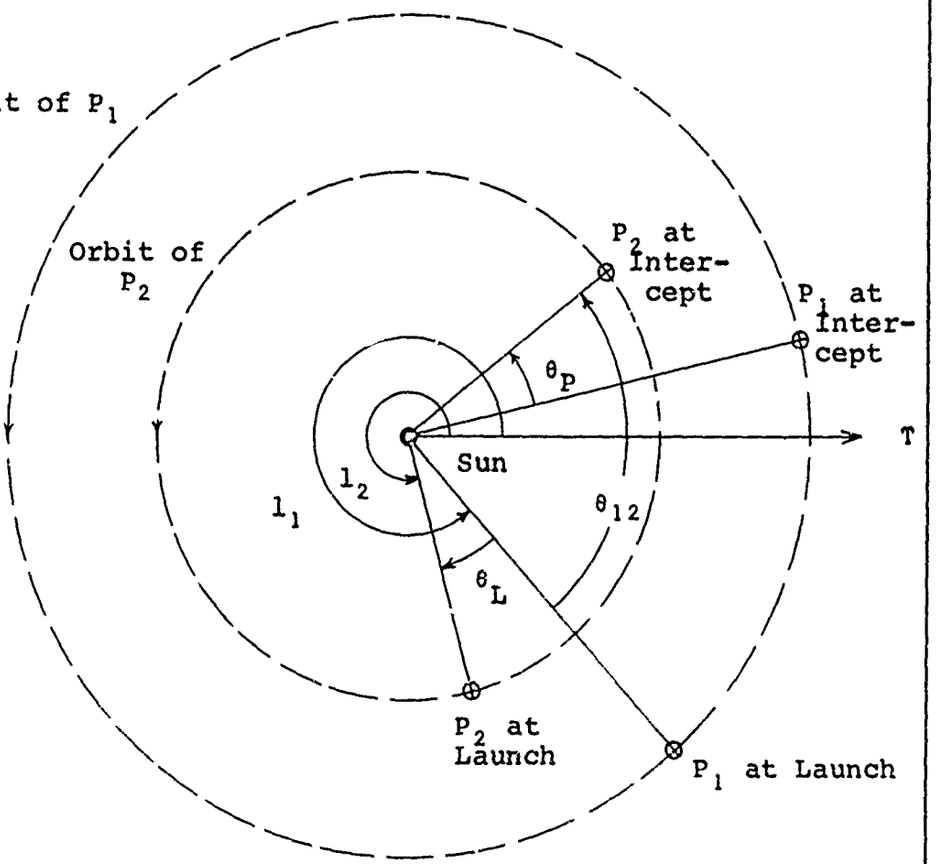

Fig. 73

Position of P_1 and P_2 at Launch and Intercept Positions

$$-\theta_L = l_1 - l_2 \tag{D-4}$$

and from Eqs (D-1) and (D-2), for $t = t_L$,

$$-\theta_L = l_{10} + \omega_1 (t_L - t_o) - l_{20} - \omega_2 (t_L - t_o) \tag{D-5}$$

Finally, after rearranging Eq (D-5),

$$t_L = \frac{1}{(\omega_2 - \omega_1)} \left[(l_{10} - l_{20}) + (\omega_2 - \omega_1)\, t_o + \theta_L\right] \tag{D-6}$$

which gives the first possible launch time near t_o. In this thesis the epoch t_o was taken as 1.5 Jan 1960 which is Julian day number 2,436,935.

Successive launch dates for the given transfer orbit may be generated by adding multiples of the synodic period to t_L. Thus, for n launch dates in addition to the date t_L from Eq (D-6),

$$\begin{aligned} t_{L_1} &= t_L + S \\ t_{L_2} &= t_L + 2S \\ &\vdots \qquad\quad \vdots \\ t_{L_n} &= t_L + nS \end{aligned} \tag{D-7}$$

where S is the synodic period of P_1 and P_2.

The angle θ_P, measured from P_1 to P_2 at the time of intercept, is given by

$$\theta_P = \theta_{12} - \omega_1 T_{12} \tag{D-8}$$

Launch dates are generated with Program 8 for ecliptic and out-of-ecliptic orbits. The method for calculating θ_{12} and T_{12} is similar to that used in Program 6 for the ecliptic and that used in Program 7 for the out-of-ecliptic trajectories. Eqs (D-1) through (D-8) apply to both types of trajectories.

Appendix E

Computer Programs

Program 1

```
$JOB            0,5,10000      67-012,LT MYERS,AFIT-SE
$IBJOB          MAP
$IBFTC MAIN     M94/2,XR7
C DIRECT-TRANSFER TRAJECTORIES FOR SOLAR PROBES
      TIME(A,G,E,T)=(2.*ATAN(SQRT((1.-E)/(1.+E))*TAN(T*R/2.))-E*SQRT(1.-
     1E**2)*SIN(T*R)/(1.+E*COS(T*R)))*SQRT((A**3)/G)/86400.
      READ(5,1)GCS,GCP1,RP1,VP1,RADP1
    1 FORMAT(5E10.0)
      VB=36000.
      PI=3.14159
      R=PI/180.
      M=72
      N=9
      L=19
      DO 2 I=1,M
      T=VB**2-2.*GCP1/RADP1
      IF(T)102,103,103
  102 WRITE(6,104)VB
  104 FORMAT(1HA,10X,3HVB=,F10.1,21HBELOW ESCAPE VELOCITY)
      GO TO 31
  103 VINFP1=SQRT(T)
      WRITE(6,105)
  105 FORMAT(1H ,2X,66H**********************************************************
     1**********)
      PH0=90.
      DO 3 J=1,N
      PH0R=PH0*R
      WRITE(6,100)VB,VINFP1,PH0
  100 FORMAT(1HA,10X,3HVB=,F10.1,5X,7HVINFP1=,F9.1,5X,3HPH=,F5.1//4X,2HX
     1I,8X,2HF0,8X,2HA1,8X,2HE1,7X,5HTIMOP,6X,2HRP)
      XI=0.
      DO 4 K=1,L
      XIR=XI*R
      IF((VP1*SIN(PH0R)*COS(XIR))**2+VINFP1**2-VP1**2)5,5,6
    5 WRITE(6,7)VB,PH0,XI
    7 FORMAT(1HA, 4X,17HNO ESCAPE FOR VB=,F10.1,7HAT PH0=,F7.2,6HAND I=,
     1F6.2)
      GO TO 30
    6 V0=VP1*SIN(PH0R)*COS(XIR)-SQRT((VP1*SIN(PH0R)*COS(XIR))**2+VINFP1*
     1*2-VP1**2)
      RP1V0=RP1*V0**2/GCS
      TANF0=RP1V0*COS(PH0R)*SIN(PH0R)/(1.-RP1V0*SIN(PH0R)**2)
      IF(TANF0)8,9,9
    8 F0=ATAN(TANF0)/R
      GO TO 10
    9 F0=(ATAN(TANF0)-PI)/R



   10 A1=RP1/(2.-RP1V0)
      A1AU=A1/(92901000.*5280.)
      E1=SQRT(((RP1V0-1.)*SIN(PH0R))**2+COS(PH0R)**2)
      RPER1=A1*(1.-E1)
      RPAU=RPER1/(92901000.*5280.)
      TIMOP=-TIME(A1,GCS,E1,F0)
      WRITE(6,101)XI,F0,A1AU,E1,TIMOP,RPAU
  101 FORMAT(6F10.4)
      XI=XI+5.
    4 CONTINUE
   30 PH0=PH0-10.
    3 CONTINUE
   31 VB=VB+1000.
    2 CONTINUE
      STOP
      END
$DATA
 4.6868E21 1.4077E16 4.9052E11 9.7751E04 2.0902E07
$EOF
```

Program 1 Output

****

VB= 42000.0 VINFP1= 20421.7 PH= 90.0

XI	FO	A1	E1	TIMOP	RP
0.	-179.9999	0.7277	0.3742	113.2736	0.4554
5.0000	-179.9999	0.7409	0.3498	116.3526	0.4817
10.0000	-179.9998	0.8030	0.2454	131.2852	0.6059

NO ESCAPE FOR VB= 42000.0AT PHO= 90.00AND I= 15.00

VB= 42000.0 VINFP1= 20421.7 PH= 88.0

XI	FO	A1	E1	TIMOP	RP
0.	-176.6150	0.7297	0.3719	109.3978	0.4583
5.0000	-176.2300	0.7432	0.3471	112.1644	0.4852
10.0000	-173.6313	0.8082	0.2398	125.1468	0.6144

NO ESCAPE FOR VB= 42000.0AT PHO= 88.00AND I= 15.00

VB= 42000.0 VINFP1= 20421.7 PH= 86.0

XI	FO	A1	E1	TIMOP	RP
0.	-172.9760	0.7359	0.3648	106.2147	0.4674
5.0000	-172.1182	0.7506	0.3388	108.7804	0.4963
10.0000	-165.5901	0.8264	0.2209	120.4026	0.6439

NO ESCAPE FOR VB= 42000.0AT PHO= 86.00AND I= 15.00

VB= 42000.0 VINFP1= 20421.7 PH= 84.0

XI	FO	A1	E1	TIMOP	RP
0.	-168.7244	0.7474	0.3520	103.5780	0.4843
5.0000	-167.1456	0.7647	0.3235	106.0049	0.5173
10.0000	-149.7241	0.8747	0.1767	114.6357	0.7202

NO ESCAPE FOR VB= 42000.0AT PHO= 84.00AND I= 15.00

VB= 42000.0 VINFP1= 20421.7 PH= 82.0

XI	FO	A1	E1	TIMOP	RP
0.	-163.1628	0.7671	0.3313	101.3462	0.5129
5.0000	-160.1405	0.7900	0.2978	103.5839	0.5547

NO ESCAPE FOR VB= 42000.0AT PHO= 82.00AND I= 10.00

****

Program 2

```
$JOB            0,3,6000        67-012,MYERS,APIT-SE
$IBJOB          MAP
$IBFTC MAIN     M94/2,XR7
C VENUS ASSISTED TRAJECTORIES IN THE ECLIPTIC
      TIME(A,G,E,T)=(2.*ATAN(SQRT((1.-E)/(1.+E))*TAN(T*R/2.))-E*SQRT(1.-
     1E**2)*SIN(T*R)/(1.+E*COS(T*R)))*SQRT((A**3)/G)/86400.
C CALCULATION OF DEPARTURE ORBITS
      READ(5,1)GCS,GCP1,GCP2,RP1,RP2,VP1,VP2,RADP1,RADP2
    1 FORMAT(9E10.0/4E10.0)
      PI=3.14159
      R=PI/180.
C DIMENSION FOR ONE GREATER THAN REQUIRED
      DIMENSION VB(162),PH(162,10),FO(162,10),VO(162,10),A(162,10),AD(16
     12,10),ET(162,10),VINFP1(162),D(22),E2(22),XNUDEG(22),PSIDEG(22),V3
     2(22),F3(22),A3(22),E3(22),OM(22),J1(162),TOP(22)
C VB(1) MUST BE GREATER THAN ESCAPE VEL = 36700 FT/SEC FOR EARTH
      VB(1)=38000.
      M=39
      N=7
      L=21
      DO 2 I=1,M
      VINFP1(I)=SQRT (VB(I)**2-2.*GCP1/RADP1)
      PH(I,1)=90.
      DO 3 J=1,N
      PHR=PH(I,J)*R
      IF(VINFP1(I)**2-(VP1*COS(PHR))**2)24,24,23
   24 J1(I)=J-1
      GO TO 29
   23 TANETP=VP1*COS (PHR)/(SQRT (VINFP1(I)**2-(VP1*COS (PHR))**2))
      J1(I)=J
      ET(I,J)=(PI-ATAN(TANETP))/R
      A(I,J)=PI/2.-ET(I,J)*R+PHR
      AD(I,J)=A(I,J)/R
      IF(PH(I,J)-90.)19,20,19
   20 VO(I,J)=VP1-VINFP1(I)
      GO TO 21
   19 VO(I,J)=VINFP1(I)*SIN (A(I,J))/COS (PHR)
   21 RPVO=RP1*(VO(I,J)**2)/GCS
      TANFO=RPVO*COS (PHR)*SIN (PHR)/(1.-RPVO*SIN (PHR)**2)
      FO(I,J)=(ATAN (TANFO)-PI)/R
      PH(I,J+1)=PH(I,J)-5.
    3 CONTINUE
   29 VB(I+1)=VB(I)+1000.
    2 CONTINUE
      WRITE(6,4)
    4 FORMAT(1H1,50X,21HEARTH DEPARTURE ORBIT)



      DO 6 I=1,M
      J2=J1(I)
      WRITE(6,5)VB(I),VINFP1(I),(PH(I,J),FO(I,J),VO(I,J),AD(I,J),ET(I,J)
     1,J=1,J2)
    5 FORMAT(1HA,25X,3HVB=,F10.0,33X,7HVINFP1=,F10.0/17X,2HPH,18X,2HFO,1
     18X,2HVO,18X,1HA,19X,2HET//(5F20.2))
    6 CONTINUE
C CALCULATION OF PRE-ASSIST ELLIPSE
      DO 13 I=1,M
      J2=J1(I)
      D(1)=0.
      DO 13 J=1,J2
      A1=RP1/(2.-RP1*(VO(I,J)**2)/GCS)
      A1AU=A1/(92901000.*5280.)
      E1=SQRT ((1-RP1*(VO(I,J)**2)/GCS-1.)*SIN (PH(I,J)*R))**2+COS (PH(I,
     1J)*R)**2)
      RPER1=A1*(1.-E1)
      IF(RPER1-RP2)15,15,16
   16 WRITE(6,17)
   17 FORMAT(1HA,31HVB INSUFFICIENT TO INTERCEPT P2)
      GO TO 13
   15 V1=SQRT (GCS*(2./RP2-1./A1))
      SPHI1=SQRT ((A1**2)*(1.-E1**2)/(RP2*(2.*A1-RP2)))
      CPHI1=SQRT (1.-SPHI1**2)
      TANF1=(RP2*(V1**2)/GCS)*CPHI1*SPHI1/(1.-(RP2*(V1**2)/GCS)*SPHI1**2
     1)
      IF(TANF1)40,40,41
   40 F1=ATAN(TANF1)/R
      GO TO 42
   41 F1=(ATAN (TANF1)-PI)/R
   42 THT12=F1-FO(I,J)
      TIM12=TIME(A1,GCS,E1,F1)-TIME(A1,GCS,E1,FO(I,J))
C CALCULATION OF HYPERBOLIC PASS TRAJECTORY
      VINF=SQRT (V1**2+VP2**2-2.*V1*VP2*SPHI1)
      A2=GCP2/(VINF**2)
      IF(VP2-V1*SPHI1)8,7,9
    7 WRITE(6,14)
   14 FORMAT(1HA,26HVP2=V1*SPHI1 FOR THIS CASE)
      GO TO 13
    8 TANNPH=-V1*CPHI1/SQRT (VINF**2-(V1*CPHI1)**2)
      GO TO 10
    9 TANNPH=V1*CPHI1/SQRT (VINF**2-(V1*CPHI1)**2)
   10 DO 11 K=1,L
      E2(K)=(RADP2+D(K)*6080.27*A2)/A2
      XNU=ATAN (1./SQRT (E2(K)**2-1.))
      XNUDEG(K)=XNU/R
```

Program 2 (Contd.)

```
      IF(VP2-V1*SPHI1)44,44,43
   44 PSI=ATAN(TANNPH)-2.*XNU+PI
      GO TO 50
   43 PSI=ATAN (TANNPH)-2.*XNU
   50 PSIDEG(K)=PSI/R
      V3(K)=SQRT (VP2**2+VINF**2-2.*VP2*VINF*COS (PSI))
      CPHI3=VINF*SIN (PSI)/V3(K)
      SPHI3=SQRT (1.-CPHI3**2)
      RPV3=RP2*(V3(K)**2)/GCS
      TANF3=RPV3*CPHI3*SPHI3/(1.-RPV3*SPHI3**2)
      IF(TANF3)45,46,46
   45 F3(K)=(ATAN(TANF3))/R
      GO TO 47
   46 F3(K)=(ATAN (TANF3)-PI)/R
   47 A3(K)=(RP2/(2.-RPV3))/(92901000.*5280.)
      E3(K)=SQRT (((RPV3-1.)*SPHI3)**2+CPHI3**2)
      AA=RP2/(2.-RPV3)
      TOP(K)=TIM12-TIME(AA,GCS,E3(K),F3(K))
      QM(K)=A3(K)*(1.-E3(K))
      D(K+1)=D(K)+100.
   11 CONTINUE
      WRITE(6,12)VB(I),PH(I,J),(THT12,F1,A1AU,E1,V1,VINF,D(K),F3(K),A3(K
     1),E3(K),V3(K),XNUDEG(K),E2(K),PSIDEG(K),TIM12,TOP(K),QM(K),K=1,L)
   12 FORMAT(1HA,2(X,3HVB=,F10.0,47X,3HPH=,F10.2//1X,4HTH12,9X,2HF1,9X,2
     1HA1,9X,2HE1,7X,2HV1,6X,4HVINF,4X,4HDOCA,6X,2HF3,6X,2HA3,9X,2HE3,6X
     2,2HV3,9X,2HNU,9X,2HE2,9X,3HPSI,4X,5HTIM12,9X,5HTOP,4X,2HQM//(F7.2,
     3F8.2,2F7.4,2F9.1,F8.0,F8.2,2F7.4,F9.1,F6.2,F8.3,F8.2,F7.1,F7.1,F8.
     45))
   13 CONTINUE
      STOP
      END
$DATA
 4.6868E21 1.4077E16 1.1488E16 4.9052E11 3.9480E11
 9.7751E04 1.1493E05 2.0902E07 2.0013E07
$EOF
```

Program 2 Output

VB= 45000. PH= 90.00

TH12	F1	A1	E1	V1	VINF	DOCA	F3	A3	E3	V3	NU	E2	PSI	TIM12	TOP	OM
56.35	-123.65	0.6841	0.4618	111590.5	53593.7	0.	-150.26	0.5419	0.5483	93738.2	9.59	6.004	53.69	62.6	104.1	0.24479
56.35	-123.65	0.6841	0.4618	111590.5	53593.7	100.	-149.76	0.5444	0.5457	94180.2	9.35	6.156	54.17	62.6	104.1	0.24733
56.35	-123.65	0.6841	0.4618	111590.5	53593.7	200.	-149.28	0.5469	0.5433	94601.1	9.12	6.308	54.62	62.6	104.1	0.24977
56.35	-123.65	0.6841	0.4618	111590.5	53593.7	300.	-148.82	0.5493	0.5410	95002.4	8.91	6.460	55.06	62.6	104.2	0.25212
56.35	-123.65	0.6841	0.4618	111590.5	53593.7	400.	-148.37	0.5516	0.5389	95385.5	8.70	6.612	55.47	62.6	104.2	0.25438
56.35	-123.65	0.6841	0.4618	111590.5	53593.7	500.	-147.94	0.5539	0.5368	95751.4	8.50	6.764	55.86	62.6	104.2	0.25656
56.35	-123.65	0.6841	0.4618	111590.5	53593.7	600.	-147.52	0.5560	0.5348	96101.4	8.31	6.916	56.24	62.6	104.2	0.25866
56.35	-123.65	0.6841	0.4618	111590.5	53593.7	700.	-147.11	0.5581	0.5329	96436.4	8.13	7.068	56.60	62.6	104.2	0.26069
56.35	-123.65	0.6841	0.4618	111590.5	53593.7	800.	-146.72	0.5602	0.5311	96757.4	7.96	7.220	56.95	62.6	104.2	0.26265
56.35	-123.65	0.6841	0.4618	111590.5	53593.7	900.	-146.34	0.5621	0.5294	97065.2	7.80	7.372	57.28	62.6	104.2	0.26454
56.35	-123.65	0.6841	0.4618	111590.5	53593.7	1000.	-145.98	0.5640	0.5277	97360.5	7.64	7.524	57.59	62.6	104.2	0.26637
56.35	-123.65	0.6841	0.4618	111590.5	53593.7	1100.	-145.62	0.5659	0.5262	97644.3	7.49	7.676	57.90	62.6	104.2	0.26813
56.35	-123.65	0.6841	0.4618	111590.5	53593.7	1200.	-145.28	0.5677	0.5247	97917.0	7.34	7.828	58.19	62.6	104.2	0.26984
56.35	-123.65	0.6841	0.4618	111590.5	53593.7	1300.	-144.94	0.5694	0.5232	98179.3	7.20	7.980	58.47	62.6	104.2	0.27149
56.35	-123.65	0.6841	0.4618	111590.5	53593.7	1400.	-144.62	0.5711	0.5218	98431.9	7.06	8.132	58.74	62.6	104.2	0.27310
56.35	-123.65	0.6841	0.4618	111590.5	53593.7	1500.	-144.30	0.5727	0.5205	98675.1	6.93	8.284	59.00	62.6	104.2	0.27465
56.35	-123.65	0.6841	0.4618	111590.5	53593.7	1600.	-144.00	0.5743	0.5192	98909.6	6.81	8.436	59.25	62.6	104.2	0.27615
56.35	-123.65	0.6841	0.4618	111590.5	53593.7	1700.	-143.70	0.5759	0.5180	99135.8	6.69	8.588	59.50	62.6	104.2	0.27761
56.35	-123.65	0.6841	0.4618	111590.5	53593.7	1800.	-143.41	0.5774	0.5168	99354.2	6.57	8.740	59.73	62.6	104.2	0.27902
56.35	-123.65	0.6841	0.4618	111590.5	53593.7	1900.	-143.13	0.5789	0.5156	99565.0	6.46	8.892	59.95	62.6	104.2	0.28039
56.35	-123.65	0.6841	0.4618	111590.5	53593.7	2000.	-142.85	0.5803	0.5145	99768.7	6.35	9.044	60.17	62.6	104.1	0.28172

VB= 45000. PH= 85.00

TH12	F1	A1	E1	V1	VINF	DOCA	F3	A3	E3	V3	NU	E2	PSI	TIM12	TOP	OM
51.93	-121.96	0.6917	0.4525	112275.7	52690.8	0.	-149.78	0.5447	0.5390	94221.9	9.87	5.837	54.07	55.7	97.7	0.25110
51.93	-121.96	0.6917	0.4525	112275.7	52690.8	100.	-149.26	0.5473	0.5364	94666.6	9.62	5.984	54.56	55.7	97.7	0.25371
51.93	-121.96	0.6917	0.4525	112275.7	52690.8	200.	-148.77	0.5498	0.5340	95090.2	9.39	6.130	55.02	55.7	97.7	0.25623
51.93	-121.96	0.6917	0.4525	112275.7	52690.8	300.	-148.29	0.5523	0.5317	95494.2	9.17	6.277	55.47	55.7	97.7	0.25865
51.93	-121.96	0.6917	0.4525	112275.7	52690.8	400.	-147.82	0.5547	0.5295	95879.9	8.95	6.424	55.89	55.7	97.7	0.26098
51.93	-121.96	0.6917	0.4525	112275.7	52690.8	500.	-147.37	0.5569	0.5274	96248.5	8.75	6.571	56.29	55.7	97.7	0.26323
51.93	-121.96	0.6917	0.4525	112275.7	52690.8	600.	-146.94	0.5592	0.5254	96601.1	8.56	6.718	56.68	55.7	97.7	0.26540
51.93	-121.96	0.6917	0.4525	112275.7	52690.8	700.	-146.52	0.5613	0.5234	96938.7	8.38	6.865	57.05	55.7	97.7	0.26749
51.93	-121.96	0.6917	0.4525	112275.7	52690.8	800.	-146.12	0.5634	0.5216	97262.2	8.20	7.012	57.40	55.7	97.7	0.26951
51.93	-121.96	0.6917	0.4525	112275.7	52690.8	900.	-145.72	0.5654	0.5199	97572.4	8.03	7.159	57.74	55.7	97.7	0.27147
51.93	-121.96	0.6917	0.4525	112275.7	52690.8	1000.	-145.34	0.5674	0.5182	97870.3	7.87	7.306	58.06	55.7	97.7	0.27335
51.93	-121.96	0.6917	0.4525	112275.7	52690.8	1100.	-144.97	0.5693	0.5166	98156.4	7.71	7.453	58.38	55.7	97.7	0.27518
51.93	-121.96	0.6917	0.4525	112275.7	52690.8	1200.	-144.61	0.5711	0.5151	98431.4	7.56	7.600	58.68	55.7	97.7	0.27694
51.93	-121.96	0.6917	0.4525	112275.7	52690.8	1300.	-144.26	0.5729	0.5136	98696.1	7.42	7.747	58.96	55.7	97.7	0.27865
51.93	-121.96	0.6917	0.4525	112275.7	52690.8	1400.	-143.93	0.5746	0.5122	98950.9	7.28	7.894	59.24	55.7	97.7	0.28031
51.93	-121.96	0.6917	0.4525	112275.7	52690.8	1500.	-143.60	0.5763	0.5108	99196.4	7.14	8.041	59.51	55.7	97.7	0.28191
51.93	-121.96	0.6917	0.4525	112275.7	52690.8	1600.	-143.28	0.5779	0.5095	99433.0	7.02	8.188	59.77	55.7	97.7	0.28346
51.93	-121.96	0.6917	0.4525	112275.7	52690.8	1700.	-142.97	0.5795	0.5083	99661.3	6.89	8.335	60.02	55.7	97.7	0.28497
51.93	-121.96	0.6917	0.4525	112275.7	52690.8	1800.	-142.67	0.5811	0.5071	99881.7	6.77	8.482	60.26	55.7	97.7	0.28643
51.93	-121.96	0.6917	0.4525	112275.7	52690.8	1900.	-142.38	0.5826	0.5059	100094.6	6.66	8.628	60.49	55.7	97.7	0.28784
51.93	-121.96	0.6917	0.4525	112275.7	52690.8	2000.	-142.09	0.5841	0.5048	100300.3	6.54	8.775	60.71	55.7	97.7	0.28922

Program 3

```
$JOB          0,5,8000       67-012,MYERS,AFIT-SE
$IBJOB        MAP
$IBFTC MAIN   M94/2,XR7,MODECK
C VENUS-MERCURY PERIHELION ASSISTED TRAJECTORIES
C CALCULATION OF DEPARTURE ORBITS
      TIME(A,G,E,T)=(2.*ATAN(SQRT((1.-E)/(1.+E))*TAN(T*R/2.))-E*SQRT(1.-
     1E**2)*SIN(T*R)/(1.+E*COS(T*R)))*SQRT((A**3)/G)/86400.
      READ(5,1)GCS,GCP1,GCP2,RP1,RP2,VP1,VP2,RADP1,RADP2
    1 FORMAT(5E10.0/4E10.0)
  101 READ(5,100)GCP3,RADP3,RP3,RA3
  100 FORMAT(4E10.0)
C DIMENSION FOR ONE GREATER THAN REQUIRED
      DIMENSION VB(162),PH(162,10),FO(162,10),VO(162,10),A(162,10),AD(16
     12,10),ET(162,10),VINFP1(162),D(22),E2(22),XNUDEG(22),PSIDEG(22),V2
     2(22),F3(22),A3(22),E3(22),OMM(22),J1(162),AA(22),T(22)
      DIMENSION D3(10),E4(10),XN4DEG(10),PSI4DG(10),V4(10),F7(10),A5(10)
     1,A5AU(10),E5(10),OMM(10),THT3P(10),T3P(10),THTOT(10),TIMOP(10)
C VB(1) MUST BE GREATER THAN ESCAPE VEL = 36700 FT/SEC FOR EARTH
      VB(1)=38000.
      PI=3.14159
      R=PI/180.
      VP3=SQRT(2.*GCS*RA3/(RP3*(RA3+RP3)))
      M=28
      N=4
      L=6
      L1=6
      DO 2 I=1,M
      VINFP1(I)=SQRT (VB(I)**2-2.*GCP1/RADP1)
      PH(I,1)=90.
      DO 3 J=1,N
      PHR=PH(I,J)*R
      IF(VINFP1(I)**2-(VP1*COS(PHR))**2)24,24,23
   24 J1(I)=J-1
      GO TO 29
   23 TANETP=VP1*COS (PHR)/(SQRT (VINFP1(I)**2-(VP1*COS (PHR))**2))
      J1(I)=J
      ET(I,J)=(PI-ATAN(TANETP))/R
      A(I,J)=PI/2.-ET(I,J)*R+PHR
      AD(I,J)=A(I,J)/R
      IF(PH(I,J)-90.)19,20,19
   20 VO(I,J)=VP1-VINFP1(I)
      GO TO 21
   19 VO(I,J)=VINFP1(I)*SIN (A(I,J))/COS (PHR)
   21 RPVO=RP1*(VO(I,J)**2)/GCS
      TANFO=RPVO*COS (PHR)*SIN (PHR)/(1.-RPVO*SIN (PHR)**2)
      FO(I,J)=(ATAN (TANFO)-PI)/R
      PH(I,J+1)=PH(I,J)-5.
    3 CONTINUE
   29 VB(I+1)=VB(I)+1000.
    2 CONTINUE
      WRITE-6,4)
    4 FORMAT(1H1,50X,21HEARTH DEPARTURE ORBIT)
      DO 6 I=1,M
      J2=J1(I)
      WRITE(6,5)VB(I),VINFP1(I),(PH(I,J),FO(I,J),VO(I,J),AD(I,J),ET(I,J)
     1,J=1,J2)
    5 FORMAT(1HA,25X,3HVB=,F10.0,33X,7HVINFP1=,F10.0/17X,2HPH,18X,2HFO,1
     18X,2HVO,18X,1HA,19X,2HET//(5F20.2))
    6 CONTINUE
C CALCULATION OF PRE-ASSIST ELLIPSE
      DO 13 I=1,M
      J2=J1(I)
      D(1)=0.
      DO 13 J=1,J2
      A1=RP1/(2.-RP1*(VO(I,J)**2)/GCS)
      A1AU=A1/(92901000.*5280.)
      E1=SQRT (((RP1*(VO(I,J)**2)/GCS-1.)*SIN (PH(I,J)*R))**2+COS (PH(I,
     1J)*R)**2)
      RPER1=A1*(1.-E1)
      IF(RPER1-RP2)15,15,16
   16 WRITE(6,17)
   17 FORMAT(1HA,31HVB INSUFFICIENT TO INTERCEPT P2)
      GO TO 13
   15 V1=SQRT (GCS*(2./RP2-1./A1))
      SPHI1=SQRT ((A1**2)*(1.-E1**2)/(RP2*(2.*A1-RP2)))
      CPHI1=SQRT (1.-SPHI1**2)
      TANF1=(RP2*(V1**2)/GCS)*CPHI1*SPHI1/(1.-(RP2*(V1**2)/GCS)*SPHI1**2
     1)
      IF(TANF1)40,40,41
   40 F1=ATAN(TANF1)/R
      GO TO 42
   41 F1=(ATAN (TANF1)-PI)/R
   42 THT12=F1-FO(I,J)
      TIM12=TIME(A1,GCS,E1,F1)-TIME(A1,GCS,E1,FO(I,J))
C CALCULATION OF HYPERBOLIC PASS TRAJECTORY
      VINF=SQRT (V1**2+VP2**2-2.*V1*VP2*SPHI1)
      A2=GCP2/(VINF**2)
      IF(VP2-V1*SPHI1)8,7,9
    7 WRITE-6,14)
   14 FORMAT(1HA,26HVP2=V1*SPHI1 FOR THIS CASE)
      GO TO 13
    8 TANPH=-V1*CPHI1/SQRT (VINF**2-(V1*CPHI1)**2)
```

Program 3 (Contd.)

```
      GO TO 10
    9 TANMPH=V1*CPHI1/SQRT (VINF**2-(V1*CPHI1)**2)
   10 DO 11 K=1,L
      E2(K)=(RADP2+D(K)*6080.27+A2)/A2
      XNU=ATAN (1./SQRT (E2(K)**2-1.))
      XNUDEG(K)=XNU/R
      IF(VP2-V1*SPHI1)44,44,43
   44 PSI=ATAN(TANMPH)-2.*XNU+PI
      GO TO 50
   43 PSI=ATAN (TANMPH)-2.*XNU
   50 PSIDEG(K)=PSI/R
      V2(K)=SQRT (VP2**2+VINF**2-2.*VP2*VINF*COS (PSI))
      CPHI3=VINF*SIN (PSI)/V2(K)
      SPHI3=SQRT (1.-CPHI3**2)
      RPV3=RP2*(V2(K)**2)/GCS
      TANF3=RPV3*CPHI3*SPHI3/(1.-RPV3*SPHI3**2)
      IF(TANF3)45,46,46
   45 F3(K)=(ATAN(TANF3))/R
      GO TO 47
   46 F3(K)=(ATAN (TANF3)-PI)/R
   47 A3(K)=(RP2/(2.-RPV3))
      AA(K)=A3(K)/(92901000.*5280.)
      E3(K)=SQRT ((RPV3-1.)*SPHI3)**2+CPHI3**2)
      QM(K)=AA(K)*(1.-E3(K))
      T2P=-TIME(A3(K),GCS,E3(K),F3(K))
      T(K)=T2P+TIM12
      D(K+1)=D(K)+100.
   11 CONTINUE
      WRITE(6,12)VB(I),PH(I,J),(THT12,F1,A1AU,E1,V1,T(K),D(K),F3(K),AA(K
     1),E3(K),V2(K),XNUDEG(K),TIM12,PSIDEG(K),QM(K),K=1,L)
   12 FORMAT(1HA,23X,3HVB=,F10.0,47X,3HPH=,F10.2//1X,4HTH12,9X,2HF1,5X,2
     1hA1,5X,2HE1,7X,2HV1,8X,4HTTOT,5X,4HDOCA,4X,2HF3,6X,2HA3,5X,2HE3,6X
     2,2HV3,8X,1HN,5X,3HT12,5X,3HPSI,6X,2HQM//(F7.2,F8.2,2F7.4,2F10.1,F7
     3.1,F8.2,2F7.4,F11.1,F8.2,F7.2,F8.2,F8.5))
  102 DO 13 K=1,L
      IF(QM(K)*92901000.*5280.-RP3)104,104,121
  121 WRITE(6,103)
  103 FORMAT(1HA,31HVB INSUFFICIENT TO INTERCEPT P3)
      GO TO 13
  104 D3(1)=0.
      V3=SQRT(GCS*(2./RP3-1./A3(K)))
      SPHI5=SQRT((A3(K)**2)*(1.-E3(K)**2)/(RP3*(2.*A3(K)-RP3)))
      CPHI5=SQRT(1.-SPHI5**2)
C HYPERBOLIC TRAJECTORY AT P3
      VINF3=SQRT(V3**2+VP3**2-2.*V3*VP3*SPHI5)
      TANF5=(RP3*(V3**2)/GCS)*CPHI5*SPHI5/(1.-(RP3*(V3**2)/GCS)*SPHI5**2


     1)
      IF(TANF5)105,105,106
  105 F5=ATAN(TANF5)/R
      GO TO 107
  106 F5=(ATAN(TANF5)-PI)/R
  107 THT23=F5-F3(K)
      T23=TIME(A3(K),GCS,E3(K),F5)-TIME(A3(K),GCS,E3(K),F3(K))
      A4=GCP3/(VINF3**2)
      IF(VP3-V3*SPHI5)108,109,110
  109 WRITE(6,111)
  111 FORMAT(1HA,26HVP3=V3*SPHI5 FOR THIS CASE)
      GO TO 13
  108 TANMP4=-V3*CPHI5/SQRT(VINF3**2-(V3*CPHI5)**2)
      GO TO 112
  110 TANMP4=V3*CPHI5/SQRT(VINF3**2-(V3*CPHI5)**2)
  112 DO 120 K1=1,L1
      E4(K1)=(RADP3+D3(K1)*6080.27+A4)/A4
      XNU4=ATAN(1./SQRT(E4(K1)**2-1.))
      XN4DEG(K1)=XNU4/R
      IF(VP3-V3*SPHI5)113,113,114
  113 PSI4=ATAN(TANMP4)-2.*XNU4+PI
      GO TO 115
  114 PSI4=ATAN(TANMP4)-2.*XNU4
  115 PSI4DG(K1)=PSI4/R
      V4(K1)=SQRT(VP3**2+VINF3**2-2.*VP3*VINF3*COS(PSI4))
      CPHI7=VINF3*SIN(PSI4)/V4(K1)
      SPHI7=SQRT(1.-CPHI7**2)
      RPV4=RP3*(V4(K1)**2)/GCS
      TANF7=RPV4*CPHI7*SPHI7/(1.-RPV4*(SPHI7**2))
      IF(TANF7)116,117,117
  116 F7(K1)=ATAN(TANF7)/R
      GO TO 118
  117 F7(K1)=(ATAN(TANF7)-PI)/R
  118 A5(K1)=RP3/(2.-RPV4)
      A5AU(K1)=A5(K1)/(92901000.*5280.)
      E5(K1)=SQRT((RPV4-1.)*SPHI7)**2+CPHI7**2)
      QMM(K1)=A5AU(K1)*(1.-E5(K1))
      THT3P(K1)=-F7(K1)
      T3P(K1)=-TIME(A5(K1),GCS,E5(K1),F7(K1))
      THTOT(K1)= THT12+THT23+THT3P(K1)
      TIMOP(K1)=TIM12+T23+T3P(K1)
      D3(K1+1)=D3(K1)+100.
  120 CONTINUE
      WRITE(6,122)VB(I),PH(I,J),D(K),QM(K),(THT23,F5,V3,VINF3,T23,D3(K1)
     1,F7(K1),A5AU(K1),E5(K1),V4(K1),XN4DEG(K1),PSI4DG(K1),THTOT(K1),TIM
     2OP(K1),QMM(K1),K1=1,L1)


  122 FORMAT(1HA,'9X,3HVB=,F10.0,5X,3HPH=,F7.2,5X,2HD=,F7.1,5X,3HQM=,F8.
     15//2X,4HTH2>,4X,2HF5,6X,2HV5,7X,5HVINF5,4X,3HT23,5X,2HD$,5X,2HF7,6
     2X,2HA5,5X,2HE5,6X,2HV7,6X,2HN4,4X,4HPSI4,4X,4HTHOP,4X,3HTOP,5X,3HQ
     3MM//(2F8.2,2F10.1,F7.2,F7.1,F8.2,2F7.4,F10.1,F4.2,2F8.2,F7.2,F8.5)
     4)
   13 CONTINUE
      STOP
      END
$DATA
 4.6868E21 1.4077E16 1.1488E16 4.9052E11 5.5483E11
 9.7751E04 1.1493E05 2.0902E07 2.0013E07
 7.7230E14 7.9393E06 1.5083E11 2.2893E11
$EOF
```

Program 3 Output

VB= 50000. PH= 90.00

TH12	F1	A1	E1	V1	TTOT	DOCA	F3	A3	E3	V3	N	TI2	PSI	QM
44.26	-135.74	0.6353	0.5741	106675.2	92.2	0.	-152.78	0.5289	0.6464	91283.8	6.74	55.41	52.50	0.18679
44.26	-135.74	0.6353	0.5741	106675.2	92.2	100.0	-152.42	0.5305	0.6464	91689.0	6.57	55.41	52.86	0.18863
44.26	-135.74	0.6353	0.5741	106675.2	92.2	200.0	-152.07	0.5325	0.6425	92073.5	6.40	55.41	53.19	0.19040
44.26	-135.74	0.6353	0.5741	106675.2	92.2	300.0	-151.74	0.5346	0.6407	92438.8	6.24	55.41	53.51	0.19209
44.26	-135.74	0.6353	0.5741	106675.2	92.2	400.0	-151.42	0.5365	0.6389	92786.5	6.09	55.41	53.81	0.19372
44.26	-135.74	0.6353	0.5741	106675.2	92.2	500.0	-151.11	0.5383	0.6373	93117.6	5.94	55.41	54.10	0.19528

VB= 50000. PH= 90.00 D= 0. QM= 0.18679

TH23	F5	V5	VINF5	T23	D3	F7	A5	E5	V7	N4	PSI4	THOP	TOP	QMM
62.79	-89.99	209905.1	115243.2	28.40	0.	-91.66	0.5102	0.6391	208933.3	0.42	80.55	198.72	92.26	0.18411
62.79	-89.99	209905.1	115243.2	28.40	100.0	-91.55	0.5114	0.6396	208681.8	0.39	80.61	198.60	92.26	0.18430
62.79	-89.99	209905.1	115243.2	28.40	200.0	-91.44	0.5125	0.6401	208575.8	0.36	80.66	198.49	92.25	0.18447
62.79	-89.99	209905.1	115243.2	28.40	300.0	-91.35	0.5135	0.6405	208650.4	0.34	80.70	198.40	92.25	0.18461
62.79	-89.99	209905.1	115243.2	28.40	400.0	-91.27	0.5143	0.6408	208731.2	0.32	80.74	198.32	92.24	0.18474
62.79	-89.99	209905.1	115243.2	28.40	500.0	-91.20	0.5151	0.6411	208796.0	0.30	80.78	198.25	92.24	0.18485

VB= 50000. PH= 90.00 D= 100.0 QM= 0.18863

TH23	F5	V5	VINF5	T23	D3	F7	A5	E5	V7	N4	PSI4	THOP	TOP	QMM
63.20	-89.22	210081.6	114286.7	28.42	0.	-90.92	0.5121	0.6369	208537.2	0.[illegible]	80.85	198.37	92.27	0.18594
63.20	-89.22	210081.6	114286.7	28.42	100.0	-90.80	0.5133	0.6374	208646.5	0.[illegible]9	80.91	198.25	92.27	0.18613
63.20	-89.22	210081.6	114286.7	28.42	200.0	-90.69	0.5144	0.6379	208741.4	0.37	80.96	198.15	92.26	0.18629
63.20	-89.22	210081.6	114286.7	28.42	300.0	-90.60	0.5154	0.6383	208824.6	0.34	81.00	198.06	92.26	0.18644
63.20	-89.22	210081.6	114286.7	28.42	400.0	-90.52	0.5162	0.6386	208898.0	0.32	81.04	197.98	92.25	0.18657
63.20	-89.22	210081.6	114286.7	28.42	500.0	-90.45	0.5170	0.6389	208963.3	0.31	81.08	197.90	92.25	0.18668

VB= 50000. PH= 90.00 D= 200.0 QM= 0.19040

TH23	F5	V5	VINF5	T23	D3	F7	A5	E5	V7	N4	PSI4	THOP	TOP	QMM
63.59	-88.48	210249.7	113367.5	28.44	0.	-90.20	0.5139	0.6348	208692.9	0.43	81.13	198.05	92.29	0.18769
63.59	-88.48	210249.7	113367.5	28.44	100.0	-90.07	0.5151	0.6353	208803.2	0.40	81.20	197.92	92.28	0.18788
63.59	-88.48	210249.7	113367.5	28.44	200.0	-89.97	0.5163	0.6357	208898.8	0.37	81.25	197.82	92.27	0.18805
63.59	-88.48	210249.7	113367.5	28.44	300.0	-89.88	0.5172	0.6362	208982.6	0.35	81.29	197.73	92.27	0.18819
63.59	-88.48	210249.7	113367.5	28.44	400.0	-89.80	0.5181	0.6365	209056.6	0.33	81.34	197.65	92.26	0.18832
63.59	-88.48	210249.7	113367.5	28.44	500.0	-89.72	0.5189	0.6368	209122.4	0.31	81.37	197.57	92.26	0.18844

VB= 50000. PH= 90.00 D= 300.0 QM= 0.19209

TH23	F5	V5	VINF5	T23	D3	F7	A5	E5	V7	N4	PSI4	THOP	TOP	QMM
63.97	-87.77	210409.9	112483.5	28.46	0.	-89.50	0.5156	0.6327	208841.1	0.44	81.41	197.73	92.30	0.18937
63.97	-87.77	210409.9	112483.5	28.46	100.0	-89.38	0.5169	0.6333	208952.2	0.41	81.47	197.61	92.29	0.18956
63.97	-87.77	210409.9	112483.5	28.46	200.0	-89.27	0.5180	0.6337	209048.6	0.38	81.53	197.50	92.28	0.18973
63.97	-87.77	210409.9	112483.5	28.46	300.0	-89.18	0.5190	0.6341	209133.0	0.36	81.58	197.41	92.28	0.18988
63.97	-87.77	210409.9	112483.5	28.46	400.0	-89.10	0.5199	0.6345	209207.6	0.34	81.62	197.33	92.27	0.19001
63.97	-87.77	210409.9	112483.5	28.46	500.0	-89.02	0.5207	0.6348	209273.9	0.32	81.65	197.25	92.27	0.19012

VB= 50000. PH= 90.00 D= 400.0 QM= 0.19372

TH23	F5	V5	VINF5	T23	D3	F7	A5	E5	V7	N4	PSI4	THOP	TOP	QMM
64.34	-87.08	210562.9	111632.7	28.48	0.	-88.83	0.5172	0.6308	208982.4	0.44	81.68	197.43	92.31	0.19098
64.34	-87.08	210562.9	111632.7	28.48	100.0	-88.71	0.5185	0.6313	209094.3	0.41	81.74	197.31	92.30	0.19117
64.34	-87.08	210562.9	111632.7	28.48	200.0	-88.60	0.5197	0.6318	209191.4	0.39	81.80	197.20	92.29	0.19134
64.34	-87.08	210562.9	111632.7	28.48	300.0	-88.51	0.5207	0.6322	209276.4	0.36	81.85	197.10	92.28	0.19149
64.34	-87.08	210562.9	111632.7	28.48	400.0	-88.42	0.5216	0.6326	209351.5	0.34	81.89	197.02	92.28	0.19162
64.34	-87.08	210562.9	111632.7	28.48	500.0	-88.35	0.5224	0.6330	209418.4	0.32	81.93	196.95	92.28	0.19174

VB= 50000. PH= 90.00 D= 500.0 QM= 0.19528

TH23	F5	V5	VINF5	T23	D3	F7	A5	E5	V7	N4	PSI4	THOP	TOP	QMM
64.69	-86.42	210709.0	110813.1	28.50	0.	-88.19	0.5188	0.6289	209117.0	0.45	81.94	197.14	92.32	0.19253
64.69	-86.42	210709.0	110813.1	28.50	100.0	-88.06	0.5201	0.6295	209229.7	0.42	82.01	197.01	92.31	0.19272
64.69	-86.42	210709.0	110813.1	28.50	200.0	-87.95	0.5213	0.6300	209327.5	0.39	82.06	196.91	92.30	0.19289
64.69	-86.42	210709.0	110813.1	28.50	300.0	-87.86	0.5223	0.6304	209413.2	0.37	82.11	196.81	92.29	0.19304
64.69	-86.42	210709.0	110813.1	28.50	400.0	-87.77	0.5232	0.6308	209488.8	0.35	82.15	196.73	92.29	0.19317
64.69	-86.42	210709.0	110813.1	28.50	500.0	-87.70	0.5240	0.6312	209556.2	0.33	82.19	196.65	92.28	0.19329

Program 4

```
$JOB          0,8,4000       67-012,LT HYERS,AFIT-SE
$IBJOB        MAP
$IBFTC MAIN   M94/2,XR7,NODECK
C DOUBLE ASSIST AT VENUS
      TIME(A,G,E,T)=(2.*ATAN(SQRT((1.-E)/(1.+E))*TAN(T*R/2.))-E*SQRT(1.-
     1E**2)*SIN(T*R)/(1.+E*COS(T*R)))*SQRT((A**3)/G)/86400.
      READ(5,1)GCS,GCP1,GCP2,RP1,RP2,VP1,VP2,RADP1,RADP2
    1 FORMAT(5E10.0/4E10.0)
C DIMENSION FOR ONE GREATER THAN REQUIRED
      DIMENSION VB(162),PH(162,10),FO(162,10),VO(162,10),AI(162,10),AD(16
     12,10),ET(162,10),VINFP1(162),J1(162)
      DIMENSION D2(25),E4(25),XN4DEG(25),PSI4DG(25),V4(25),F5(25),A5(25)
     1,A5AU(25),E5(25),QH2(25),THTOT(25),TIHOP(25)
C VB(1) MUST BE GREATER THAN ESCAPE VEL = 36700 FT/SEC FOR EARTH
      VB(1)=38000.
      PI=3.14159
      R=PI/180.
      M=33
      N=1
      L2=21
      L=1
      TAUP2=2.*PI*SQRT(RP2**3/GCS)/86400.
C CALCULATION OF DEPARTURE ORBITS
      DO 2 I=1,M
      VINFP1(I)=SQRT (VB(I)**2-2.*GCP1/RADP1)
      PH(I,1)=90.
      DO 3 J=1,M
      PHR=PH(I,J)*R
      IF(VINFP1(I)**2-(VP1*COS(PHR))**2)24,24,23
   24 J1(I)=J-1
      GO TO 29
   23 TANETP=VP1*COS (PHR)/(SQRT (VINFP1(I)**2-(VP1*COS (PHR))**2))
      J1(I)=J
      ET(I,J)=(PI-ATAN(TANETP))/R
      A(I,J)=PI/2.-ET(I,J)*R+PHR
      AD(I,J)=A(I,J)/R
      IF(PH(I,J)-90.)19,20,19
   20 VO(I,J)=VP1-VINFP1(I)
      GO TO 21
   19 VO(I,J)=VINFP1(I)*SIN (A(I,J))/COS (PHR)
   21 RPVO=RP1*(VO(I,J)**2)/GCS
      TANFO=RPVO*COS (PHR)*SIN (PHR)/(1.-RPVO*SIN (PHR)**2)
      FO(I,J)=(ATAN (TANFO)-PI)/R
      PH(I,J+1)=PH(I,J)-2.
    3 CONTINUE
   29 VB(I+1)=VB(I)+1000.
    2 CONTINUE
      WRITE(6,4)
    4 FORMAT(1H1,50X,21HEARTH DEPARTURE ORBIT)
      DO 6 I=1,M
      J2=J1(I)
      WRITE(6,5)VB(I),VINFP1(I),(PH(I,J),FO(I,J),VO(I,J),AD(I,J),ET(I,J)
     1,J=1,J2)
    5 FORMAT(1HA,25X,3HVB=,F10.0,33X,7HVINFP1=,F10.0/17X,2HPH,18X,2HFO,1
     18X,2HVO,18X,1HA,19X,2HET//(5F20.2))
    6 CONTINUE
C CALCULATION OF PRE-ASSIST ELLIPSE
      DO 13 I=1,M
      J2=J1(I)
      DO 13 J=1,J2
      D=0.
      A1=RP1/(2.-RP1*(VO(I,J)**2)/GCS)
      A1AU=A1/(92901000.*5280.)
      E1=SQRT (((RP1*(VO(I,J)**2)/GCS-1.)*SIN (PH(I,J)*R))**2+COS (PH(I,
     1J)*R)**2)
      RPER1=A1*(1.-E1)
      IF(RPER1-RP2)15,15,16
   16 WRITE(6,17)
   17 FORMAT(1HA,31HVB INSUFFICIENT TO INTERCEPT P2)
      GO TO 13
   15 V1=SQRT (GCS*(2./RP2-1./A1))
      SPHI1=SQRT ((A1**2)*(1.-E1**2)/(RP2*(2.*A1-RP2)))
      CPHI1=SQRT (1.-SPHI1**2)
      TANF1=(RP2*(V1**2)/GCS)*CPHI1*SPHI1/(1.-(RP2*(V1**2)/GCS)*SPHI1**2
     1)
      IF(TANF1)40,40,41
   40 F1=ATAN(TANF1/R
      GO TO 42
   41 F1=(ATAN (TANF1)-PI)/R
   42 THT12=F1-FO(I,J)
      TIM12=TIME(A1,GCS,E1,F1)-TIME(A1,GCS,E1,FO(I,J))
C CALCULATION OF HYPERBOLIC PASS TRAJECTORY--FIRST PASS
      VINF=SQRT (V1**2+VP2**2-2.*V1*VP2*SPHI1)
      A2=GCP2/(VINF**2)
   10 E2=(RADP2+D*6080.27+A2)/A2
      XNU=ATAN(1./SQRT(E2**2-1.))
      XNUDEG=XNU/R
      IF(VP2-V1*SPHI1)8,7,9
    7 WRITE(6,14)
   14 FORMAT(1HA,26HVP2=V1*SPHI1 FOR THIS CASE)
      GO TO 13
    8 TANPH=-V1*CPHI1/SQRT (VINF**2-(V1*CPHI1)**2)
```

Program 4 (Contd.)

```
   44 PSI=ATAN(TANNPH)-2.*XNU+PI
      GO TO 30
    9 TANNPH=V1*CPHI1/SQRT (VINF**2-(V1*CPHI1)**2)
   43 PSI=ATAN (TANNPH)-2.*XNU
   50 PSIDEG   =PSI/R
      V2    =SQRT (VP2**2+VINF**2-2.*VP2*VINF*COS (PSI))
      CPHI3=VINF*SIN (PSI)/V2
      SPHI3=SQRT (1.-CPHI3**2)
      RPV3=RP2*(V2    **2)/GCS
      TANF3=RPV3*CPHI3*SPHI3/(1.-RPV3*SPHI3**2)
      IF(TANF3)45,46,46
   45 F3.   =(ATAN(TANF3))/R
      GO TO 47
   46 F3    =(ATAN (TANF3)-PI)/R
   47 A3    =(RP2/(2.-RPV3))
      AA    =A3    /(92901000.*5280.)
      E3    =SQRT (((RPV3-1.)*SPHI3)**2+CPHI3**2)
      AP3=A3*(1.+E3)
      IF(AP3-RP2)216,215,215
  216 WRITE(6,217)
  217 FORMAT(1HA,5X,34HAPHELION TOO SMALL FOR SECOND PASS)
      GO TO 13
  215 QM=AA*(1.-E3)
      T2P=-TIME(A3,GCS,E3,F3)
      T=T2P+TIM12
      TAUP=2.*PI*SQRT(A3**3/GCS)/86400.
      DO 200 MP1=1,5
      DO 200 NSP=1,9
      IF(ABS(FLOAT(NSP)*TAUP-FLOAT(MP1)*TAUP2)-.1)201,200,200
  200 CONTINUE
      D=D+5.
      IF(D-5000.)10,10,202
  202 WRITE(6,203)VB(I),PH(I,J)
  203 FORMAT(1HA,5X,25HNO  MORE  TRAJECTORIES FOR VB=,F10.1,2X,7HAND PH=
     1,F8.2,2X,13HBELOW 5000 MI)
      GO TO 13
C CALCULATION OF SECOND ASSIST TRAJECTORY
  201 VINF3=SQRT(V2**2+VP2**2-2.*V2*VP2*SPHI3)
      A4=GCP2/VINF3**2
      D2(1)=0.
      DO 212 K2=1,L2
      E4(K2)=(RADP2+D2(K2)*6080.27+A4)/A4
      XNU4=ATAN(1./SQRT(E4(K2)**2-1.))
      XN4DEG(K2)=XNU4/R
      IF(VP2-V2*SPHI3)206,205,204
  206 TANNP4=-V2*CPHI3/SQRT(VINF3**2-(V2*CPHI3)**2)


      PSI4=ATAN(TANNP4)-2.*XNU4+PI
      GO TO 208
  205 WRITE(6,207)
  207 FORMAT(1HA,26HVP2=V2*SPHI3 FOR THIS CASE)
      GO TO 212
  204 TANNP4= V2*CPHI3/SQRT(VINF3**2-(V2*CPHI3)**2)
      PSI4=ATAN(TANNP4)-2.*XNU4
  208 PSI4DG(K2)=PSI4/R
      V4(K2)=SQRT(VP2**2+VINF3**2-2.*VP2*VINF3*COS(PSI4))
      RPV4=RP2*(V4(K2)**2)/GCS
      IF(RPV4-2.)219,222,222
  222 L=K2+1
      GO TO 223
  219 CPHI5=VINF3*SIN(PSI4)/V4(K2)
      SPHI5=SQRT(1.-CPHI5**2)
      TANF5=RPV4*CPHI5*SPHI5/(1.-RPV4*SPHI5**2)
      IF(PSI4)327,328,328
  327 F5(K2)=(ATAN(TANF5)+PI)/R
      GO TO 211
  328 IF(TANF5)209,210,210
  209 F5(K2)=(ATAN(TANF5))/R
      GO TO 211
  210 F5(K2)=(ATAN(TANF5)-PI)/R
  211 A5(K2)=RP2/(2.-RPV4)
      A5AU(K2)=A5(K2)/(92901000.*5280.)
      E5(K2)=SQRT(((RPV4-1.)*SPHI5)**2+CPHI5**2)
      QM2(K2)=A5AU(K2)*(1.-E5(K2))
      IF(PSI4)329,330,330
  329 THTOT(K2)=THT12-F5(K2)+360.
      TIMOP(K2)=TIM12+FLOAT(NSP)*TAUP-TIME(A5(K2),GCS,E5(K2),F5(K2))+TAU
     1P
      GO TO 223
  330 THTOT(K2)=THT12-F5(K2)
      TIMOP(K2)=TIM12+FLOAT(NSP)*TAUP-TIME(A5(K2),GCS,E5(K2),F5(K2))
  223 D2(K2+1)=D2(K2)+10000.
  212 CONTINUE
      WRITE(6,213)VB(I),PH(I,J),D,TAUP2,NP1,NSP,THT12,F1,A1AU,E1,V1,TIM1
     12,T,F3,AA,E3,V2,XNUDEG,PSIDEG,TAUP,QM,(D2(K2),VINF3,V4(K2),XN4DEG(
     2K2),PSI4DG(K2),F5(K2),THTOT(K2),TIMOP(K2),A5AU(K2),E5(K2),QM2(K2),
     3K2=L,L2)
  213 FORMAT(1HA,5X,3HVB=,F10.1,5X,3HPH=,F10.2,5X,6HDOCA1=,F8.2,5X,6HTAU
     1P2=,F7.1,5X,4HMP1=,I3,5X,4HNSP=,I3//2X,4HTH12,5X,2HF1,6X,2HA1,5X,2
     2HE1,6X,2HV1,6X,3HT12,5X,1HT,6X,2HF3,6X,2HA3,5X,2HE3,6X,2HV3,7X,1HM
     3,7X,3HPSI,4X,4HTAUP,4X,2HQM//2F8.2,2F7.4,F10.1,2F7.1,F8.2,2F7.4,F1
     40.1,2F8.2,F7.1,F8.5//3X,5HDOCA2,5X,5HVINF3,7X,2HV3,8X,2HN4,6X,4HP
     5SI4,6X,2HF5,6X,5HTHTOT,3X,5HTIMOP,5X,2HA5,6X,2HE5,6X,3HQM2//(F9.0,


     62F11.1,4F9.2,F8.1,2F8.4,F9.5))
      D=D+15.
      GO TO 10
   13 CONTINUE
      STOP
      END
$DATA
 4.6098E21 1.4077E16 1.1488E16 4.9052E11 3.5480E11
 9.7791E04 1.1493E05 2.0902E07 2.0013E07
$EOF
```

Program 4 Output

VB= 51000.0 PH= 90.00 DOCA1= 165.00 TAUP2= 224.5 MP1= 5 NSP= 8

TH12	F1	A1	E1	V1	T12	T	F3	A3	E3	V3	N	PSI	TAUP	QM
42.46	-137.54	0.6276	0.5933	105811.0	54.4	90.5	-152.67	0.5287	0.6603	91337.9	6.14	52.64	140.3	0.17960

DOCA2	VINF3	V5	N4	PSI4	F5	THTOT	TIMOP	A5	E5	QM2
0.	67782.7	76470.3	6.38	39.88	-163.53	205.99	1213.0	0.4685	0.7303	0.12527
1000.00	67782.7	79594.3	5.02	42.60	-161.62	204.08	1212.9	0.4757	0.7163	0.13495
2000.00	67782.7	81640.1	4.14	44.37	-160.28	202.74	1212.8	0.4837	0.7069	0.14175
3000.00	67782.7	83082.0	3.52	45.60	-159.30	201.76	1212.8	0.4896	0.7002	0.14677
4000.00	67782.7	84152.5	3.06	46.52	-158.55	201.01	1212.8	0.4941	0.6952	0.15062
5000.00	67782.7	84978.3	2.71	47.22	-157.95	200.41	1212.8	0.4977	0.6912	0.15367
6000.00	67782.7	85634.8	2.43	47.78	-157.47	199.93	1212.8	0.5006	0.6881	0.15614
7000.00	67782.7	86169.0	2.20	48.23	-157.07	199.53	1212.8	0.5030	0.6856	0.15818
8000.00	67782.7	86612.3	2.01	48.61	-156.74	199.20	1212.8	0.5051	0.6836	0.15990
9000.00	67782.7	86985.9	1.86	48.93	-156.45	198.91	1212.8	0.5068	0.6818	0.16136
10000.00	67782.7	87305.2	1.72	49.20	-156.21	198.67	1212.8	0.5083	0.6801	0.16262
11000.00	67782.7	87581.1	1.60	49.43	-155.99	198.45	1212.8	0.5096	0.6787	0.16372
12000.00	67782.7	87821.9	1.50	49.64	-155.80	198.26	1212.8	0.5108	0.6776	0.16468
13000.00	67782.7	88033.9	1.41	49.82	-155.64	198.10	1212.8	0.5118	0.6766	0.16554
14000.00	67782.7	88222.1	1.33	49.97	-155.49	197.95	1212.8	0.5127	0.6756	0.16630
15000.00	67782.7	88390.1	1.26	50.12	-155.36	197.81	1212.8	0.5135	0.6748	0.16698
16000.00	67782.7	88541.1	1.20	50.24	-155.23	197.69	1212.8	0.5143	0.6741	0.16760
17000.00	67782.7	88677.5	1.14	50.36	-155.13	197.58	1212.8	0.5149	0.6734	0.16816
18000.00	67782.7	88801.4	1.09	50.47	-155.03	197.48	1212.8	0.5155	0.6728	0.16867
19000.00	67782.7	88914.3	1.04	50.56	-154.93	197.39	1212.8	0.5161	0.6723	0.16913
20000.00	67782.7	89017.8	0.99	50.65	-154.85	197.31	1212.8	0.5166	0.6718	0.16956

VB= 51000.0 PH= 90.00 DOCA1= 1660.00 TAUP2= 224.5 MP1= 2 NSP= 3

TH12	F1	A1	E1	V1	T12	T	F3	A3	E3	V3	N	PSI	TAUP	QM
42.46	-137.54	0.6276	0.5933	105811.0	54.4	90.5	-149.16	0.5520	0.6405	95438.9	4.41	56.08	149.6	0.19843

DOCA2	VINF3	V5	N4	PSI4	F5	THTOT	TIMOP	A5	E5	QM2
0.	67782.7	80430.4	6.38	43.33	-161.08	203.54	1212.4	0.4789	0.7125	0.13768
1000.00	67782.7	83600.8	5.02	46.03	-158.94	201.40	1212.3	0.4917	0.6978	0.14862
2000.00	67782.7	85669.3	4.14	47.81	-157.45	199.90	1212.3	0.5008	0.6879	0.15627
3000.00	67782.7	87124.0	3.52	49.04	-156.35	198.81	1212.3	0.5075	0.6810	0.16190
4000.00	67782.7	88202.2	3.06	49.96	-155.50	197.96	1212.3	0.5126	0.6757	0.16622
5000.00	67782.7	89033.3	2.71	50.66	-154.84	197.30	1212.4	0.5167	0.6717	0.16963
6000.00	67782.7	89693.2	2.43	51.22	-154.30	196.76	1212.4	0.5200	0.6685	0.17238
7000.00	67782.7	90230.0	2.20	51.67	-153.85	196.31	1212.4	0.5228	0.6659	0.17466
8000.00	67782.7	90675.2	2.01	52.05	-153.48	195.94	1212.4	0.5251	0.6637	0.17658
9000.00	67782.7	91050.2	1.86	52.37	-153.16	195.62	1212.4	0.5270	0.6619	0.17820
10000.00	67782.7	91370.6	1.72	52.64	-152.88	195.34	1212.4	0.5287	0.6603	0.17961
11000.00	67782.7	91647.3	1.60	52.87	-152.64	195.10	1212.4	0.5302	0.6590	0.18083
12000.00	67782.7	91888.9	1.50	53.08	-152.43	194.89	1212.4	0.5315	0.6578	0.18190
13000.00	67782.7	92101.5	1.41	53.26	-152.24	194.70	1212.4	0.5327	0.6567	0.18285
14000.00	67782.7	92290.1	1.33	53.42	-152.08	194.54	1212.4	0.5337	0.6558	0.18370
15000.00	67782.7	92458.5	1.26	53.56	-151.93	194.39	1212.4	0.5347	0.6550	0.18446
16000.00	67782.7	92609.8	1.20	53.69	-151.79	194.25	1212.4	0.5355	0.6543	0.18514
17000.00	67782.7	92746.5	1.14	53.80	-151.67	194.13	1212.4	0.5363	0.6536	0.18576
18000.00	67782.7	92870.6	1.09	53.91	-151.56	194.02	1212.4	0.5370	0.6530	0.18633
19000.00	67782.7	92983.8	1.04	54.00	-151.46	193.92	1212.4	0.5376	0.6524	0.18685
20000.00	67782.7	93087.4	0.99	54.09	-151.36	193.82	1212.4	0.5382	0.6519	0.18732

VB= 51000.0 PH= 90.00 DOCA1= 4960.00 TAUP2= 224.5 MP1= .5 NSP= 7

TH12	F1	A1	E1	V1	T12	T	F3	A3	E3	V3	N	PSI	TAUP	QM
42.46	-137.54	0.6276	0.5933	105811.0	54.4	90.6	-145.08	0.5780	0.6214	99436.4	2.72	59.47	160.3	0.21880

DOCA2	VINF3	V5	N4	PSI4	F5	THTOT	TIMOP	A5	E5	QM2
0.	67782.7	84382.7	6.38	46.71	-158.38	200.84	1212.8	0.4951	0.6941	0.15144
1000.00	67782.7	87582.2	5.02	49.43	-155.99	198.45	1212.8	0.5096	0.6787	0.16372
2000.00	67782.7	89663.3	4.14	51.20	-154.32	196.78	1212.9	0.5199	0.6686	0.17226
3000.00	67782.7	91124.1	3.52	52.43	-153.09	195.55	1212.9	0.5274	0.6615	0.17853
4000.00	67782.7	92205.5	3.06	53.34	-152.15	194.61	1212.9	0.5329	0.6562	0.18332
5000.00	67782.7	93038.2	2.71	54.05	-151.41	193.87	1212.9	0.5379	0.6522	0.18710
6000.00	67782.7	93699.0	2.43	54.61	-150.81	193.26	1212.9	0.5417	0.6489	0.19015
7000.00	67782.7	94236.3	2.20	55.06	-150.31	192.77	1212.9	0.5448	0.6463	0.19267
8000.00	67782.7	94681.5	2.01	55.44	-149.89	192.35	1213.0	0.5474	0.6442	0.19478
9000.00	67782.7	95056.6	1.86	55.76	-149.53	191.99	1213.0	0.5496	0.6423	0.19653
10000.00	67782.7	95376.8	1.72	56.03	-149.22	191.68	1213.0	0.5516	0.6408	0.19813
11000.00	67782.7	95653.4	1.60	56.26	-148.96	191.42	1213.0	0.5533	0.6395	0.19948
12000.00	67782.7	95894.8	1.50	56.46	-148.72	191.18	1213.0	0.5548	0.6383	0.20066
13000.00	67782.7	96107.2	1.41	56.64	-148.51	190.97	1213.0	0.5561	0.6373	0.20170
14000.00	67782.7	96295.5	1.33	56.80	-148.33	190.79	1213.0	0.5572	0.6364	0.20266
15000.00	67782.7	96463.7	1.26	56.95	-148.16	190.62	1213.0	0.5583	0.6355	0.20347
16000.00	67782.7	96614.8	1.20	57.07	-148.01	190.47	1213.0	0.5593	0.6348	0.20423
17000.00	67782.7	96751.3	1.14	57.19	-147.87	190.33	1213.0	0.5601	0.6342	0.20491
18000.00	67782.7	96875.2	1.09	57.29	-147.75	190.21	1213.0	0.5609	0.6336	0.20553
19000.00	67782.7	96988.2	1.04	57.39	-147.63	190.09	1213.0	0.5616	0.6330	0.20610
20000.00	67782.7	97091.6	0.99	57.48	-147.53	189.99	1213.0	0.5623	0.6325	0.20662

NO MORE TRAJECTORIES FOR VB= 51000.0 AND PH= 90.00 BELOW 5000 MI

Program 5

```
$JOB          0,25,7000      67-012,LT MYERS,AFIT-SE
$IBJOB        MAP
$IBFTC MAIN   M94/2,XR7
C TRIPLE ASSIST AT VENUS
      TIME(A,G,E,T)=(2.*ATAN(SQRT((1.-E)/(1.+E))*TAN(T*R/2.))-E*SQRT(1.-
     1E**2)*SIN(T*R)/(1.+E*COS(T*R)))*SQRT((A**3)/G)/86400.
      READ(5,1)GCS,GCP1,GCP2,RP1,RP2,VP1,VP2,RADP1,RADP2
    1 FORMAT(5E10.0/4E10.0)
C DIMENSION FOR ONE GREATER THAN REQUIRED
      DIMENSION VB(162),PH(162,10),F0(162,10),V0(162,10),A(162,10),AD(16
     12,10),ET(162,10),VINFP1(162),J1(162)
      DIMENSION D4(25),E6(25),XN6DEG(25),P316DG(25),V6(25),F7(25),A7(25)
     1,A7AU(25),E7(25),QM4(25),THT02(25),TIM02(25)
C VB(1) MUST BE GREATER THAN ESCAPE VEL = 36700 FT/SEC FOR EARTH
      VB(1)=38000.
      PI=3.14159
      R=PI/180.
      M=99
      N=1
      L2=21
      L=1
      TAUP2=2.*PI*SQRT(RP2**3/GCS)/86400.
C CALCULATION OF DEPARTURE ORBITS
      DO 2 I=1,M
      VINFP1(I)=SQRT (VB(I)**2-2.*GCP1/RADP1)
      PH(I,1)=90.
      DO 3 J=1,N
      PHR=PH(I,J)*R
      IF(VINFP1(I)**2-(VP1*COS(PHR))**2)24,24,23
   24 J1(I)=J-1
      GO TO 29
   23 TANETP=VP1*COS (PHR)/(SQRT (VINFP1(I)**2-(VP1*COS (PHR))**2))
      J1(I)=J
      ET(I,J)=(PI-ATAN(TANETP))/R
      A(I,J)=PI/2.-ET(I,J)*R+PHR
      AD(I,J)=A(I,J)/R
      IF(PH(I,J)-90.)19,20,19
   20 V0(I,J)=VP1-VINFP1(I)
      GO TO 21
   19 V0(I,J)=VINFP1(I)*SIN (A(I,J))/COS (PHR)
   21 RPV0=RP1*(V0(I,J)**2)/GCS
      TANF0=RPV0*COS (PHR)*SIN (PHR)/(1.-RPV0*SIN (PHR)**2)
      F0(I,J)=(ATAN (TANF0)-PI)/R
      PH(I,J+1)=PH(I,J)-2.
    3 CONTINUE
   29 VB(I+1)=VB(I)+1000.
    2 CONTINUE
      WRITE(6,4)
    4 FORMAT(1H1,50X,21HEARTH DEPARTURE ORBIT)
      DO 6 I=1,M
      J2=J1(I)
      WRITE(6,5)VB(I),VINFP1(I),(PH(I,J),F0(I,J),V0(I,J),AD(I,J),ET(I,J)
     1,J=1,J2)
    5 FORMAT(1HA,25X,3HVB=,F10.0,33X,7HVINFP1=,F10.0/17X,2HPH,18X,2HF0,1
     18X,2HV0,16X,1HA,19X,2HET//(5F20.2))
    6 CONTINUE
C CALCULATION OF PRE-ASSIST ELLIPSE
      DO 13 I=1,M
      J2=J1(I)
      DO 13 J=1,J2
      D=0.
      A1=RP1/(2.-RP1*(V0(I,J)**2)/GCS)
      A1AU=A1/(92901000.*3280.)
      E1=SQRT (((RP1*(V0(I,J)**2)/GCS-1.)*SIN (PH(I,J)*R))**2+COS (PH(I,
     1J)*R)**2)
      RPER1=A1*(1.-E1)
      IF(RPER1-RP2)15,15,16
   16 WRITE(6,17)
   17 FORMAT(1HA,31HVB INSUFFICIENT TO INTERCEPT P2)
      GO TO 13
   15 V1=SQRT (GCS*(2./RP2-1./A1))
      SPHI1=SQRT ((A1**2)*(1.-E1**2)/(RP2*(2.*A1-RP2)))
      CPHI1=SQRT (1.-SPHI1**2)
      TANF1=(RP2*(V1**2)/GCS)*CPHI1*SPHI1/(1.-(RP2*(V1**2)/GCS)*SPHI1**2
     1)
      IF(TANF1)40,40,41
   40 F1=ATAN(TANF1)/R
      GO TO 42
   41 F1=(ATAN (TANF1)-PI)/R
   42 THT12=F1-F0(I,J)
      TIM12=TIME(A1,GCS,E1,F1)-TIME(A1,GCS,E1,F0(I,J))
C CALCULATION OF HYPERBOLIC PASS TRAJECTORY--FIRST PASS
      VINF=SQRT (V1**2+VP2**2-2.*V1*VP2*SPHI1)
      A2=GCP2/(VINF**2)
   10 E2=(RADP2+D*R/4.2)*A2)/A2
      XNU=ATAN(1./(E2**2-1.))
      XNUDEG=XNU/R
      IF(VP2-V1*SPHI1)8,7,9
    7 WRITE(6,14)
   14 FORMAT(1HA,26HVP2=V1*SPHI1 FOR THIS CASE)
      GO TO 13
    8 TANPHI=-V1*CPHI1/SQRT (VINF**2-(V1*CPHI1)**2)
```

Program 5 (Contd.)

```
   44 PSI=ATAN(TANNPH)-2.*XNU+PI
      GO TO 50
    9 TANNPH=V1*CPHI1/SQRT (VINF**2-(V1*CPHI1)**2)
   43 PSI=ATAN (TANNPH)-2.*XNU
   50 PSIDEG   =PSI/R
      V2    =SQRT (VP2**2+VINF**2-2.*VP2*VINF*COS (PSI))
      CPHI3=VINF*SIN (PSI)/V2
      SPHI3=SQRT (1.-CPHI3**2)
      RPV3=RP2*(V2    **2)/GCS
      TANF3=RPV3*CPHI3*SPHI3/(1.-RPV3*SPHI3**2)
      IF(TANF3)45,46,46
   45 F3    =(ATAN(TANF3))/R
      GO TO 47
   46 F3    =(ATAN (TANF3)-PI)/R
   47 A3    =(RP2/(2.-RPV3));
      AA    =A3    /(92901000.*5280.)
      E3    =SQRT (((RPV3-1.)*SPHI3)**2+CPHI3**2)
      AP3=A3*(1.+E3)
      IF(AP3-RP2)216,215,215
  216 WRITE(6,217)
  217 FORMAT(1HA,5X,34HAPHELION TOO SMALL FOR SECOND PASS)
      GO TO 13
  215 OM=AA*(1.-E3)
      T2P=-TIME(A3,GCS,E3,F3)
      T=T2P+TIM12
      TAUP=2.*PI*SQRT(A3**3/GCS)/86400.
      DO 200 MP1=1,5
      DO 200 NSP=1,9
      IF(ABS(FLOAT(NSP)*TAUP-FLOAT(MP1)*TAUP2)-.1)201,200,200
  200 CONTINUE
  212 D=D+5.
      IF(D-5000.)10,10,202
  202 WRITE(6,203)VB(I),PH(I,J,
  203 FORMAT(1HA,5X,30HNO  MORE  TRAJECTORIES FOR VB=,F10.1,2X,7HAND PH=
     1,F5.2,2X,13HBELOW 5000 MI)
      GO TO 13
C CALCULATION OF SECOND ASSIST TRAJECTORY
  201 VINF3=SQRT(V2**2+VP2**2-2.*V2*VP2*SPHI3)
      A4=GCP2/VINF3**2
      D2=0.
  310 E4      =(RAD*2+D2*6080.27  +A4)/A4
      XNU4=ATAN(1./SQRT(E4     **2-1.))
      XN4DEG    =XNU4/R
      IF(VP2-V2*SPHI3)206,205,204
  206 TANNP4=-V2*CPHI3/SQRT(VINF3**2-(V2*CPHI3)**2)
      PSI4=ATAN(TANNP4)-2.*XNU4+PI
      GO TO 208
  205 WRITE-6,207)
  207 FORMAT(1HA,26HVP2=V2*SPHI3 FOR THIS CASE)
      GO TO 212
  204 TANNP4= V2*CPHI3/SQRT(VINF3**2-(V2*CPHI3)**2)
      PSI4=ATAN(TANNP4)-2.*XNU4
  208 PSI4DG    =PSI4/R
      V4      =SQRT(VP2**2+VINF3**2-2.*VP2*VINF3*COS(PSI4))
      RPV4=RP2*(V4     **2)/GCS
      IF(RPV4-2.)219,223,223
  219 CPHI5=VINF3*SIN(PSI4)/V4
      SPHI5=SQRT(1.-CPHI5**2)
      TANF5=RPV4*CPHI5*SPHI5/(1.-RPV4*SPHI5**2)
      IF(PSI4)327,328,328
  327 F5=(ATAN(TANF5)+PI)/R
      GO TO 211
  328 IF(TANF5)209,210,210
  209 F5    =(ATAN(TANF5))/R
      GO TO 211
  210 F5    =(ATAN(TANF5)-PI)/R
  211 A5    =RP2/(2.-RPV4)
      A5AU    =A5    /(92901000.*5280.)
      E5    =SQRT(((RPV4-1.)*SPHI5)**2+CPHI5**2)
      OM2    =A5AU    *(1.-E5    )
      IF(PSI4)529,530,530
  529 THTOT=THT12-F5+360.
      TIMOP    =TIM12+FLOAT(NSP)*TAUP-TIME(A5,GCS,E5,F5)+TAUP
      GO TO 523
  530 THTOT    =THT12-F5
      TIMOP    =TIM12+FLOAT(NSP)*TAUP-TIME(A5,GCS,E5,F5)
  523 TAUPP=2.*PI*SQRT(A5**3/GCS)/86400.
      DO 300 MP2=1,5
      DO 300 NS2=1,9
      IF(ABS(FLOAT(NS2)*TAUPP-FLOAT(MP2)*TAUP2)-.2)301,300,300
  300 CONTINUE
  223 D2=D2+5.
      IF(D2-5000.)310,310,202
C CALCULATION OF THIRD ASSIST TRAJECTORY
  301 VINF5=SQRT(V4**2+VP2**2-2.*V4*VP2*SPHI5)
      A6=GCP2/VINF5**2
      D4(1)=0.
      DO 312 K2=1,L2
      E6(K2)=(RAD*2+D4(K2)*6080.27+A6)/A6
      XNU6=ATAN(1./SQRT(E6(K2)**2-1.))
      XN6DEG(K2)=XNU6/R
      IF(VP2-V4*SPHI5)306,305,304
```

Program 5 (Contd.)

```
  306 TANMP6=-V4*CPHI5/SQRT(VINF5**2-(V4*CPHI5)**2)
      PSI6=ATAN(TANMP6)-2.*XNU6+PI
      GO TO 309
  305 WRITE(6,307)
  307 FORMAT(1HA,26HVP2=V4*SPHI5 FOR THIS CASE)
      GO TO 312
  304 TANMP6= V4*CPHI5/SQRT(VINF5**2-(V4*CPHI5)**2)
      PSI6=ATAN(TANMP6)-2.*XNU6
  309 PSI6DG(K2)=PSI6/R
      V6(K2)=SQRT(VP2**2+VINF5**2-2.*VP2*VINF5*COS(PSI6))
      RPV6=RP2*(V6(K2)**2)/GCS
      IF(RPV6-2.)319,322,322
  322 L=K2+1
      GO TO 329
  319 CPHI7=VINF5*SIN(PSI6)/V6(K2)
      SPHI7=SQRT(1.-CPHI7**2)
      TANF7=RPV6*CPHI7*SPHI7/(1.-RPV6*SPHI7**2)
      IF(PSI6)329,329,309
  329 IF(TANF7)829,829,309
  829 F7(K2)=(ATAN(TANF7)+PI)/R
      GO TO 311
  330 IF(TANF7)309,325,325
  309 F7(K2)=(ATAN(TANF7))/R
      GO TO 311
  325 F7(K2)=(ATAN(TANF7)-PI)/R
  311 A7(K2)=RP2/(2.-RPV6)
      A7AU(K2)=A7(K2)/(92901000.*5280.)
      E7(K2)=SQRT(((RPV6-1.)*SPHI7)**2+CPHI7**2)
      QM4(K2)=A7AU(K2)*(1.-E7(K2))
      IF(PSI6)629,630,630
  629 THT02(K2)=THT12-F7(K2)+360.
      TIM02(K2)=TIM12+FLOAT(NSP)*TAUP-TIME(A7(K2),GCS,E7(K2),F7(K2))+FLO
     1AT(NS2)*TAUPP+TAUPP
      GO TO 329
  630 THT02=K2)=THT12-F7(K2)
      TIM02(K2)=TIM12+FLOAT(NSP)*TAUP-TIME(A7(K2),GCS,E7(K2),F7(K2))+FLO
     1AT(NS2)*TAUPP
  329 D4(K2+1)=D4(K2)+100.
  312 CONTINUE
      WRITE(6,213)VB(I),PH(I,J),D,TAUP2,MP1,NSP,THT12,F1,A1AU,E1,V1,TIM1
     12,T,F3,AA,E3,V2,XNUDEG,PSIDEG,TAUP,QM,D2,VINF3,V4,XN4DEG,PSI4DG,F5
     2,THT0T,TIM0P,A5AU,E5,TAUPP,MP2,NS2,QM2,(D4(K2),VINF5,V6(K2),XN6DEG
     3(K2),PSI6DG(K2),F7(K2),THT02(K2),TIM02(K2),A7AU(K2),E7(K2),QM4(K2)
     4,K2=L,L2)
  213 FORMAT(1HA,5X,3HVB=,F10.1,5X,3HPH=,F10.2,5X,6HDOCA1=,F8.2,5X,6HTAU
     1P2=,F7.1,5X,4HMP1=,I3,5X,4HNSP=,I3//2X,4HTH12,5X,2HF1,6X,2HA1,5X,2
     2HE1,6X,2HV1,6X,3HT12,5X,1HT,6X,2HF3,6X,2HA3,5X,2HE3,6X,2HV3,7X,1HN
     3,7X,3HPSI,4X,4HTAUP,4X,2HQM//2F8.2,2F7.4,F10.1,2F7.1,F8.2,2F7.4,F1
     40.1,2F8.2,F7.1,F8.5///3X,5HDOCA2,5X,5HVINF3,7X,2HV5,8X,2HN4,6X,4HP
     5SI4,6X,2HF5,6X,5HTHTOT,3X,5HTIM0P,5X,2HA5,6X,2HE5,4X,5HTAUPP,2X,3H
     6MP2,1X,3HNS2,3X,3HQM2//F9.2,2F11.1,4F9.2,F8.1,2F8.4,F7.1,214,F9.5/
     7/3X,5HDOCA3,3X,5HVINF5,7X,2HV7,8X,2HN6,6X,4HPSI6,6X,2HF7,6X,5HTHT0
     82,3X,5HTIM02,5X,2HA7,6X,2HE7,6X,3HQM3//(F9.0,2F11.1,4F9.2,F8.1,2F8
     9.4,F9.5))
       D=D+25.
       GO TO 10
   13 CONTINUE
      STOP
      END
$DATA
 4.6868E21 1.4077E16 1.1488E16 4.9052E11 3.5480E11
 9.7791E04 1.1495E05 2.0902E07 2.0019E07
$EOF
```

Program 5 Output

VB= 45000.0 PH= 90.00 DOCA1= 415.00 TAUP2= 224.5 MP1= 3 NSP= 3

TH12	F1	A1	E1	V1	T12	T	F3	A3	E3	V3	N	PSI	TAUP	QM
56.35	-123.65	0.6841	0.4618	111590.5	62.6	104.2	-148.30	0.5520	0.5385	95641.4	8.67	55.7	149.7	0.25471

DOCA2	VINF3	V3	N4	PSI4	F5	THTOT	TIMOP	A5	E5	TAUPP	MP2	NS2	QM2
1480.00	53593.7	82860.7	8.96	41.61	-160.69	217.04	559.2	0.4888	0.6101	124.7	5	9	0.19059

DOCA3	VINF5	V7	N6	PSI6	F7	THT02	TIM02	A7	E7	QM3
0.	53593.7	68517.8	9.59	22.44	-171.48	227.83	1677.4	0.4398	0.6838	0.13906
1000.	53593.7	70999.3	7.64	26.34	-169.68	226.03	1676.8	0.4469	0.6721	0.14556
2000.	53593.7	72787.6	6.35	28.92	-168.39	224.74	1676.5	0.4524	0.6633	0.15250
3000.	53593.7	74122.1	5.43	30.75	-167.43	223.78	1676.3	0.4566	0.6567	0.15678
4000.	53593.7	75151.2	4.75	32.12	-166.69	223.03	1676.1	0.4600	0.6514	0.16036
5000.	53593.7	75967.0	4.22	33.19	-166.09	222.44	1676.0	0.4627	0.6472	0.16324
6000.	53593.7	76628.8	3.79	34.03	-165.60	221.95	1676.0	0.4650	0.6438	0.16563
7000.	53593.7	77176.1	3.44	34.72	-165.19	221.54	1675.9	0.4669	0.6409	0.16765
8000.	53593.7	77635.9	3.16	35.30	-164.85	221.19	1675.9	0.4686	0.6385	0.16937
9000.	53593.7	78027.7	2.91	35.79	-164.55	220.90	1675.8	0.4700	0.6365	0.17085
10000.	53593.7	78365.3	2.70	36.21	-164.29	220.64	1675.8	0.4712	0.6347	0.17214
11000.	53593.7	78659.2	2.52	36.57	-164.07	220.42	1675.8	0.4723	0.6331	0.17327
12000.	53593.7	78917.4	2.36	36.89	-163.87	220.22	1675.8	0.4732	0.6317	0.17427
13000.	53593.7	79146.0	2.22	37.16	-163.70	220.04	1675.7	0.4741	0.6305	0.17516
14000.	53593.7	79349.7	2.10	37.41	-163.54	219.89	1675.7	0.4748	0.6294	0.17596
15000.	53593.7	79532.5	1.99	37.63	-163.40	219.74	1675.7	0.4755	0.6284	0.17668
16000.	53593.7	79697.4	1.89	37.83	-163.27	219.61	1675.7	0.4761	0.6275	0.17734
17000.	53593.7	79846.8	1.80	38.01	-163.15	219.50	1675.7	0.4767	0.6267	0.17793
18000.	53593.7	79983.0	1.72	38.18	-163.04	219.39	1675.7	0.4772	0.6260	0.17848
19000.	53593.7	80107.5	1.64	38.33	-162.95	219.29	1675.7	0.4777	0.6253	0.17898
20000.	53593.7	80221.8	1.57	38.47	-162.86	219.20	1675.7	0.4781	0.6247	0.17944

VB= 45000.0 PH= 90.00 DOCA1= 1840.00 TAUP2= 224.5 MP1= 5 NSP= 7

TH12	F1	A1	E1	V1	T12	T	F3	A3	E3	V3	N	PSI	TAUP	QM
56.35	-123.65	0.6841	0.4618	111590.5	62.6	104.2	-143.29	0.5760	0.5163	99639.4	6.52	59.82	160.4	0.27957

DOCA2	VINF3	V3	N4	PSI4	F5	THTOT	TIMOP	A5	E5	TAUPP	MP2	NS2	QM2
210.00	53593.7	82897.4	9.10	41.62	-160.69	217.04	1226.7	0.4888	0.6100	124.7	5	9	0.19062

DOCA3	VINF5	V7	N6	PSI6	F7	THT02	TIM02	A7	E7	QM3
0.	53593.7	68522.4	9.59	22.44	-171.48	227.83	2351.1	0.4398	0.6838	0.13908
1000.	53593.7	71004.5	7.64	26.35	-169.67	226.02	2350.5	0.4470	0.6720	0.14458
2000.	53593.7	72793.2	6.35	28.92	-168.39	224.74	2350.1	0.4524	0.6633	0.15252
3000.	53593.7	74127.8	5.43	30.76	-167.43	223.78	2349.9	0.4566	0.6566	0.15679
4000.	53593.7	75157.0	4.75	32.13	-166.68	223.03	2349.8	0.4600	0.6514	0.16036
5000.	53593.7	75973.0	4.22	33.19	-166.08	222.43	2349.7	0.4628	0.6472	0.16326
6000.	53593.7	76634.9	3.79	34.04	-165.60	221.94	2349.6	0.4650	0.6438	0.16566
7000.	53593.7	77182.2	3.44	34.73	-165.19	221.54	2349.5	0.4669	0.6409	0.16767
8000.	53593.7	77642.1	3.16	35.31	-164.84	221.19	2349.5	0.4684	0.6385	0.16939
9000.	53593.7	78033.9	2.91	35.80	-164.55	220.89	2349.5	0.4700	0.6364	0.17087
10000.	53593.7	78371.5	2.70	36.21	-164.29	220.64	2349.4	0.4712	0.6346	0.17216
11000.	53593.7	78665.5	2.52	36.58	-164.07	220.41	2349.4	0.4723	0.6331	0.17329
12000.	53593.7	78923.7	2.36	36.89	-163.87	220.21	2349.4	0.4732	0.6317	0.17429

13000.	53593.7	79162.3	2.22	37.17	-163.69	220.04	2349.4	0.4741	0.6305	0.17519
14000.	53593.7	79356.1	2.10	37.42	-163.53	219.88	2349.4	0.4748	0.6294	0.17599
15000.	53593.7	79538.9	1.99	37.65	-163.39	219.74	2349.3	0.4755	0.6284	0.17671
16000.	53593.7	79703.8	1.89	37.84	-163.26	219.61	2349.3	0.4762	0.6275	0.17736
17000.	53593.7	79853.3	1.80	38.02	-163.15	219.49	2349.3	0.4767	0.6267	0.17796
18000.	53593.7	79989.4	1.72	38.19	-163.04	219.39	2349.3	0.4772	0.6260	0.17850
19000.	53593.7	80113.9	1.64	38.34	-162.94	219.29	2349.3	0.4777	0.6253	0.17900
20000.	53593.7	80228.2	1.57	38.47	-162.85	219.20	2349.3	0.4782	0.6247	0.17946

VB= 45000.0 PH= 90.00 DOCA1= 3415.00 TAUP2= 224.5 MP1= 3 NSP= 4

TH12	F1	A1	E1	V1	T12	T	F3	A3	E3	V3	N	PSI	TAUP	QM
56.35	-123.65	0.6841	0.4618	111590.5	62.6	104.1	-139.46	0.5970	0.5024	102057.0	5.12	62.62	168.3	0.29706

DOCA2	VINF3	V3	N4	PSI4	F5	THTOT	TIMOP	A5	E5	TAUPP	MP2	NS2	QM2
140.00	53593.7	85061.1	9.26	44.11	-158.84	215.18	777.6	0.4981	0.5979	128.3	4	7	0.20026

DOCA3	VINF5	V7	N6	PSI6	F7	THT02	TIM02	A7	E7	QM3
0.	53593.7	70071.0	9.59	24.93	-170.35	226.70	1677.1	0.4442	0.6765	0.14370
1000.	53593.7	72725.9	7.64	28.83	-168.44	224.79	1676.5	0.4522	0.6636	0.15210
2000.	53593.7	74614.4	6.35	31.41	-167.98	223.42	1676.2	0.4582	0.6542	0.15847
3000.	53593.7	76013.4	5.43	33.24	-166.04	222.40	1676.1	0.4629	0.6470	0.16340
4000.	53593.7	77087.2	4.75	34.61	-165.24	221.61	1675.9	0.4666	0.6414	0.16732
5000.	53593.7	77935.7	4.22	35.68	-164.62	220.97	1675.9	0.4696	0.6369	0.17050
6000.	53593.7	78622.4	3.79	36.52	-164.10	220.45	1675.8	0.4721	0.6333	0.17319
7000.	53593.7	79189.2	3.44	37.22	-163.66	220.01	1675.8	0.4742	0.6303	0.17539
8000.	53593.7	79664.7	3.16	37.79	-163.29	219.64	1675.7	0.4760	0.6277	0.17721
9000.	53593.7	80069.3	2.91	38.28	-162.98	219.32	1675.7	0.4775	0.6255	0.17882
10000.	53593.7	80417.7	2.70	38.70	-162.70	219.05	1675.7	0.4789	0.6234	0.18023
11000.	53593.7	80720.8	2.52	39.06	-162.46	218.81	1675.7	0.4801	0.6220	0.18144
12000.	53593.7	80986.8	2.36	39.38	-162.25	218.60	1675.6	0.4811	0.6205	0.18255
13000.	53593.7	81222.2	2.22	39.66	-162.06	218.41	1675.6	0.4820	0.6193	0.18352
14000.	53593.7	81431.9	2.10	39.91	-161.89	218.24	1675.6	0.4829	0.6181	0.18440
15000.	53593.7	81619.9	1.99	40.13	-161.74	218.09	1675.6	0.4836	0.6171	0.18518
16000.	53593.7	81789.4	1.89	40.33	-161.60	217.95	1675.6	0.4843	0.6161	0.18589
17000.	53593.7	81943.1	1.80	40.51	-161.48	217.82	1675.6	0.4849	0.6153	0.18654
18000.	53593.7	82083.0	1.72	40.67	-161.36	217.71	1675.6	0.4855	0.6145	0.18713
19000.	53593.7	82210.8	1.64	40.82	-161.26	217.60	1675.6	0.4860	0.6138	0.18767
20000.	53593.7	82328.2	1.57	40.96	-161.16	217.51	1675.6	0.4865	0.6132	0.18817

NO MORE TRAJECTORIES FOR VB= 45000.0 AND PH= 90.00 BELOW 5000 MI

Program 6

```
$JOB          0,5,9G00      67-012,LT MYERS,AFIT-SE
$IBJOB        MAP
$IBFTC MAIN   M94/2,XR7
C VENUS CATEGORY 1 OUT-OF-ECLIPTIC TRAJECTORIES
      TIME(A,G,E,T)=(2.*ATAN(SQRT((1.-E)/(1.+E))*TAN(T*R/2.))-E*SQRT(1.-
     1E**2)*SIN(T*R)/(1.+E*COS(T*R)))*SQRT((A**3)/G)/86400.
      READ(5,1)GCS,GCP1,GCP2,RP1,RP2,VP1,VP2,RADP1,RADP2,RHO
    1 FORMAT(5E10.0/5E10.0)
      DIMENSION D(25),E2(25),XNU(25),VINFOX(25),VINFOY(25),VINFOZ(25),DX
     1(25),DY(25),DZ(25),V2X(25),V2Y(25),V2Z(25),V2(25),PH3(25),XI2(25),
     2F3(25),A3AU(25),E3(25),TOP(25),OM(25)
      VB=38000.
      PI=3.14159
      R=PI/180.
      M=99
      N=1
      L=1
      MB=10
      MD=11
C DEPARTURE ORBITS
      DO 2 I=1,M
      VINFP1=SQRT(VB**2-2.*GCP1/RADP1)
      PH0=90.
      DO 3 J=1,N
      XI=0.
      DO 4 K=1,L
      PH0R=PH0*R
      XIR=XI*R
      IF((VP1*SIN(PH0R)*COS(XIR))**2+VINFP1**2-VP1**2)5,5,6
    5 WRITE(6,7)VB,PH0,XI
    7 FORMAT(1HA,20X,17HNO ESCAPE FOR VB=,F10.1,7HAT PH0=,F7.2,6HAND I=,
     1F6.2)
      GO TO 31
    6 V0=VP1*SIN(PH0R)*COS(XIR)-SQRT((VP1*SIN(PH0R)*COS(XIR))**2+VINFP1*
     1*2-VP1**2)
      V0X=V0*SIN(PH0R)*COS(XIR)
      V0Y=V0*COS(PH0R)
      V0Z=V0*SIN(PH0R)*SIN(XIR)
C PRE-ASSIST TRAJECTORY
      RP1V0=RP1*V0**2/GCS
      TANF0=RP1V0*COS(PH0R)*SIN(PH0R)/(1.-RP1V0*SIN(PH0R)**2)
      IF(TANF0)8,9,9
    8 F0=ATAN(TANF0)/R
      GO TO 10
    9 F0=(ATAN(TANF0)-PI)/R
   10 A1=RP1/(2.-RP1V0)
      A1AU=A1/(92901000.*5280.)
      E1=SQRT(((RP1V0-1.)*SIN(PH0R))**2+COS(PH0R)**2)
      RPER1=A1*(1.-E1)
      IF(RPER1-RP2)11,11,12
   12 WRITE(6,13)VB,PH0,XI
   13 FORMAT(1HA,10X,3HVB=,F10.1,36HINSUFFICIENT TO INTERCEPT P2 AT PH0=
     1,F7.2,6HAND I=,F7.2)
      GO TO 31
   11 V1=SQRT(GCS*(2./RP2-1./A1))
      PH1R=ARSIN(SQRT(A1**2*(1.-E1**2)/(RP2*(2.*A1-RP2))))
      PH1=PH1R/R
      RP2V1=RP2*V1**2/GCS
      TANF1=RP2V1*COS(PH1R)*SIN(PH1R)/(1.-RP2V1*SIN(PH1R)**2)
      IF(TANF1)14,14,15
   14 F1=ATAN(TANF1)/R
      GO TO 16
   15 F1=(ATAN(TANF1)-PI)/R
   16 THT12=F1-F0
      THR=THT12*R
      TIN12=TIME(A1,GCS,E1,F1)-TIME(A1,GCS,E1,F0)
      R1XP=-RP2*SIN(THR)*COS(XIR)
      R1XPAU=R1XP/(92901000.*5280.)
      R1YP=-RP2*COS(THR)
      R1YPAU=R1YP/(92901000.*5280.)
      R1ZP=RP2*SIN(THR)*SIN(XIR)
      R1ZPAU=R1ZP/(92901000.*5280.)
      IF(R1XP-RHO)17,18,28
   28 WRITE(6,29)XI,PH0
   29 FORMAT 1HA,10X,2HI=,F5.2,30HTOO LARGE FOR INTERCEPT AT VB=,F10.1,8
     1HAND PH0=,F8.2)
      GO TO 30
C CALCULATION OF E MATRIX
   17 ETR=THR-PI/2.
      E11=COS(ETR)*COS(THR)*COS(XIR)+SIN(ETR)*SIN(THR)
      E12=-COS(ETR)*SIN(THR)*COS(XIR)+SIN(ETR)*COS(THR)
      E13=COS(ETR)*SIN(XIR)
      E21=-SIN(ETR)*COS(THR)*COS(XIR)+COS(ETR)*SIN(THR)
      E22=SIN(ETR)*SIN(THR)*COS(XIR)+COS(ETR)*COS(THR)
      E23=-SIN(ETR)*SIN(XIR)
      E31=-COS(THR)*SIN(XIR)
      E32=SIN(THR)*SIN(XIR)
      E33=COS(XIR)
      V1X=-V1*SIN(PH1R)*E11-V1*COS(PH1R)*E12
      V1Y=-V1*SIN(PH1R)*E21-V1*COS(PH1R)*E22
      V1Z=-V1*SIN(PH1R)*E31-V1*COS(PH1R)*E32
      VINFIX=V1X
```

Program 6 (Contd.)

```
      VINFIY=V1Y+VP2
      VINFIZ=V1Z
      VINFI=SQRT(VINFIX**2+VINFIY**2+VINFIZ**2)
      VINFXY=SQRT(VINFIX**2+VINFIY**2)
      PSIR=ARCOS(-VINFIY/VINFXY)
      PSI=PSIR/R
      IF(V1Z)18,18,19
   18 ALPR=ARCOS(VINFXY/VINFI)
      GO TO 20
   19 ALPR=-ARCOS(VINFXY/VINFI)
   20 ALP=ALPR/R
      VINFO=VINFI
      A2=GCP2/VINFI**2
      A2P=A2/RADP2
      WRITE(6,32)
   32 FORMAT(1HA,10X,100H**********************************************
     1**********************************************)
      WRITE(6,21)VB,PHO,XI,VINFP1,V0,V0X,V0Y,V0Z,V1,V1X,V1Y,V1Z,THY1Z,F0
     1,A1AU,E1,PH1,R1XPAU,R1YPAU,R1ZPAU,TIM12,VINFI,VINFXY,PSI,ALP
   21 FORMAT(1HA,45X,3HVB=,F10.1,5X,4HPHO=,F6.1///3X,1HI,5X,6HVINFP1,3X,
     12HV0,8X,3HV0X,7X,3HV0Y,7X,3HV0Z,7X,2HV1,8X,3HV1X,7X,3HV1Y,7X,3HV1
     22//F7.3,5F10.1,10X,4F10.1///2X,4HTH12,5X,2HF0,6X,2HA1,5X,2HE1,5X,3
     3HPH1,4X,4HR1XP,4X,4HR1YP,4X,4HR1ZP,4X,5HTIM12,4X,5HVINFI,4X,6HVINF
     4XY,5X,3HPSI,5X,3HALP//2F8.2,2F8.4,F8.2,3F8.4,F3.2,2F10.1,2F8.2)
      BET=0.
      DO 22 IB=1,MB
      BETR=BET*R
C CALCULATION OF F MATRIX
      F11=COS(BETR)*COS(PSIR)-SIN(BETR)*SIN(ALPR)*SIN(PSIR)
      F12=-COS(ALPR)*SIN(PSIR)
      F13=SIN(BETR)*COS(PSIR)+COS(BETR)*SIN(ALPR)*SIN(PSIR)
      F21=COS(BETR)*SIN(PSIR)+SIN(BETR)*SIN(ALPR)*COS(PSIR)
      F22=COS(ALPR)*COS(PSIR)
      F23=SIN(BETR)*SIN(PSIR)-COS(BETR)*SIN(ALPR)*COS(PSIR)
      F31=-SIN(BETR)*COS(ALPR)
      F32=SIN(ALPR)
      F33=COS(BETR)*COS(ALPR)
C HYPERBOLIC PASS TRAJECTORY
      D(1)=0.
      DO 23 ID=1,MD
      E2(ID)=(RADP2+D(ID)*6080.27+A2)/A2
      XNUR=ARSIN(1./E2(ID))
      XNU(ID)=XNUR/R
      VNFOX=VINFO*COS(PI/2.-2.*XNUR)
      VNFOY=-VINFO*SIN(PI/2.-2.*XNUR)
      VNFOZ=0.


      VINFOX(ID)=VNFOX*F11+VNFOY*F12+VNFOZ*F13
      VINFOY(ID)=VNFOX*F21+VNFOY*F22+VNFOZ*F23
      VINFOZ(ID)=VNFOX*F31+VNFOY*F32+VNFOZ*F33
      D2X=(A2+D(ID)*6080.27+RADP2)*COS(XNUR)/RADP2
      D2Y=(A2+D(ID)*6080.27+RADP2)*SIN(XNUR)/RADP2
      D2Z=0.
      DX(ID)=D2X*F11+D2Y*F12+D2Z*F13
      DY(ID)=D2X*F21+D2Y*F22+D2Z*F23
      DZ(ID)=D2X*F31+D2Y*F32+D2Z*F33
      V2X(ID)=VINFOX(ID)
      V2Y(ID)=VINFOY(ID)-VP2
      V2Z(ID)=VINFOZ(ID)
      V2(ID)=SQRT(V2X(ID)**2+V2Y(ID)**2+V2Z(ID)**2)
      PH3R=ARCOS(V2X(ID)/V2(ID))
      PH3(ID)=PH3R/R
      XI2(ID)=ATAN(V2Z(ID)/V2Y(ID))/R
      RP2V2=RP2*V2(ID)**2/GCS
      TANF3=RP2V2*COS(PH3R)*SIN(PH3R)/(1.-RP2V2*SIN(PH3R)**2)
      IF(TANF3)24,25,25
   24 F3(ID)=(ATAN(TANF3))/R
      GO TO 26
   25 F3(ID)=(ATAN(TANF3)-PI)/R
   26 A3=RP2/(1.-RP2V2)
      A3AU(ID)=A3/(93900100.*5280.)
      E3(ID)=SQRT(((RP2V2-1.)*SIN(PH3R))**2+COS(PH3R)**2)
      TOP(ID)=TIM12-TIME(A3,GCS,E3(ID),F3(ID))
      QM(ID)=A3AU(ID)*(1.-E3(ID))
      D(ID+1)=D(ID)+10000.
   23 CONTINUE
      WRITE(6,27)BET,A2P,(D(ID),XNU(ID),V2(ID),V2X(ID),V2Y(ID),V2Z(ID),D
     1X(ID),DY(ID),DZ(ID),TOP(ID),PH3(ID),F3(ID),A3AU(ID),E3(ID),XI2(ID)
     2,QM(ID),ID=1,MD)
   27 FORMAT(1HA,45X,5HBETA=,F7.2,3X,3HA2=,F7.2///4X,4HDOCA,4X,2HXU,6X,2
     1HV3,6X,3HV2X,6X,3HV3Y,6X,3HV3Z,5X,2HDX,4X,2HDY,4X,2HDZ,4X,3HTOP,4X
     2,3HPH3,5X,2HF3,6X,2HA3,5X,2HE3,5X,2HI3,5X,2HQM//(F9.1,F7.2,4F9.1,3
     3F6.2,F7.1,F7.2,F8.2,2F7.4,F7.3,F8.5))
      BET=BET+10.
   22 CONTINUE
      XI=XI+.1
    4 CONTINUE
   30 PHO=PHO-2.
    3 CONTINUE
   31 VB=VB+1000.
    2 CONTINUE
      STOP
      END


$DATA
 4.6868E21 1.4077E16 1.1488E16 4.9052E11 3.5480E11
 9.7751E04 1.1493E05 2.0902E07 2.0013E07 2.0200E09
$EOF
```

Program 6 Output

VB= 48000.0 PHO= 90.0

I	VIAFP1	V0	V0X	V0Y	V0Z	V1	V1X	V1Y	V1Z
0.	30936.2	66814.8	66814.8	0.1	0.	108508.5	56832.2	-92373.2	0.

TM12	F0	A1	E1	PH1	R1XP	R1YP	R1ZP	TIM12	VINF1	VINFXY	PSI	ALP
48.35	-180.00	0.6524	0.5328	58.35	-0.5405	0.4307	0.	57.75	61237.9	61237.9	111.61	-0.

BETA= 0. A2= 0.15

ECCA	AU	V3	V3X	V3Y	V3Z	DX	DY	DZ	TOP	PH3	F3	A3	E3	I3	QR
0.	7.63	92266.5	48989.7	-78186.4	-0.	-0.56	1.01	-0.	96.2	57.93	-151.64	0.5336	0.6105	0.	0.20785
100.0	7.43	92686.2	49241.2	-78524.1	-0.	-0.57	1.03	-0.	96.2	57.91	-151.24	0.5359	0.6083	0.	0.20993
200.0	7.24	93084.9	49477.8	-78846.4	-0.	-0.59	1.06	-0.	96.2	57.89	-150.84	0.5382	0.6062	0.	0.21194
300.0	7.07	93464.2	49700.8	-79154.2	-0.	-0.60	1.09	-0.	96.2	57.88	-150.47	0.5403	0.6042	0.	0.21386
400.0	6.90	93825.4	49911.4	-79448.4	-0.	-0.61	1.12	-0.	96.2	57.86	-150.11	0.5424	0.6023	0.	0.21571
500.0	6.74	94169.7	50110.4	-79730.1	-0.	-0.62	1.15	-0.	96.2	57.85	-149.74	0.5444	0.6005	0.	0.21748
600.0	6.58	94498.4	50298.8	-79959.9	-0.	-0.63	1.18	-0.	96.2	57.84	-149.42	0.5463	0.5988	0.	0.21919
700.0	6.44	94812.5	50477.4	-80258.5	-0.	-0.64	1.21	-0.	96.2	57.83	-149.10	0.5482	0.5971	0.	0.22084
800.0	6.29	95112.8	50647.0	-80506.7	-0.	-0.65	1.23	-0.	96.2	57.83	-148.78	0.5500	0.5956	0.	0.22242
900.0	6.16	95400.3	50808.2	-80745.0	-0.	-0.66	1.26	-0.	96.2	57.82	-148.48	0.5517	0.5941	0.	0.22395
1000.0	6.03	95675.5	50961.0	-80974.0	-0.	-0.68	1.29	-0.	96.2	57.82	-148.19	0.5534	0.5927	0.	0.22543

BETA= 10.00 A2= 0.15

ECCA	AU	V3	V3X	V3Y	V3Z	DX	DY	DZ	TOP	PH3	F3	A3	E3	I3	QR
0.	7.63	92549.6	49079.9	-78414.1	-2798.3	-0.56	0.99	-0.20	96.2	57.97	-151.37	0.5352	0.6083	2.044	0.20960
100.0	7.43	92960.9	49329.1	-78746.0	-2727.7	-0.57	1.02	-0.20	96.2	57.95	-150.96	0.5375	0.6062	1.984	0.21165
200.0	7.24	93351.7	49563.6	-79062.8	-2660.6	-0.58	1.05	-0.21	96.2	57.93	-150.58	0.5397	0.6042	1.927	0.21361
300.0	7.07	93723.5	49784.5	-79365.4	-2596.6	-0.59	1.07	-0.21	96.2	57.91	-150.20	0.5418	0.6023	1.874	0.21549
400.0	6.90	94077.7	49993.1	-79654.7	-2535.6	-0.60	1.10	-0.22	96.2	57.90	-149.85	0.5439	0.6004	1.823	0.21730
500.0	6.74	94415.3	50190.2	-79931.6	-2477.4	-0.61	1.13	-0.23	96.2	57.89	-149.50	0.5458	0.5987	1.775	0.21904
600.0	6.59	94737.7	50376.9	-80196.9	-2421.8	-0.62	1.16	-0.23	96.2	57.88	-149.17	0.5477	0.5970	1.730	0.22071
700.0	6.44	95045.7	50553.8	-80451.2	-2368.6	-0.63	1.19	-0.24	96.2	57.87	-148.85	0.5494	0.5955	1.686	0.22233
800.0	6.29	95340.2	50721.7	-80695.2	-2317.7	-0.65	1.21	-0.24	96.2	57.86	-148.54	0.5514	0.5939	1.645	0.22388
900.0	6.16	95622.4	50881.3	-80929.6	-2269.0	-0.66	1.24	-0.25	96.2	57.85	-148.24	0.5531	0.5925	1.606	0.22538
1000.0	6.03	95892.7	51033.1	-81154.8	-2222.2	-0.67	1.27	-0.25	96.2	57.85	-147.95	0.5547	0.5911	1.568	0.22682

BETA= 20.00 A2= 0.15

ECCA	AU	V3	V3X	V3Y	V3Z	DX	DY	DZ	TOP	PH3	F3	A3	E3	I3	QR
0.	7.63	93385.2	49347.7	-79090.0	-5511.6	-0.54	0.94	-0.39	96.3	58.10	-150.53	0.5399	0.6021	3.984	0.21484
100.0	7.43	93771.9	49590.1	-79404.8	-5372.6	-0.55	0.97	-0.40	96.3	58.07	-150.14	0.5421	0.6002	3.871	0.21675
200.0	7.24	94139.8	49818.2	-79705.4	-5240.3	-0.56	1.00	-0.41	96.3	58.05	-149.77	0.5442	0.5984	3.762	0.21858
300.0	7.07	94489.5	50033.0	-79992.5	-5114.3	-0.57	1.02	-0.42	96.3	58.03	-149.41	0.5463	0.5966	3.658	0.22034
400.0	6.90	94822.5	50235.7	-80267.1	-4994.2	-0.58	1.05	-0.43	96.3	58.01	-149.07	0.5482	0.5950	3.560	0.22204
500.0	6.74	95141.0	50427.3	-80530.0	-4879.6	-0.59	1.08	-0.44	96.3	57.99	-148.74	0.5502	0.5934	3.468	0.22367
600.0	6.58	95444.7	50608.6	-80781.8	-4770.1	-0.60	1.10	-0.45	96.3	57.98	-148.42	0.5520	0.5919	3.379	0.22524
700.0	6.44	95735.0	50780.4	-81023.3	-4665.3	-0.61	1.13	-0.46	96.3	57.97	-148.11	0.5538	0.5905	3.295	0.22675
800.0	6.29	96012.8	50943.5	-81255.0	-4565.1	-0.62	1.16	-0.47	96.3	57.95	-147.81	0.5555	0.5892	3.214	0.22821
900.0	6.16	96278.9	51098.4	-81477.6	-4469.0	-0.63	1.18	-0.49	96.3	57.95	-147.52	0.5571	0.5879	3.139	0.22962
1000.0	6.03	96533.9	51245.8	-81691.5	-4376.8	-0.64	1.21	-0.50	96.3	57.94	-147.25	0.5587	0.5866	3.067	0.23097

Program 7

```
$JOB            0,2,7000        67-012,LT MYERS,AFIT-SE
$IBJOB          MAP
$IBFTC MAIN     M94/2,XR7
C VENUS CATEGORY 2 OUT-OF-ECLIPTIC TRAJECTORIES
      TIME(A,G,E,T)=(2.*ATAN(SQRT((1.-E)/(1.+E))*TAN(T*R/2.))-E*SQRT 1.-
     1E**2)*SIN(T*R)/(1.+E*COS(T*R)))*SQRT((A**3)/G)/86400.
      READ(5,1)GCS,GCP1,GCP2,RP1,RP2,VP1,VP2,RADP1,RADP2,RHO
    1 FORMAT(5E10.0/5E10.0)
      DIMENSION D(25),E2(25),XNU(25),VINFOX(25),VINFOY(25),VINFOZ(25),DX
     1(25),DY(25),DZ(25),V2X(25),V2Y(25),V2Z(25),V2(25),PH3(25),XI2(25),
     2F3(25),A3AU(25),E3(25),TOP(25),GM(25)
      VB=38000.
      PI=3.14159
      R=PI/180.
      M=39
      N=1
      MB=10
      MD=11
      R12=RP1/RP2
      A=(1.-R12)/(1.+R12)
C DEPARTURE ORBITS
      DO 2 I=1,M
      VINFP1=SQRT(VB**2-2.*GCP1/RADP1)
      PH0=90.
      DO 3 J=1,M
      PH0R=PH0*R
      E1=SQRT(A**2+(1.-SIN(PH0R)**2)*(1.+2.*A))/SIN(PH0R)
   40 A1=RP1*SIN(PH0R)*(SIN(PH0R)-SQRT(E1**2+SIN(PH0R)**2-1.))/(1.-E1**2
     1)
      V0=SQRT(GCS*(2./RP1-1./A1))
      VEL=(V0**2+VP1**2-VINFP1**2)/(2.*VP1*V0*SIN(PH0R))
      IF(ABS(VEL)-1.)42,42,30
   42 A1AU=A1/(92901000.*5280.)
      XIR=ARCOS((V0**2+VP1**2-VINFP1**2)/(2.*VP1*V0*SIN(PH0R)))
      XI=XIR/R
  102 V0X=V0*SIN(PH0R)*COS(XIR)
      V0Y=V0*COS(PH0R)
      V0Z=V0*SIN(PH0R)*SIN(XIR)
C PRE-ASSIST TRAJECTORY
      RP1V0=RP1*V0**2/GCS
      TANF0=RP1V0*COS(PH0R)*SIN(PH0R)/(1.-RP1V0*SIN(PH0R)**2)
      IF(TANF0)8,9,9
    8 F0=ATAN(TANF0)/R
      GO TO 11
    9 F0=(ATAN(TANF0)-PI)/R
   11 V1=SQRT(GCS*(2./RP2-1./A1))



      PH1R=ARSIN(SQRT(A1**2*(1.-E1**2)/(RP2*(2.*A1-RP2))))
      PH1=PH1R/R
      RP2V1=RP2*V1**2/GCS
      TANF1=RP2V1*COS(PH1R)*SIN(PH1R)/(1.-RP2V1*SIN(PH1R)**2)
      IF(TANF1)14,14,15
   14 F1=ATAN(TANF1)/R
      GO TO 16
   15 F1=(ATAN(TANF1)-PI)/R
   16 F1=-F1
      PH1R=PI-PH1R
      PH1=PH1R/R
      THT12=F1-F0
   34 THR=THT12*R
      TIM12=TIME(A1,GCS,E1,F1)-TIME(A1,GCS,E1,F0)
      R1XP=-RP2*SIN(THR)*COS(XIR)
      R1XPAU=R1XP/(92901000.*5280.)
      R1YP=RP2*COS(THR)
      R1YPAU=R1YP/(92901000.*5280.)
      R1ZP=RP2*SIN(THR)*SIN(XIR)
      R1ZPAU=R1ZP/(92901000.*5280.)
      IF(R1ZP-RHO)17,28,28
   28 WRITE(6,29)XI,VB,PH0
   29 FORMAT(1HA,10X,2HI=,F9.2,30HTOO LARGE FOR INTERCEPT AT VB=,F10.1,8
     1HAND PH0=,F8.2)
      GO TO 30
C CALCULATION OF E MATRIX
   17 ETR=THR-PI/2.
      E11=COS(ETR)*COS(THR)*COS(XIR)+SIN(ETR)*SIN(THR)
      E12=-COS(ETR)*SIN(THR)*COS(XIR)+SIN(ETR)*COS(THR)
      E13=COS(ETR)*SIN(XIR)
      E21=-SIN(ETR)*COS(THR)*COS(XIR)+COS(ETR)*SIN(THR)
      E22=SIN(ETR)*SIN(THR)*COS(XIR)+COS(ETR)*COS(THR)
      E23=-SIN(ETR)*SIN(XIR)
      E31=-COS(THR)*SIN(XIR)
      E32=SIN(THR)*SIN(XIR)
      E33=COS(XIR)
      V1X=-V1*SIN(PH1R)*E11-V1*COS(PH1R)*E12
      V1Y=-S1*SIN(PH1R)*E21-V1*COS(PH1R)*E22
      V1Z=-V1*SIN(PH1R)*E31-V1*COS(PH1R)*E32
      VINFIX=V1X
      VINFIY=V1Y+VP2
      VINFIZ=V1Z
      VINFI=SQRT(VINFIX**2+VINFIY**2+VINFIZ**2)
      VINFXY=SQRT(VINFIX**2+VINFIY**2)
      IF(VINFIY)800,800,801
  800 PSIR=0.
```

Program 7 (Contd.)

```
      PSI=0.
      GO TO 802
  801 PSIR=PI
      PSI=180.
  802 IF(V1Z)18,18,19
   18 ALPR=ARCOS(VINFXY/VINFI)
      GO TO 20
   19 ALPR=-ARCOS(VINFXY/VINFI)
   20 ALP=ALPR/R
      VINFO=VINFI
      A2=GCP2/VINFI**2
      A2P=A2/RADP2
      WRITE(6,32)
   32 FORMAT(1HA,10X,...00H**********...**********)
      WRITE(6,21)VB,PHO,XI,VINFP1,VO,VOX,VOY,VOZ,V1,V1X,V1Y,V1Z,TMT12,F0
     1,A1AU,E1,PH1,R1XPAU,R1YPAU,R1ZPAU,TIM12,VINFI,VINFXY,PSI,ALP
   21 FORMAT(1HA,45X,3HVB=,F10.1,5X,4HPHO=,F6.1///3X,1HI,5X,6HVINFP1,6X,
     12HVO,8X,3HVOX,7X,3HVOY,7X,3HVOZ,17X,2HV1,8X,3HV1X,7X,3HV1Y,7X,3HV1
     2Z//F7.3,5F10.1,10X,4F10.1///2X,4HTH12,5X,2HFO,6X,2HA1,6X,2HE1,6X,3
     3HPH1,4X,4HR1XP,4X,4HR1YP,4X,4HR1ZP,4X,5HTIM12,4X,5HVINFI,4X,6HVINF
     4XY,5X,3HPSI,5X,3HALP//2F8.2,2F8.4,F8.2,3F8.4,F8.2,2F10.1,2F8.2)
      BET=0.
      DO 22 IB=1,MB
      BETR=BET*R
C CALCULATION OF F MATRIX
      F11=COS(BETR)*COS(PSIR)-SIN(BETR)*SIN(ALPR)*SIN(PSIR)
      F12=-COS(ALPR)*SIN(PSIR)
      F13=SIN(BETR)*COS(PSIR)+COS(BETR)*SIN(ALPR)*SIN(PSIR)
      F21=COS(BETR)*SIN(PSIR)+SIN(BETR)*SIN(ALPR)*COS(PSIR)
      F22=COS(ALPR)*COS(PSIR)
      F23=SIN(BETR)*SIN(PSIR)-COS(BETR)*SIN(ALPR)*COS(PSIR)
      F31=-SIN(BETR)*COS(ALPR)
      F32=SIN(ALPR)
      F33=COS(BETR)*COS(ALPR)
C HYPERBOLIC PASS TRAJECTORY
      D(1)=0.
      DO 23 ID=1,MD
      E2(ID)=(RADP2+D(ID)*6080.27+A2)/A2
      XNUR=ARSIN(1./E2(ID))
      XNU(ID)=XNUR/R
      VNFOX=VINFO*COS(PI/2.-2.*XNUR)
      VNFOY=-VINFO*SIN(PI/2.-2.*XNUR)
      VNFOZ=0.
      VINFOX(ID)=VNFOX*F11+VNFOY*F12+VNFOZ*F13
      VINFOY(ID)=VNFOX*F21+VNFOY*F22+VNFOZ*F23
      VINFOZ(ID)=VNFOX*F31+VNFOY*F32+VNFOZ*F33
      D2X=(A2+D(ID)*6080.27+RADP2)*COS(XNUR)/RADP2
      D2Y=(A2+D(ID)*6080.27+RADP2)*SIN(XNUR)/RADP2
      D2Z=0.
      DX(ID)=D2X*F11+D2Y*F12+D2Z*F13
      DY(ID)=D2X*F21+D2Y*F22+D2Z*F23
      DZ(ID)=D2X*F31+D2Y*F32+D2Z*F33
      V2X(ID)=VINFOX(ID)
      V2Y(ID)=VINFOY(ID)-VP2
      V2Z(ID)=VINFOZ(ID)
      V2(ID)=SQRT(V2X(ID)**2+V2Y(ID)**2+V2Z(ID)**2)
      PH3R=ARCOS(V2X(ID)/V2(ID))
      PH3(ID)=PH3R/R
      XI2(ID)=ATAN(V2Z(ID)/V2Y(ID))/R
      RP2V2=RP2*V2(ID)**2/GCS
      TANF3=RP2V2*COS(PH3R)*SIN(PH3R)/(1.-RP2V2*SIN(PH3R)**2)
      IF(TANF3)24,25,25
   24 F3(ID)=(ATAN(TANF3))/R
      GO TO 26
   25 F3(ID)=(ATAN(TANF3)-PI)/R
   26 A3=RP2/(2.-RP2V2)
      A3AU(ID)=A3/(92901000.*5280.)
      E3(ID)=SQRT(((RP2V2-1.)*SIN(PH3R))**2+COS(PH3R)**2)
      TOP(ID)=TIM12-TIME(A3,GCS,E3(ID),F3(ID))
      QM(ID)=A3AU(ID)*(1.-E3(ID))
      D(ID+1)=D(ID)+100.
   23 CONTINUE
      WRITE(6,27)BET,A2P,(D(ID),XNU(ID),V2(ID),V2X(ID),V2Y(ID),V2Z(ID),D
     1X(ID),DY(ID),DZ(ID),TOP(ID),PH3(ID),F3(ID),A3AU(ID),E3(ID),XI2(ID)
     2,QM(ID),ID=1,MD)
   27 FORMAT(1HA,45X,5HBETA=,F7.2,3X,5HA2=,F7.2///4X,4HDOCA,4X,2HNU,7X,2
     1HV3,7X,3HV3X,7X,3HV3Y,7X,3HV3Z,5X,2HDX,4X,2HDY,4X,2HDZ,4X,3HTOP,4X
     2,3HPH3,5X,2HF3,6X,2HA3,5X,2HE3,6X,2HI3,5X,2HQM//(F9.1,F7.2,4F10.1,
     33F6.2,F7.1,F7.2,F8.2,2F7.4,F8.4,F8.5))
      BET=BET+10.
   22 CONTINUE
   30 PHO=PHO-2.
    3 CONTINUE
   31 VB=VB+1000.
    2 CONTINUE
      STOP
      END
$DATA
 4.6668E21 1.4077E16 1.1488E16 4.9052E11 9.5428E11
 9.7791E04 1.1493E05 2.0902E07 2.0019E07 2.0200E09
$EOF
```

Program 7 Output

VR= 41000.0 PHG= 90.0

I	VIAFPI	VO	VOX	VOY	VOZ	VI	V1X	V1Y	V1Z
10.018	18277.0	89558.3	88193.0	0.1	15578.6	123816.7	-18.9	-121929.1	-21537.8

TH12	FO	A1	E1	PH1	R1XP	R1YP	R1ZP	TIM12	VINFI	VINFXY	PSI	ALP
180.07	-180.00	0.8617	0.1606	90.01	0.0009	-0.7233	-0.0002	145.98	22646.5	6999.1	0.15	72.00

BETA= 0. A2= 1.12

DCCA	NU	V3	V3X	V3Y	V3Z	DX	DY	DZ	TOP	PH3	F3	A3	E3	I3	OM
0.	31.88	120085.4	20320.9	-117969.9	-9522.7	1.80	0.35	..06	183.3	80.26	-71.65	0.7963	0.1918	4.6150	0.64356
1000.0	27.51	120965.1	18566.6	-118892.3	-12346.8	2.15	0.35	..06	180.0	81.17	-64.09	0.8106	0.1868	5.9289	0.65922
2000.0	24.23	121564.6	16964.9	-119525.1	-14280.8	2.49	0.35	1.06	177.2	81.98	-57.91	0.8208	0.1825	6.8134	0.67100
3000.0	21.67	121992.2	15558.2	-119978.0	-15662.8	2.82	0.35	..06	174.8	82.67	-52.77	0.8282	0.1790	7.4378	0.67994
4000.0	19.61	122307.6	14335.5	-120313.4	-16684.6	3.14	0.35	1.06	172.7	83.27	-48.44	0.8337	0.1762	7.8952	0.68686
5000.0	17.92	122547.4	13273.0	-120568.6	-17461.3	3.46	0.36	..06	170.8	83.78	-44.74	0.8380	0.1739	8.2405	0.69220
6000.0	16.49	122733.7	12346.2	-120767.4	-18065.4	3.78	0.36	1.06	169.2	84.23	-41.54	0.8414	0.1721	8.5077	0.69660
7000.0	15.28	122881.5	11533.4	-120925.3	-18544.5	4.09	0.36	..06	167.7	84.61	-38.76	0.8441	0.1706	8.7187	0.70010
8000.0	14.24	123000.7	10816.3	-121052.8	-18931.0	4.41	0.36	1.06	166.4	84.96	-36.33	0.8463	0.1694	8.8883	0.70296
9000.0	13.33	123098.2	10180.1	-121157.3	-19247.1	4.72	0.36	1.06	165.3	85.26	-34.17	0.8481	0.1683	9.0266	0.70533
10000.0	12.53	123179.1	9612.3	-121243.9	-19509.0	5.03	0.36	..06	164.3	85.52	-32.25	0.8496	0.1675	9.1410	0.70731

BETA= 10.00 A2= 1.12

DCCA	NU	V3	V3X	V3Y	V3Z	DX	DY	DZ	TOP	PH3	F3	A3	E3	I3	OM
0.	31.88	116631.6	20002.3	-114616.1	-10612.9	1.77	0.65	0.97	191.4	80.14	-89.01	0.7482	0.1743	5.2902	0.61780
1000.0	27.51	116018.4	18276.4	-115828.7	-13342.7	2.11	0.71	0.95	187.9	81.09	-79.77	0.7649	0.1639	6.5711	0.63954
2000.0	24.23	118889.7	16699.8	-116726.2	-15190.6	2.45	0.76	0.93	184.5	81.93	-71.81	0.7778	0.1566	7.4147	0.65395
3000.0	21.67	119549.9	15315.1	-117411.5	-16497.0	2.77	0.81	0.91	181.4	82.64	-64.97	0.7879	0.1517	7.9981	0.66435
4000.0	19.61	120065.4	14111.6	-117948.9	-17453.2	3.09	0.87	0.90	178.6	83.25	-59.10	0.7960	0.1484	8.4171	0.67183
5000.0	17.92	120477.0	13065.7	-118379.7	-18172.8	3.41	0.93	0.88	176.1	83.77	-54.06	0.8026	0.1463	8.7275	0.68518
6000.0	16.49	120812.3	12153.4	-118731.6	-18727.1	3.72	0.98	0.86	173.9	84.23	-49.72	0.8081	0.1450	8.9632	0.69095
7000.0	15.28	121089.9	11353.3	-119023.8	-19162.6	4.03	1.03	0.84	171.9	84.62	-45.95	0.8127	0.1442	9.1481	0.69559
8000.0	14.24	121323.1	10647.5	-119269.7	-19510.5	4.34	1.09	0.83	170.2	84.97	-42.66	0.8166	0.1437	9.2904	0.69926
9000.0	13.33	121521.5	10021.1	-119479.3	-19792.5	4.65	1.14	0.81	168.6	85.27	-39.79	0.8200	0.1436	9.4060	0.70229
10000.0	12.53	121692.0	9462.2	-119659.7	-20024.0	4.95	1.19	0.79	167.2	85.54	-37.25	0.8229	0.1436	9.4999	0.70479

BETA= 20.00 A2= 1.12

DCCA	NU	V3	V3X	V3Y	V3Z	DX	DY	DZ	TOP	PH3	F3	A3	E3	I3	OM
0.	31.88	113589.3	19078.1	-111366.0	-11669.9	1.69	0.94	0.07	199.2	80.33	-107.44	0.7049	0.1695	5.9821	0.58706
1000.0	27.51	115090.7	17431.3	-112859.6	-14308.3	2.02	1.05	0.86	196.3	81.29	-97.69	0.7253	0.1515	7.2254	0.61543
2000.0	24.23	116237.4	15927.7	-114013.7	-16072.7	2.33	1.16	0.80	192.9	82.12	-88.51	0.7402	0.1389	8.0202	0.63741
3000.0	21.67	117134.4	14607.1	-114924.3	-17305.9	2.64	1.27	0.77	189.4	82.84	-80.06	0.7524	0.1305	8.5436	0.65524
4000.0	19.61	117851.5	13459.3	-115617.4	-18198.4	2.95	1.38	0.73	185.9	83.44	-72.46	0.7625	0.1251	8.9420	0.66713
5000.0	17.92	118436.1	12461.9	-116258.4	-18862.7	3.25	1.48	0.70	182.7	83.96	-65.72	0.7710	0.1219	9.2158	0.67705
6000.0	16.49	118920.6	11591.8	-116758.7	-19368.8	3.55	1.58	0.66	179.7	84.41	-59.81	0.7783	0.1202	9.4189	0.68474
7000.0	15.28	119329.0	10828.7	-117181.0	-19762.0	3.84	1.69	0.63	177.0	84.79	-54.67	0.7845	0.1194	9.5726	0.69078
8000.0	14.24	119674.9	10155.6	-117541.7	-20072.5	4.14	1.79	0.60	174.6	85.13	-50.19	0.7898	0.1193	9.6909	0.69557
9000.0	13.33	119973.6	9556.2	-117853.1	-20321.4	4.43	1.89	0.57	172.5	85.43	-46.29	0.7945	0.1197	9.7833	0.69942
10000.0	12.53	120233.5	9025.2	-118124.4	-20523.1	4.73	2.00	0.53	170.7	85.70	-42.89	0.7987	0.1204	9.8564	0.70256

Program 8

```
$JOB            0:4,9000        67-012,LT MYERS,AFIT-SE
$IBJOB          MAP
$IBFTC MAIN     M94/2,XR7
C LAUNCH OPPORTUNITIES FOR VENUS-ASSISTED TRAJECTORIES
      TIME(A,G,E,T)=(2.*ATAN(SQRT((1.-E)/(1.+E))*TAN(T*R/2.))-E*SQRT(1.-
     1E**2)*SIN(T*R)/(1.+E*COS(T*R)))*SQRT((A**3)/G)/86400.
      READ(5,1)GCS,GCP1,GCP2,RP1,RP2,VP1,VP2,RADP1,RADP2,RHO
    1 FORMAT(5E10.0/5E10.0)
      READ(5,60)W1,W2,XL10,XL20,S,T0
   60 FORMAT(4F12.6,F10.2,F12.2)
      DIMENSION TL(50)
      VB=38000.
      PI=3.14159
      R=PI/180.
      M=39
      N=4
      L=4
      ITT=15
C DEPARTURE ORBITS
      DO 2 I=1,M
      VINFP1=SQRT(VB**2-2.*GCP1/RADP1)
      PH0=90.
      WRITE(6,32)
   32 FORMAT(1HA,10X,100H**************************************************
     1**************************************************)
      DO 3 J=1,N
      XI=0.
      DO 4 K=1,L
      PH0R=PH0*R
      XIR=XI*R
      IF((VP1*SIN(PH0R)*COS(XIR))**2+VINFP1**2-VP1**2)5,5,6
    5 WRITE(6,7)VB,PH0,XI
    7 FORMAT(1HA,20X,17HNO ESCAPE FOR VB=,F10.1,7HAT PH0=,F7.2,6HAND I=,
     1F6.2)
      GO TO 31
    6 V0=VP1*SIN(PH0R)*COS(XIR)-SQRT((VP1*SIN(PH0R)*COS(XIR))**2+VINFP1*
     1*2-VP1**2)
C PRE-ASSIST TRAJECTORY
      RP1V0=RP1*V0**2/GCS
      TANF0=RP1V0*COS(PH0R)*SIN(PH0R)/(1.-RP1V0*SIN(PH0R)**2)
      IF(TANF0)8,9,9
    8 F0=ATAN(TANF0)/R
      GO TO 10
    9 F0=(ATAN(TANF0)-PI)/R
   10 A1=RP1/(2.-RP1V0)
      E1=SQRT((RP1V0-1.)*SIN(PH0R))**2+COS(PH0R)**2)


      RPER1=A1*(1.-E1)
      IF(RPER1-RP2)11,11,12
   12 WRITE(6,13)VB,PH0,XI
   13 FORMAT(1HA,10X,3HVB=,F10.1,36HINSUFFICIENT TO INTERCEPT P2 AT PH0=
     1,F7.2,6HAND I=,F7.2)
      GO TO 31
   11 V1=SQRT(GCS*(2./RP2-1./A1))
      PH1R=ARSIN(SQRT(A1**2*(1.-E1**2)/(RP2*(2.*A1-RP2))))
      PH1=PH1R/R
      RP2V1=RP2*V1**2/GCS
      TANF1=RP2V1*COS(PH1R)*SIN(PH1R)/(1.-RP2V1*SIN(PH1R)**2)
      IF(TANF1)14,14,15
   14 F1=ATAN(TANF1)/R
      GO TO 16
   15 F1=(ATAN(TANF1)-PI)/R
   16 THT12=F1-F0
      THR=THT12*R
      TIM12=TIME(A1,GCS,E1,F1)-TIME(A1,GCS,E1,F0)
      R1ZP=RP2*SIN(THR)*SIN(XIR)
      IF(R1ZP-RHO)17,28,28
   28 WRITE(6,29)XI,VB,PH0
   29 FORMAT(1HA,10X,2HI=,F5.2,30HTOO LARGE FOR INTERCEPT AT VB=,F10.1,8
     1HAND PH0=,F8.2)
      GO TO 30
   17 THL=THT12-W2*TIM12
      THP=THT12-W1*TIM12
      TL(1)=(XL10-XL20+(W2-W1)*T0+THL)/(W2-W1)
      DO 50 IT=2,ITT
      TL(IT)=TL(1)+FLOAT(IT-1)*S
   50 CONTINUE
      WRITE(6,51)VB,PH0,XI,TIM12,THT12,THL,THP,(TL(IT),IT=1,ITT)
   51 FORMAT(1HA,48X,3HVB=,F10.1,2X,4HPH0=,F7.2,2X,2HI=,F6.2//39X,6HTIM1
     12=,F9.2,2X,6HTHT12=,F7.2,2X,4HTHL=,F7.2,2X,4HTHP=,F7.2//49X,12HJUL
     2IAN DATES,10X,14HCALENDAR DATES//(F60.2))
      XI=XI+.1
    4 CONTINUE
   30 PH0=PH0-2.
    3 CONTINUE
   31 VB=VB+1000.
    2 CONTINUE
      STOP
      END
$DATA
 4.6868E21 1.4077E16 1.1488E16 4.9092E11 3.5480E11
 9.7751E04 1.1493E05 2.0903E07 2.0013E07 2.0200E09
     .985609    1.602131  100.158150  174.29431     583.92  2436935.00


$EOF
```

Program 8 Output

VB= 49000.0 PHO= 90.00 I= 0.

TIM12= 56.52 THT12= 46.21 THL= -44.33 THP= -9.49

JULIAN DATES	CALENDAR DATES
2436742.79	
2437326.69	
2437910.59	See Ref 1
2438494.53	
2439078.44	
2439662.38	
2440246.28	
2440830.22	
2441414.13	
2441998.03	
2442581.97	
2443165.88	
2443749.81	
2444333.72	
2444917.66	

Vita: 1/Lt K. A. Myers

Kenneth Alan Myers was born on 11 September 1942 in Waynesboro, Pennsylvania. He spent his boyhood years in Mercersburg, Pennsylvania, and was graduated from James Buchanan High School in 1960, after which he attended The Pennsylvania State University. On 12 December 1964 he was commissioned as a Second Lieutenant in the United States Air Force as a Distinguished Military Graduate, and received a Bachelor of Science degree in Aerospace Engineering. He attended The Pennsylvania State University Graduate School prior to reporting to the Air Force Institute of Technology in June 1965.

Permanent address: 23 W. Fairview Avenue
Mercersburg, Pennsylvania 17236

This thesis was typed by Mrs. Kenneth A. Myers

UNCLASSIFIED
Security Classification

DOCUMENT CONTROL DATA - R & D

(Security classification of title, body of abstract and indexing annotation must be entered when the overall report is classified)

1. ORIGINATING ACTIVITY (Corporate author) Air Force Institute of Technology (AFIT-SE) Wright-Patterson AFB, Ohio 45433	2a. REPORT SECURITY CLASSIFICATION UNCLASSIFIED 2b. GROUP

3. REPORT TITLE

GRAVITY-ASSISTED TRAJECTORIES FOR SOLAR PROBE MISSIONS

4. DESCRIPTIVE NOTES (Type of report and inclusive dates)

AFIT Thesis

5. AUTHOR(S) (First name, middle initial, last name)

Myers, Kenneth A., 1/Lt, USAF

6. REPORT DATE	7a. TOTAL NO. OF PAGES	7b. NO. OF REFS
June 1967	198	25

8a. CONTRACT OR GRANT NO. N/A b. PROJECT NO. N/A c. d.	9a. ORIGINATOR'S REPORT NUMBER(S) AFIT Thesis GA/AE/67-4 9b. OTHER REPORT NO(S) (Any other numbers that may be assigned this report) N/A

10. DISTRIBUTION STATEMENT This document is subject to special export controls and each transmittal to foreign governments or foreign nationals may be made only with prior approval of the Dean, School of Engineering, Air Force Institute of Technology (AFIT-SE), Wright-Patterson Air Force Base, Ohio 45433.

11. SUPPLEMENTARY NOTES	12. SPONSORING MILITARY ACTIVITY
	Department of Aeronautical Engineering Air Force Institute of Technology (AFIT-SEA) Wright-Patterson AFB, Ohio 45433

13. ABSTRACT

An investigation of direct-transfer trajectories for solar probe missions indicates that expensive launch vehicles such as the $125-million Saturn V are required to achieve perihelia less than 0.25 AU and inclination angles above 20°. Methods are developed for two- and three-dimensional gravity-assisted trajectories (trajectories which pass through one or more planetary gravitational fields), and are applied to solar probe missions in an attempt to reduce launch vehicle costs. The analysis is based on the pieced-conic approximation and the assumption of circular coplanar planetary orbits. It is found that a perihelion of 0.16 AU can be obtained with the $16-million Atlas/Centaur/TE-364-3 by using a Venus assist. Even greater reductions in perihelia are attained with multiple passes at Venus; in addition, these missions allow the exploration of several regions near the Sun with a single launch. Venus-Mercury combination-assisted trajectories are of little value in solar probe missions. A Venus assist is useful for 10°-out-of-ecliptic trajectories when the pre-assist orbit lies in the ecliptic. For a pre-assist orbit out of the ecliptic, an inclination angle of 25° and a perihelion of 0.53 AU can be achieved with the Atlas/Centaur/TE-364-3 launch vehicle. Solar impact and 90°-out-of-ecliptic trajectories can be attained with a Jupiter assist; however, traversal of the asteroid belt and a three-year mission time decreases spacecraft reliability.

DD FORM 1 NOV 65 1473

UNCLASSIFIED
Security Classification

UNCLASSIFIED
Security Classification

14. KEY WORDS	LINK A		LINK B		LINK C	
	ROLE	WT	ROLE	WT	ROLE	WT
Gravity Assist Flyby Solar-Probe Missions Trajectories for Solar-Probes Interplanetary Trajectories Gravity-Assisted Trajectories Planetary Swing-By Orbits Planetary Flyby						

UNCLASSIFIED
Security Classification